TABLE OF CONTENTS

A Results 1 - Application of ball milling technology for production of co-crystals (Chapter 4)

A.1 Caffeine/oxalic acid

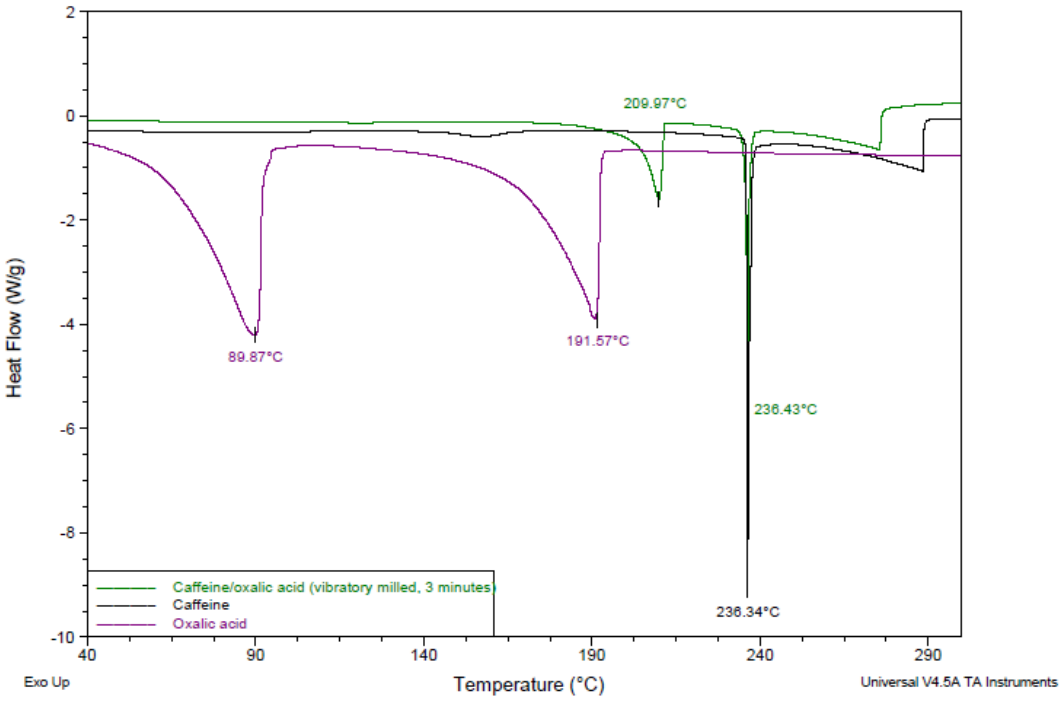

Figure A.1 - Thermal analysis of caffeine/oxalic acid produced by vibratory milling for 3 minutes with a 1:1 stoichiometry.

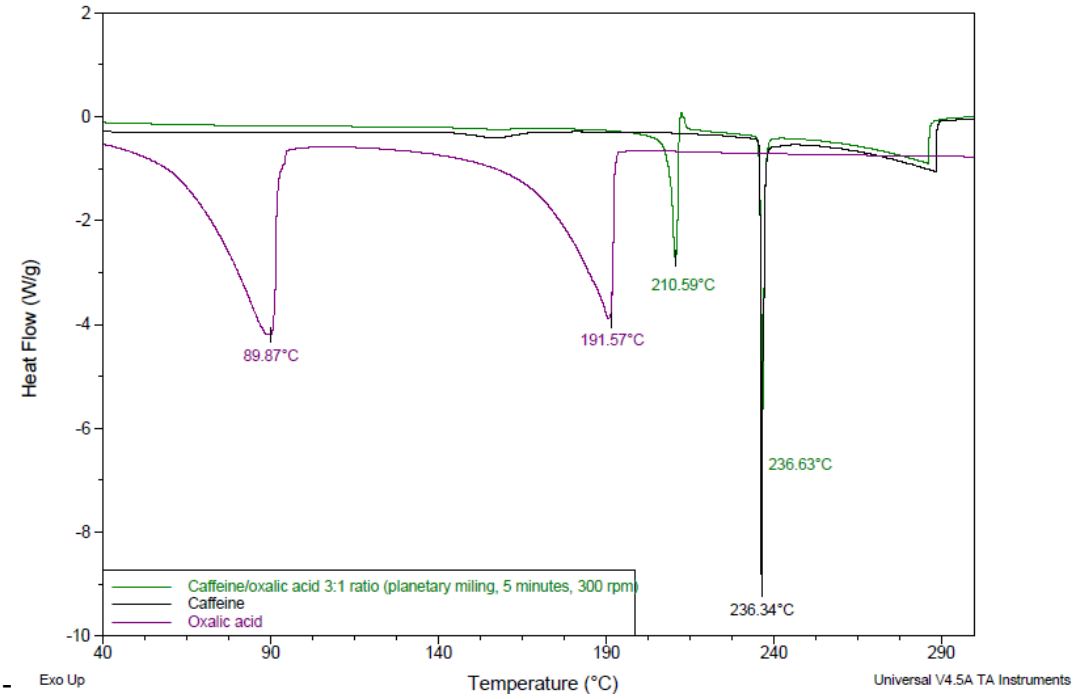

Figure A.2 - Thermal analysis of caffeine/oxalic acid produced by planetary milling for 5 minutes at 300 rpm with a 3:1 stoichiometry.

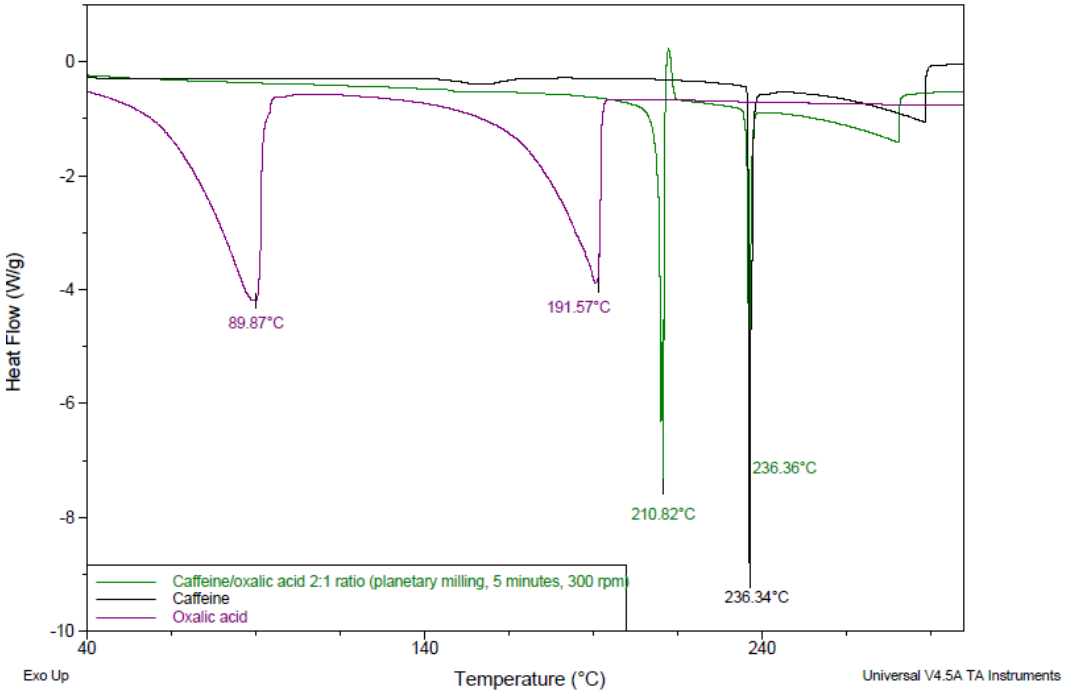

Figure A.3 - Thermal analysis of caffeine/oxalic acid produced by planetary milling for 5 minutes at 300 rpm with a 2:1 stoichiometry.

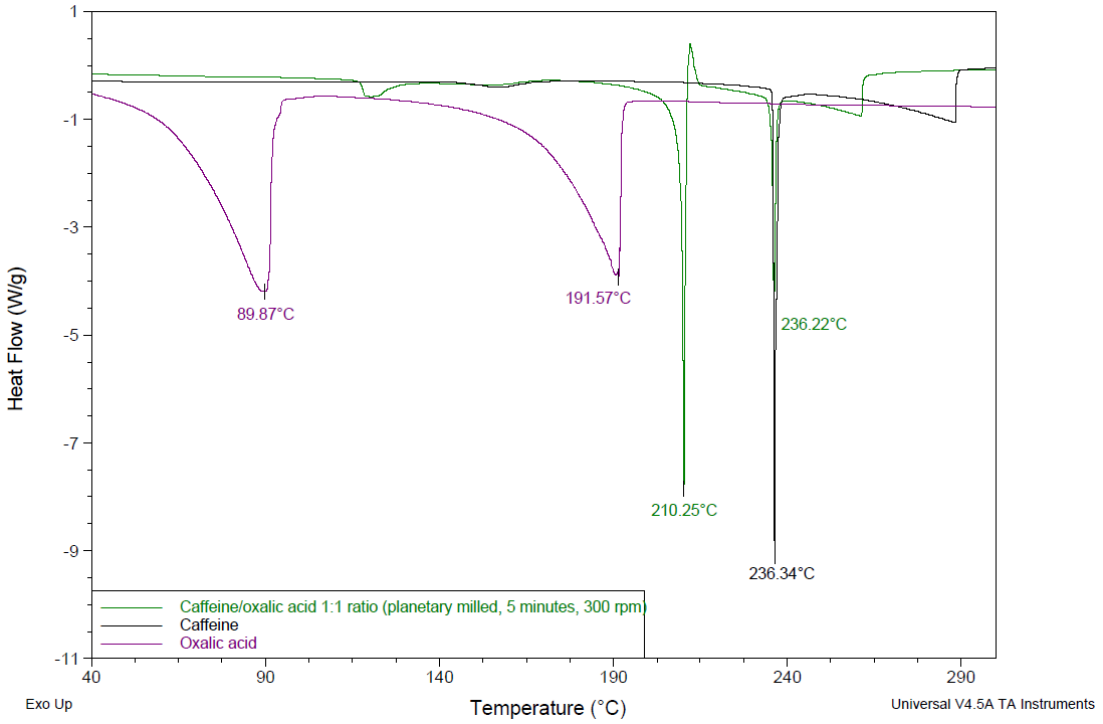

Figure A.4 - Thermal analysis of caffeine/oxalic acid produced by planetary milling for 5 minutes at 300 rpm with a 1:1 stoichiometry.

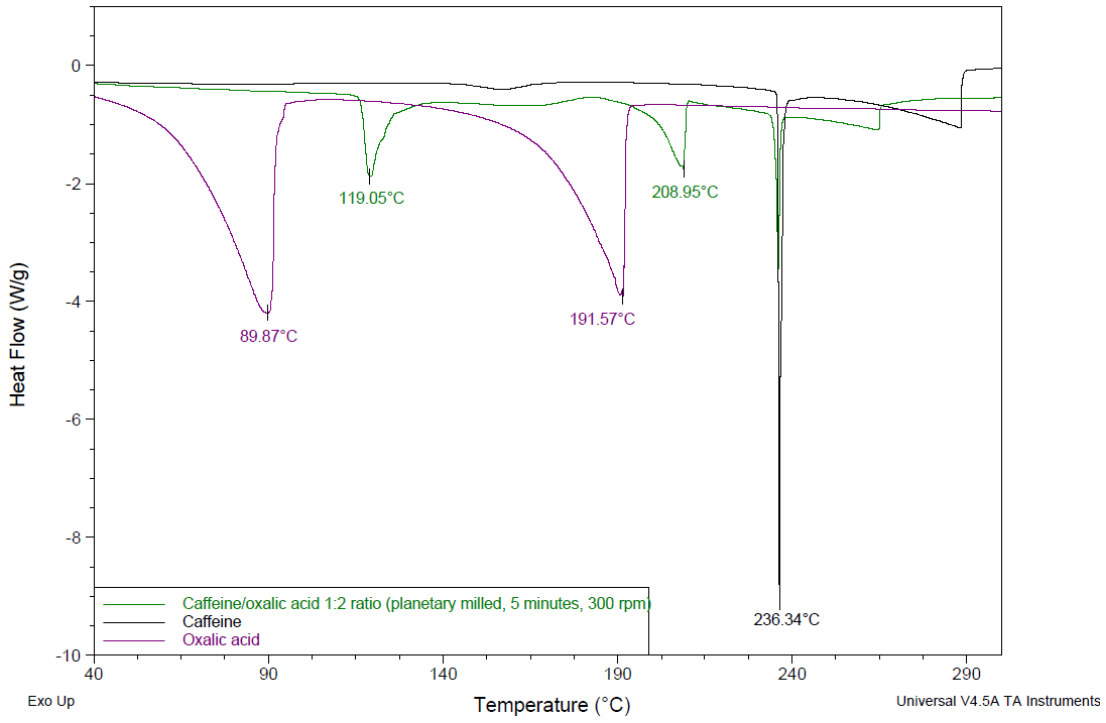

Figure A.5 - Thermal analysis of caffeine/oxalic acid produced by planetary milling for 5 minutes at 300 rpm with a 1:2 stoichiometry.

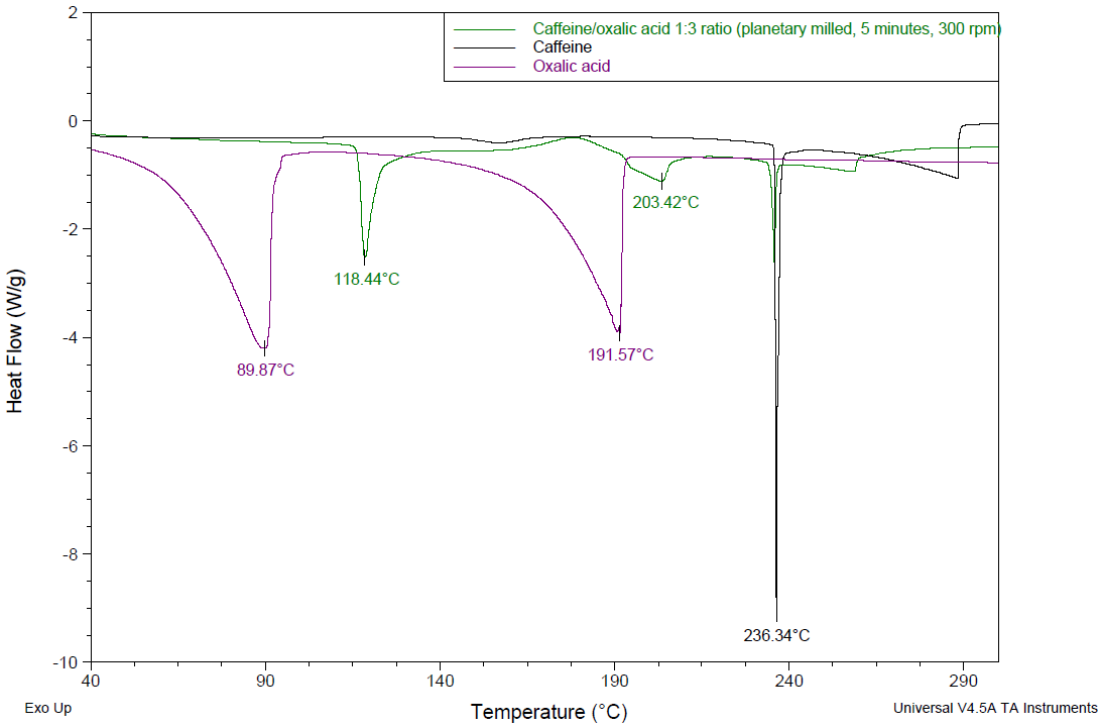

Figure A.6 - Thermal analysis of caffeine/oxalic acid produced by planetary milling for 5 minutes at 300 rpm with a 1:3 stoichiometry.

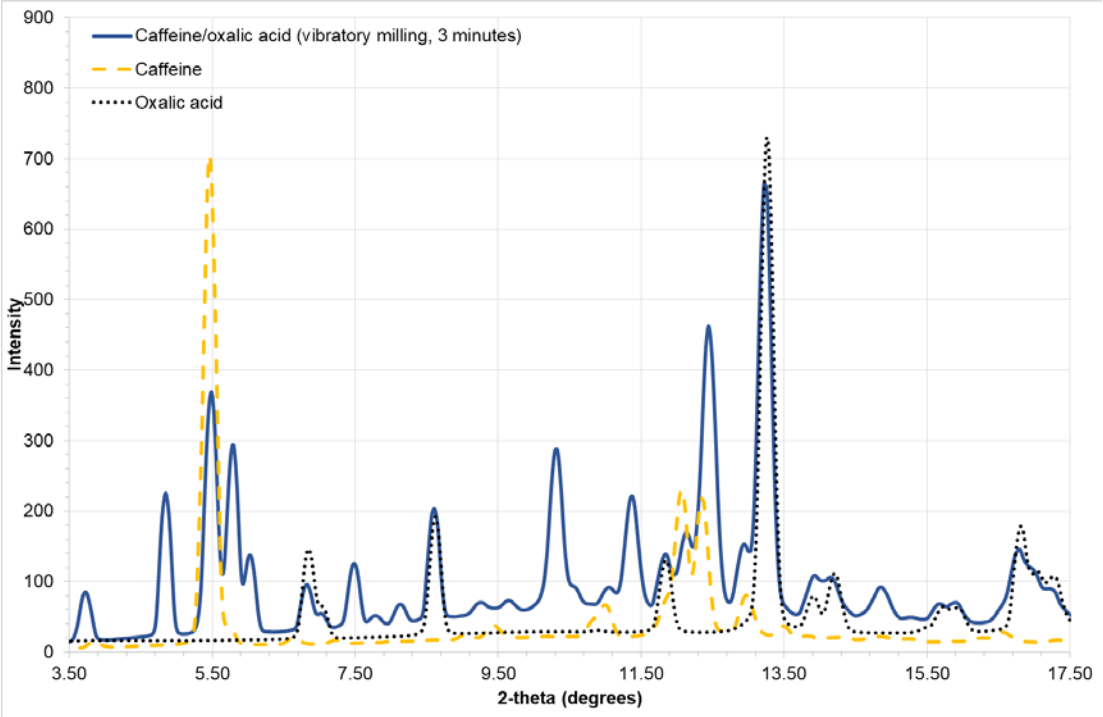

Figure A.7 - Powder x-ray pattern of caffeine/oxalic acid produced by vibratory milling for 3 minutes with a 1:1 stoichiometry (λ = 0.7107 Å).

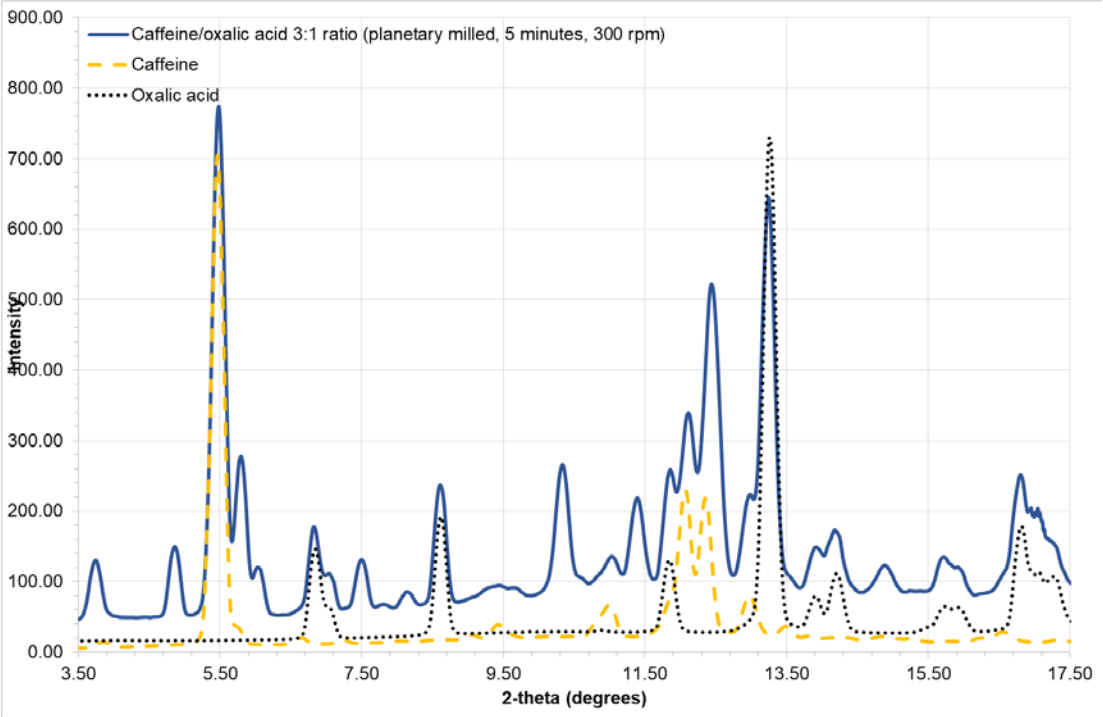

Figure A.8 - Powder x-ray pattern of caffeine/oxalic acid produced by planetary milling for 5 minutes at 300 rpm, with a 3:1 stoichiometry (λ = 0.7107 Å).

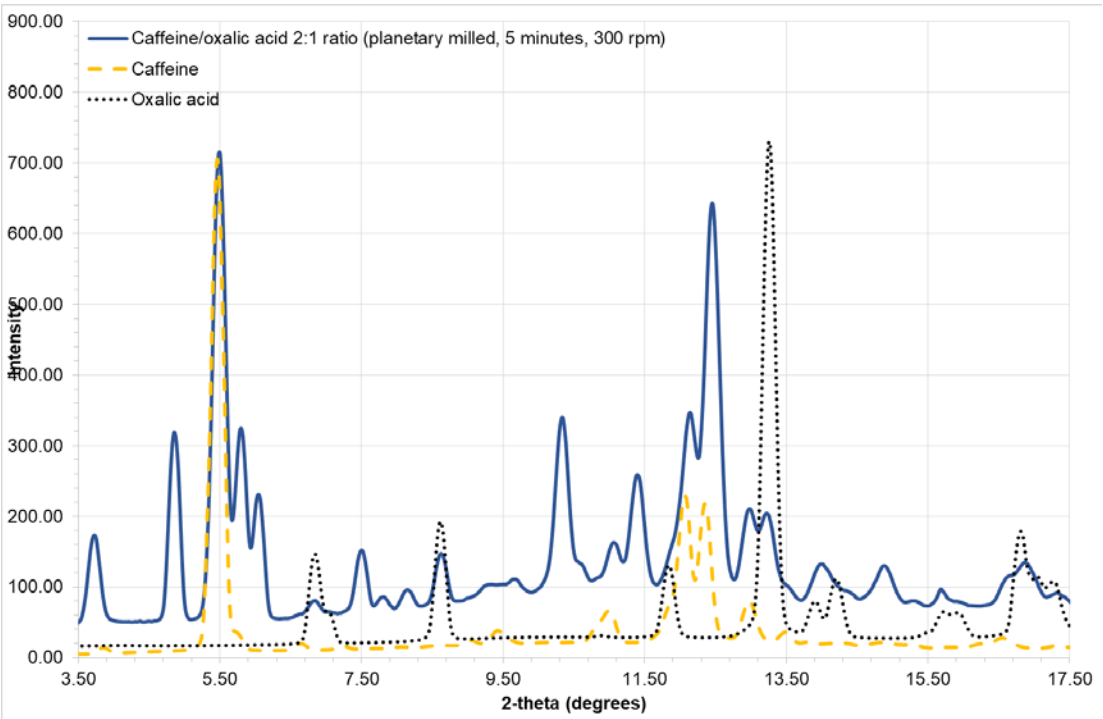

Figure A.9 - Powder x-ray pattern of caffeine/oxalic acid produced by planetary milling for 5 minutes at 300 rpm, with a 2:1 stoichiometry (λ = 0.7107 Å).

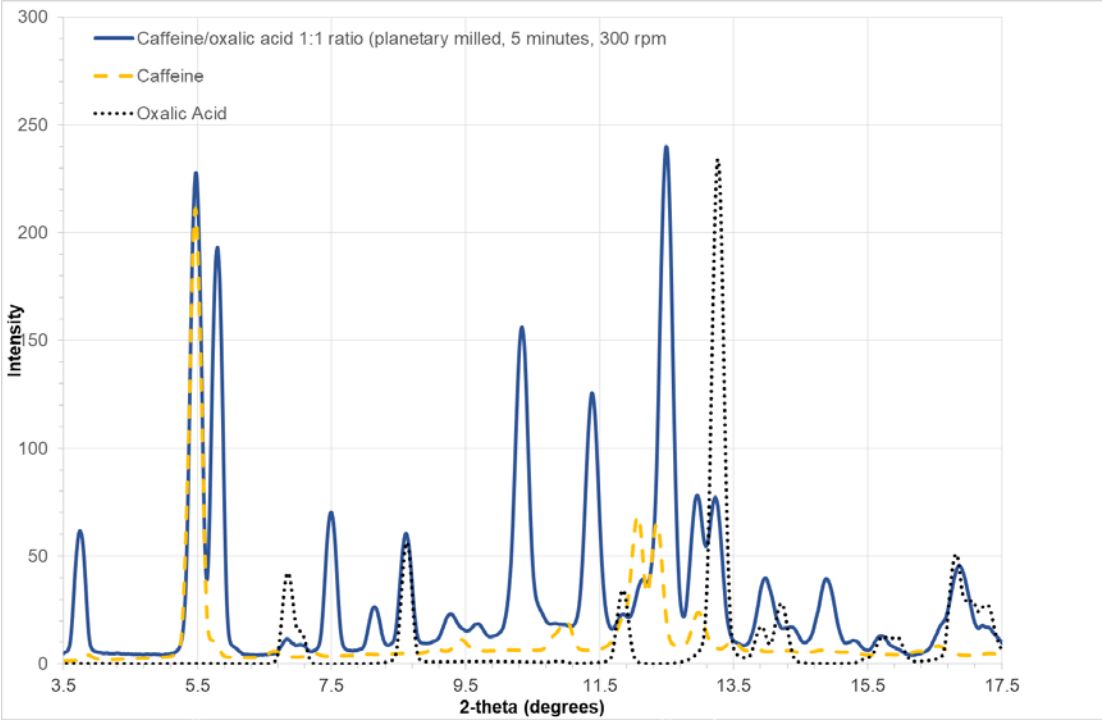

Figure A.10 - Powder x-ray pattern of caffeine/oxalic acid produced by planetary milling for 5 minutes at 300 rpm, with a 1:1 stoichiometry (λ = 0.7107 Å).

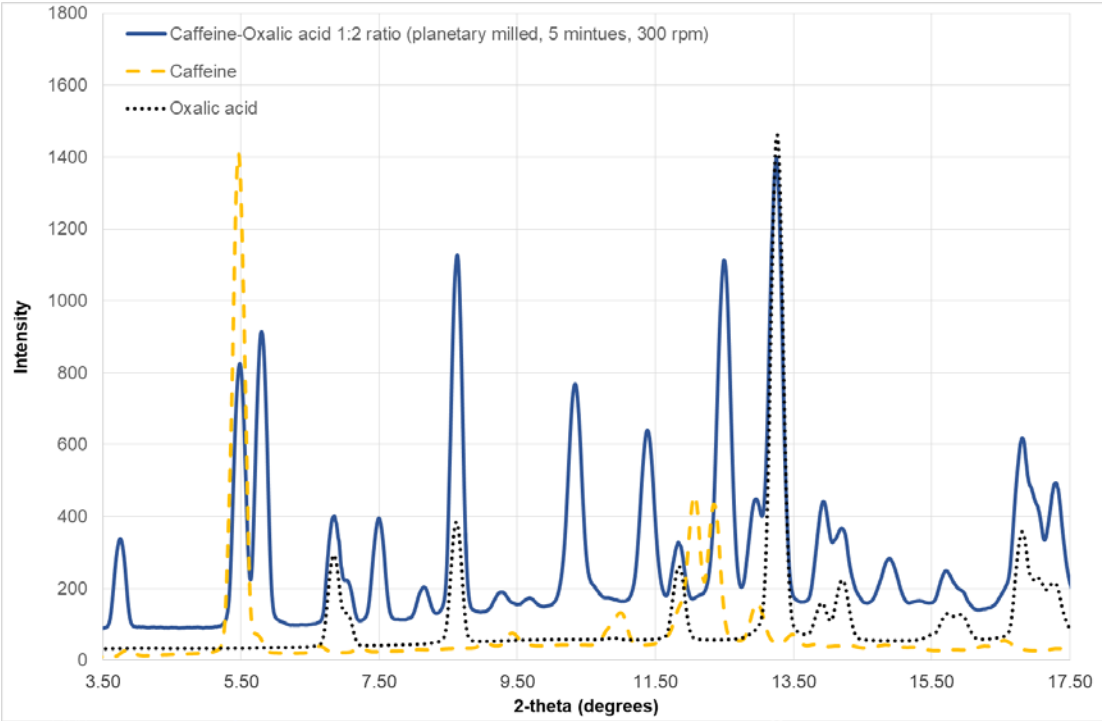

Figure A.11 - Powder x-ray pattern of caffeine/oxalic acid produced by planetary milling for 5 minutes at 300 rpm, with a 1:2 stoichiometry (λ = 0.7107 Å).

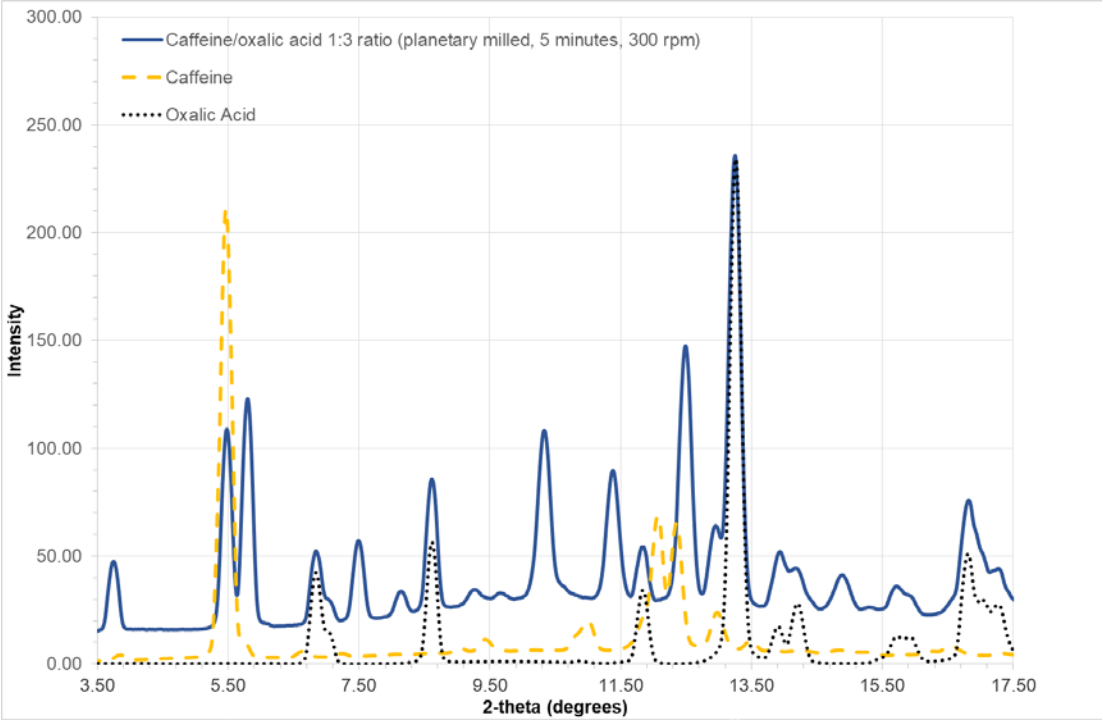

Figure A.12 - Powder x-ray pattern of caffeine/oxalic acid produced by planetary milling for 5 minutes at 300 rpm, with a 1:3 stoichiometry.

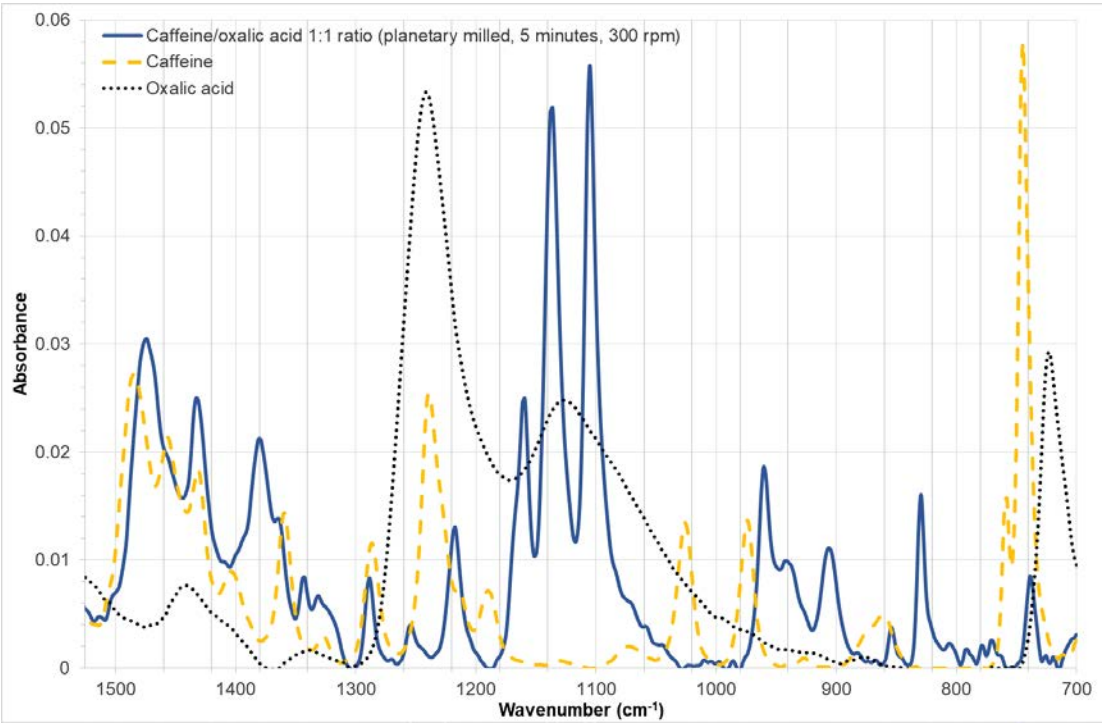

Figure A.13 - Infra-red spectra of caffeine/oxalic acid produced by planetary milling for 5 minutes at 300 rpm, with a 1:1 stoichiometry.

Table A.1 - Infrared spectra peak positions and heights of caffeine/oxalic acid produced by planetary milling for 5 minutes at 300 rpm, with a 1:1 stoichiometry.

Peak Position (cm^{-1})	Peak Height (Absorbance)
1701.86	0.03
1661.04	0.05
1543.58	0.02
1501.83	0.01
1449.3	0.01
1433.87	0.01
1286.89	0.01
1229.26	0.02
1206.15	0.03
1174.59	0.03
1029.58	0.02
1010.87	0.01
975.57	0.01
923.61	0.01
898.93	0.02
875.31	0.01
848.11	0.01
839.83	0.01
807.88	0.01
794.96	0.01
761.94	0.02
748.36	0.04
723.25	0.01
707.15	0.03

A.2 2,4,6-trinitrotoluene/naphthalene

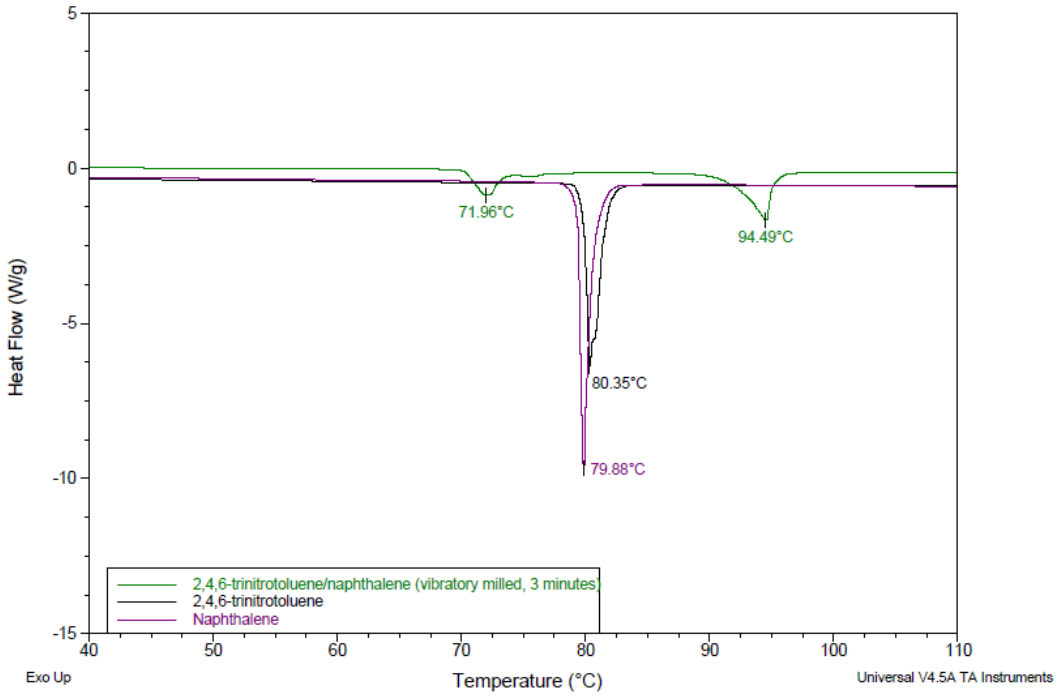

Figure A.14 - Thermal analysis of 2,4,6-trinitrotoluene/naphthalene produced by vibratory milling for 3 minutes with a 1:1 stoichiometry.

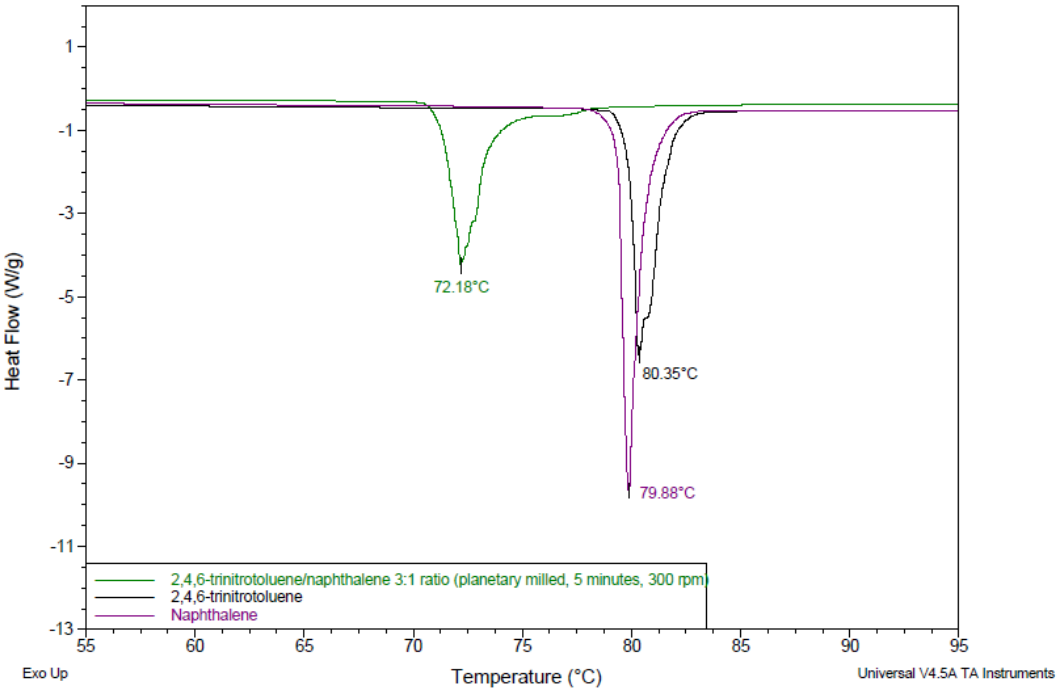

Figure A.15 - Thermal analysis of 2,4,6-trinitrotoluene/naphthalene produced by planetary milling for 5 minutes at 300 rpm, with a 3:1 stoichiometry.

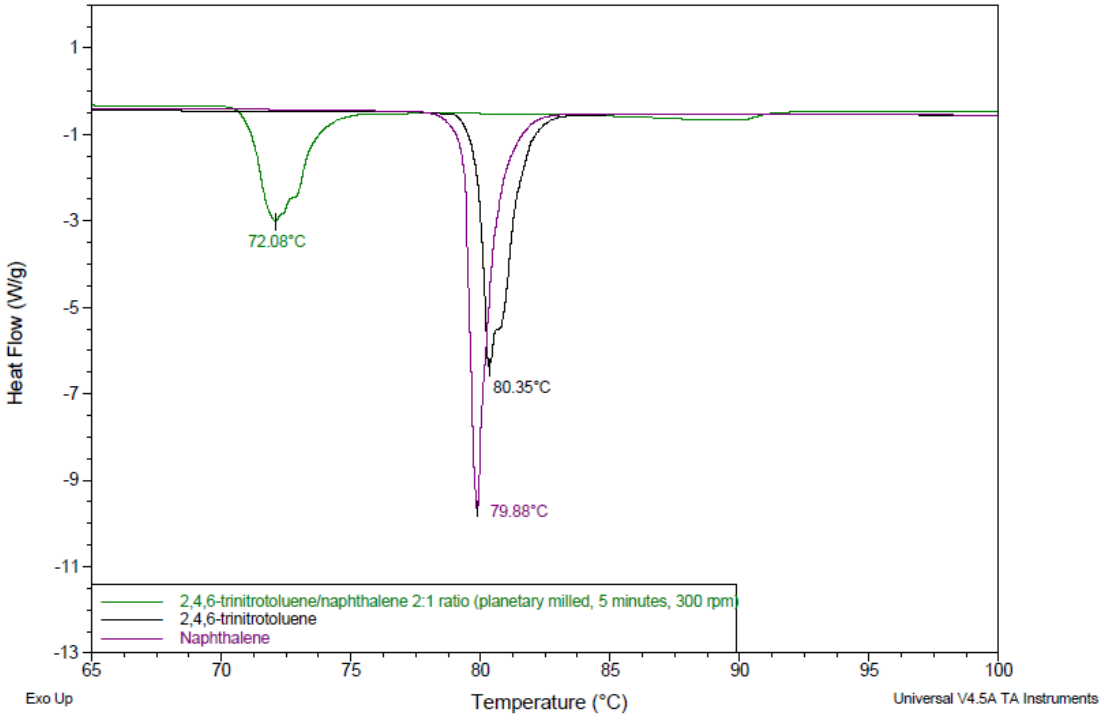

Figure A.16 - Thermal analysis of 2,4,6-trinitrotoluene/naphthalene produced by planetary milling for 5 minutes at 300 rpm, with a 2:1 stoichiometry.

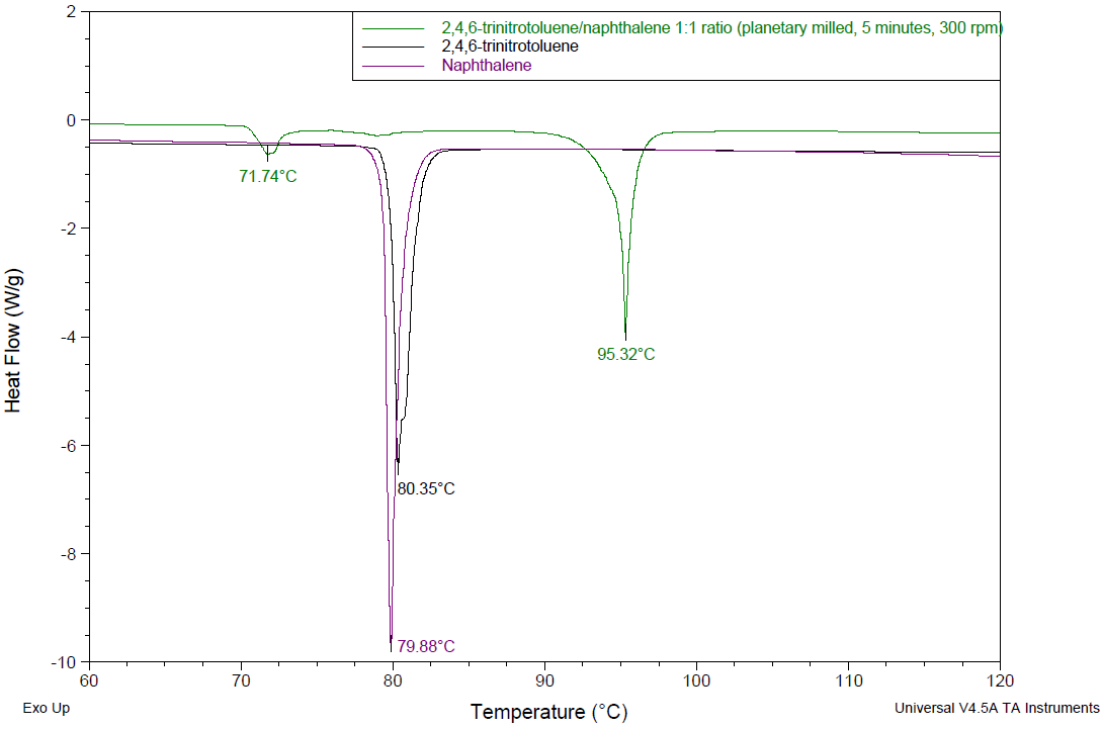

Figure A.17 - Thermal analysis of 2,4,6-trinitrotoluene/naphthalene produced by planetary milling for 5 minutes at 300 rpm, with a 1:1 stoichiometry.

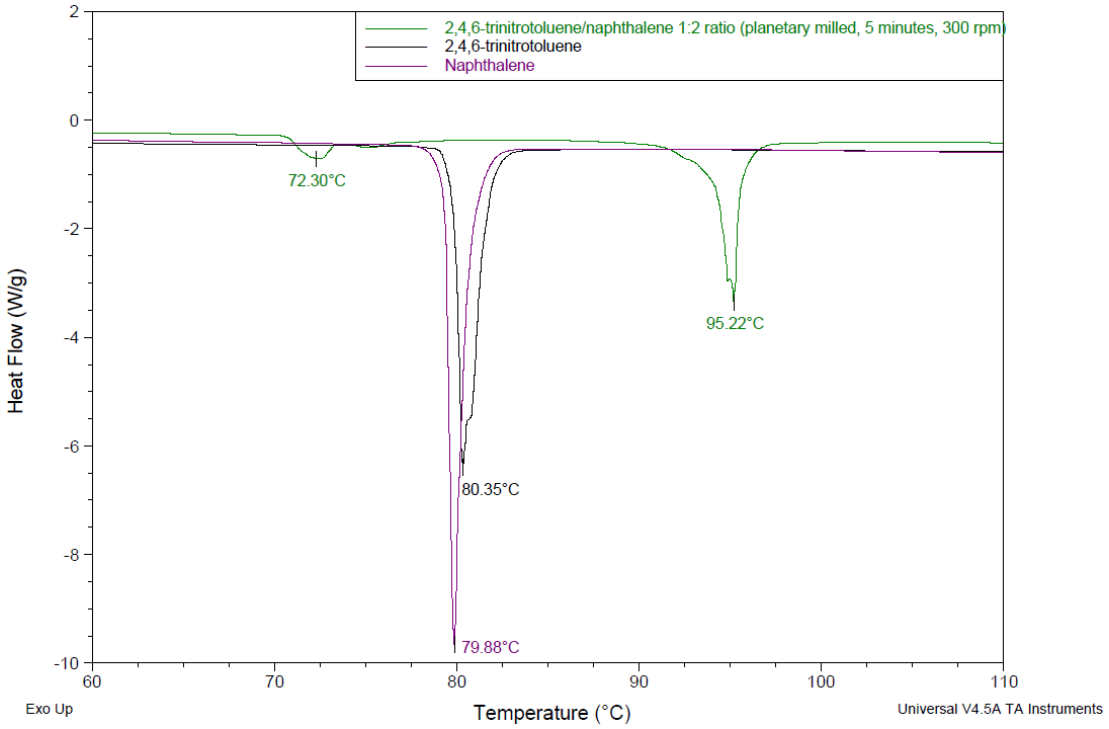

Figure A.18 - Thermal analysis of 2,4,6-trinitrotoluene/naphthalene produced by planetary milling for 5 minutes at 300 rpm, with a 1:2 stoichiometry.

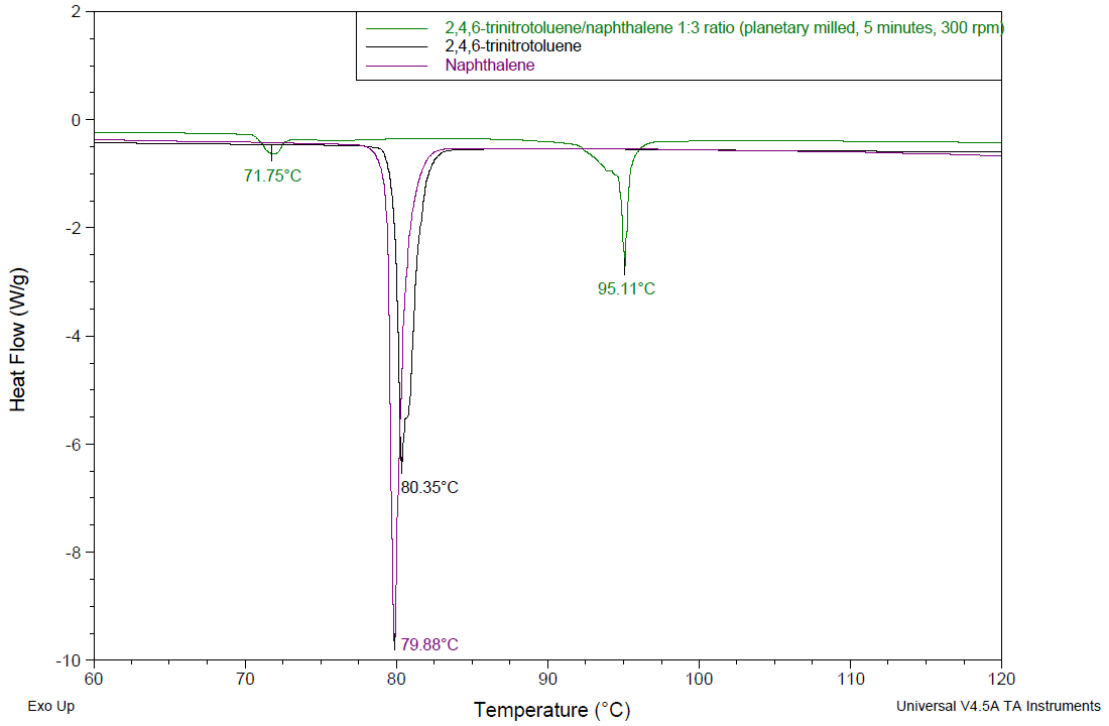

Figure A.19 - Thermal analysis of 2,4,6-trinitrotoluene/naphthalene produced by planetary milling for 5 minutes at 300 rpm, with a 1:3 stoichiometry.

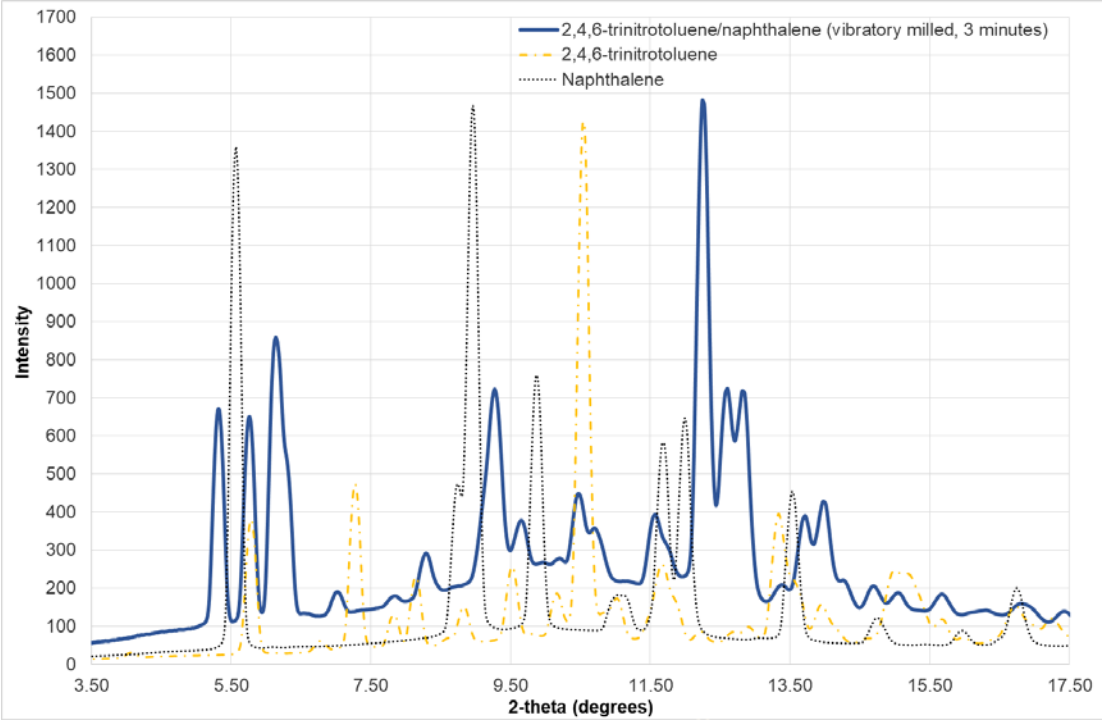

Figure A.20 - Powder x-ray pattern of 2,4,6-trinitrotoluene/naphthalene produced by vibratory milling for 3 minutes with a 1:1 stoichiometry (*λ* = 0.7107 Å).

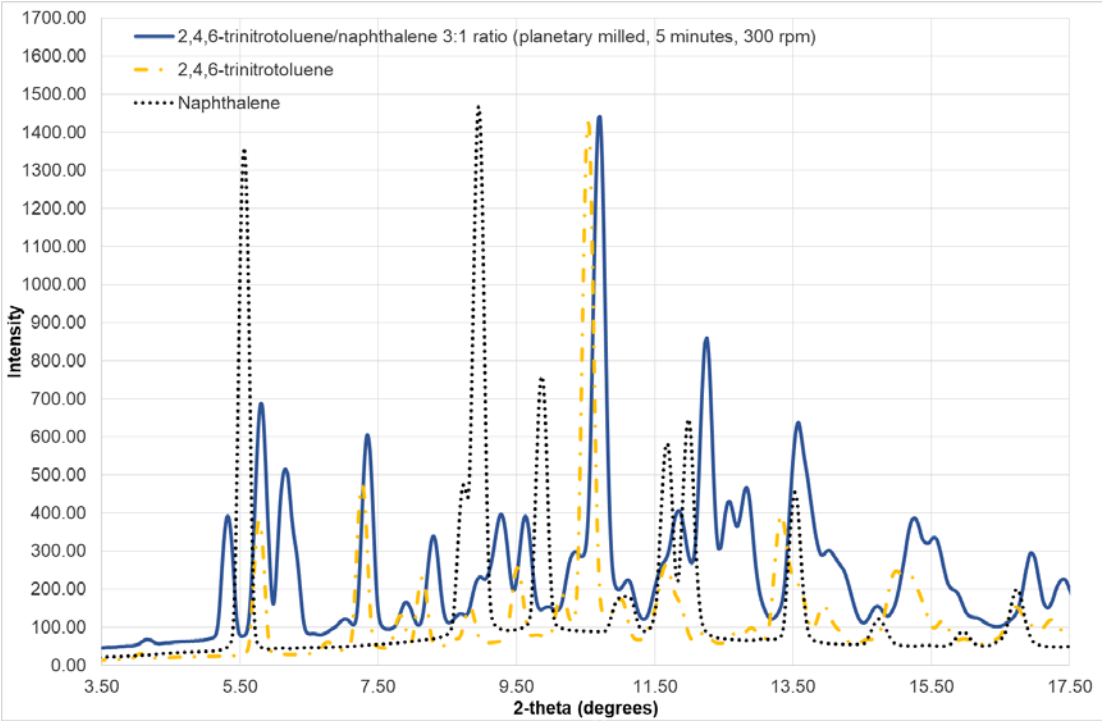

Figure A.21 - Powder x-ray pattern of 2,4,6-trinitrotoluene/naphthalene produced by planetary milling for 5 minutes at 300 rpm, with a 3:1 stoichiometry (*λ* = 0.7107 Å).

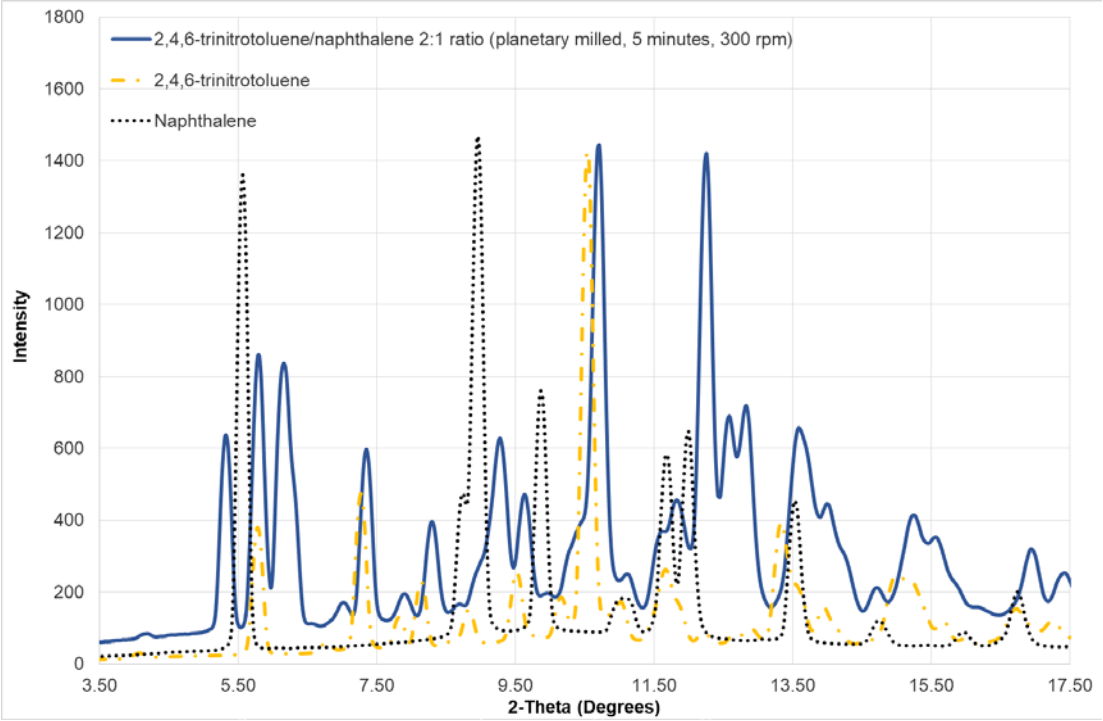

Figure A.22 - Powder x-ray pattern of 2,4,6-trinitrotoluene/naphthalene produced by planetary milling for 5 minutes at 300 rpm, with a 2:1 stoichiometry (λ = 0.7107 Å).

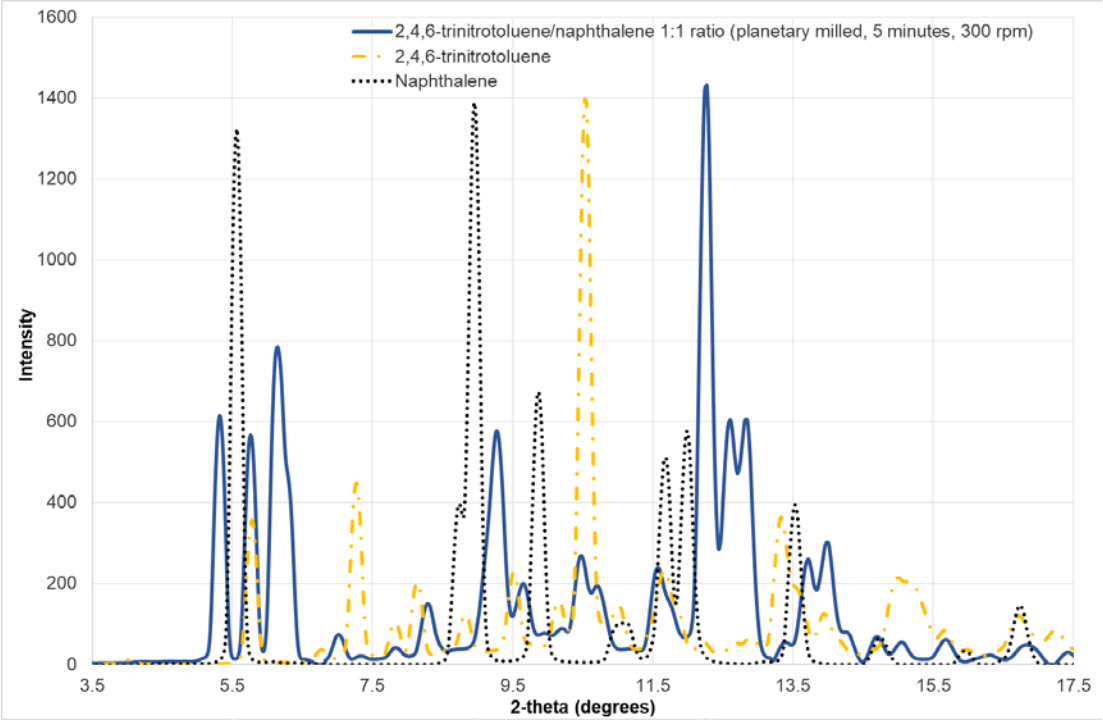

Figure A.23 - Powder x-ray pattern of 2,4,6-trinitrotoluene/naphthalene produced by planetary milling for 5 minutes at 300 rpm, with a 1:1 stoichiometry (λ = 0.7107 Å).

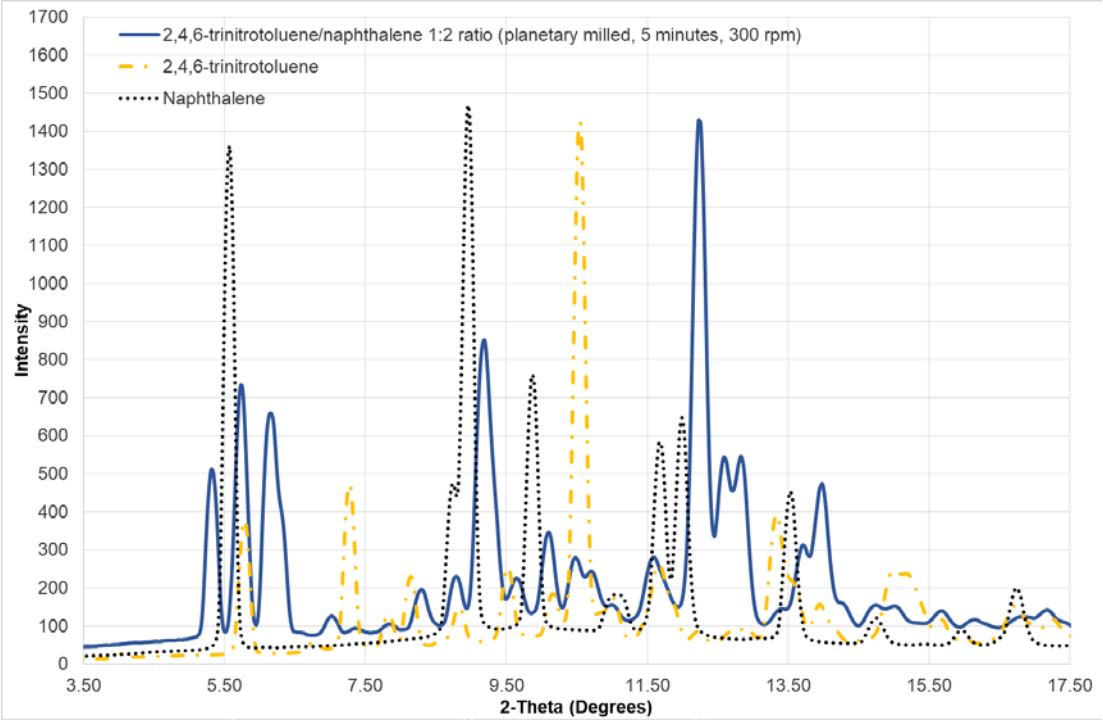

Figure A.24 - Powder x-ray pattern of 2,4,6-trinitrotoluene/naphthalene produced by planetary milling for 5 minutes at 300 rpm, with a 1:2 stoichiometry (λ = 0.7107 Å).

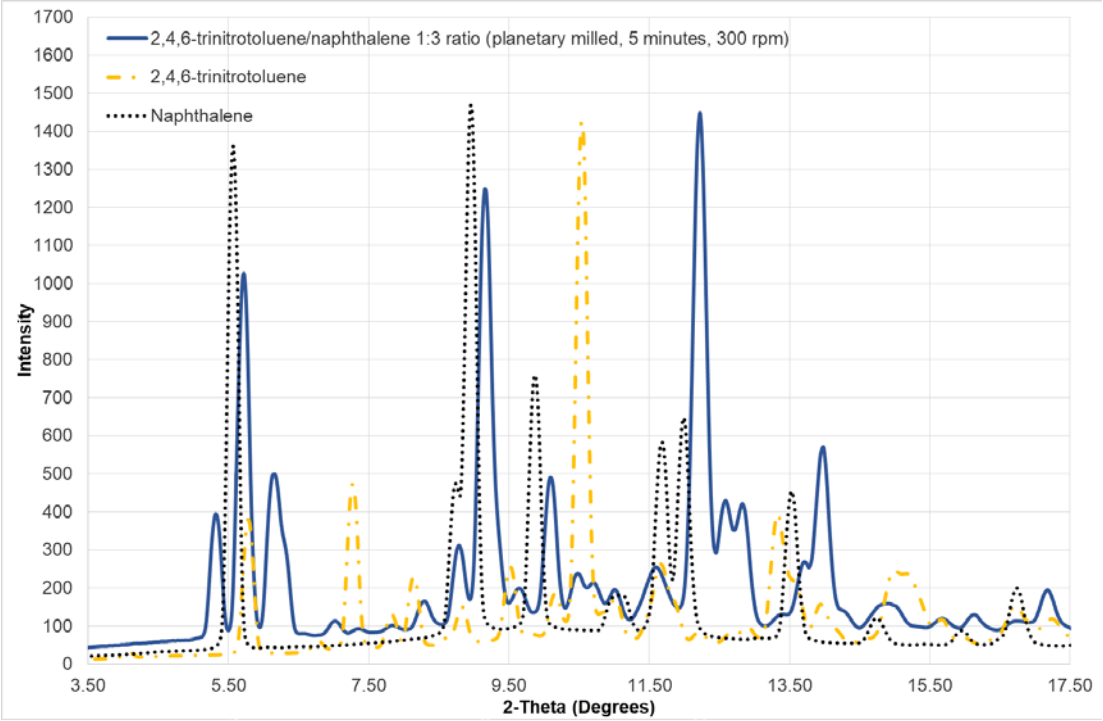

Figure A.25 - Powder x-ray pattern of 2,4,6-trinitrotoluene/naphthalene produced by planetary milling for 5 minutes at 300 rpm, with a 1:3 stoichiometry (λ = 0.7107 Å).

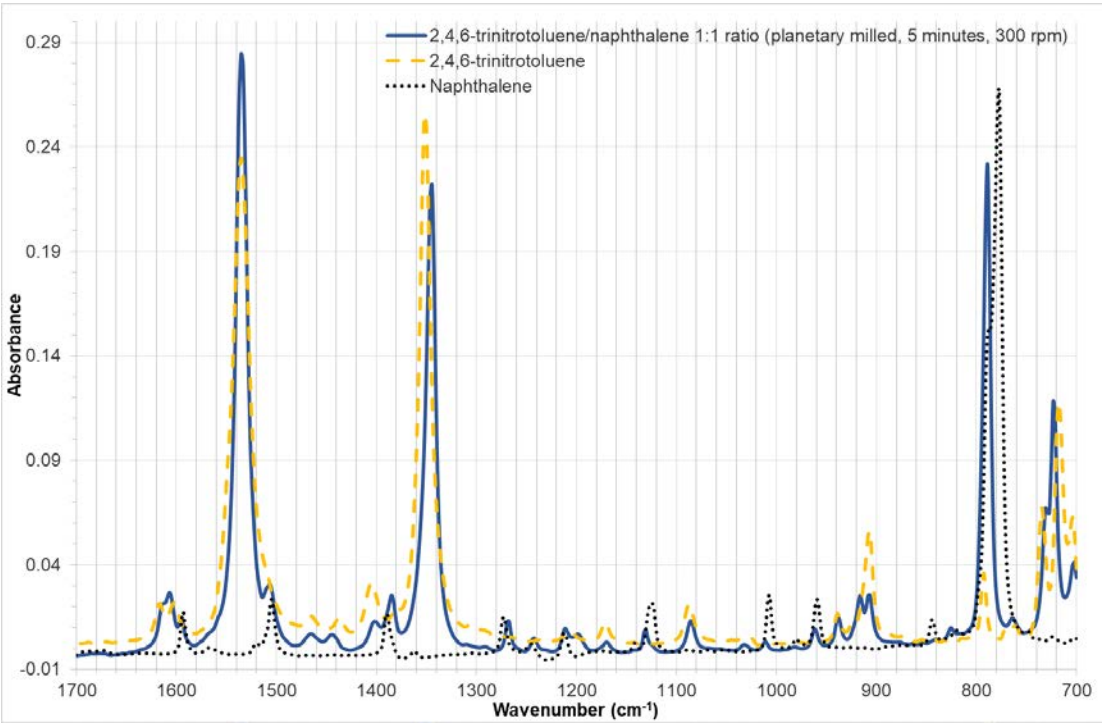

Figure A.26 - Infra-red spectra of 2,4,6-trinitrotoluene/naphthalene produced by planetary milling for 5 minutes at 300 rpm, with a 1:1 stoichiometry.

Table A.2 - Infrared spectra peak positions and heights of 2,4,6-trinitrotoluene/naphthalene produced by planetary milling for 5 minutes at 300 rpm, with a 1:1 stoichiometry.

Peak Position (cm-1)	Peak Height (Absorbance)
3098.89	0.02
1606.84	0.03
1595.19	0.01
1534.89	0.29
1506.74	0.03
1401.72	0.01
1384.79	0.03
1344.91	0.22
1268.36	0.01
1211.16	0.01
1085.71	0.01
961.68	0.01
938.01	0.01
916.21	0.03
907.19	0.03
825.44	0.01
789.1	0.23
763.91	0.01
730.5	0.07
722.86	0.12
702.58	0.04

A.3 2,4,6-trinitrotoluene/anthracene

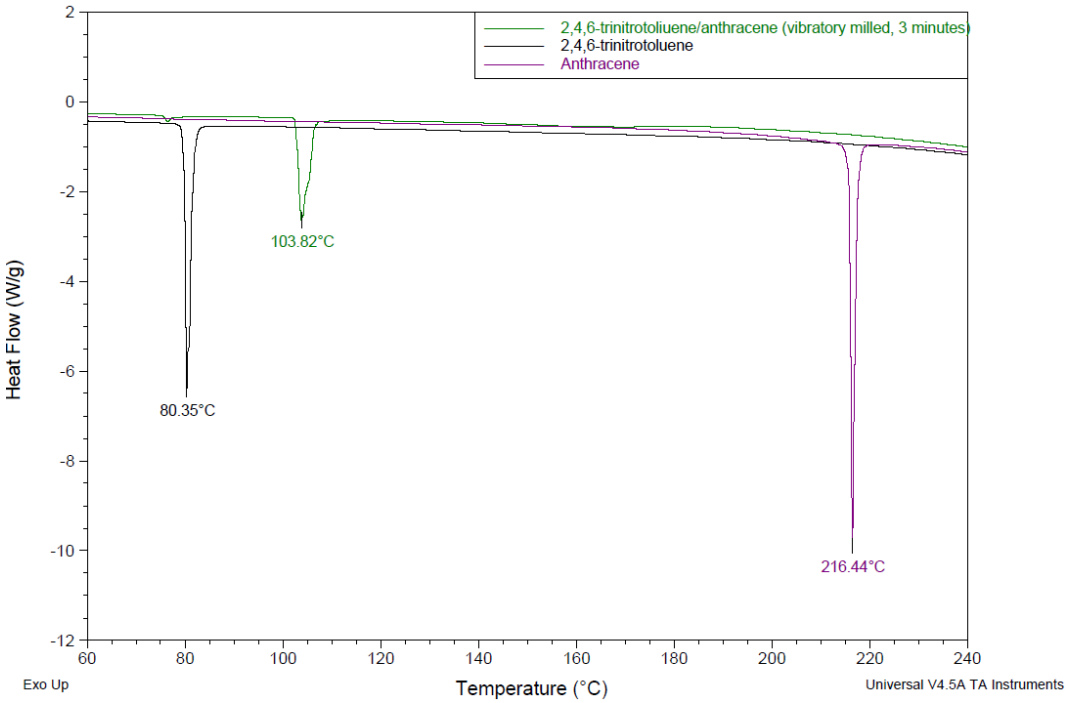

Figure A.27 - Thermal analysis of 2,4,6-trinitrotoluene/anthracene produced by vibratory milling for 3 minutes with a 1:1 stoichiometry.

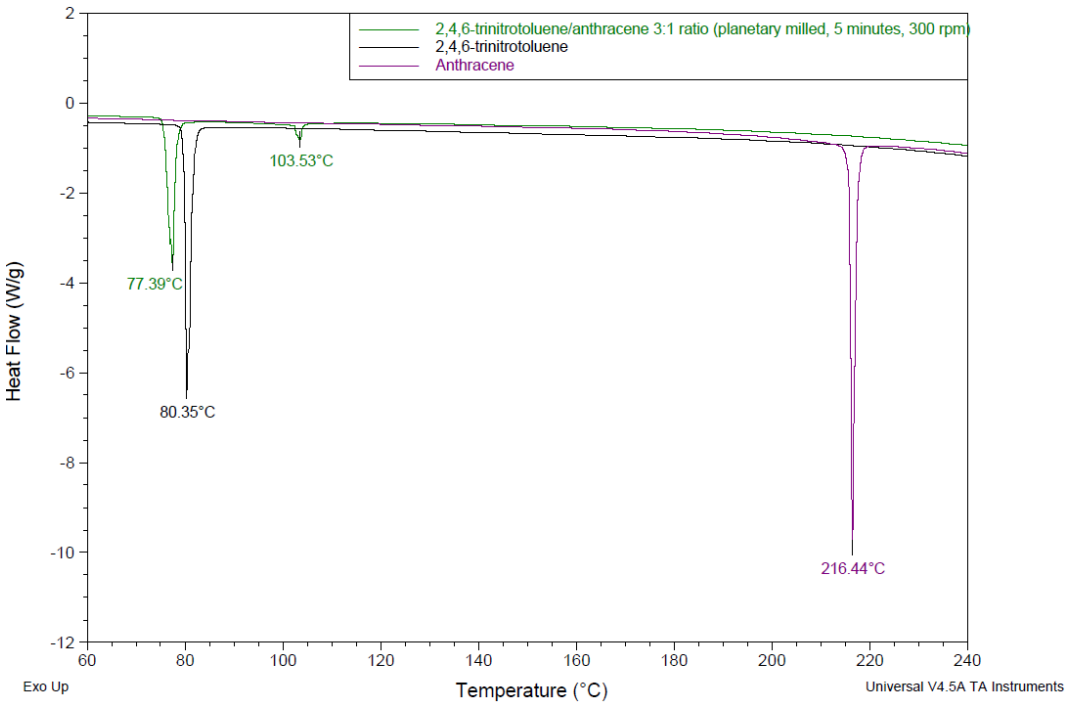

Figure A.28 - Thermal analysis of 2,4,6-trinitrotoluene/anthracene produced by planetary milling for 5 minutes at 300 rpm with a 3:1 stoichiometry.

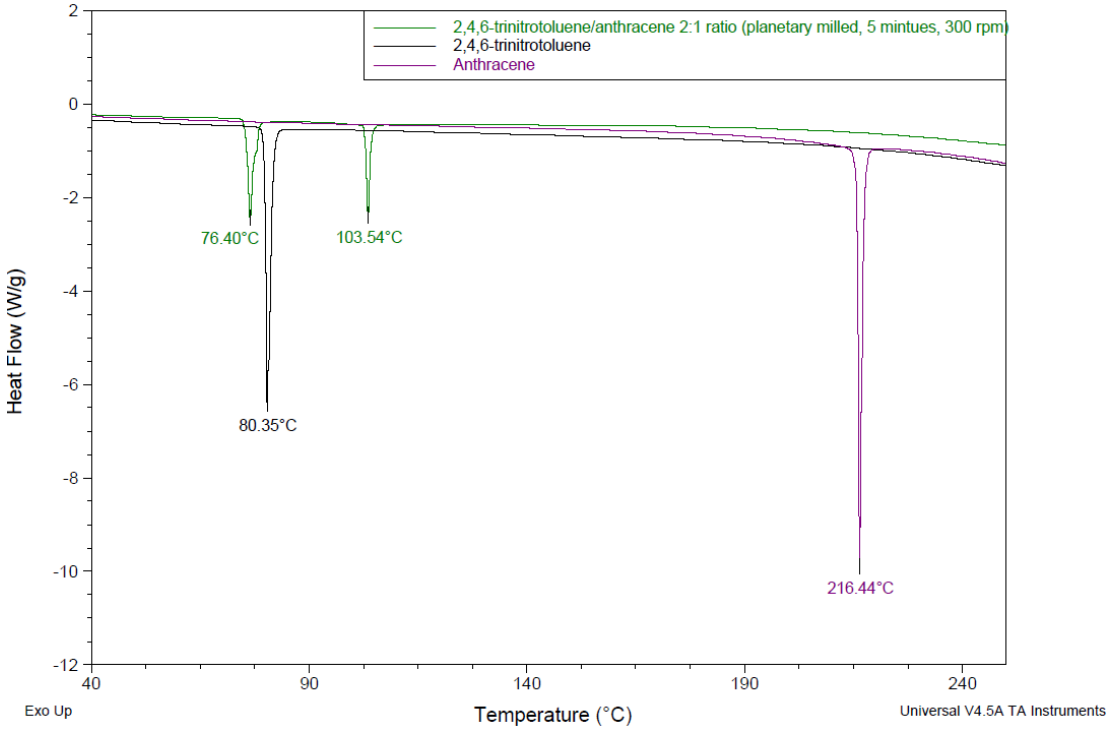

Figure A.29 - Thermal analysis of 2,4,6-trinitrotoluene/anthracene produced by planetary milling for 5 minutes at 300 rpm with a 2:1 stoichiometry.

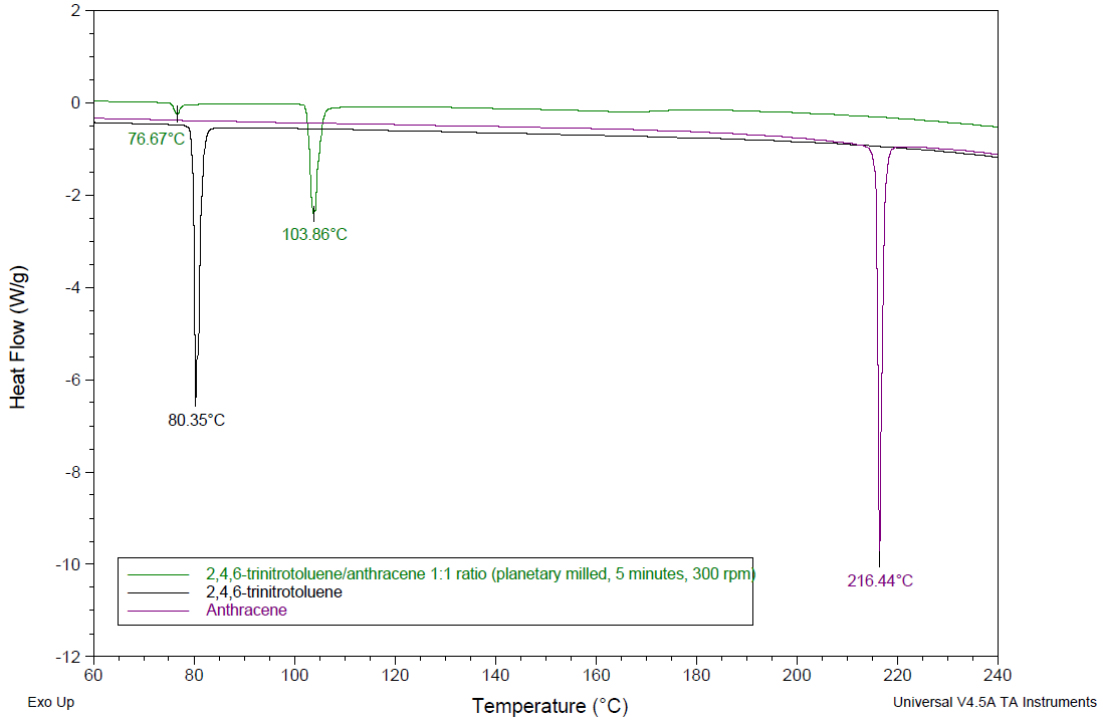

Figure A.30 - Thermal analysis of 2,4,6-trinitrotoluene/anthracene produced by planetary milling for 5 minutes at 300 rpm with a 1:1 stoichiometry.

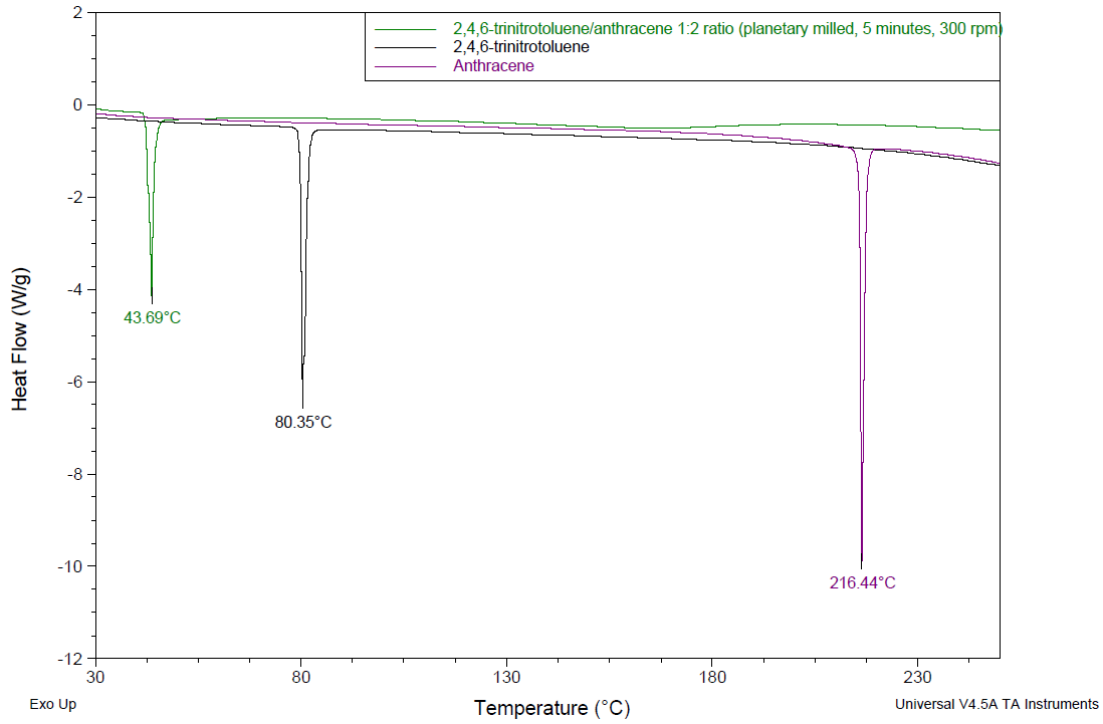

Figure A.31 - Thermal analysis of 2,4,6-trinitrotoluene/anthracene produced by planetary milling for 5 minutes at 300 rpm with a 1:2 stoichiometry.

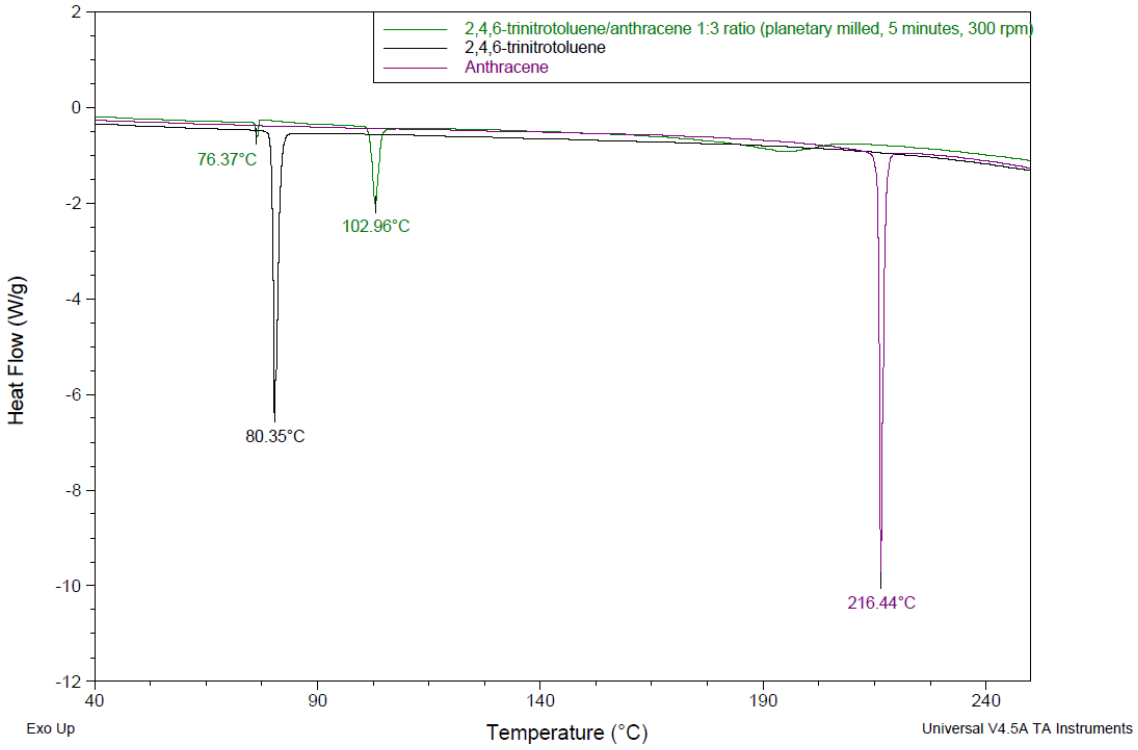

Figure A.32 - Thermal analysis of 2,4,6-trinitrotoluene/anthracene produced by planetary milling for 5 minutes at 300 rpm with a 1:3 stoichiometry.

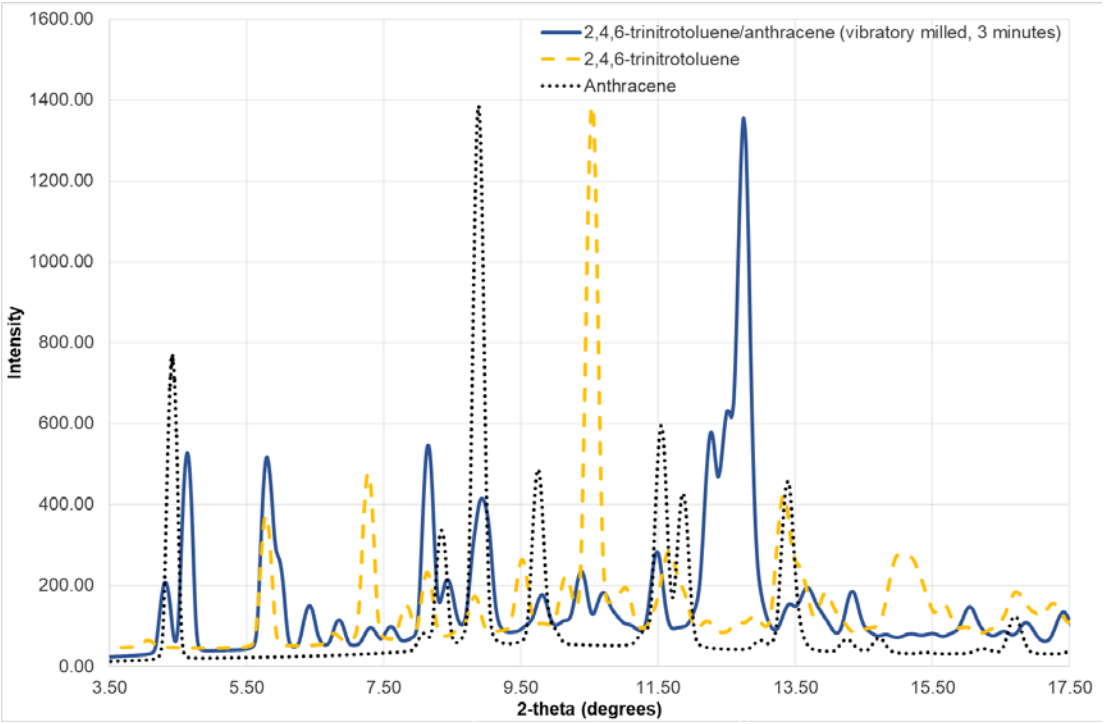

Figure A.33 - Powder x-ray pattern of 2,4,6-trinitrotoluene/anthracene produced by vibratory milling for 3 minutes with a 1:1 stoichiometry (λ = 0.7107 Å).

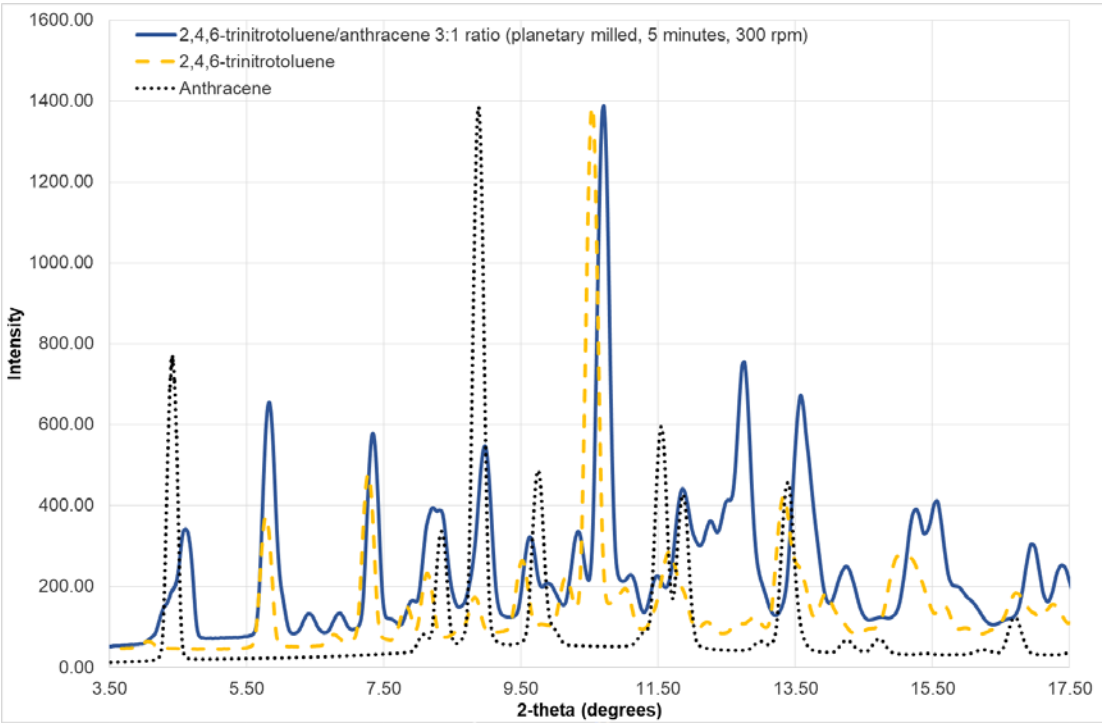

Figure A.34 - Powder x-ray pattern of 2,4,6-trinitrotoluene/anthracene produced by planetary milling for 5 minutes at 300 rpm with a 3:1 stoichiometry (λ = 0.7107 Å).

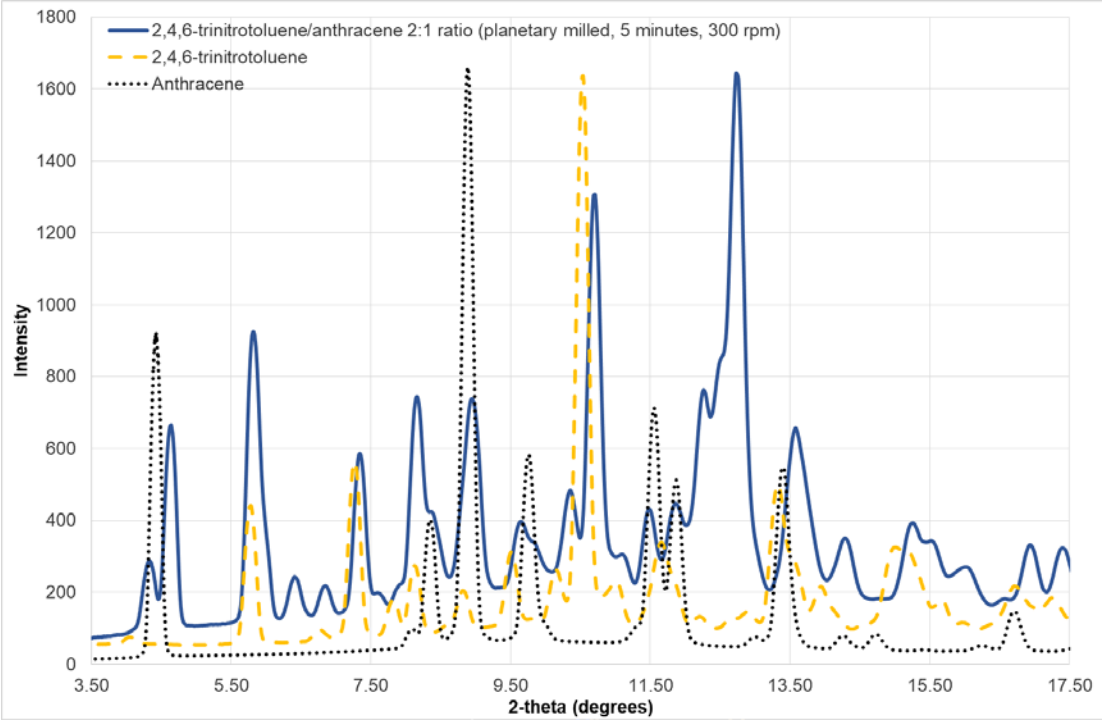

Figure A.35 - Powder x-ray pattern of 2,4,6-trinitrotoluene/anthracene produced by planetary milling for 5 minutes at 300 rpm with a 2:1 stoichiometry (λ = 0.7107 Å).

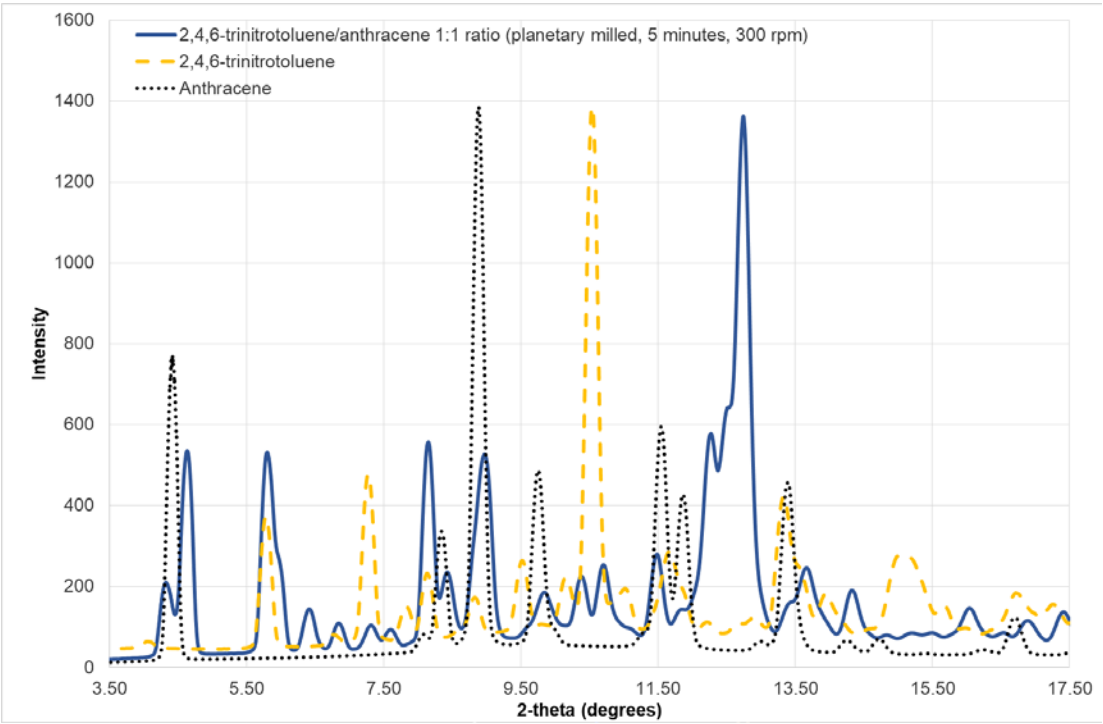

Figure A.36 - Powder x-ray pattern of 2,4,6-trinitrotoluene/anthracene produced by planetary milling for 5 minutes at 300 rpm with a 1:1 stoichiometry (λ = 0.7107 Å).

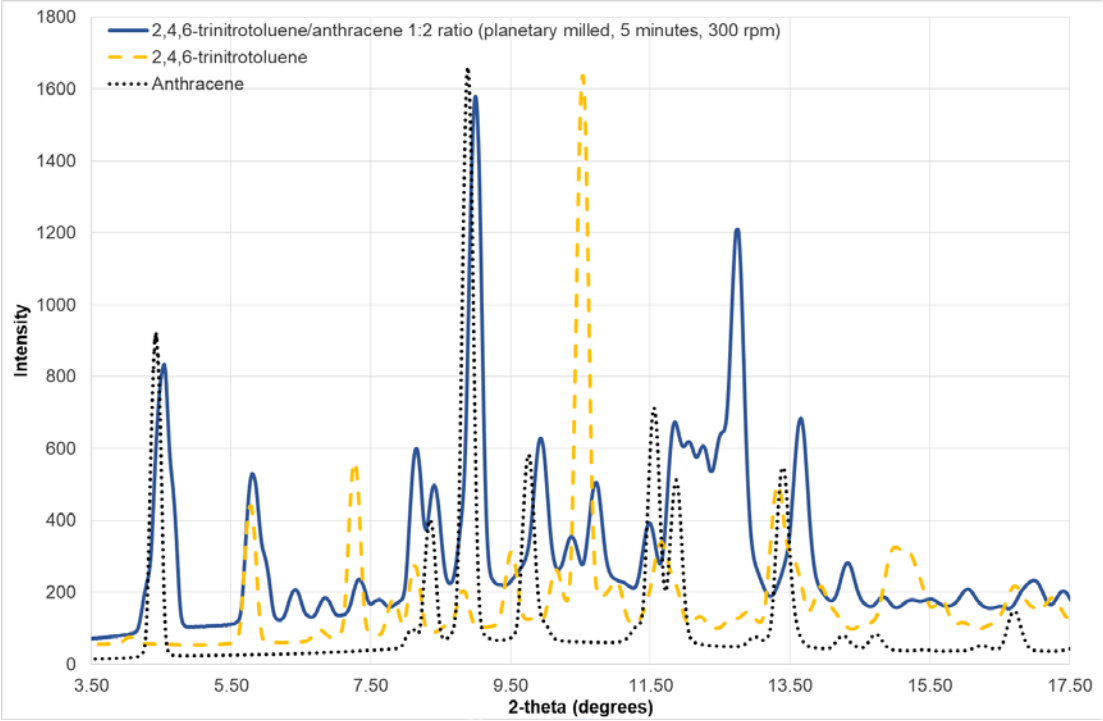

Figure A.37 - Powder x-ray pattern of 2,4,6-trinitrotoluene/anthracene produced by planetary milling for 5 minutes at 300 rpm with a 1:2 stoichiometry (λ = 0.7107 Å).

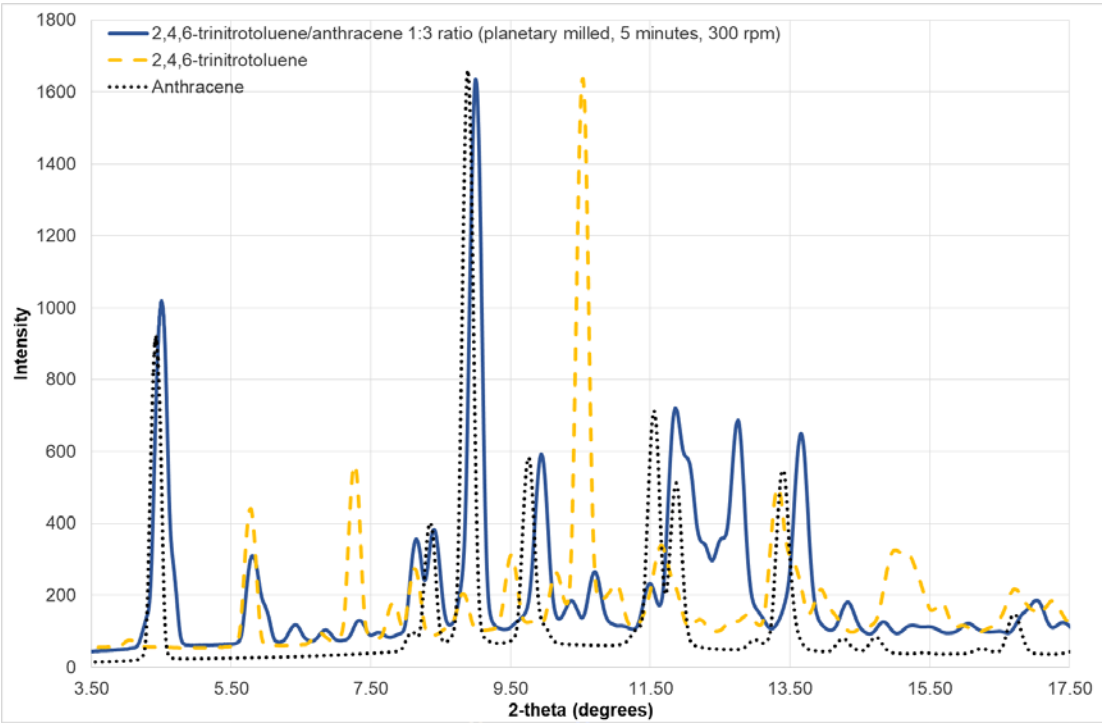

Figure A.38 - Powder x-ray pattern of 2,4,6-trinitrotoluene/anthracene produced by planetary milling for 5 minutes at 300 rpm with a 1:3 stoichiometry (λ = 0.7107 Å).

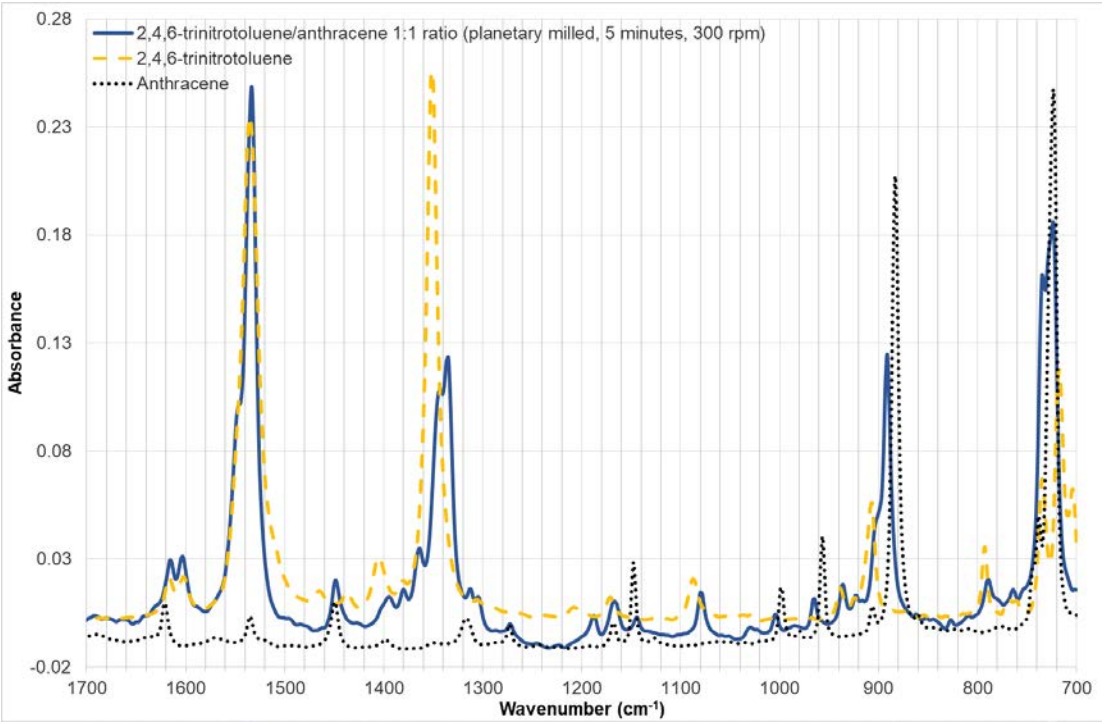

Figure A.39 - Infra-red spectra of 2,4,6-trinitrotoluene/anthracene produced by planetary milling for 5 minutes at 300 rpm, with a 1:1 stoichiometry.

Table A.3 - Infrared spectra peak positions and heights of 2,4,6-trinitrotoluene/anthracene produced by planetary milling for 5 minutes at 300 rpm, with a 1:1 stoichiometry.

Peak Position (cm^{-1})	Peak Height (Absorbance)
3107.03	0.01
1615.7	0.01
1603.45	0.02
1533.62	0.12
1448.6	0.01
1394.71	0.01
1379.86	0.01
1363.93	0.02
1343.62	0.05
1335.42	0.06
1312.92	0.01
1305.01	0.01
1166.88	0.01
1079.53	0.01
965.05	0.01
936.08	0.01
922.69	0.01
916.36	0.01
891.33	0.06
789.14	0.01
764.03	0.01
734.27	0.08
723.83	0.09
701.68	0.01

A.4 2,4,6-trinitrotoluene/1,4-dimethoxybenzene

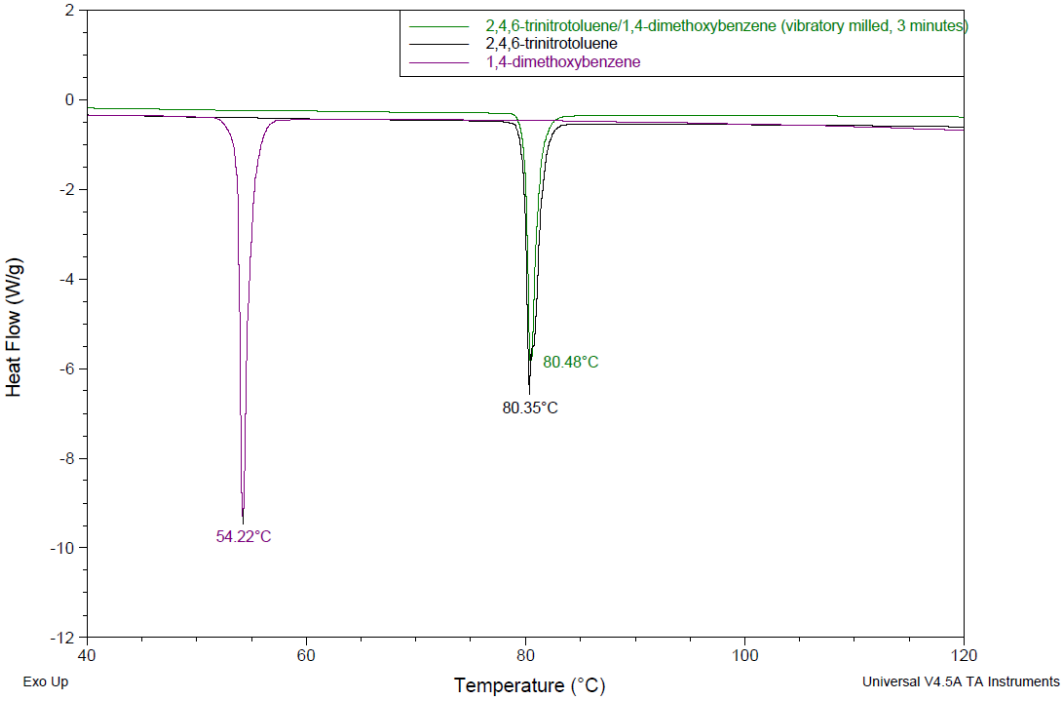

Figure A.40 - Thermal analysis of 2,4,6-trinitrotoluene/1,4-dimethoxybenzene produced by vibratory milling for 3 minutes with a 1:1 stoichiometry.

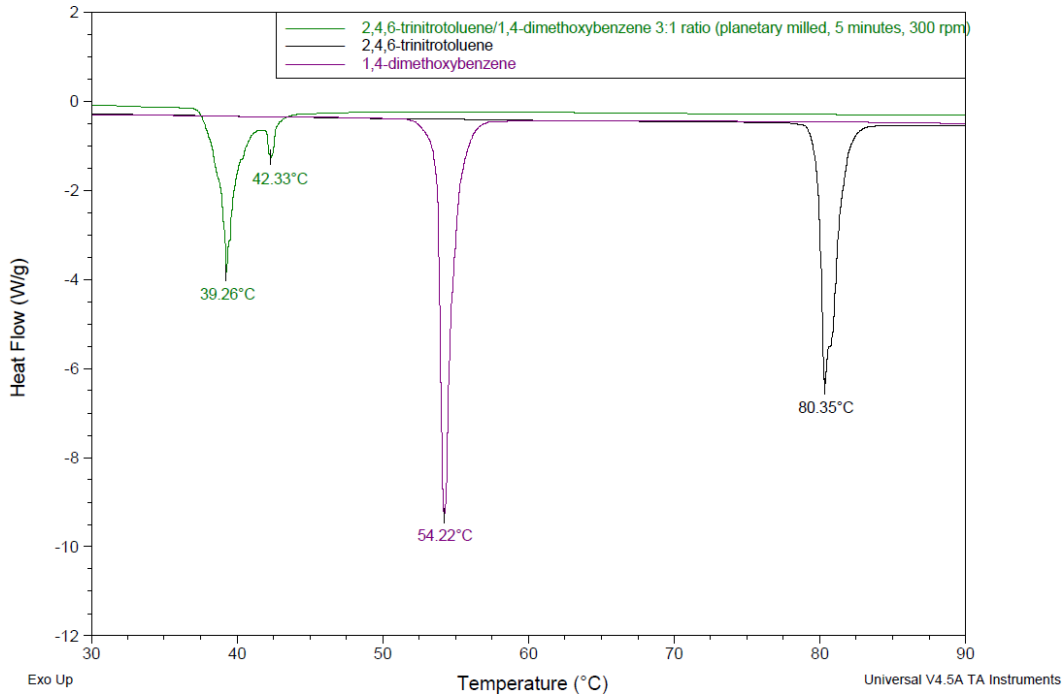

Figure A.41 - Thermal analysis of 2,4,6-trinitrotoluene/1,4-dimethoxybenzene produced by planetary milling for 5 minutes at 300 rpm with a 3:1 stoichiometry.

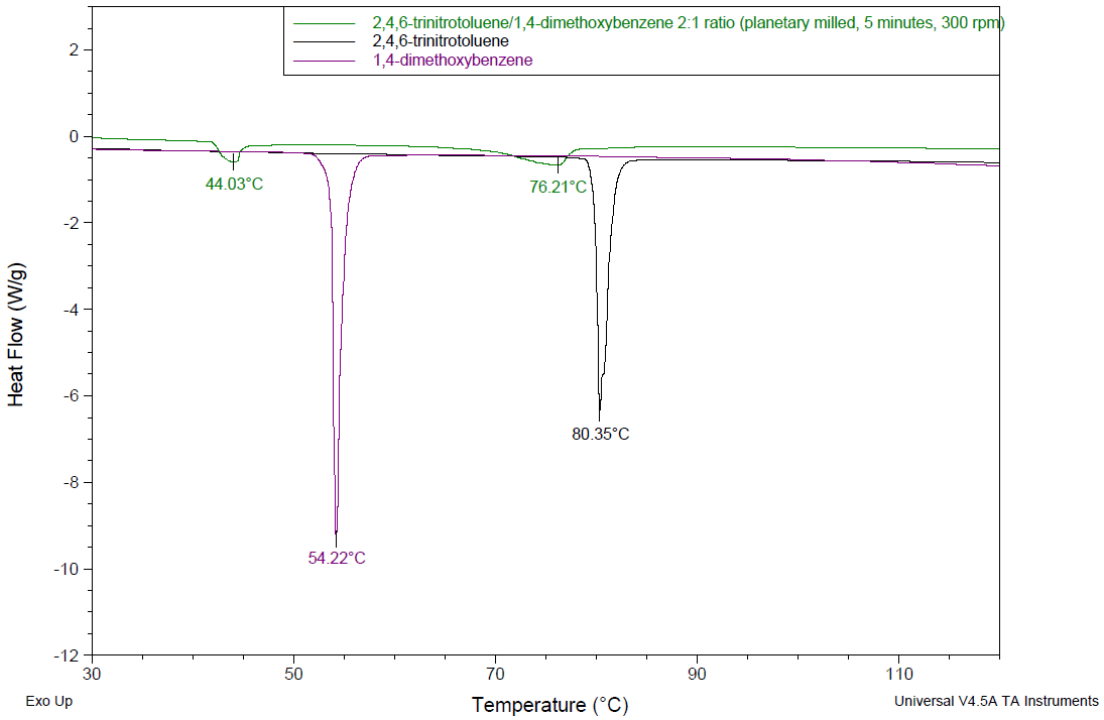

Figure A.42 - Thermal analysis of 2,4,6-trinitrotoluene/1,4-dimethoxybenzene produced by planetary milling for 5 minutes at 300 rpm with a 2:1 stoichiometry.

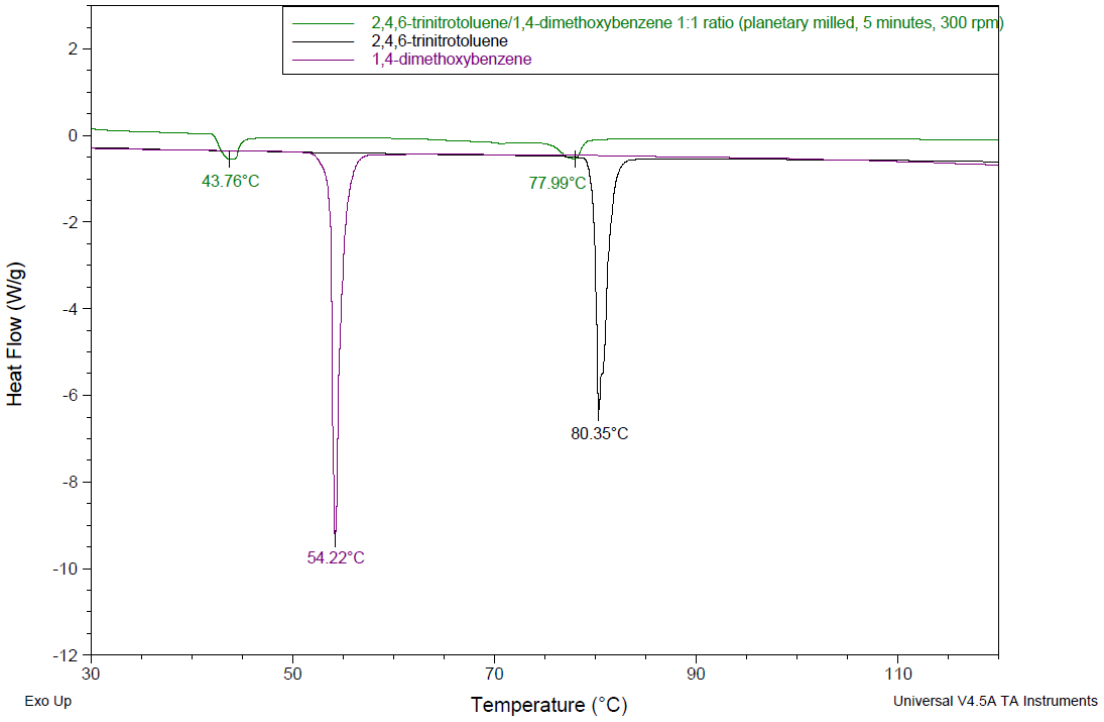

Figure A.43 - Thermal analysis of 2,4,6-trinitrotoluene/1,4-dimethoxybenzene produced by planetary milling for 5 minutes at 300 rpm with a 1:1 stoichiometry.

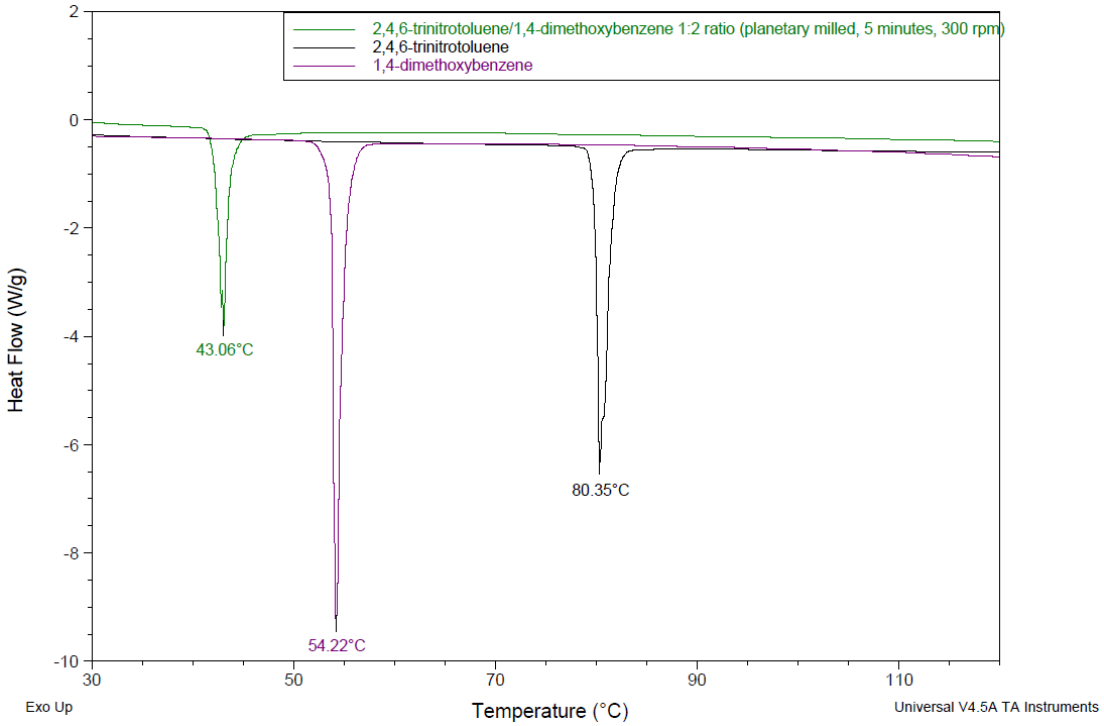

Figure A.44 - Thermal analysis of 2,4,6-trinitrotoluene/1,4-dimethoxybenzene produced by planetary milling for 5 minutes at 300 rpm with a 1:2 stoichiometry.

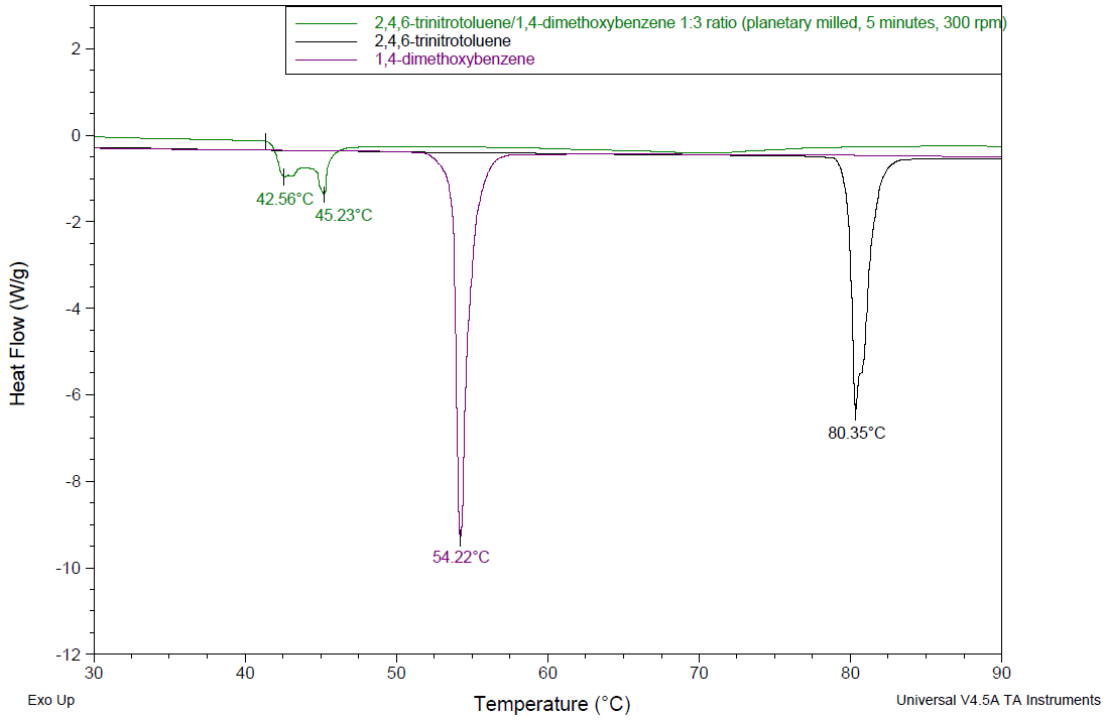

Figure A.45 - Thermal analysis of 2,4,6-trinitrotoluene/1,4-dimethoxybenzene produced by planetary milling for 5 minutes at 300 rpm with a 1:3 stoichiometry.

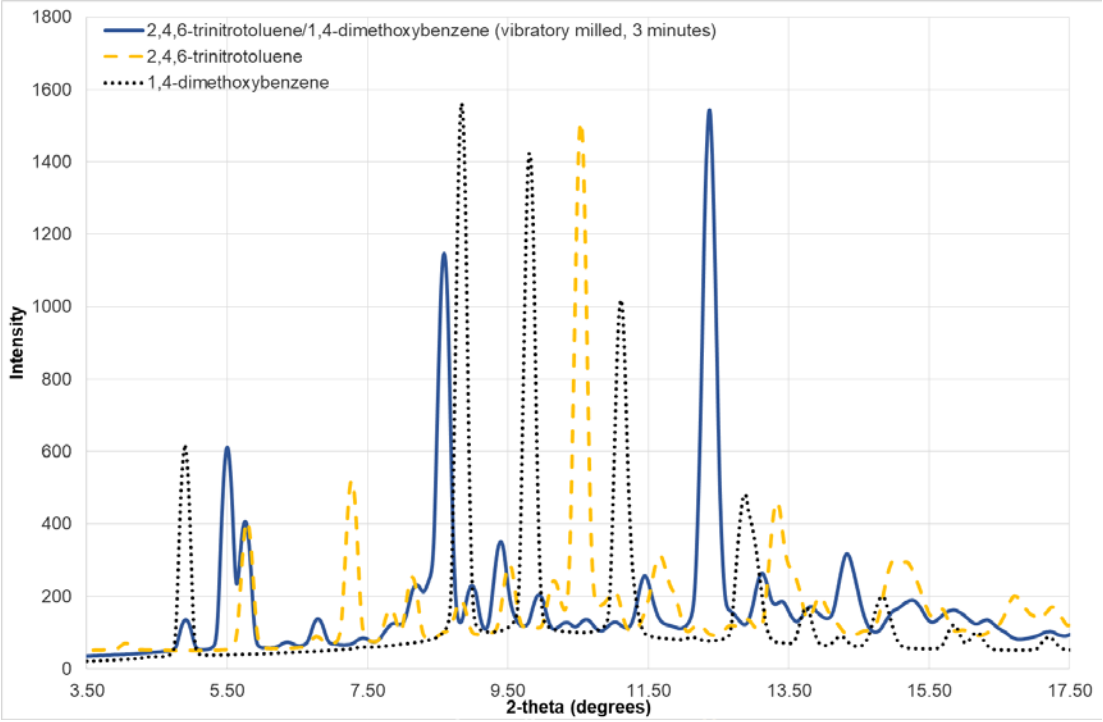

Figure A.46 - Powder x-ray pattern of 2,4,6-trinitrotoluene/1,4-dimethoxybenzene produced by vibratory milling for 3 minutes with a 1:1 stoichiometry (λ = 0.7107 Å).

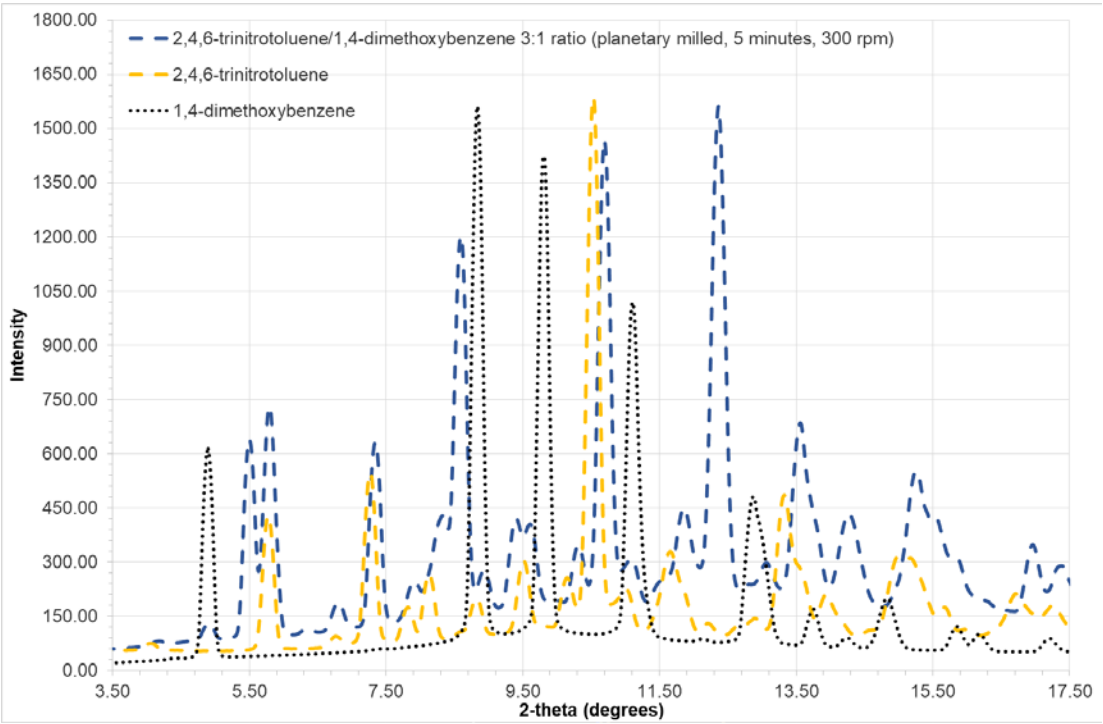

Figure A.47 - Powder x-ray pattern of 2,4,6-trinitrotoluene/1,4-dimethoxybenzene produced by planetary milling for 5 minutes at 300 rpm with a 3:1 stoichiometry (λ = 0.7107 Å).

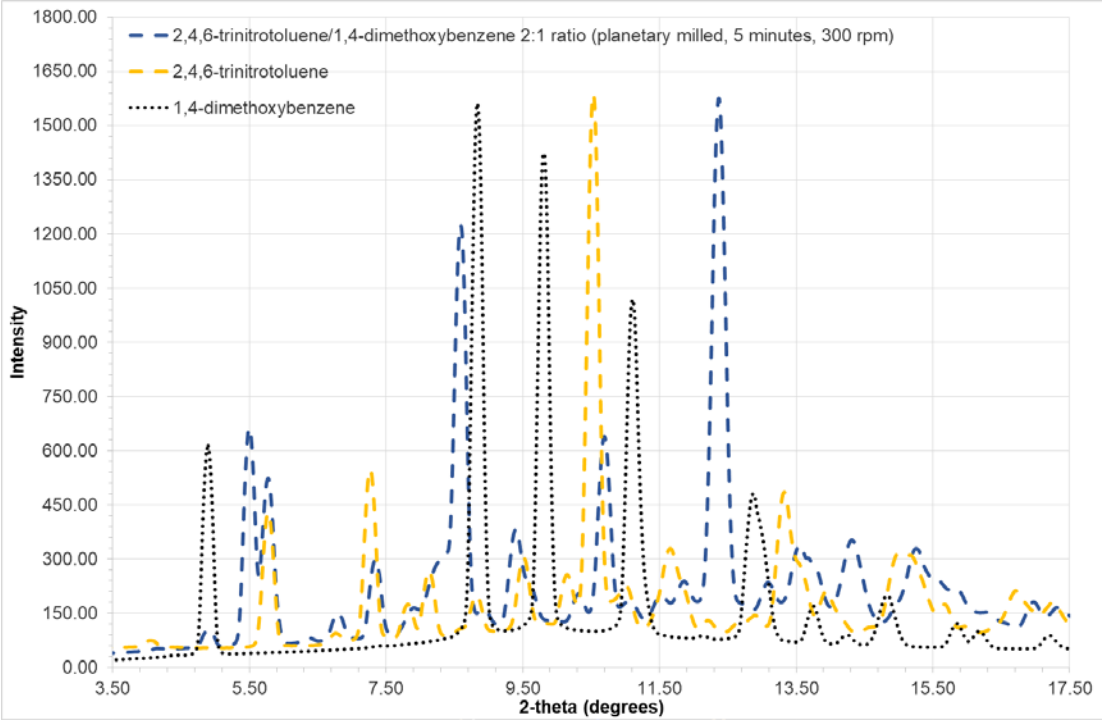

Figure A.48 - Powder x-ray pattern of 2,4,6-trinitrotoluene/1,4-dimethoxybenzene produced by planetary milling for 5 minutes at 300 rpm with a 2:1 stoichiometry (λ = 0.7107 Å).

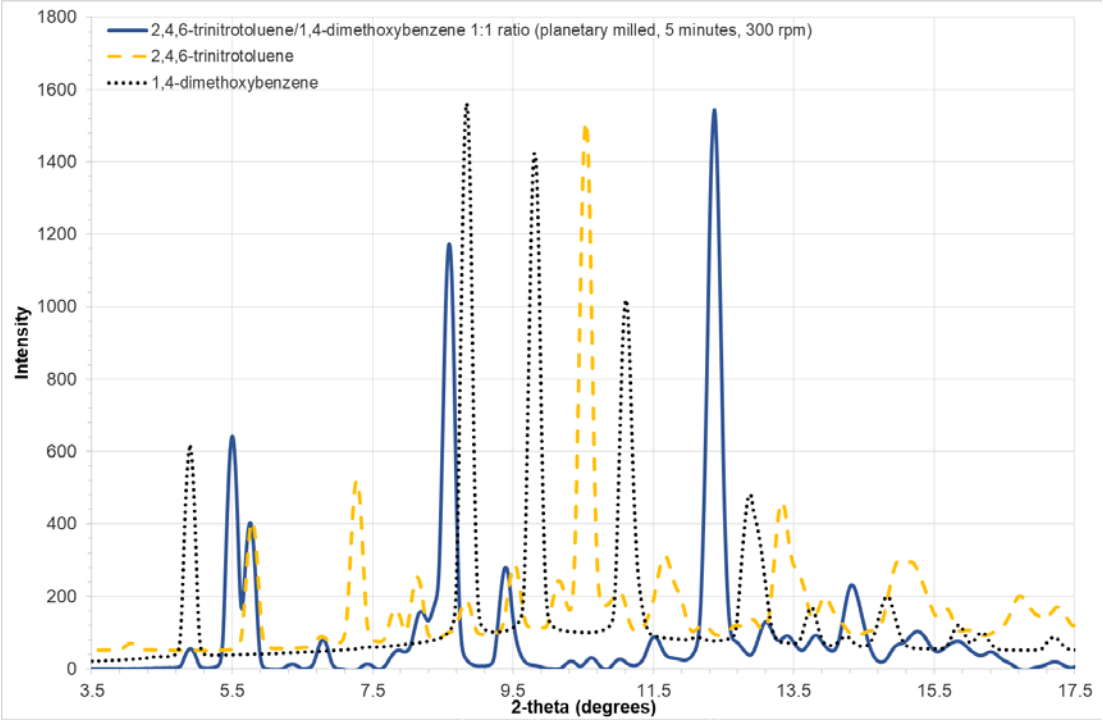

Figure A.49 - Powder x-ray pattern of 2,4,6-trinitrotoluene/1,4-dimethoxybenzene produced by planetary milling for 5 minutes at 300 rpm with a 1:1 stoichiometry (λ = 0.7107 Å).

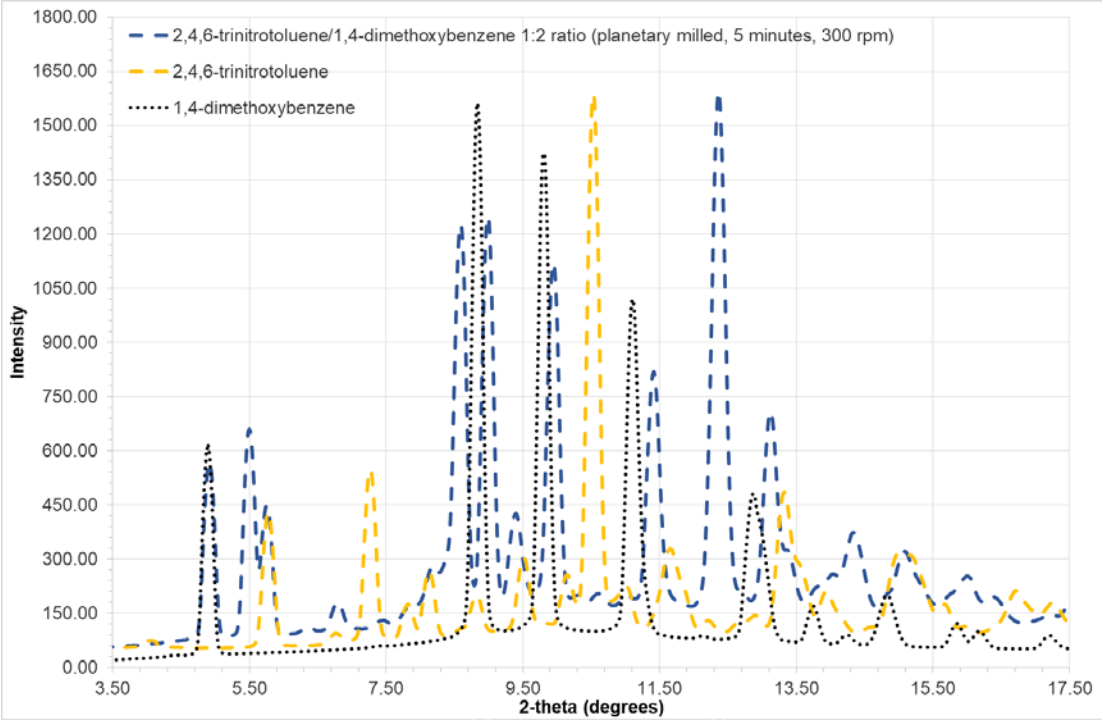

Figure A.50 - Powder x-ray pattern of 2,4,6-trinitrotoluene/1,4-dimethoxybenzene produced by planetary milling for 5 minutes at 300 rpm with a 1:2 stoichiometry (λ = 0.7107 Å).

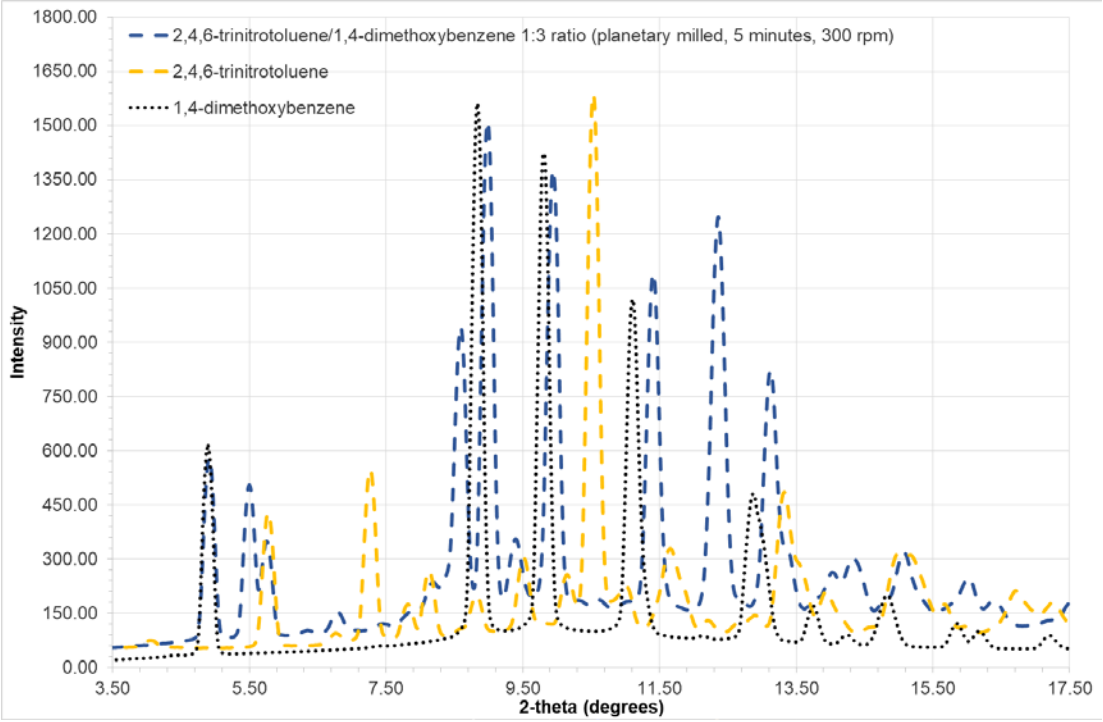

Figure A.51 - Powder x-ray pattern of 2,4,6-trinitrotoluene/1,4-dimethoxybenzene produced by planetary milling for 5 minutes at 300 rpm with a 1:3 stoichiometry (λ = 0.7107 Å).

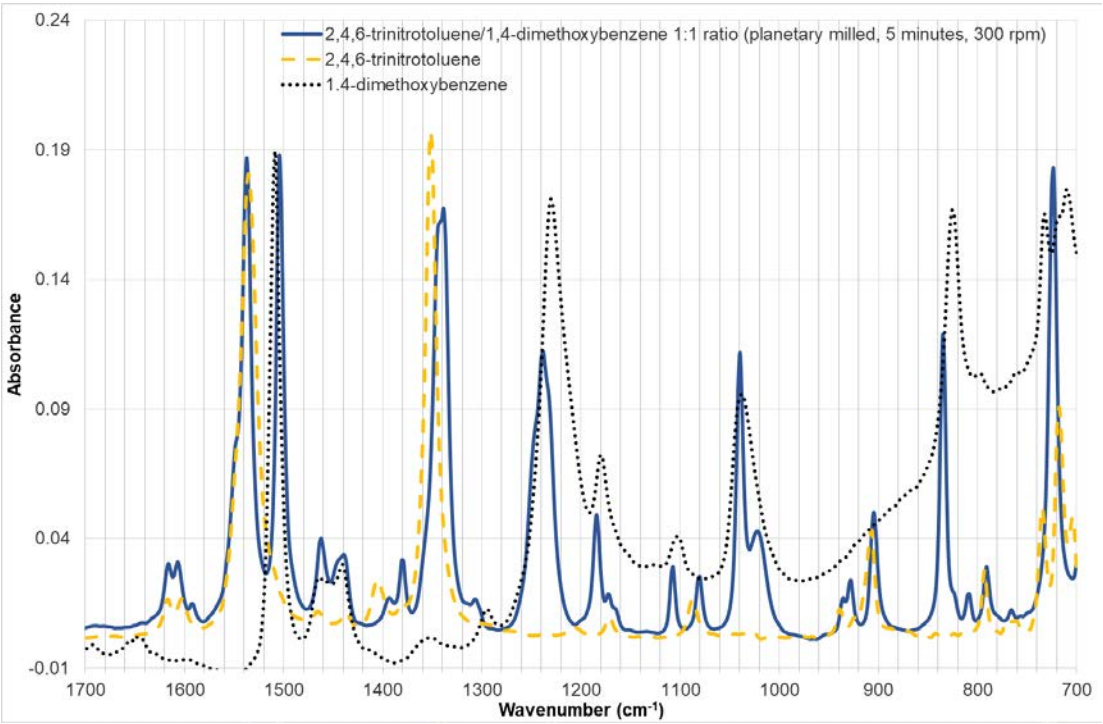

Figure A.52 – Infra-red spectra of 2,4,6-trinitrotoluene/1,4-dimethoxybenzene produced by planetary milling for 5 minutes at 300 rpm with a 1:1 stoichiometry.

Table A.4 - Infrared spectra peak positions and heights of 2,4,6-trinitrotoluene/1,4-dimethoxybenzene produced by planetary milling for 5 minutes at 300 rpm, with a 1:1 stoichiometry.

Peak Position (cm-1)	Peak Height (Absorbance)
3087.55	0.01
1616.25	0.03
1606.84	0.03
1592.56	0.01
1537.29	0.19
1504.18	0.19
1462.26	0.04
1439.38	0.03
1393.29	0.02
1380.31	0.03
1338.97	0.17
1307.13	0.02
1238.51	0.11
1184.31	0.05
1172.51	0.02
1107.47	0.03
1080.66	0.03
1039.77	0.11
1022.25	0.04
935.34	0.02
928.13	0.02
904.71	0.05
834.92	0.12
808.86	0.02

B Results 2 – Manipulation of electrostatic potential and its impact on co-crystal formation (Chapter 5)

B.1 *N*-heterocyclic co-formers investigated in this study

Co-former name (CAS No.)	Co-former name (CAS No.)
Pyrrolidine (288-13-1)	2-methylimidazole (693-98-1)
3-Pyrroline (123-75-1)	4-Methylimidazole (822-36-6)
Pyrrole (109-97-7)	Imidazol-2-amine (7720-39-0)
2-Nitropyrrole (5919-26-6)	2-Bromoimidazole (16681-56-4)
2-Methylpyrrole (636-41-9)	4-Bromoimidazole (2302-25-2)
3-Methylpyrrole (616-43-3)	2,4-Dimethylimidazole (930-62-1)
2,4-Dimethylpyrrole (625-82-1)	4,5-Dinitroimidazole (19183-14-3)
2,5-Dimethylpyrrole (625-84-3)	4,5-Dichloroimidazole (15965-30-7)
Pyrazole (288-13-1)	2,4,5-Tribromoimidazole (2034-22-2)
3-Nitropyrazole (26621-44-3)	2-Methyl-5-nitroimidazole (696-23-1)
4-Nitropyrazole (2075-46-9)	4-Methyl-5-nitroimidazole (14003-66-8)
5-Methylpyrazole (88054-14-2)	2-Bromo-5-nitroimidazole (65902-59-2)
Pyrazol-4-amine (28466-26-4)	4-Bromo-2-methylimidazole (16265-11-5)
3-Bromopyrazole (14521-80-3)	5-Bromo-4-methylimidazole (15813-08-8)
4-Bromopyrazole (2075-45-8)	4,5-Dibromo-2-methylimidazole (4002-81-7)
3,4-Dimethylpyrazole (2820-37-3)	2,5-Dibromo-4-methylimidazole (219814-29-6)
3,5-Dimethylpyrazole (67-51-6)	1,2,3-Triazole (288-35-7)
3,4,5-Tribromopyrazole (17635-44-8)	5-Nitro-1,2,3-triazole (84406-63-3)
3-Methyl-5-nitropyrazole (34334-96-8)	1,2,4-Triazole (288-88-0)
5-Methylpyrazol-3-amine (31230-17-8)	3-Methyl-1,2,4-triazole (7170-01-6)
4-Bromopyrazol-3-amine (16461-94-2)	1,2,4-Triazol-3-amine (61-82-5)
3-Bromopyrazol-5-amine	5-Bromo-1,2,4-triazole (7343-33-1)

(950739-21-6)	
3,5-Dimethylpyrazol-4-amine (5272-86-6)	1,2,4-Triazol-3,5-diamine (1455-77-2)
3,4-Dimethylpyrazol-5-amine (91159-73-8)	3,5-Dimethyl-1,2,4-triazole (7343-34-2)
3-Methyl-4-bromopyrazole (13808-64-5)	3,5-Dibromo-1,2,4-triazole (7411-23-6)
3-Bromo-5-methylpyrazole (57097-81-1)	1,2,3,4-Tetrazole (288-94-8)
4-Bromo-3,5-dimethylpyrazole (3398-16-1)	1,2,3,4-Tetrazol-5-amine (4418-61-5)
Imidazole (288-32-4)	5-Methyl-1,2,3,4-tetrazole (4076-36-2)

B.2 2-naphthol/pyrrolidine

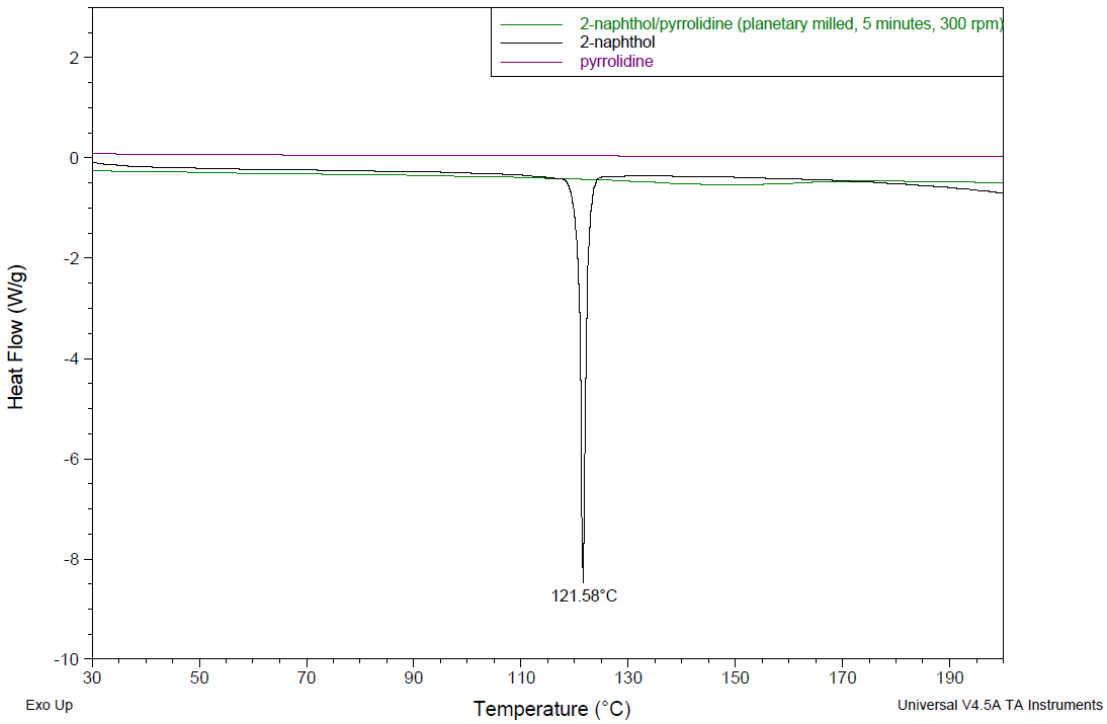

Figure B.1 - Thermal analysis of 2-naphthol/pyrrolidine produced by planetary milling for 5 minutes at 300 rpm. Pyrrolidine and the mixed system are liquids, therefore no melts are observed.

B.3 2-naphthol/3-pyrroline

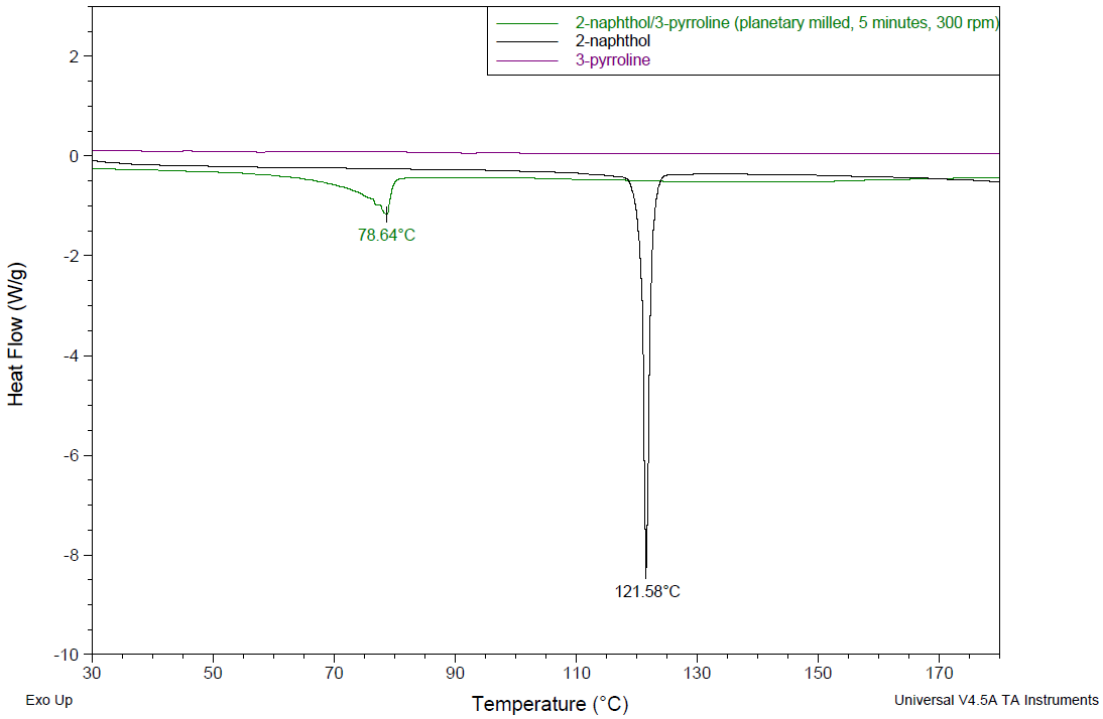

Figure B.2 - Thermal analysis of 2-naphthol/3-pyrroline produced by planetary milling for 5 minutes at 300 rpm. Pyrrole is a liquid, therefore no melt is observed.

B.4 2-naphthol/pyrrole

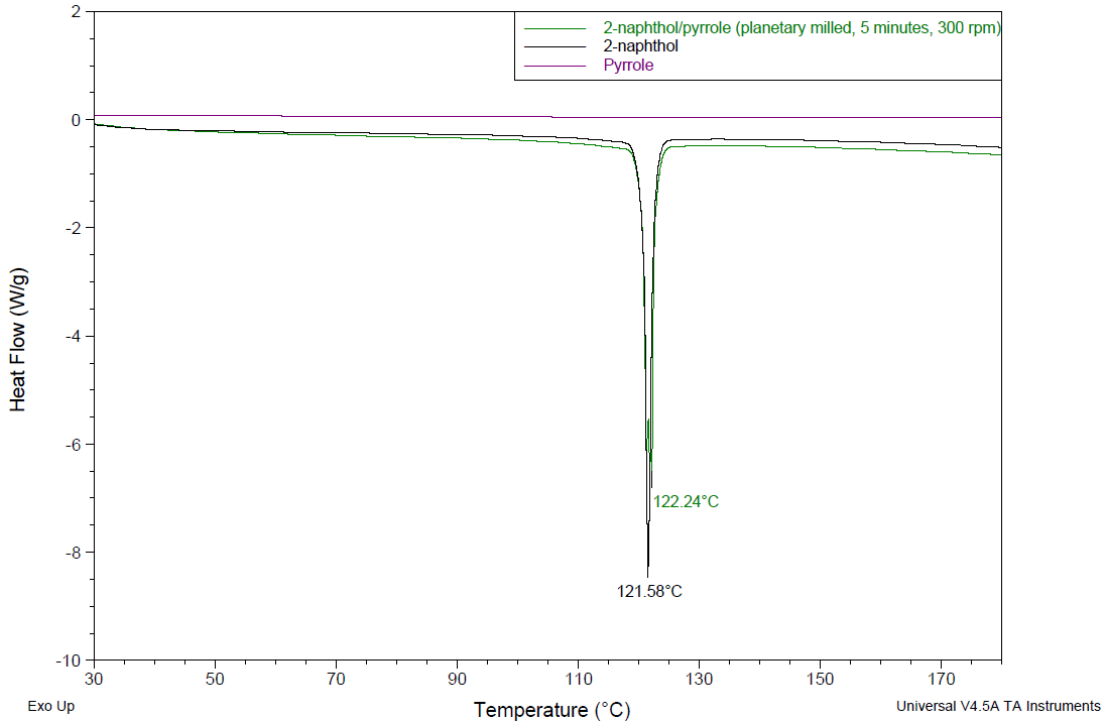

Figure B.3 – Thermal analysis of 2-naphthol/pyrrole produced by planetary milling for 5 minutes at 300 rpm. Pyrrole is a liquid, therefore no melt is observed.

B.5 2-naphthol/2-nitropyrrole

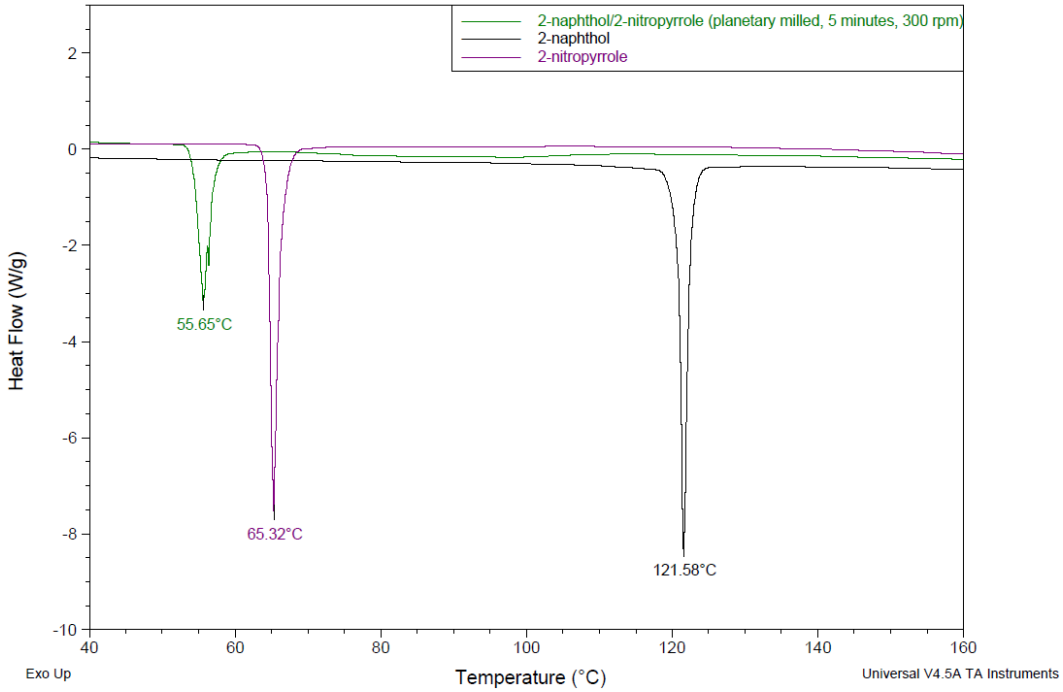

Figure B.4 – Thermal analysis of 2-napthol/2-nitropyrrole produced by planetary milling for 5 minutes at 300 rpm.

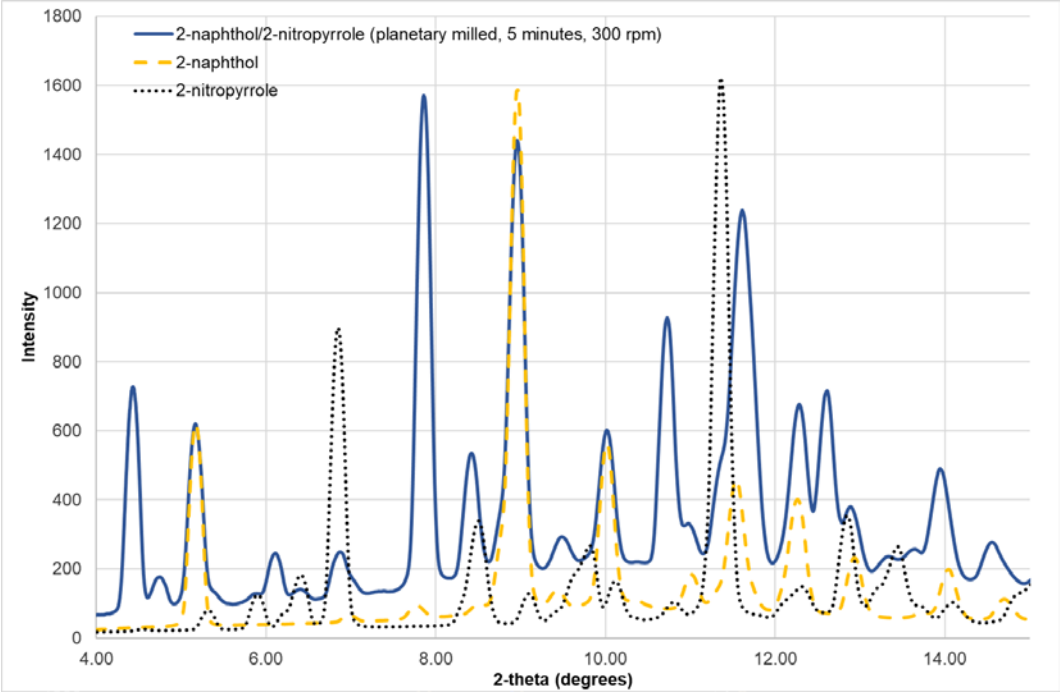

Figure B.5 - Powder x-ray pattern of 2-napthol/2-nitropyrrole produced by planetary milling for 5 minutes at 300 rpm (λ = 0.7107 Å).

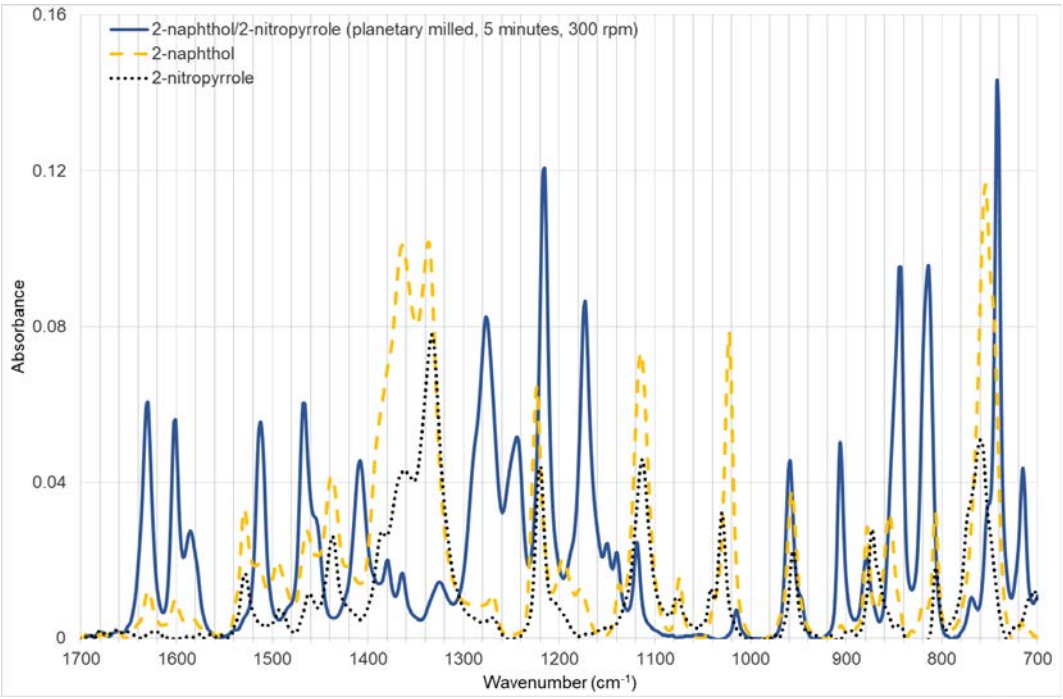

Figure B.6 – Infra-red spectra of 2-napthol/2-nitropyrrole produced by planetary milling for 5 minutes at 300 rpm.

Table B.1 - Infrared spectra peak positions and heights of 2-napthol/2-nitropyrrole produced by planetary milling for 5 minutes at 300 rpm, with a 1:1 stoichiometry.

Peak Position (cm^{-1})	Peak Height (Absorbance)	Peak Position (cm^{-1})	Peak Height (Absorbance)
3242.59	0.04	1178.14	0.03
3142.1	0.01	1137.2	0.03
3129.22	0.01	1114.8	0.15
1629.56	0.01	1074.45	0.04
1601.05	0.01	1022.37	0.16
1529.06	0.06	956.87	0.08
1514.41	0.03	904.87	0.01
1494.38	0.03	877.98	0.06
1463.76	0.05	854.64	0.07
1438.1	0.08	830.95	0.02
1422.06	0.04	819.45	0.03
1363.97	0.2	806.65	0.08
1336.69	0.2	790.41	0.02
1269.57	0.03	754.46	0.25
1223.28	0.14	716.8	0.04
1196.04	0.05	707.47	0.04

B.6 2-naphthol/2-methylpyrole

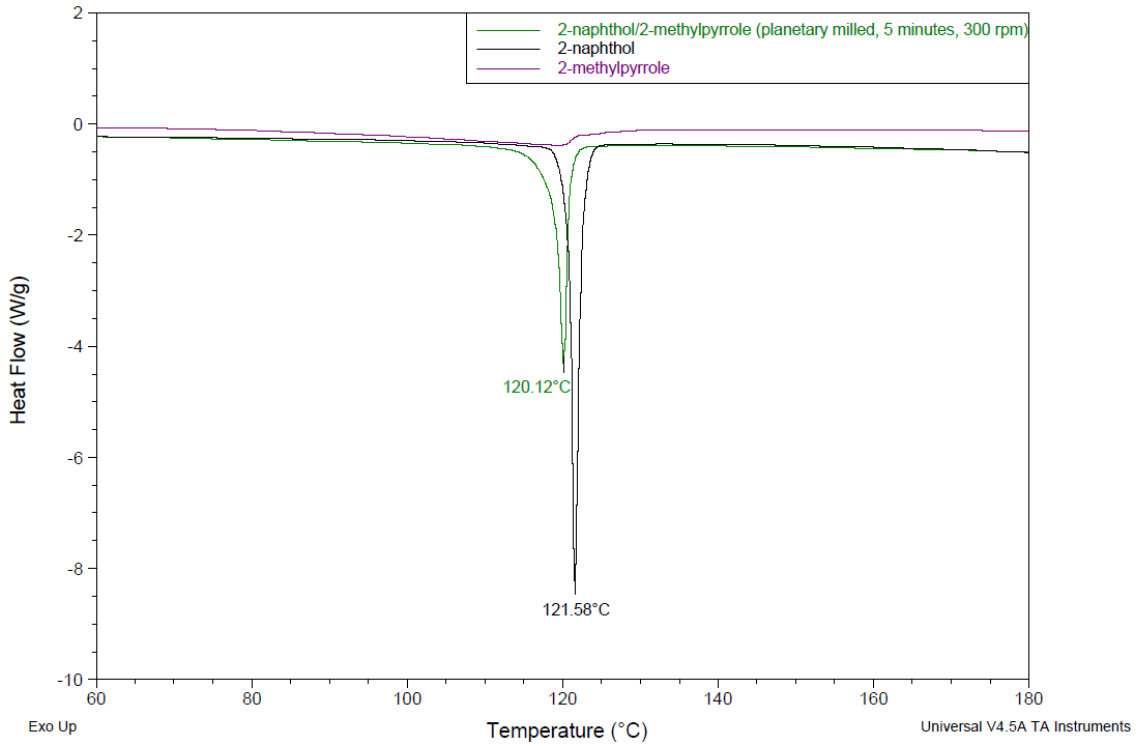

Figure B.7 - Thermal analysis of 2-napthol/2-methylpyrrole produced by planetary milling for 5 minutes at 300 rpm. 2-methylpyrrole is a liquid and showed no melt.

B.7 2-naphthol/3-methylpyrrole

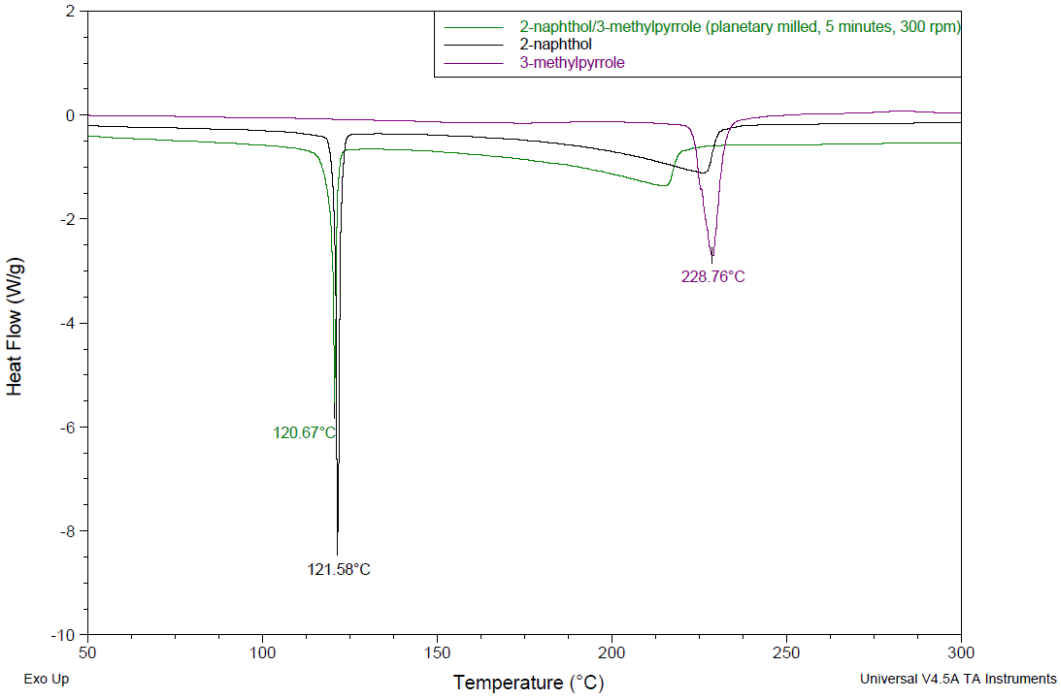

Figure B.8 - Thermal analysis of 2-napthol/3-methylpyrrole produced by planetary milling for 5 minutes at 300 rpm.

B.8 2-naphthol/2,4-dimethylpyrrole

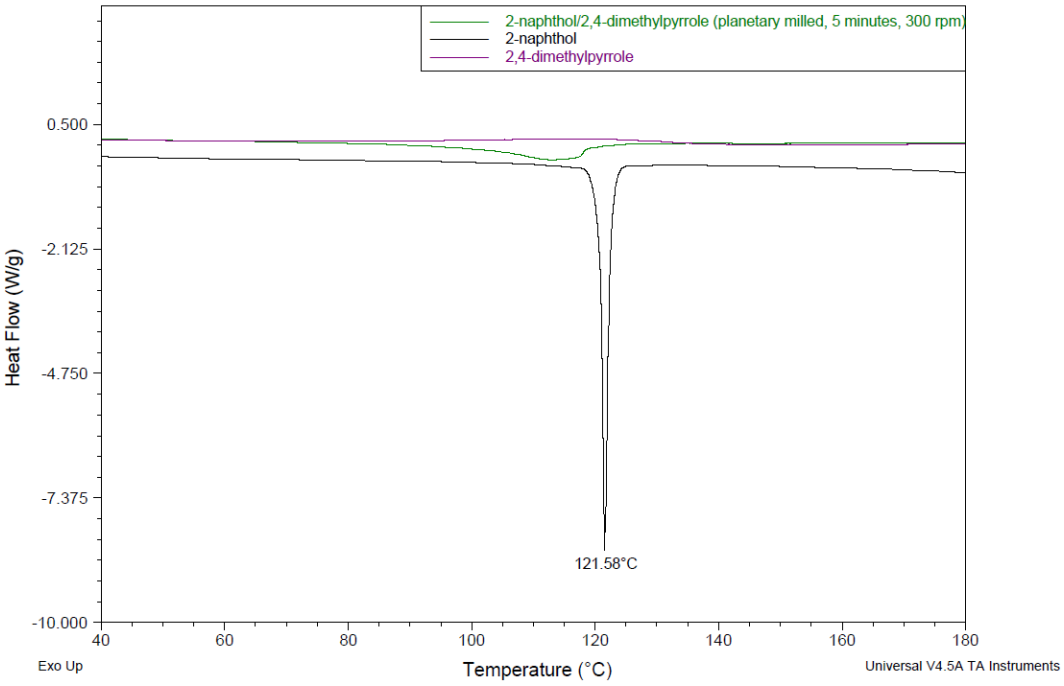

Figure B.9 - Thermal analysis of 2-napthol/2,4-dimethylpyrrole produced by planetary milling for 5 minutes at 300 rpm. 2,4-dimethylpyrazole is a liquid and did not display a melt.

B.9 2-naphthol/2,5-dimethylpyrrole

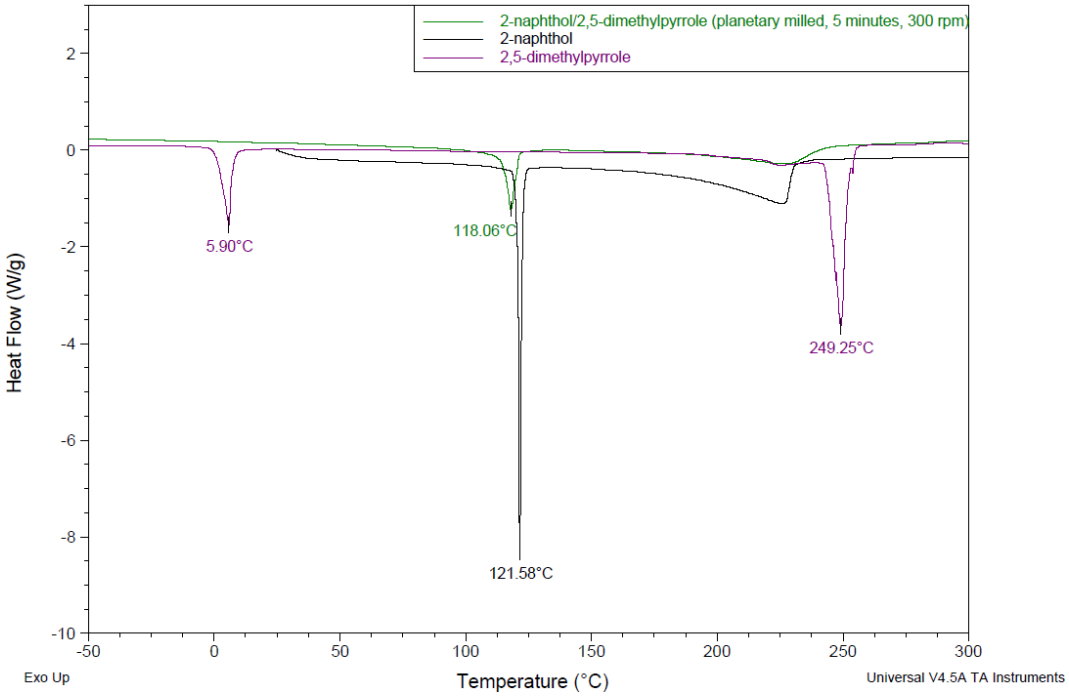

Figure B.10 - Thermal analysis of 2-napthol/2,5-dimethylpyrrole produced by planetary milling for 5 minutes at 300 rpm.

B.10 2-naphthol/pyrazole

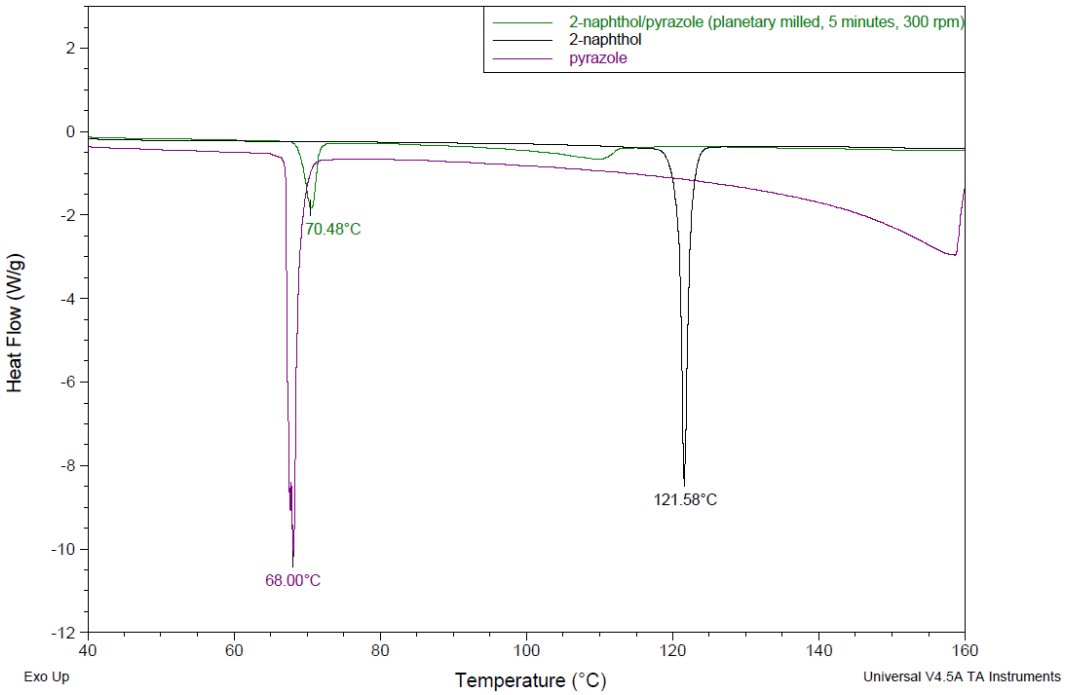

Figure B.11 – Thermal analysis of 2-naphthol/pyrazole produced by planetary milling for 5 minutes at 300 rpm.

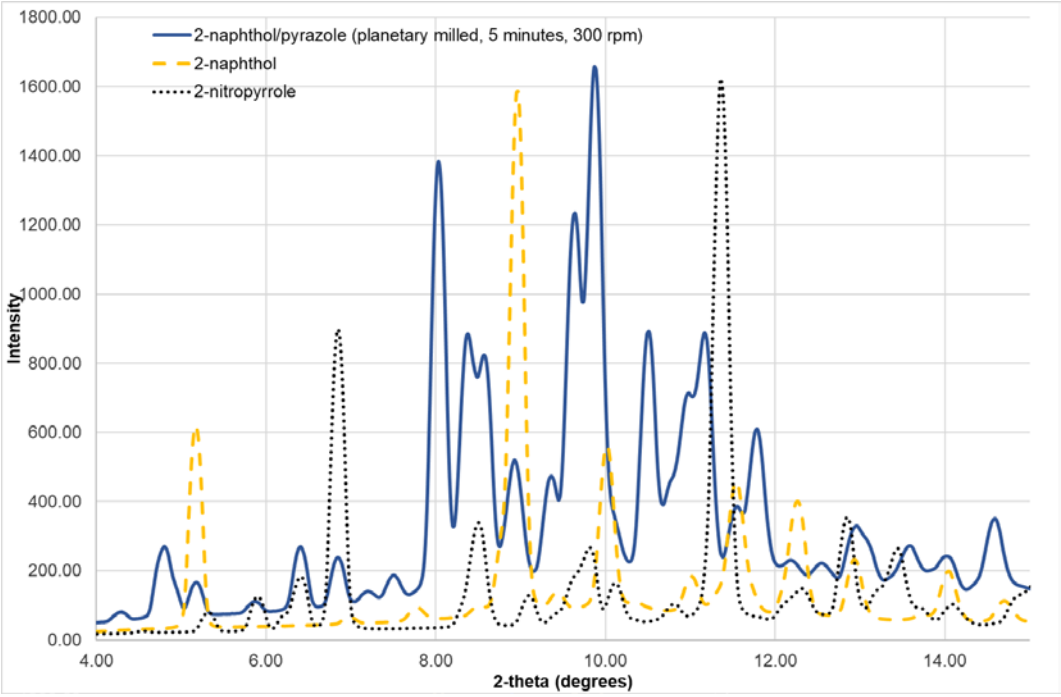

Figure B.12 - Powder x-ray pattern of 2-naphthol/pyrazole produced by planetary milling for 5 minutes at 300 rpm (λ = 0.7107 Å).

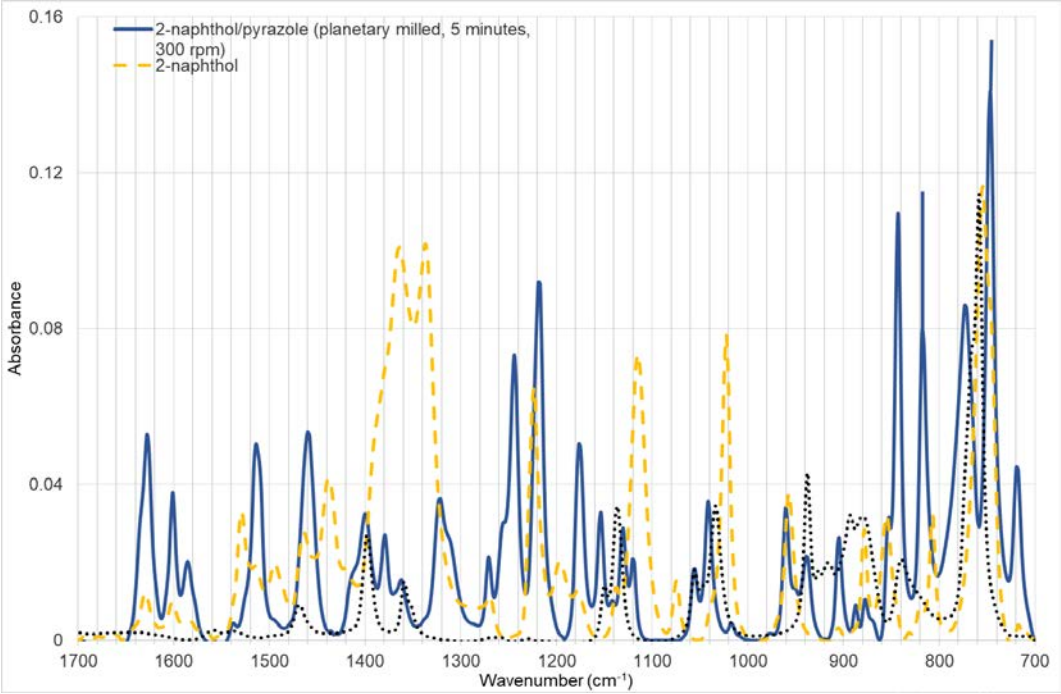

Figure B.13 – Infra-red spectra of 2-naphthol/pyrazole produced by planetary milling for 5 minutes at 300 rpm.

Table B.2 - Infrared spectra peak positions and heights of 2-napthol/pyrazole produced by planetary milling for 5 minutes at 300 rpm, with a 1:1 stoichiometry.

Peak Position (cm^{-1})	Peak Height (Absorbance)	Peak Position (cm^{-1})	Peak Height (Absorbance)
3281.05	0.02	1130.58	0.03
1627.71	0.05	1120.12	0.02
1600.98	0.04	1055.74	0.02
1585.47	0.02	1041.42	0.03
1513.79	0.05	960.3	0.04
1459.63	0.06	938.61	0.03
1399.83	0.04	904.87	0.03
1379.36	0.03	887.27	0.02
1362.19	0.02	877.4	0.02
1321.77	0.04	852.48	0.04
1270.88	0.02	843.03	0.12
1254.86	0.03	817.37	0.09
1244.11	0.08	772.81	0.1
1218.29	0.1	746.74	0.16
1176.09	0.05	718.77	0.06
1153.76	0.03		

B.11 2-naphthol/3-nitropyrazole

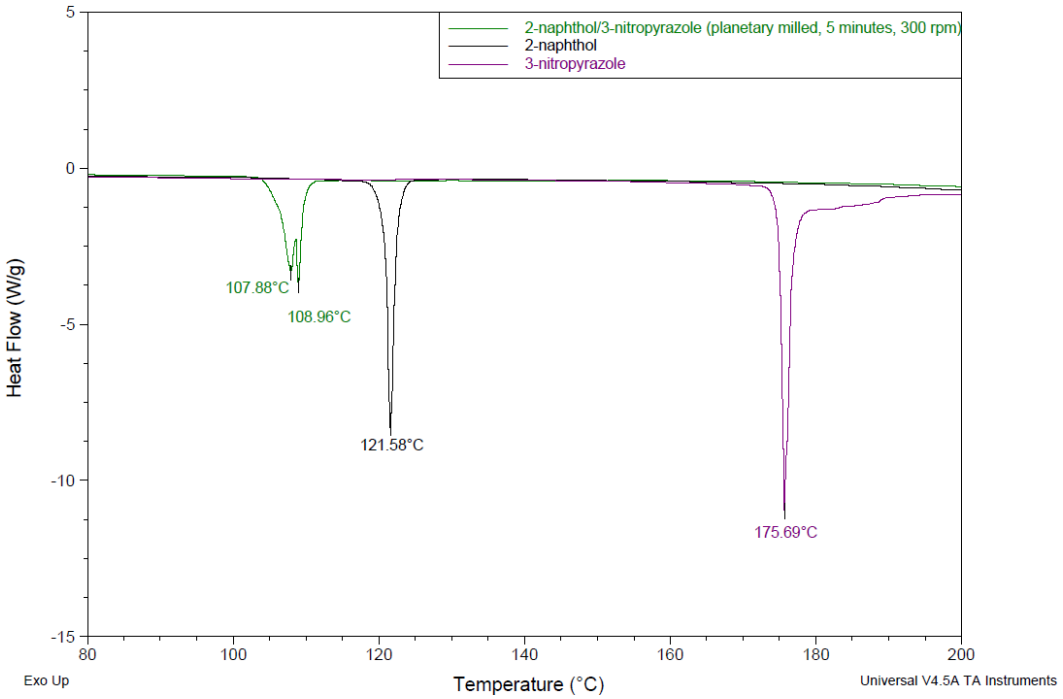

Figure B.14 - Thermal analysis of 2-naphthol/3-nitropyrazole produced by planetary milling for 5 minutes at 300 rpm.

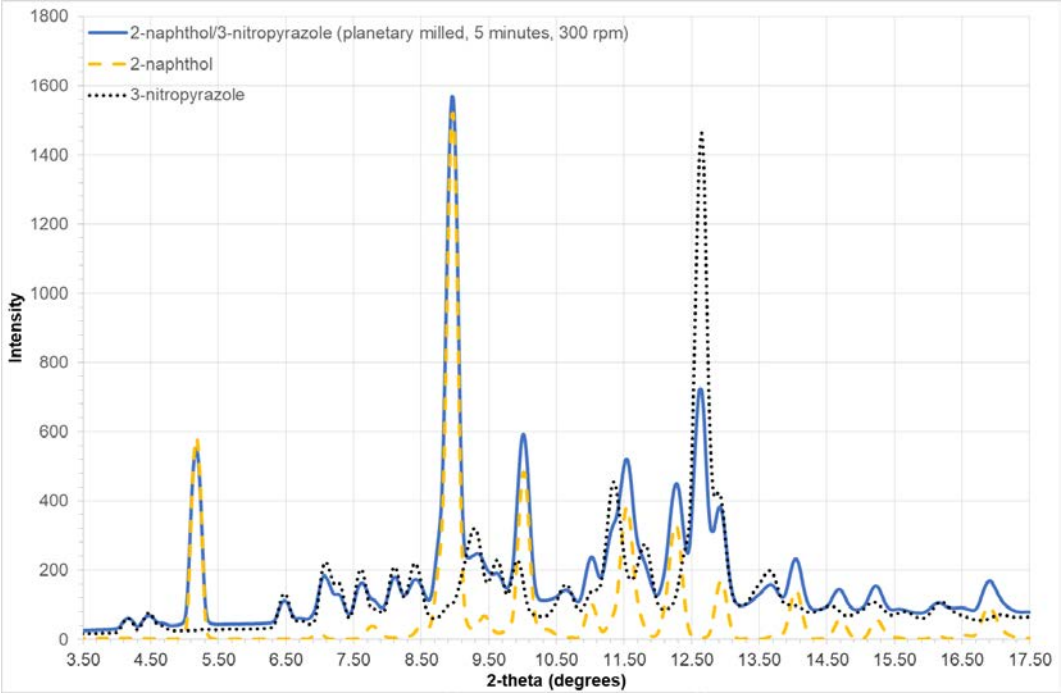

Figure B.15 – Powder x-ray pattern of 2-naphthol/3-nitropyrazole produced by planetary milling for 5 minutes at 300 rpm (λ = 0.7107 Å).

B.12 2-naphthol/4-nitropyrazole

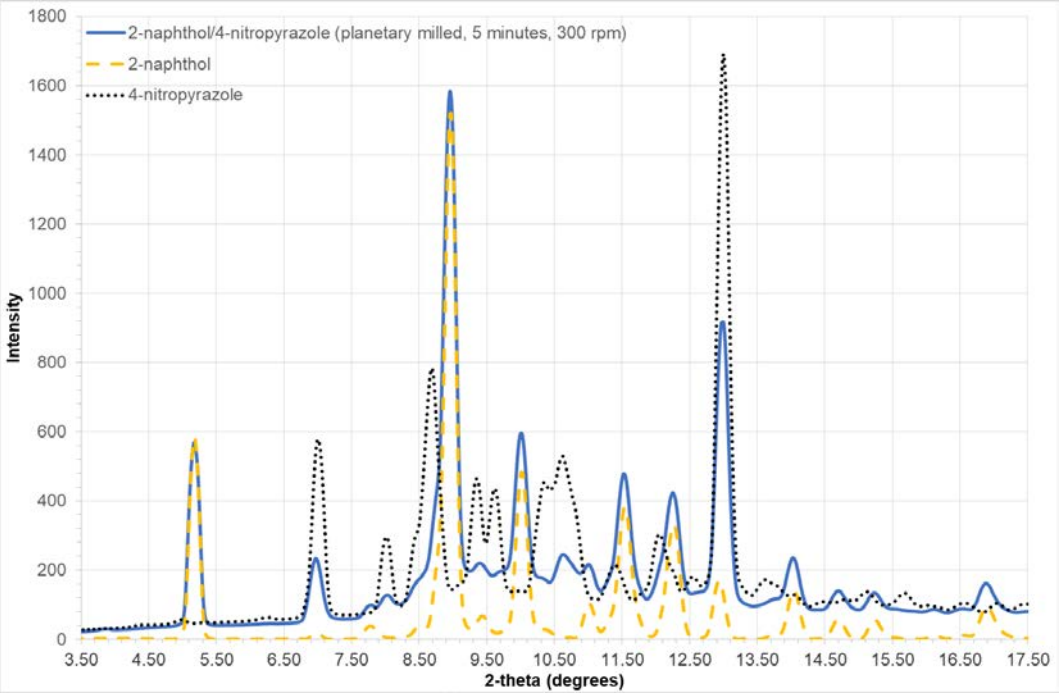

Figure B.16 - Powder x-ray pattern of 2-naphthol/4-nitropyrazole produced by planetary milling for 5 minutes at 300 rpm (λ = 0.7107 Å).

B.13 2-naphthol/5-methylpyrazole

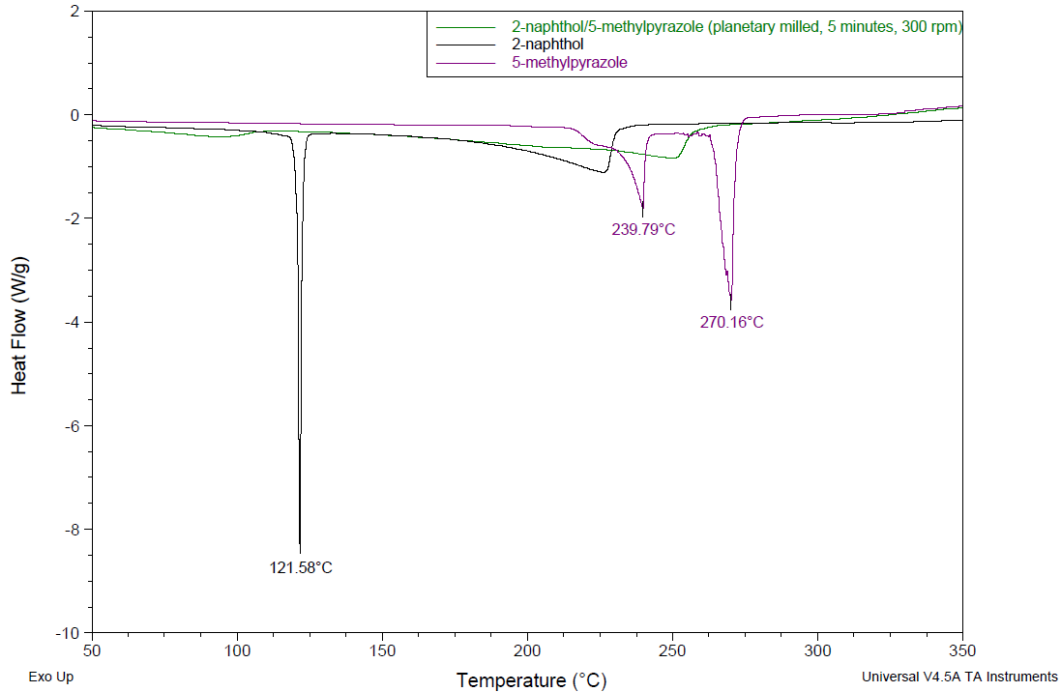

Figure B.17 - Thermal analysis of 2-naphthol/5-methylpyrazole produced by planetary milling for 5 minutes at 300 rpm.

B.14 2-naphthol/pyrazol-4-amine

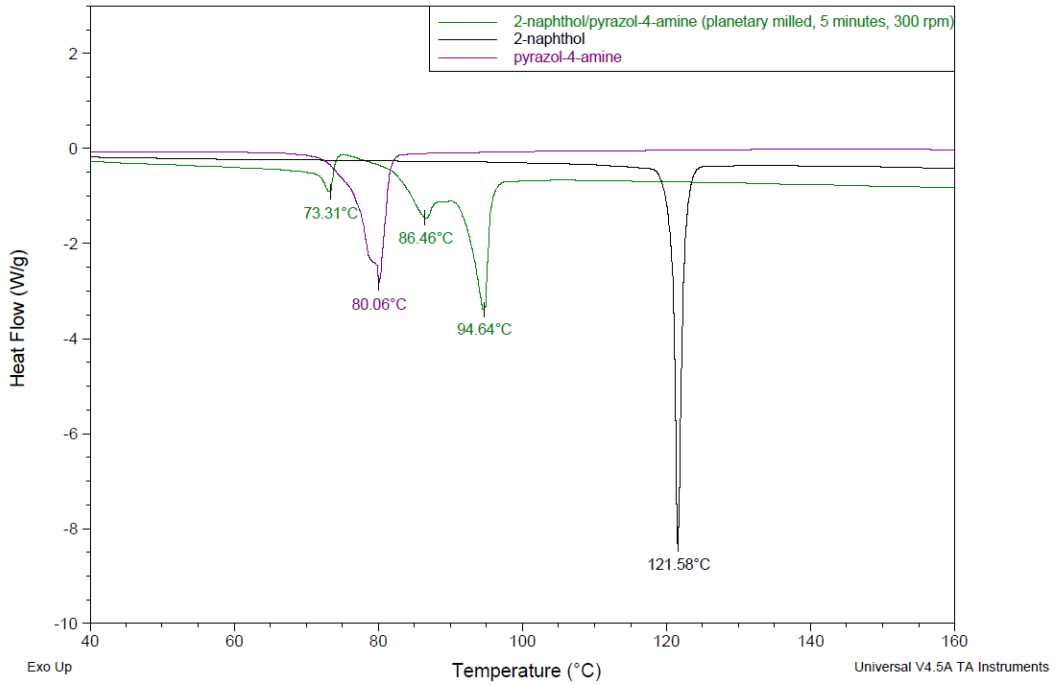

Figure B.18 - Thermal analysis of 2-naphthol/pyrazol-4-amine produced by planetary milling for 5 minutes at 300 rpm.

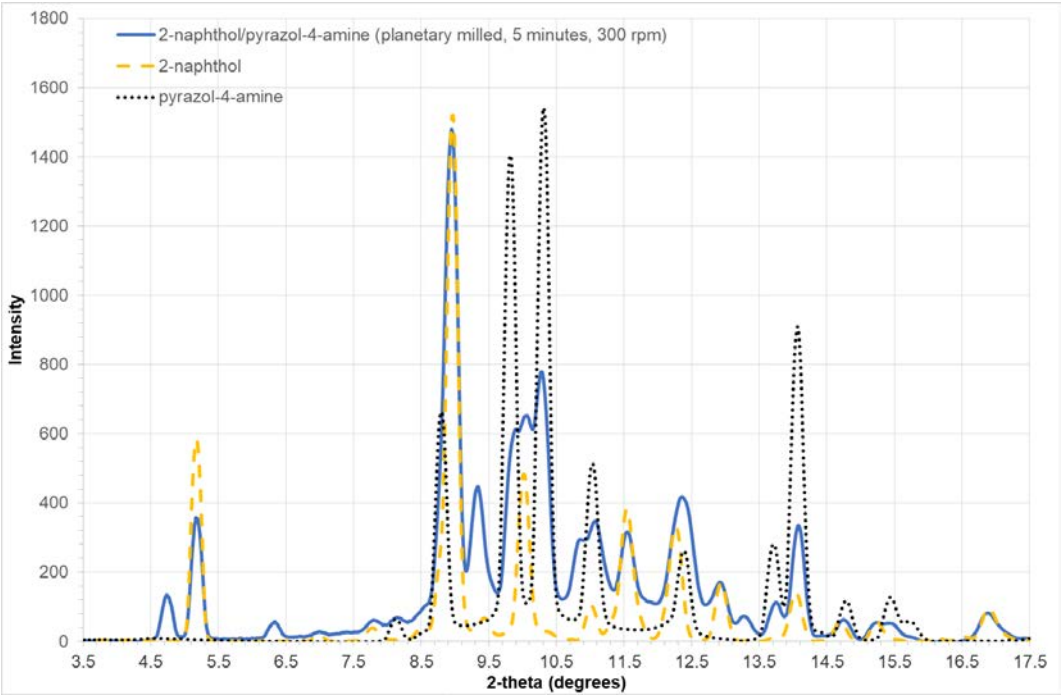

Figure B.19 – Powder x-ray pattern of 2-naphthol/pyrazol-4-amine produced by planetary milling for 5 minutes at 300 rpm (λ = 0.7107 Å).

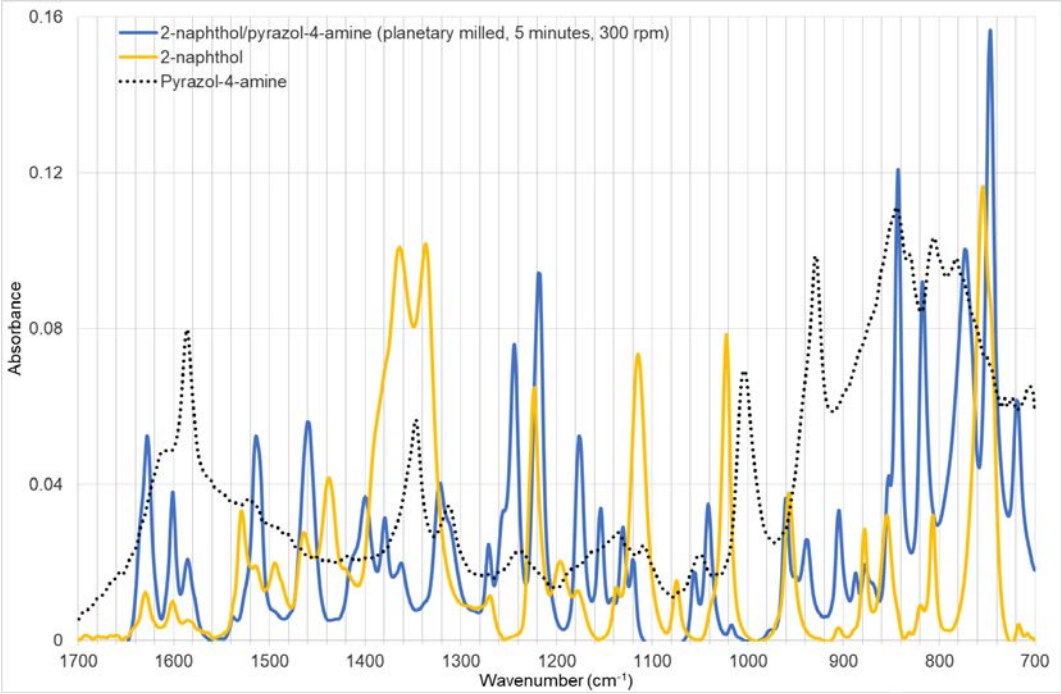

Figure B.20 - Infrared spectra of 2-napthol/pyrazol-4-amine produced by planetary milling for 5 minutes at 300 rpm, with a 1:1 stoichiometry.

Table B.3 - Infrared spectra peak positions and heights of 2-napthol/pyrazol-4-amine produced by planetary milling for 5 minutes at 300 rpm, with a 1:1 stoichiometry.

Peak Position (cm^{-1})	Peak Height (Absorbance)
1631.21	0.05
1602.2	0.04
1586.97	0.02
1558.35	-0.01
1512.87	0.02
1467.34	0.03
1408.64	0.01
1323.03	-0.01
1274.77	0.02
1250.09	0.04
1217.22	0.07
1174.04	0.03
1151.06	-0.01
1140.46	-0.01
1118.65	-0.01
1014.23	-0.01
1002.5	0
958.91	0.05
929.79	0.01
906.1	0.04
878.06	0.02
843.65	0.13
814.6	0.12
742.03	0.18
715.57	0.07

B.15 2-naphthol/3-bromopyrazole

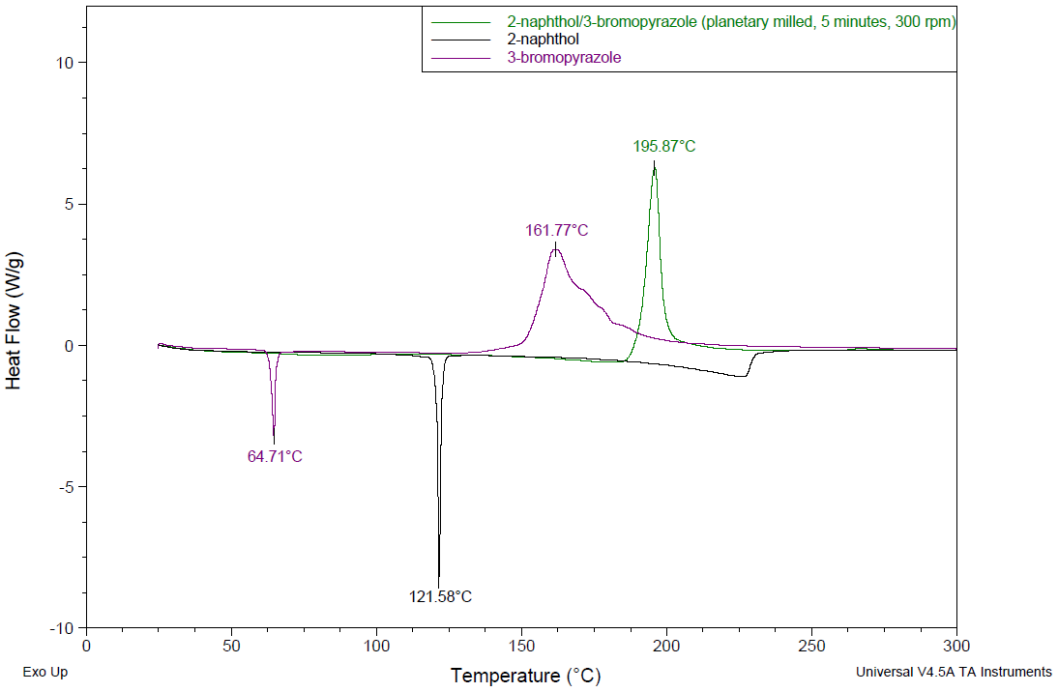

Figure B.21 - Thermal analysis of 2-naphthol/3-bromopyrazole produced by planetary milling for 5 minutes at 300 rpm.

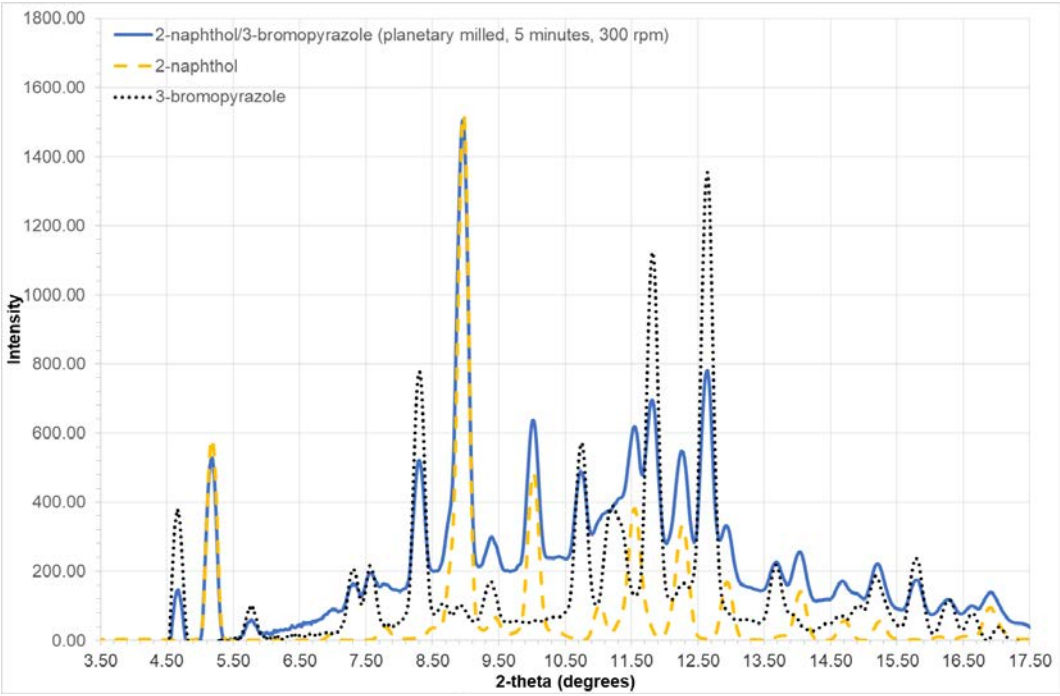

Figure B.22 – Powder x-ray pattern of 2-naphthol/3-bromopyrazole produced by planetary milling for 5 minutes at 300 rpm (λ = 0.7107 Å).

B.16 2-naphthol/4-bromopyrazole

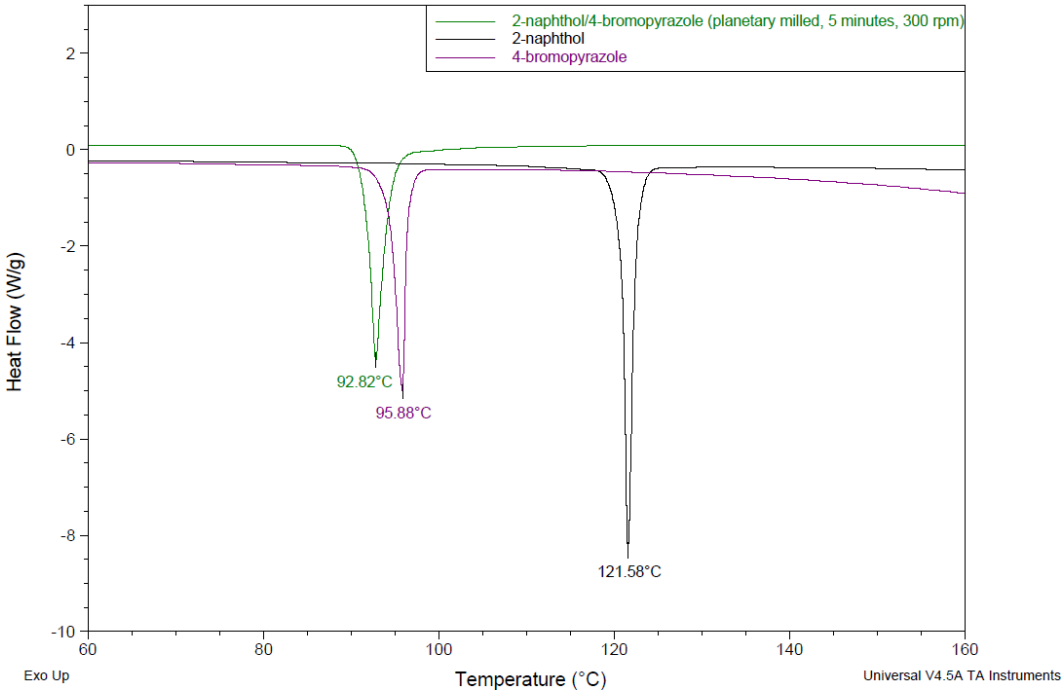

Figure B.23 - Thermal analysis of 2-naphthol/4-bromopyrazole produced by planetary milling for 5 minutes at 300 rpm.

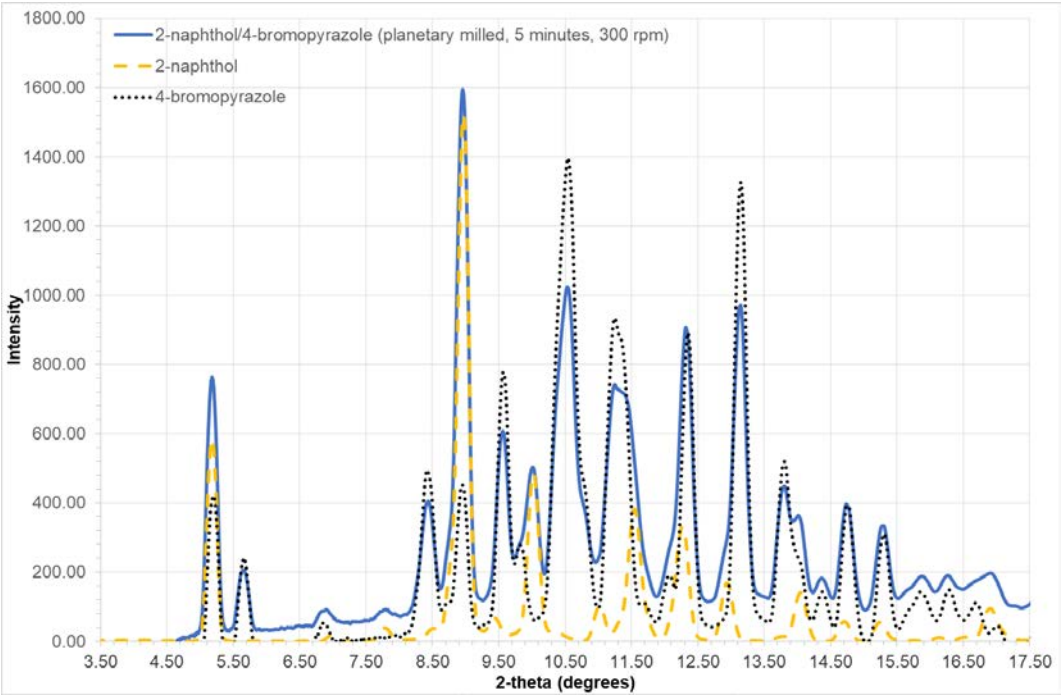

Figure B.24 – Powder x-ray pattern of 2-naphthol/4-bromopyrazole produced by planetary milling for 5 minutes at 300 rpm (λ = 0.7107 Å).

B.17 2-naphthol/3,4-dimethylpryazole

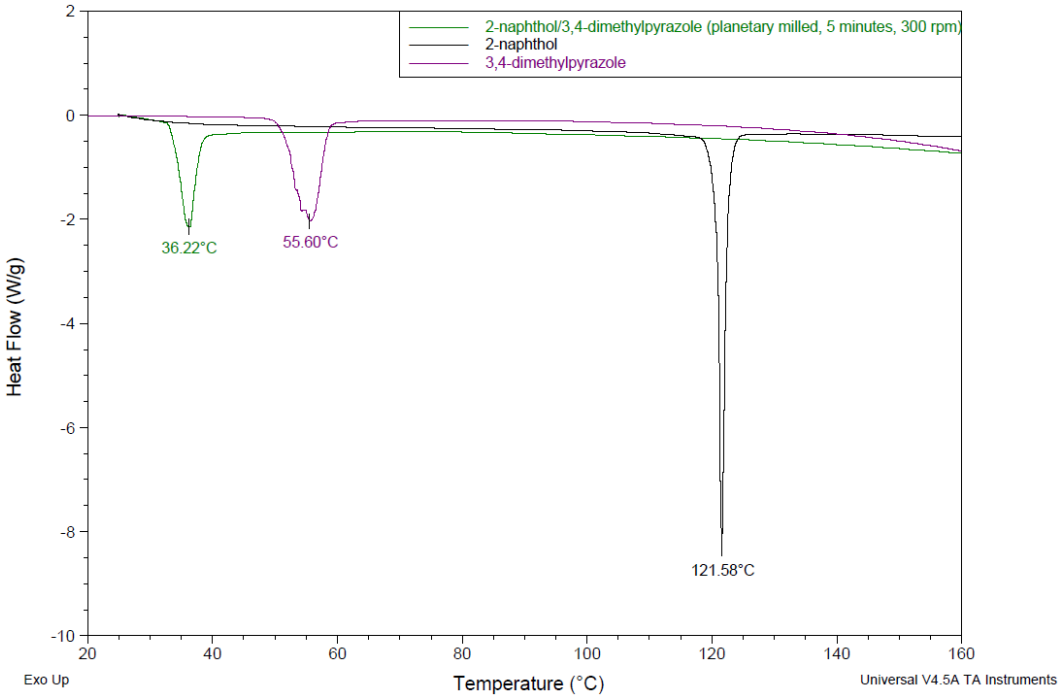

Figure B.25 - Thermal analysis of 2-naphthol/3,4-dimethylpyrazole produced by planetary milling for 5 minutes at 300 rpm.

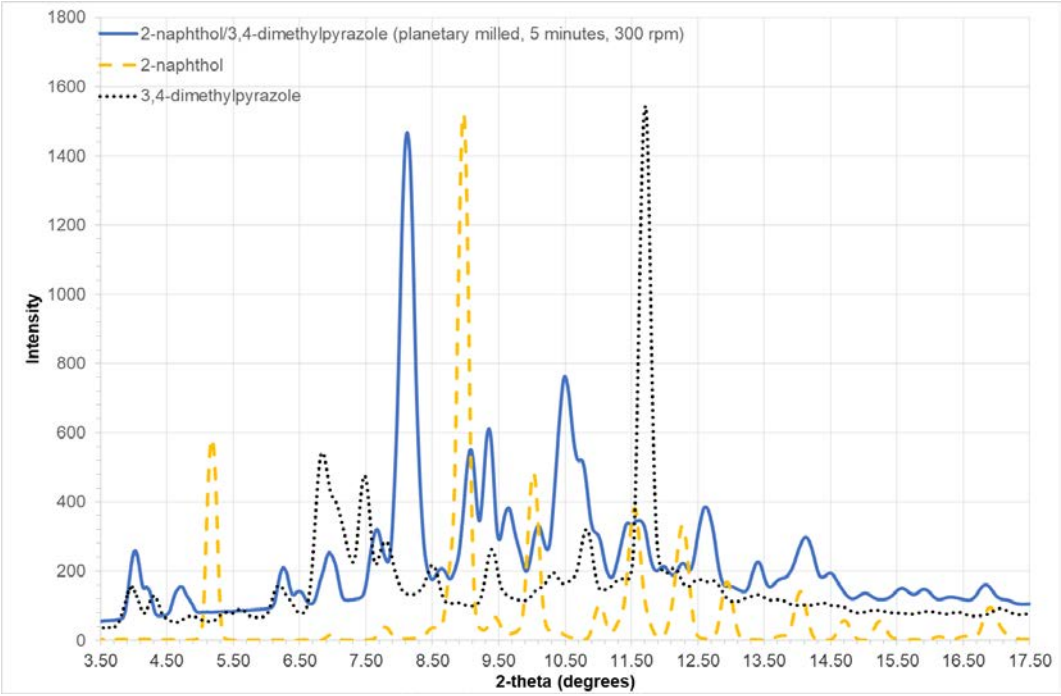

Figure B.26 – Powder x-ray pattern of 2-naphthol/3,4-dimethylpyrazole produced by planetary milling for 5 minutes at 300 rpm (λ = 0.7107 Å).

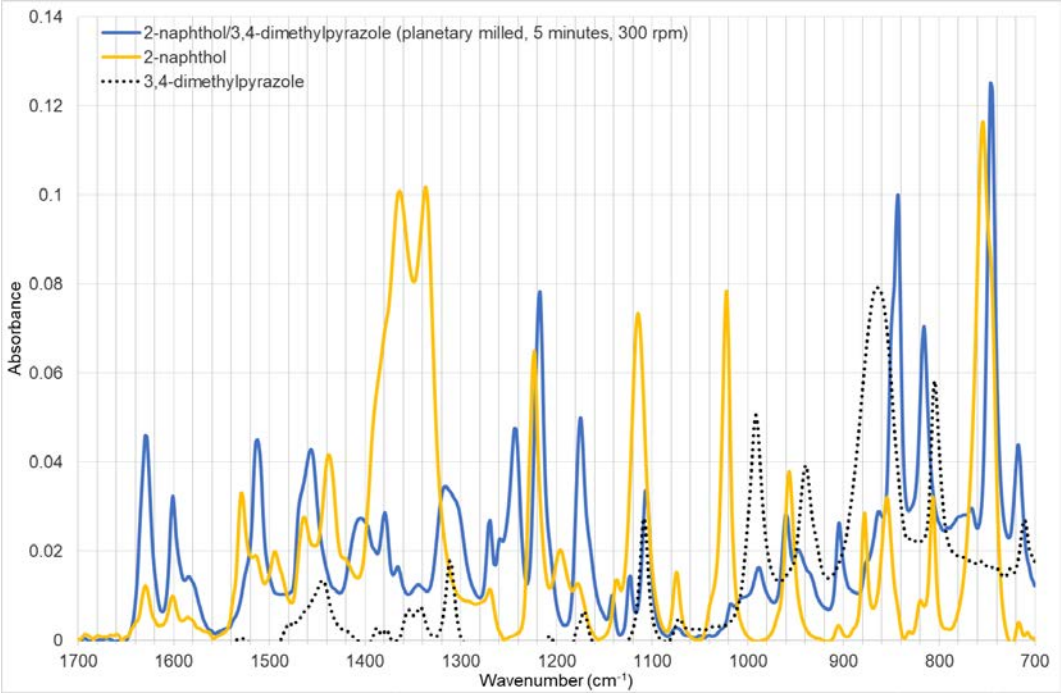

Figure B.27 – Infra-red spectra of 2-naphthol/3,4-dimethylpyrazole produced by planetary milling for 5 minutes at 300 rpm.

Table B.4- Infrared spectra peak positions and heights of 2-naphthol/3,4-dimethylpyrazole produced by planetary milling for 5 minutes at 300 rpm, with a 1:1 stoichiometry.

Peak Position (cm^{-1})	Peak Height (Absorbance)	Peak Position (cm^{-1})	Peak Height (Absorbance)
3262.11	0.03	1141.84	0.01
1629.17	0.05	1123.14	0.01
1600.9	0.03	1106.42	0.03
1584.2	0.01	1017.73	0.01
1512.72	0.05	988.68	0.02
1485.56	0.01	960.06	0.03
1456.55	0.04	947.5	0.02
1404.47	0.03	904.6	0.03
1379.36	0.03	862.94	0.03
1365.86	0.02	843.34	0.1
1344.37	0.01	816.03	0.07
1315.82	0.03	790.6	0.03
1269.65	0.03	773.28	0.03
1258.83	0.02	766.3	0.03
1243.37	0.05	745.77	0.13
1217.49	0.08	717.46	0.04
1174.82	0.05		

B.18 2-naphthol/3,5-dimethylpyrazole

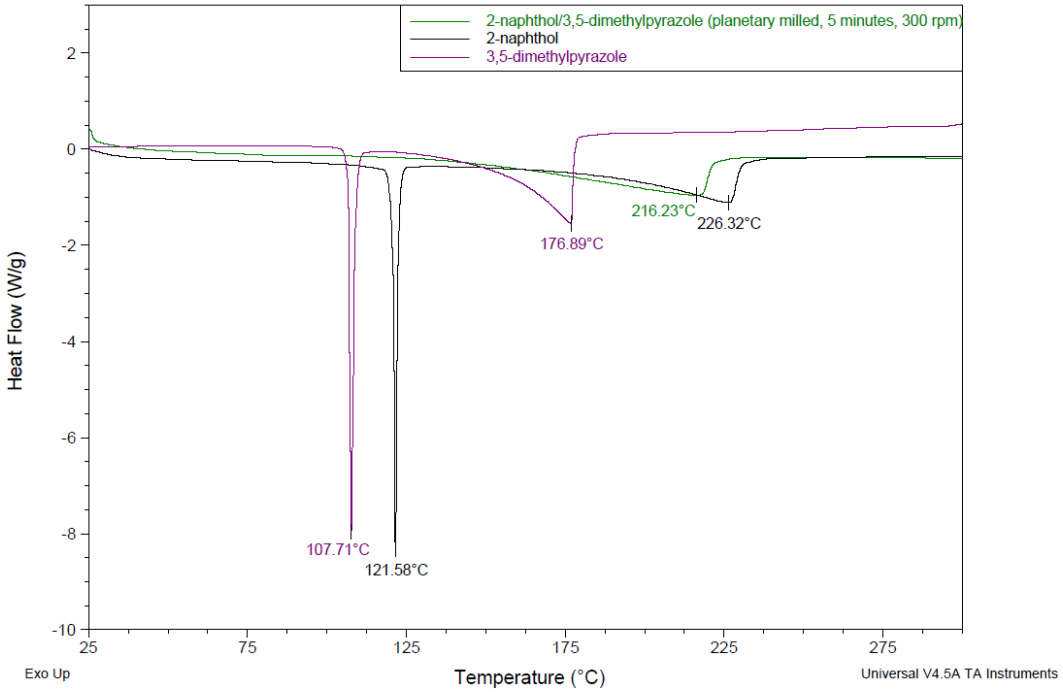

Figure B.28 - Thermal analysis of 2-naphthol/3,5-dimethylpyrazole produced by planetary milling for 5 minutes at 300 rpm. No melt is observed for the mixed system

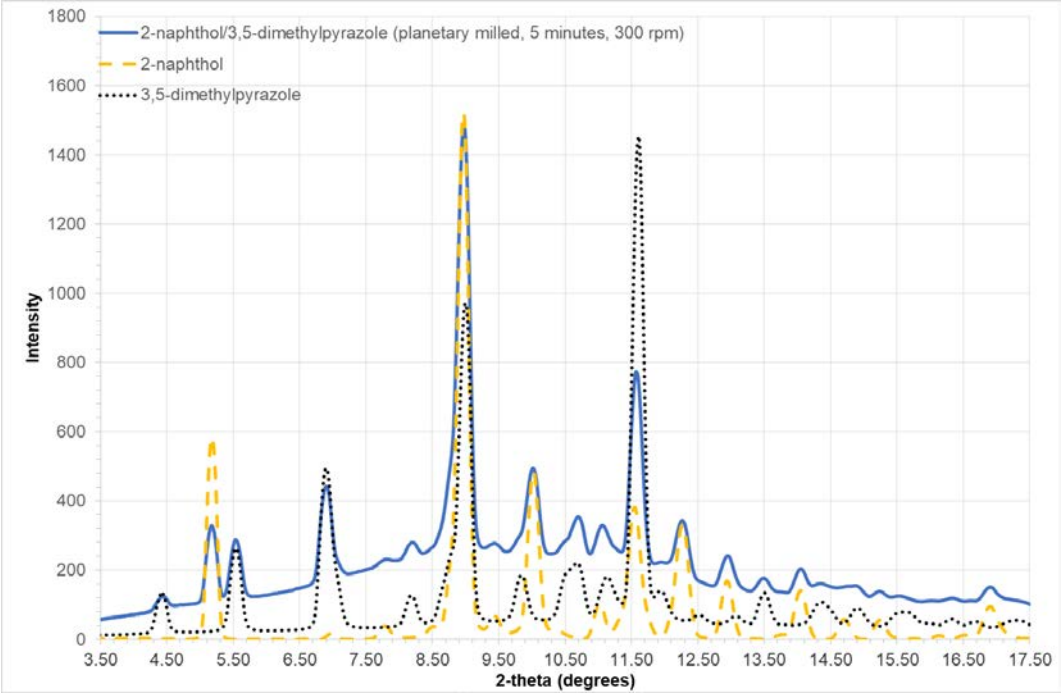

Figure B.29 – Powder x-ray pattern of 2-naphthol/3,5-dimethylpyrazole produced by planetary milling for 5 minutes at 300 rpm (λ = 0.7107 Å).

B.19 2-naphthol/3,4,5-tribromopyrazole

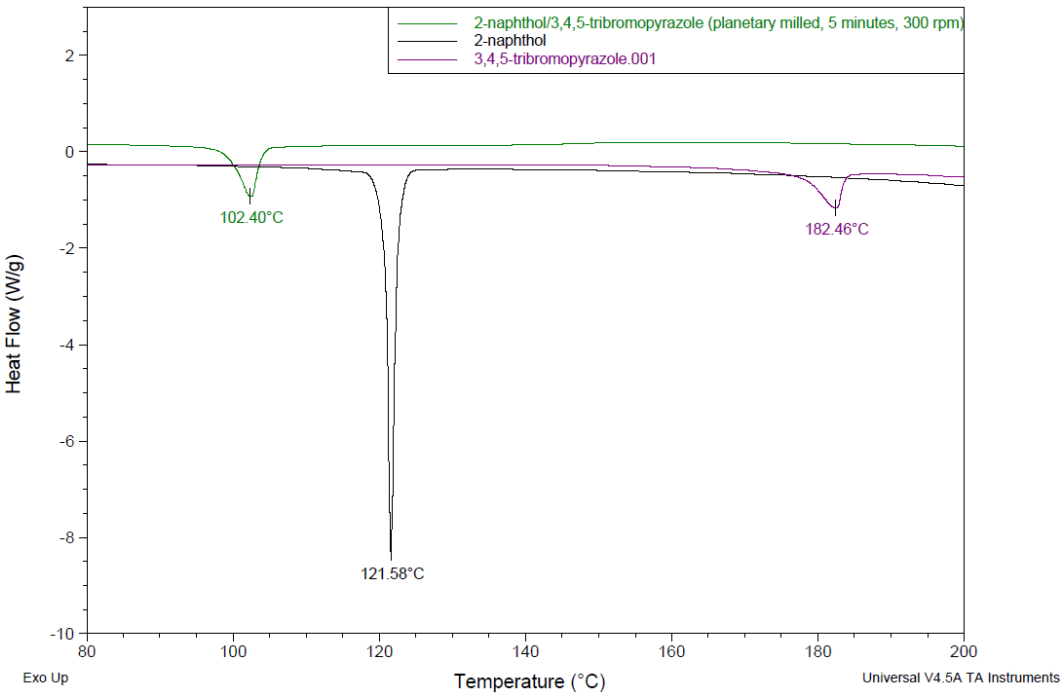

Figure B.30 - Thermal analysis of 2-naphthol/3,4.5-tribromopyrazole produced by planetary milling for 5 minutes at 300 rpm.

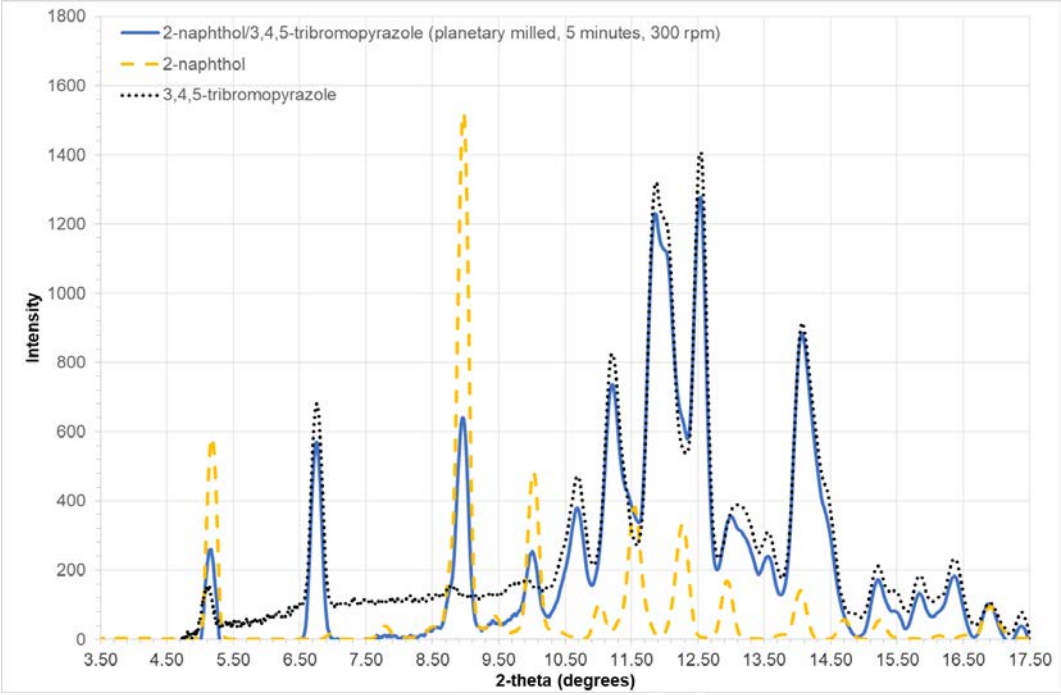

Figure B.31 – Powder x-ray pattern of 2-naphthol/3,4.5-tribromopyrazole produced by planetary milling for 5 minutes at 300 rpm (λ = 0.7107 Å).

B.20 2-naphthol/3-methyl-5-nitropyrazole

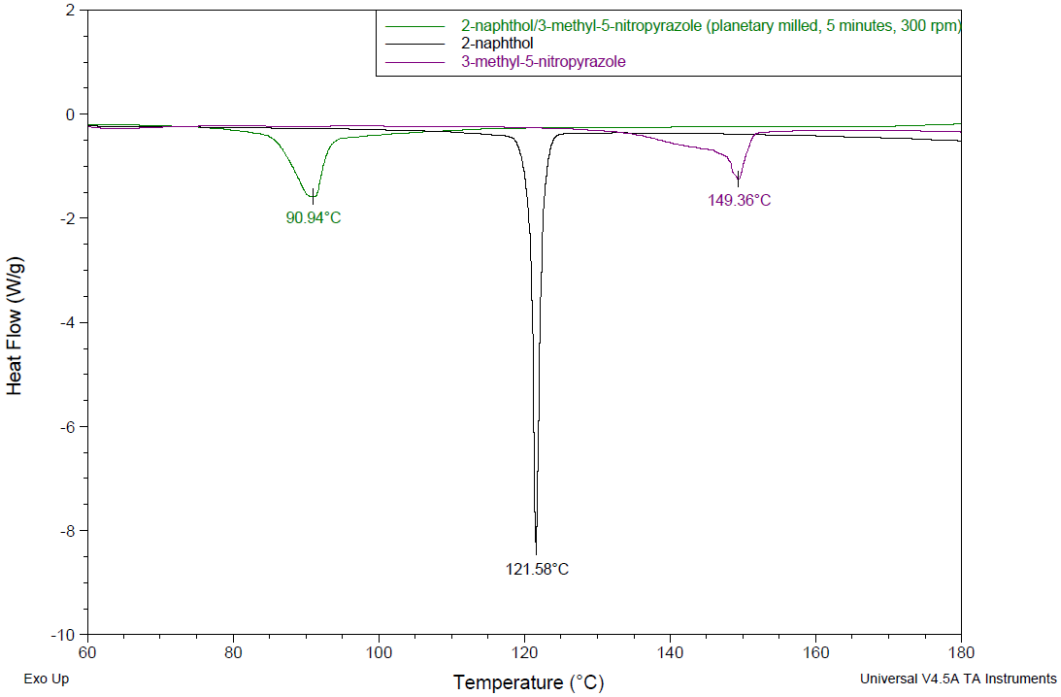

Figure B.32 - Thermal analysis of 2-naphthol/3-methyl-5-nitropyrazole produced by planetary milling for 5 minutes at 300 rpm.

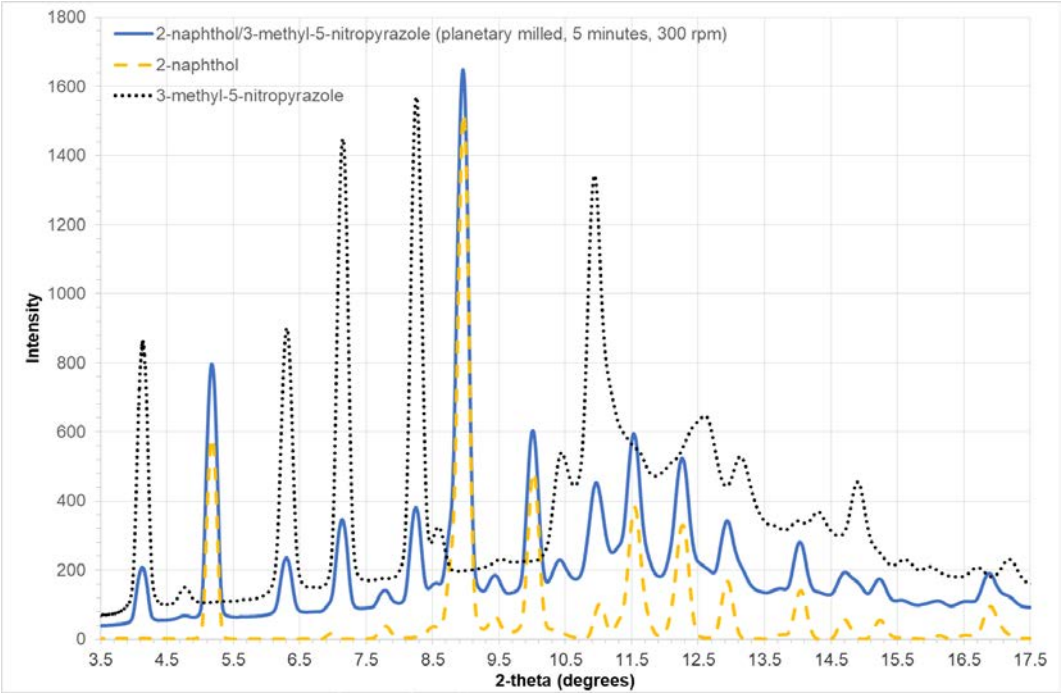

Figure B.33 – Powder x-ray pattern of 2-naphthol/3-methyl-5-nitropyrazole produced by planetary milling for 5 minutes at 300 rpm (λ = 0.7107 Å).

B.21 2-naphthol/5-methylpyrazol-3-amine

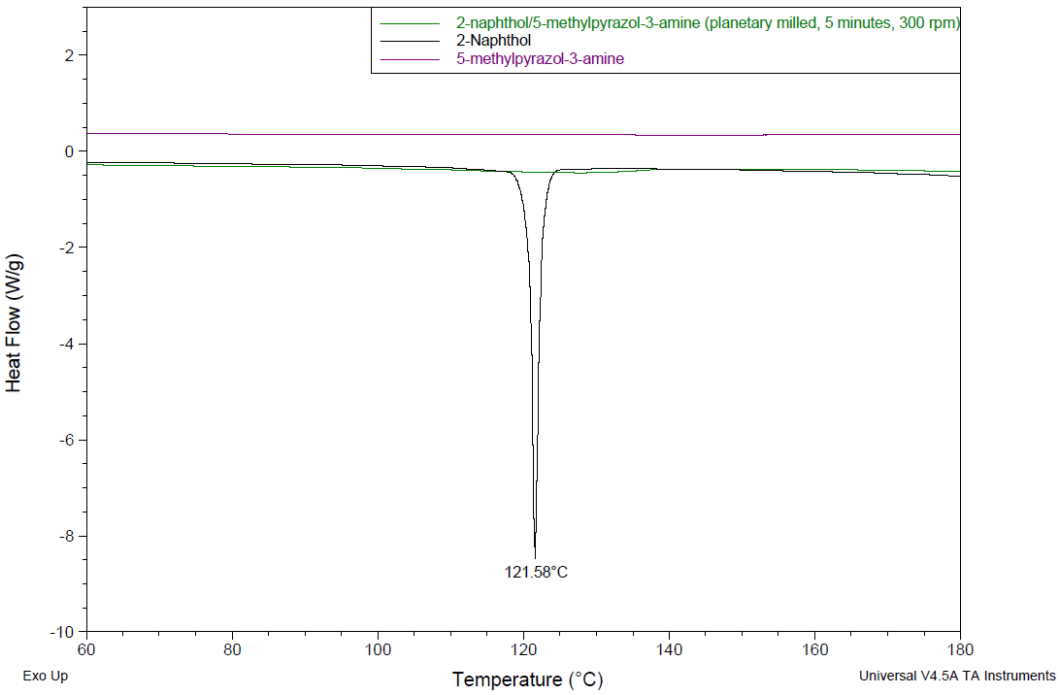

Figure B.34 - Thermal analysis of 2-naphthol/5-methylpyrazol-3-amine produced by planetary milling for 5 minutes at 300 rpm. Both 5-methylpyrazol-3-amine and the mixed system are liquids and did not display melts.

B.22 2-naphthol/4-bromopyrazol-3-amine

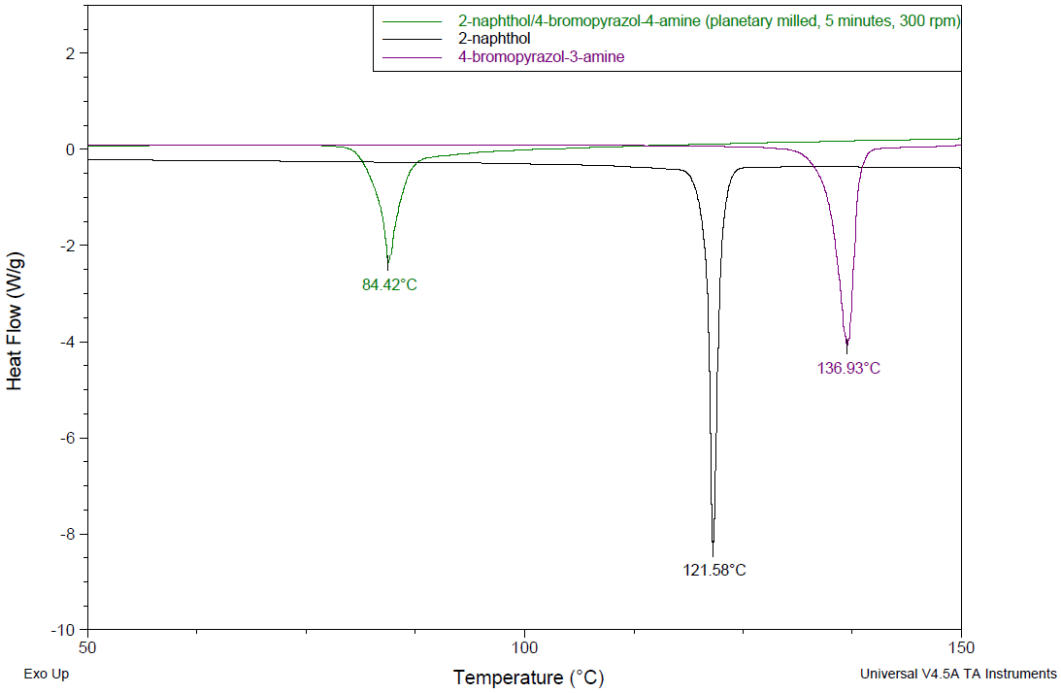

Figure B.35 - Thermal analysis of 2-naphthol/4-bromopyrazol-3-amine produced by planetary milling for 5 minutes at 300 rpm.

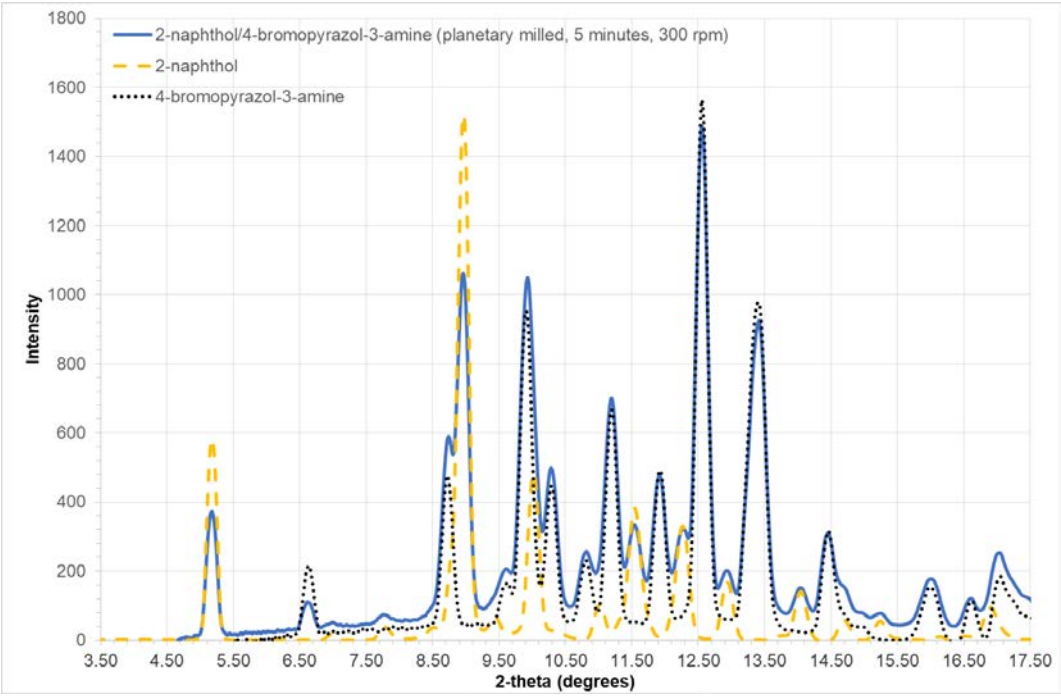

Figure B.36 – Powder x-ray pattern of 2-naphthol/4-bromopyrazol-3-amine produced by planetary milling for 5 minutes at 300 rpm (λ = 0.7107 Å).

B.23 2-naphthol/3-bromopyrazol-5-amine

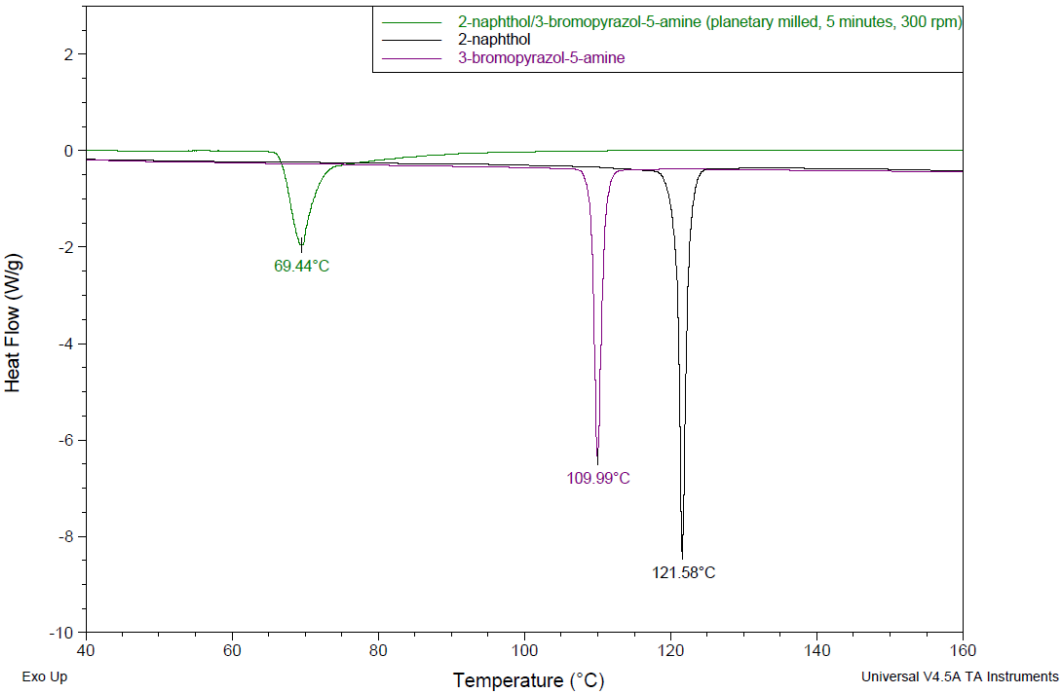

Figure B.37 - Thermal analysis of 2-naphthol/3-bromopyrazol-5-amine produced by planetary milling for 5 minutes at 300 rpm.

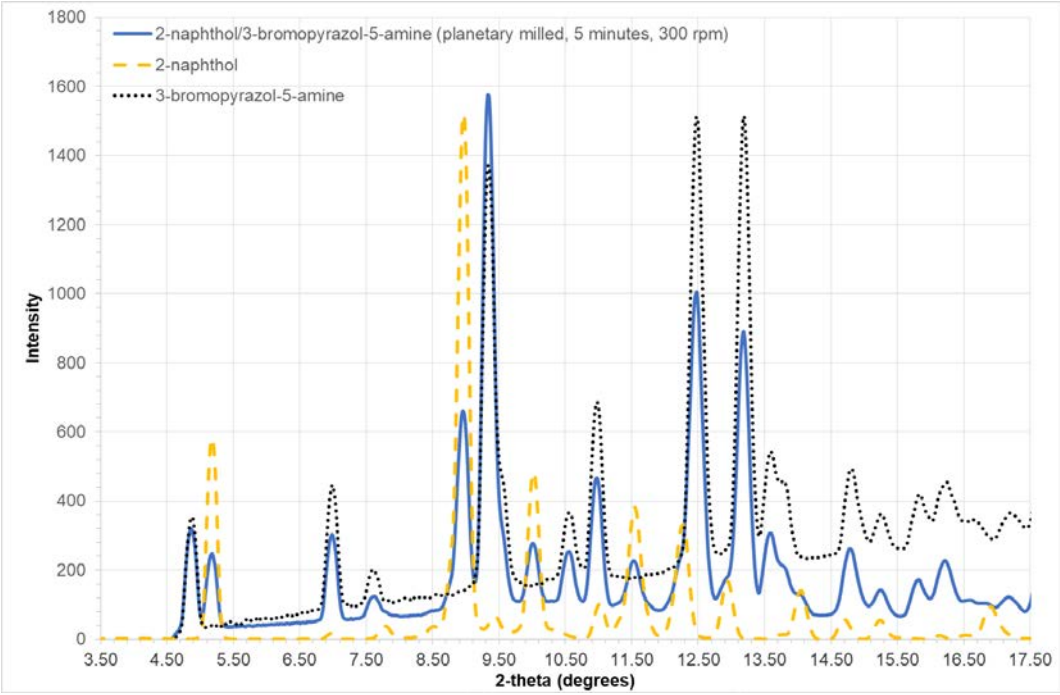

Figure B.38 – Powder x-ray pattern of 2-naphthol/3-bromopyrazol-5-amine produced by planetary milling for 5 minutes at 300 rpm (λ = 0.7107 Å).

B.24 2-naphthol/3,5-dimethylpyrazol-4-amine

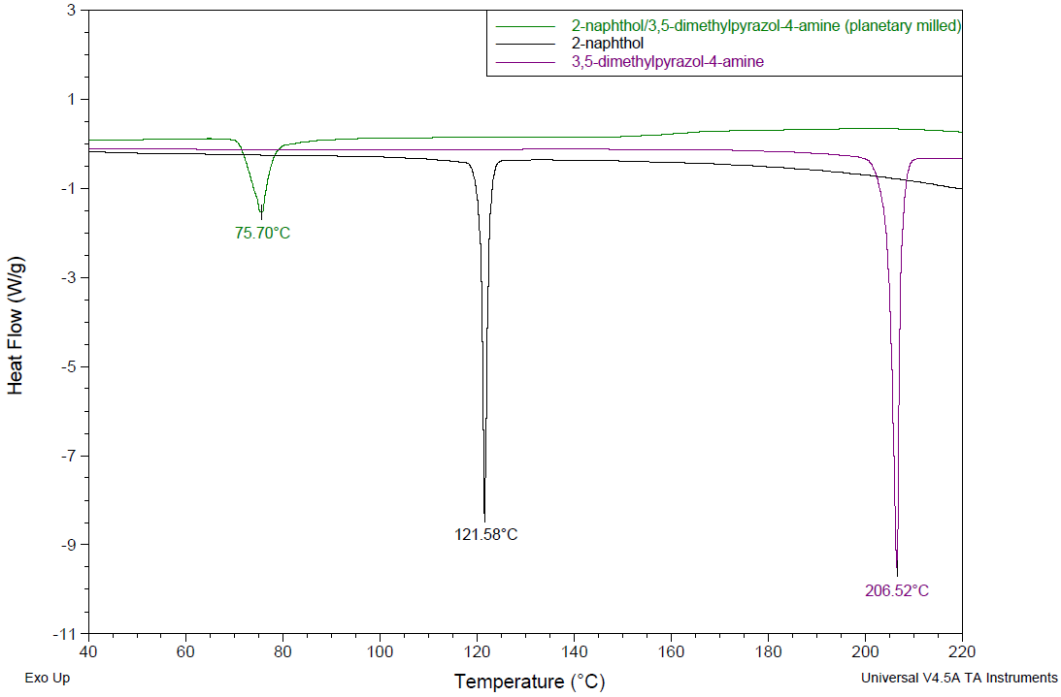

Figure B.39 - Thermal analysis of 2-naphthol/3,5-dimethylpyrazol-4-amine produced by planetary milling for 5 minutes at 300 rpm.

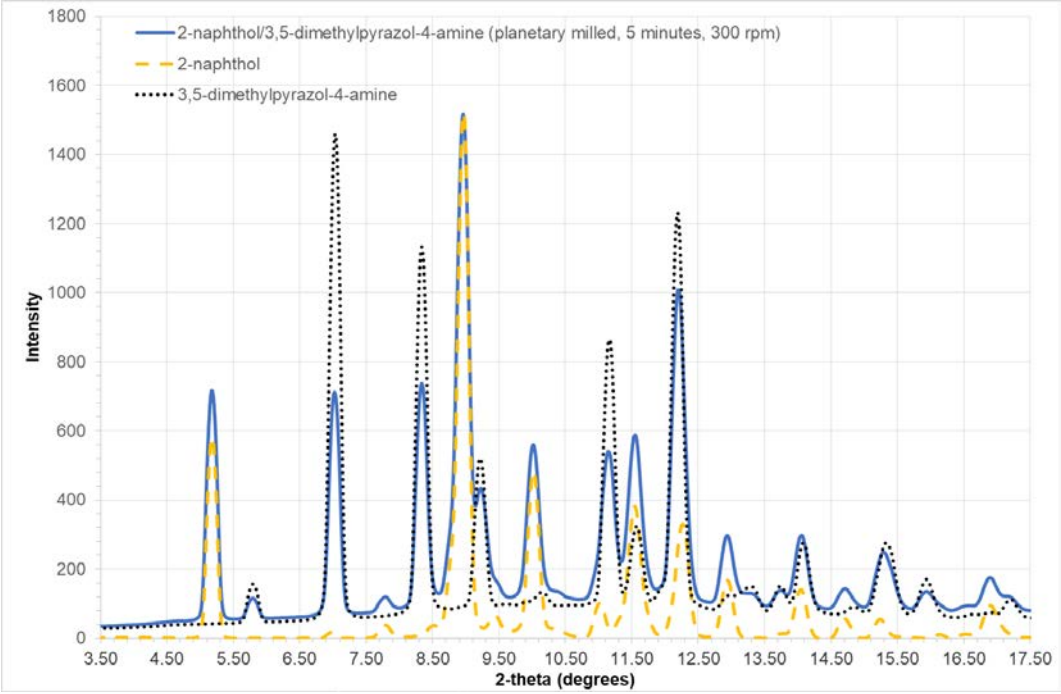

Figure B.40 – Powder x-ray pattern of 2-naphthol/3,5-dimethylpyrazol-4-amine produced by planetary milling for 5 minutes at 300 rpm (λ = 0.7107 Å).

B.25 2-naphthol/3,4-dimethylpyrazol-5-amine

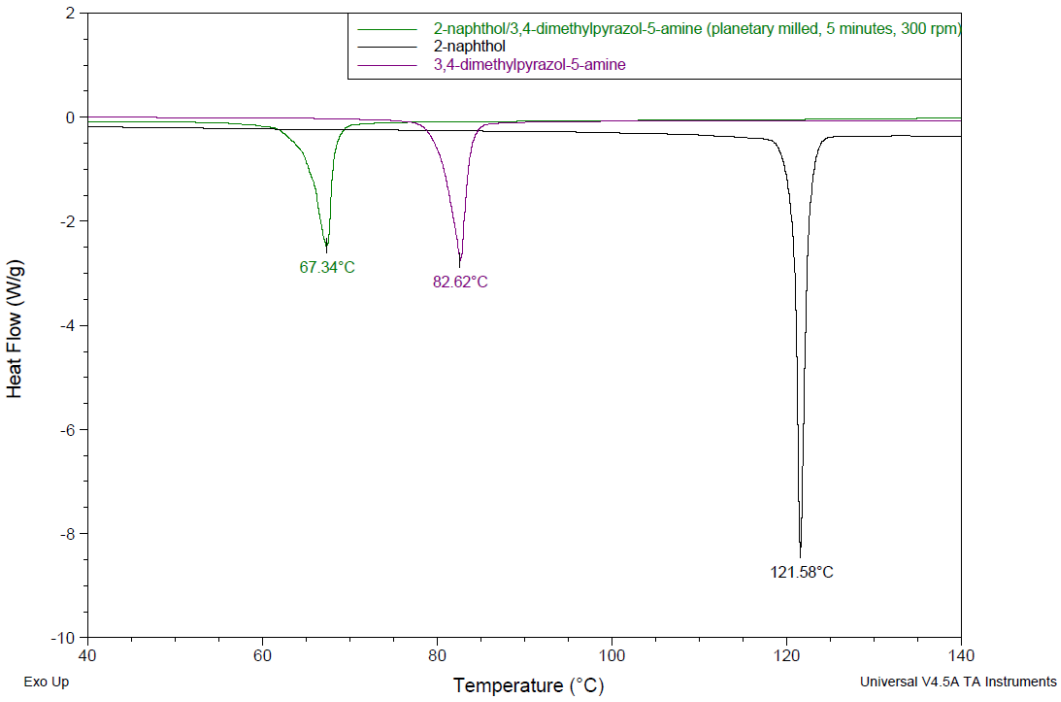

Figure B.41 - Thermal analysis of 2-naphthol/3,4-dimethylpyrazol-5-amine produced by planetary milling for 5 minutes at 300 rpm.

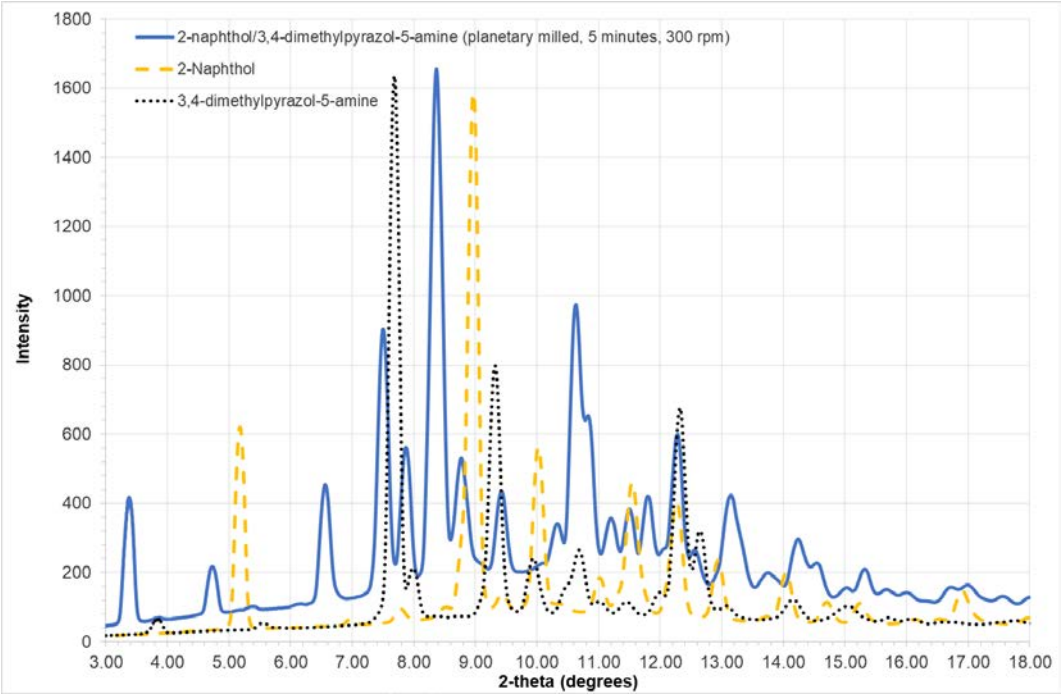

Figure B.42 – Powder x-ray pattern of 2-naphthol/3,4-dimethylpyrazol-5-amine produced by planetary milling for 5 minutes at 300 rpm (λ = 0.7107 Å).

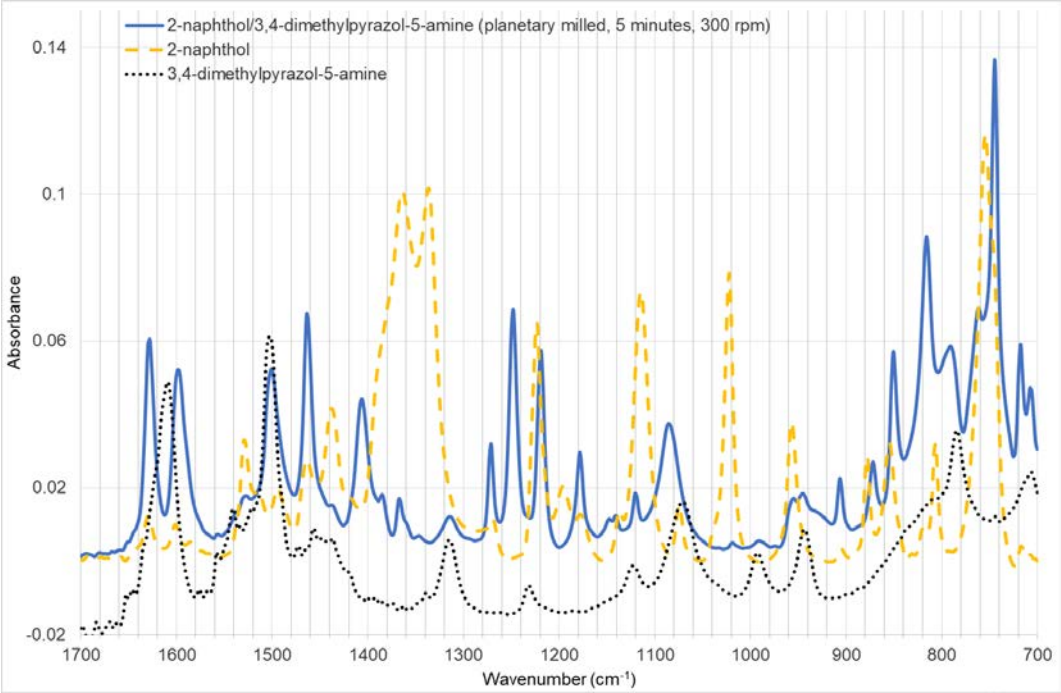

Figure B.43 – Infrared spectra of 2-naphthol/3,4-dimethylpyrazol-5-amine produced by planetary milling for 5 minutes at 300 rpm.

Table B.5 - Infrared spectra peak positions and heights of 2-naphthol/3,4-dimethylpyrazol-5-amine produced by planetary milling for 5 minutes at 300 rpm, with a 1:1 stoichiometry.

Peak Positions (cm^{-1})	Peak Height (Absorbance)	Peak Positions (cm^{-1})	Peak Height (Absorbance)
3389.11	0.02	1178.37	0.03
3321.95	0.01	1147.51	0.01
1628.41	0.06	1141.06	0.01
1598.35	0.05	1120.23	0.02
1556.73	0.01	1085.44	0.04
1527.49	0.02	991.16	0.01
1500.76	0.05	954.86	0.02
1463.52	0.07	945.33	0.02
1437.73	0.02	906.41	0.02
1406.28	0.04	871.92	0.03
1385.22	0.02	850.55	0.06
1367.12	0.02	815.87	0.09
1346.68	0.01	790.95	0.06
1314.17	0.01	761.59	0.07
1271.3	0.03	744.62	0.14
1248.16	0.07	717.62	0.06
1219.11	0.06	707.35	0.05

B.26 2-naphthol/3-methyl-4-bromopyrazole

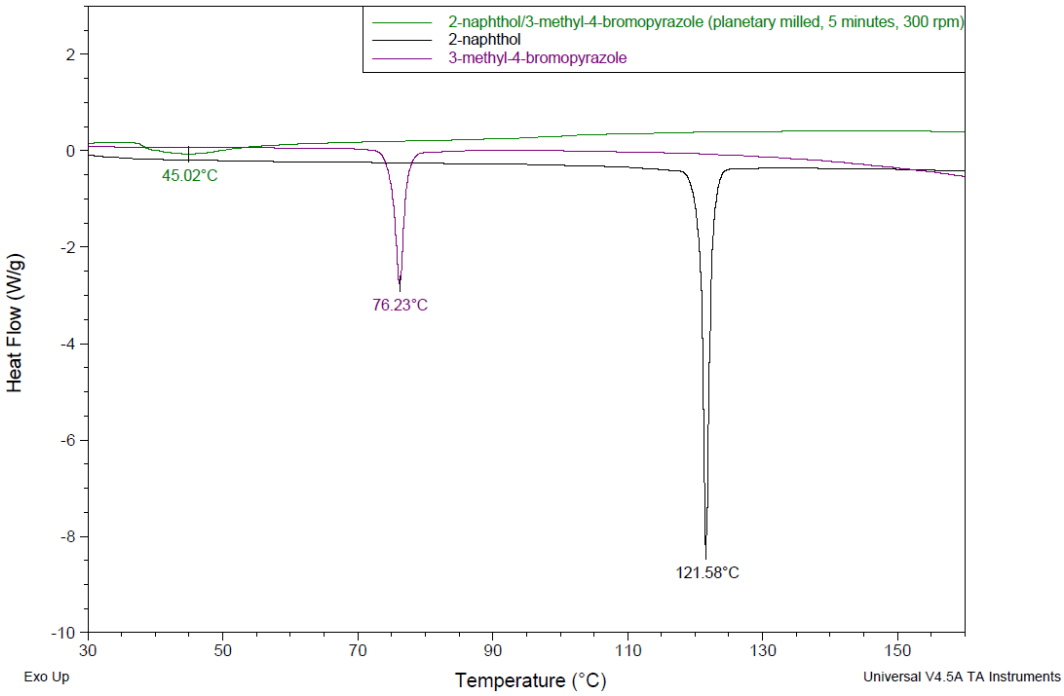

Figure B.44 - Thermal analysis of 2-naphthol/3-methyl-4-bromopyrazole produced by planetary milling for 5 minutes at 300 rpm.

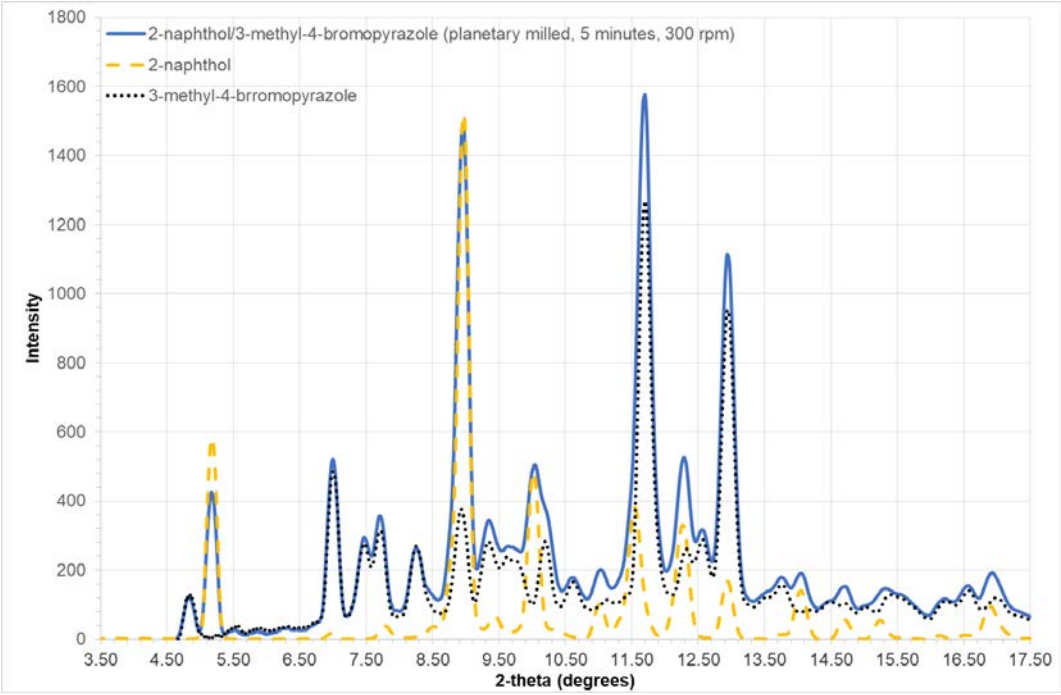

Figure B.45 – Powder x-ray pattern of 2-naphthol/3-methyl-4-bromopyrazole produced by planetary milling for 5 minutes at 300 rpm (λ = 0.7107 Å).

B.27 2-naphthol/3-bromo-5-methylpyrazole

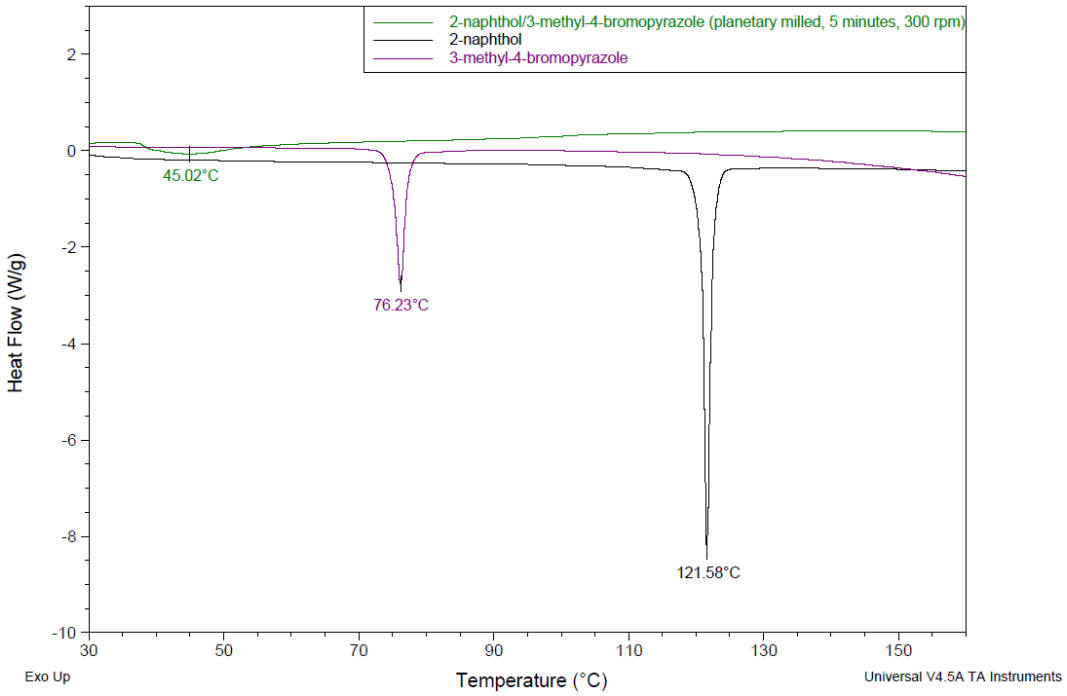

Figure B.46 - Thermal analysis of 2-naphthol/3-bromo-5-methylpyrazole produced by planetary milling for 5 minutes at 300 rpm.

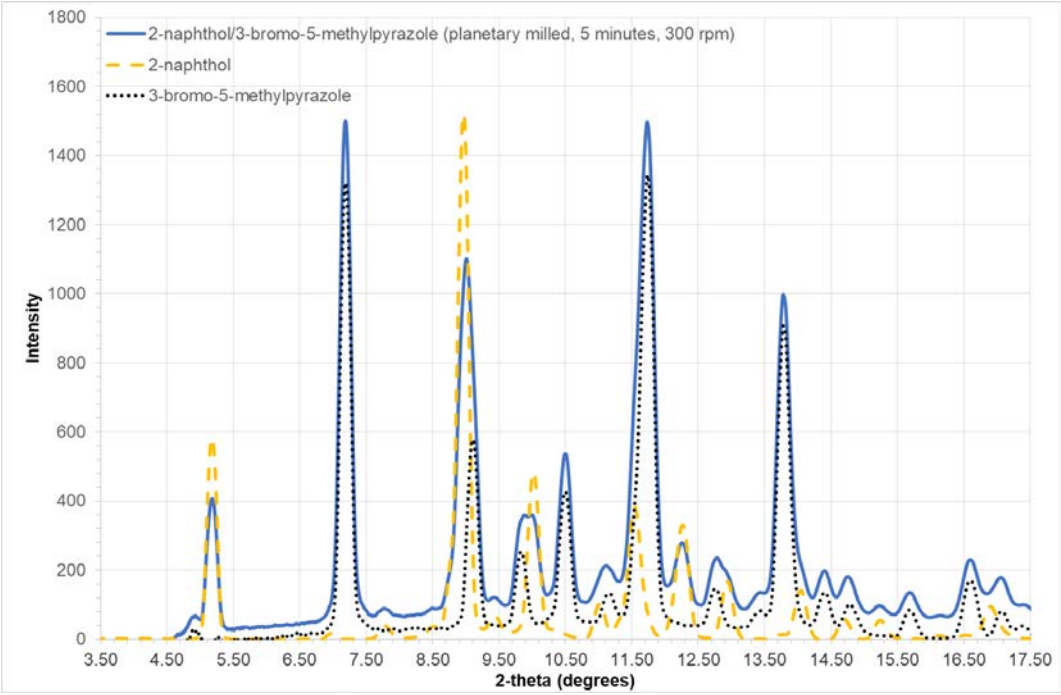

Figure B.47 – Powder x-ray pattern of 2-naphthol/3-bromo-5-methylpyrazole produced by planetary milling for 5 minutes at 300 rpm (λ = 0.7107 Å).

B.28 2-naphthol/4-bromo-3,5-dimethylpyrazole

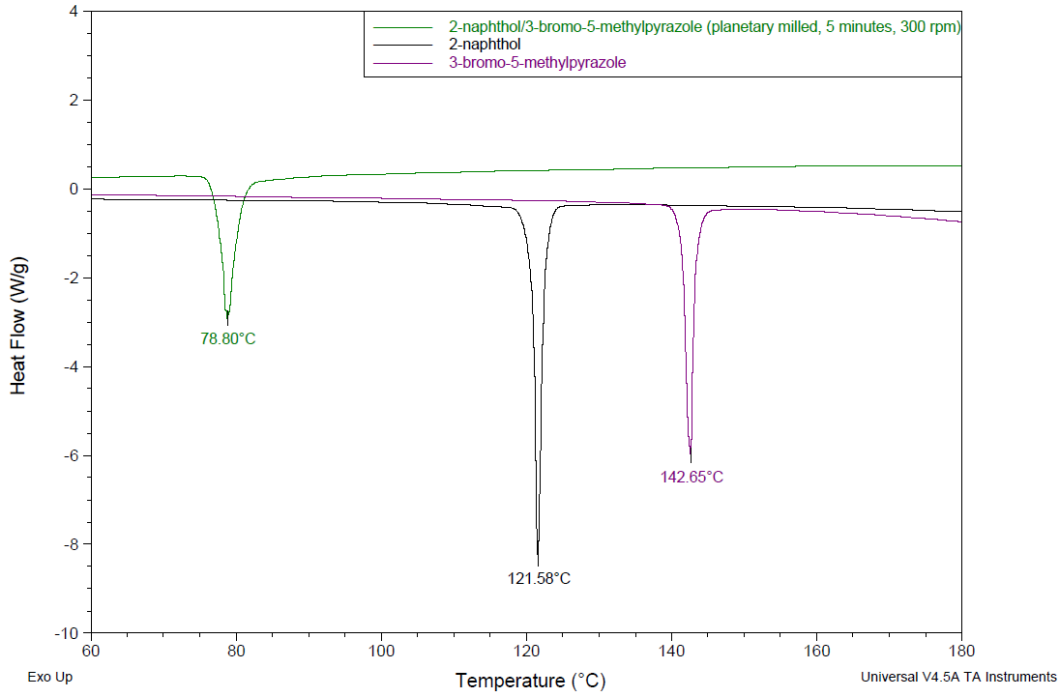

Figure B.48 - Thermal analysis of 2-naphthol/4-bromo-3,5-dimethylpyrazole produced by planetary milling for 5 minutes at 300 rpm.

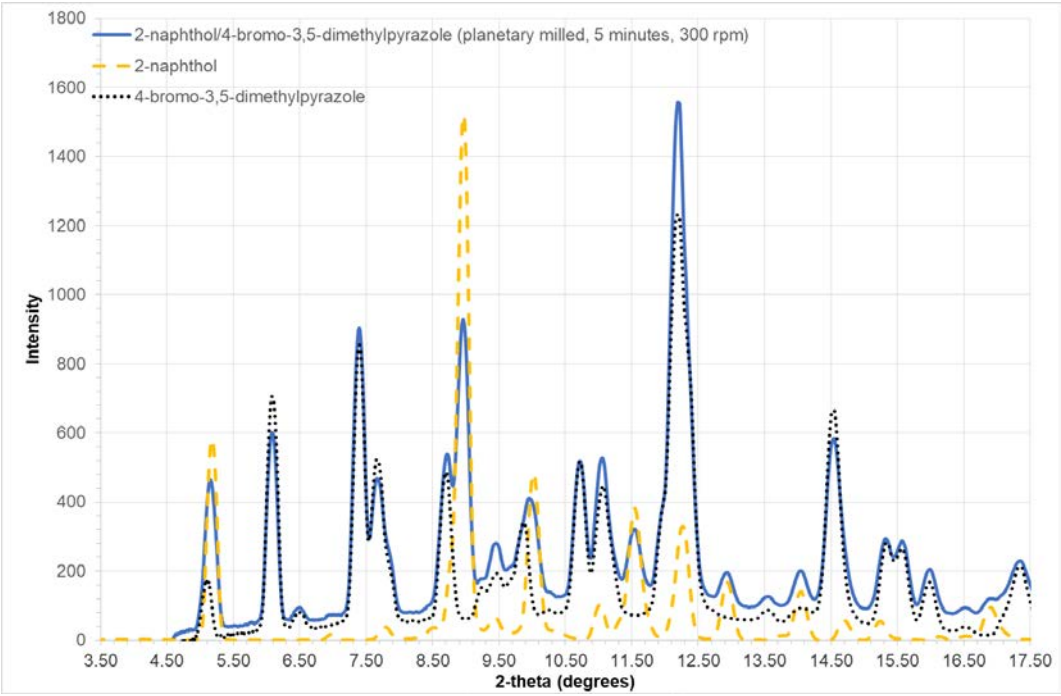

Figure B.49 – Powder x-ray pattern of 2-naphthol/4-bromo-3,5-dimethylpyrazole produced by planetary milling for 5 minutes at 300 rpm (λ = 0.7107 Å).

B.29 2-naphthol/imidazole

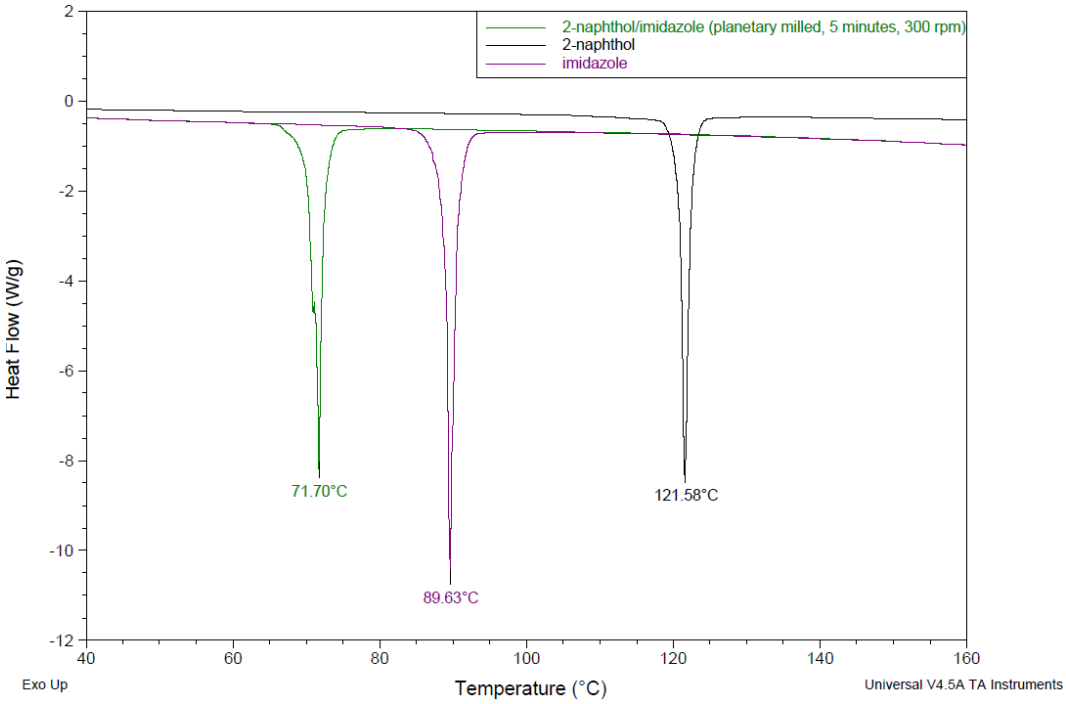

Figure B.50 - Thermal analysis of 2-naphthol/imidazole produced by planetary milling for 5 minutes at 300 rpm.

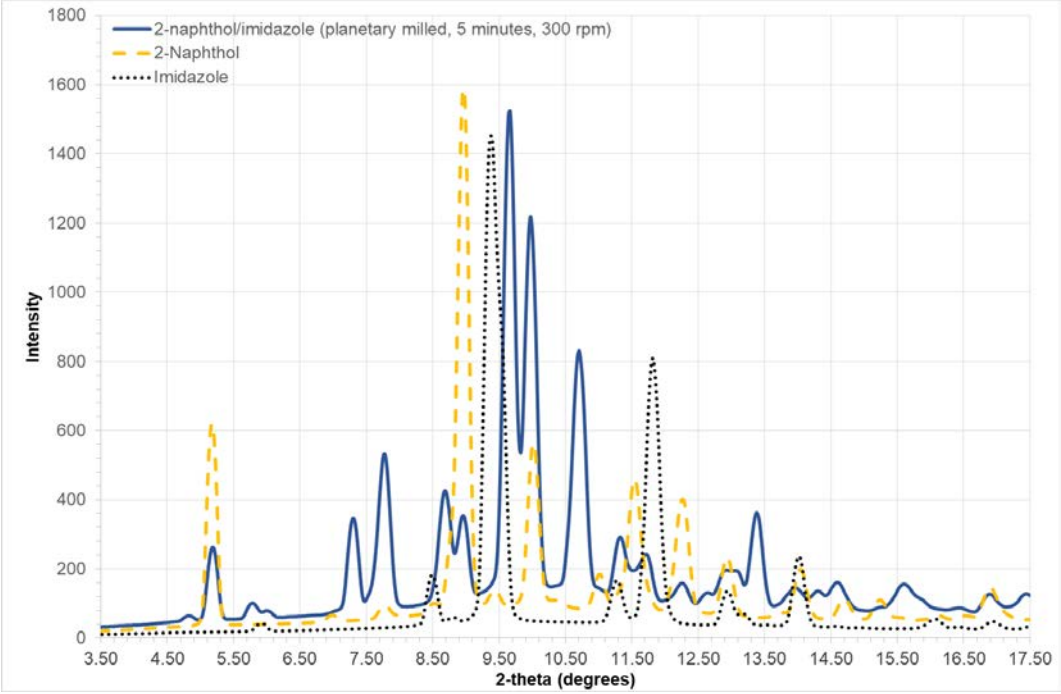

Figure B.51 – Powder x-ray pattern of 2-naphthol/imidazole produced by planetary milling for 5 minutes at 300 rpm (λ = 0.7107 Å).

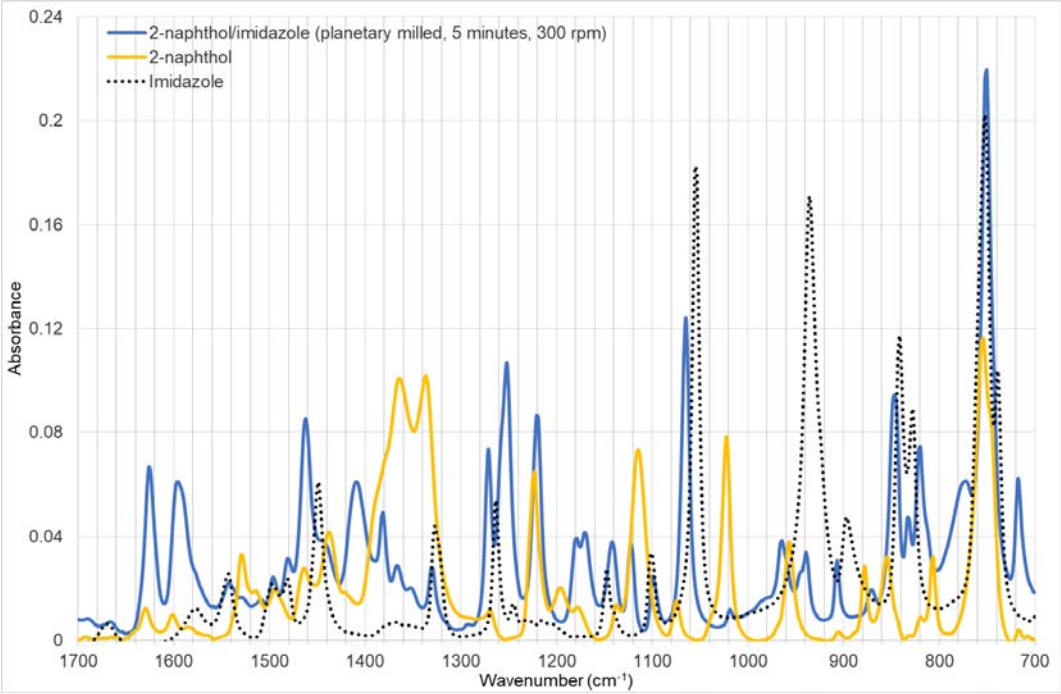

Figure B.52 – Infrared spectra of 2-naphthol/imidazole produced by planetary milling for 5 minutes at 300 rpm.

Table B.6 - Infrared spectra peak positions and heights of 2-naphthol/imidazole produced by planetary milling for 5 minutes at 300 rpm, with a 1:1 stoichiometry.

Peak Position (cm^{-1})	Peak Height (Absorbance)	Peak Position (cm^{-1})	Peak Height (Absorbance)
3221.88	0.04	1179.11	0.04
3137.85	0.03	1170.38	0.04
1625.54	0.07	1141.8	0.04
1595.77	0.06	1122.32	0.04
1542.37	0.02	1099.17	0.02
1496.2	0.02	1064.84	0.12
1480.69	0.03	964.58	0.04
1462.14	0.09	939.27	0.03
1409.17	0.06	906.72	0.03
1381.48	0.05	870.54	0.02
1366.73	0.03	846.81	0.09
1352.43	0.02	832.61	0.05
1330.28	0.03	820.39	0.08
1271.07	0.07	772.25	0.06
1252.02	0.11	750.87	0.22
1220.22	0.09	717.46	0.06

B.30 2-naphthol/2-nitroimidazole

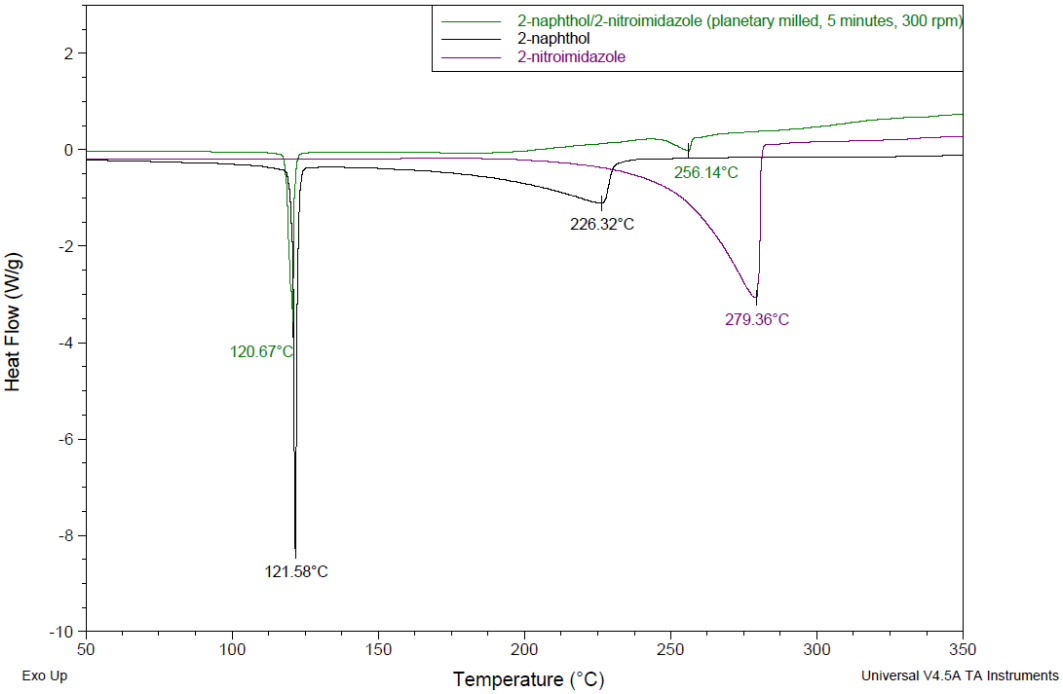

Figure B.53 - Thermal analysis of 2-naphthol/2-nitroimidazole produced by planetary milling for 5 minutes at 300 rpm.

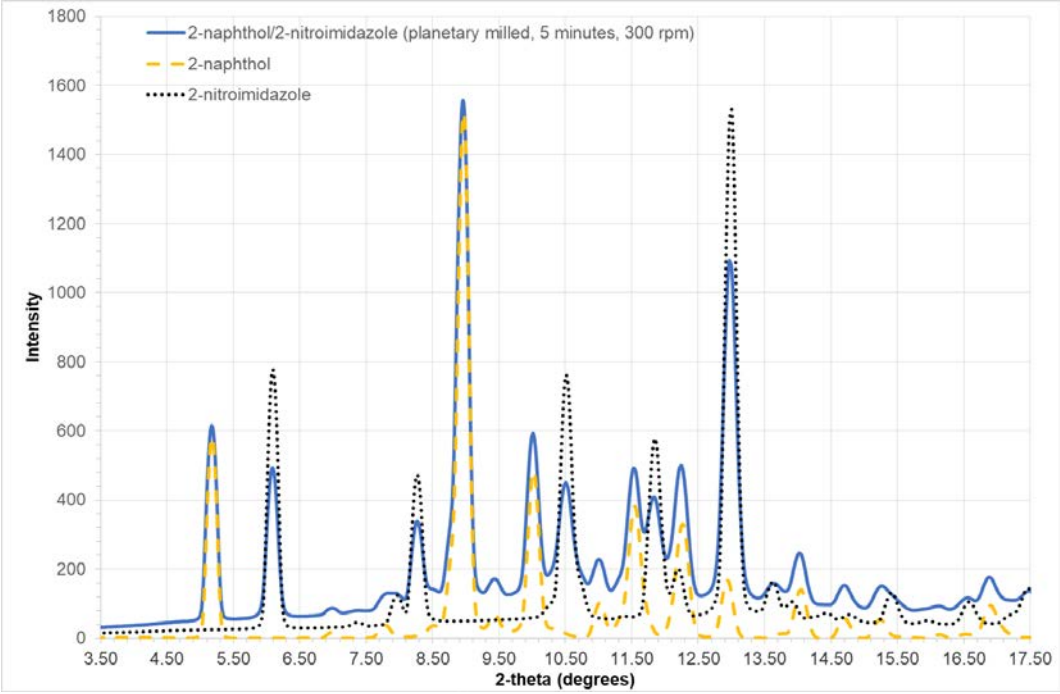

Figure B.54 – Powder x-ray pattern of 2-naphthol/2-nitroimidazole produced by planetary milling for 5 minutes at 300 rpm (λ = 0.7107 Å).

B.31 2-naphthol/2-methylimidazole

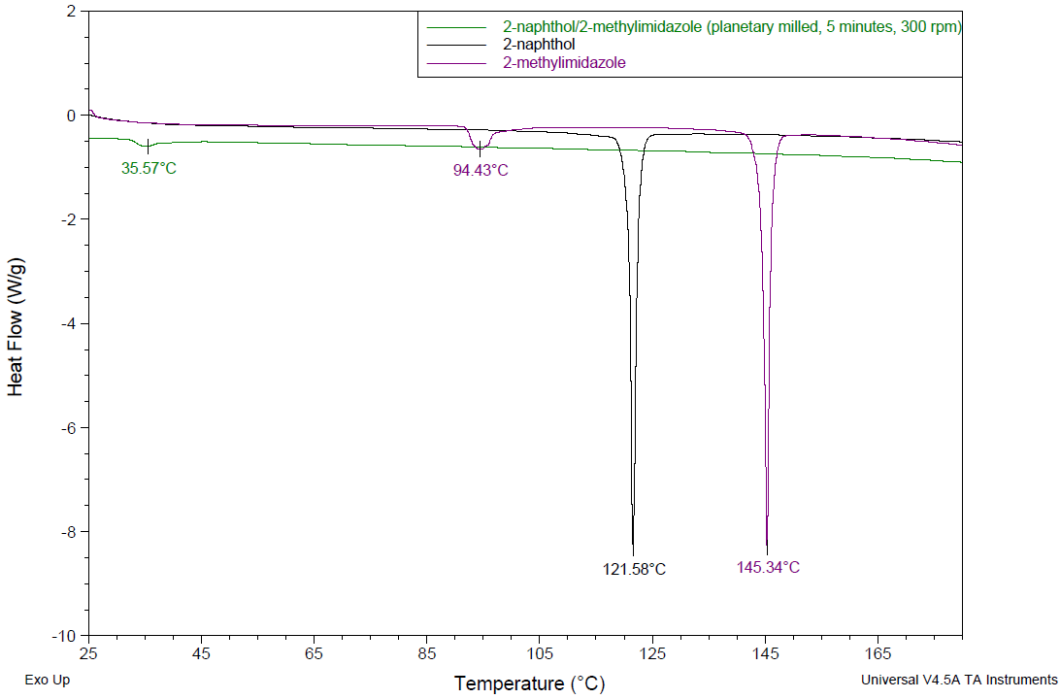

Figure B.55 - Thermal analysis of 2-naphthol/2-methylimidazole produced by planetary milling for 5 minutes at 300 rpm.

B.32 2-naphthol/4-methylimidazole

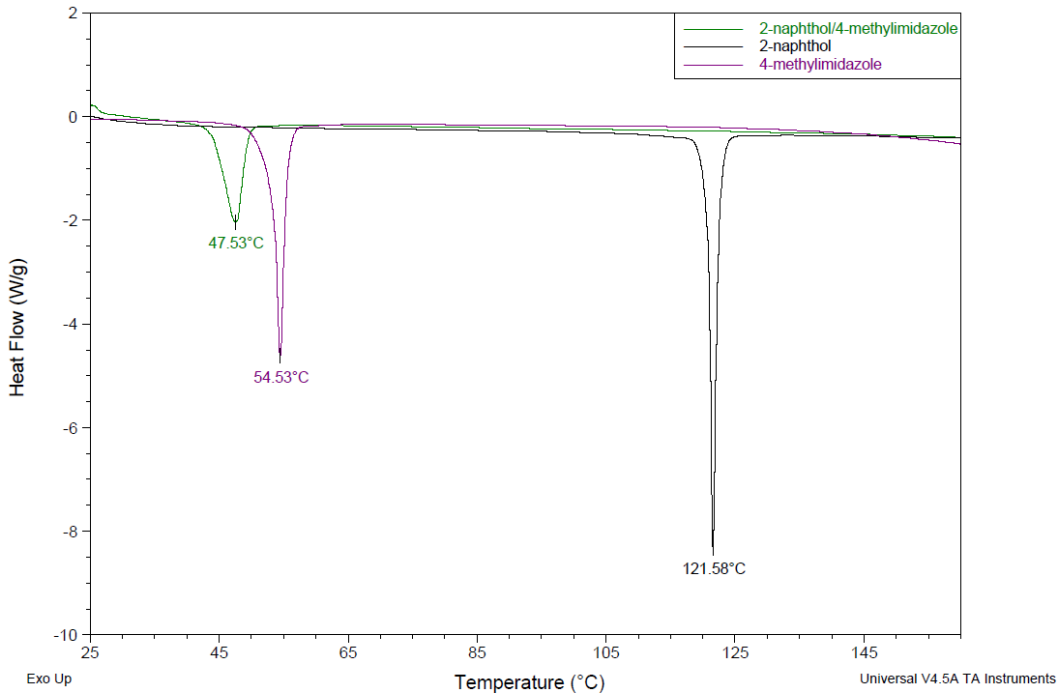

Figure B.56 - Thermal analysis of 2-naphthol/4-methylimidazole produced by planetary milling for 5 minutes at 300 rpm.

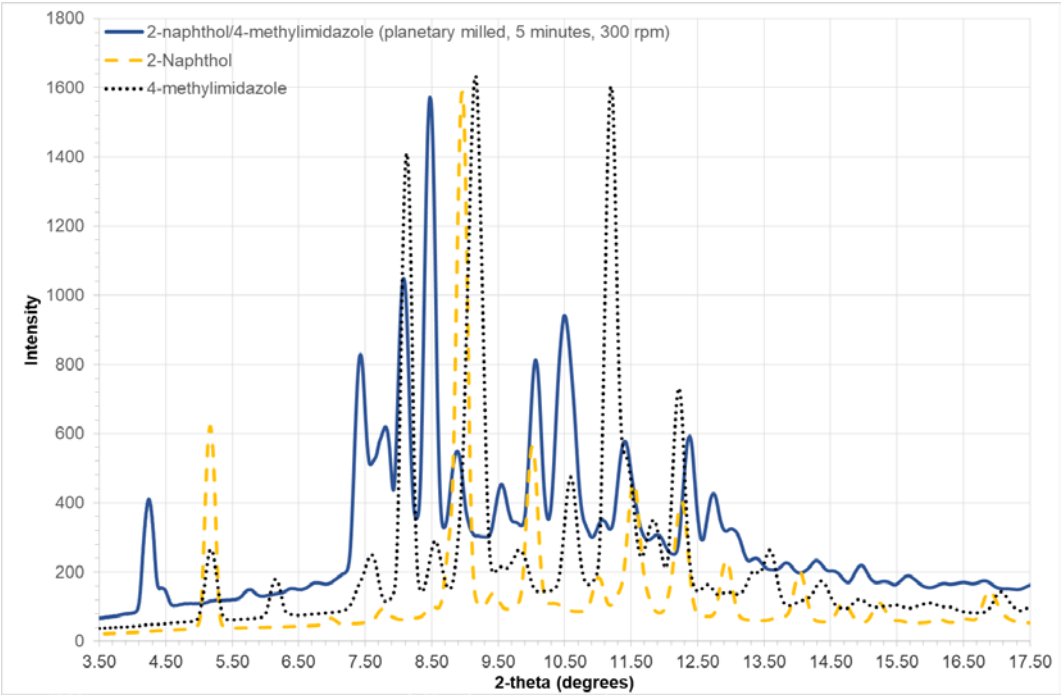

Figure B.57 – Powder x-ray pattern of 2-naphthol/4-methylimidazole produced by planetary milling for 5 minutes at 300 rpm (λ = 0.7107 Å).

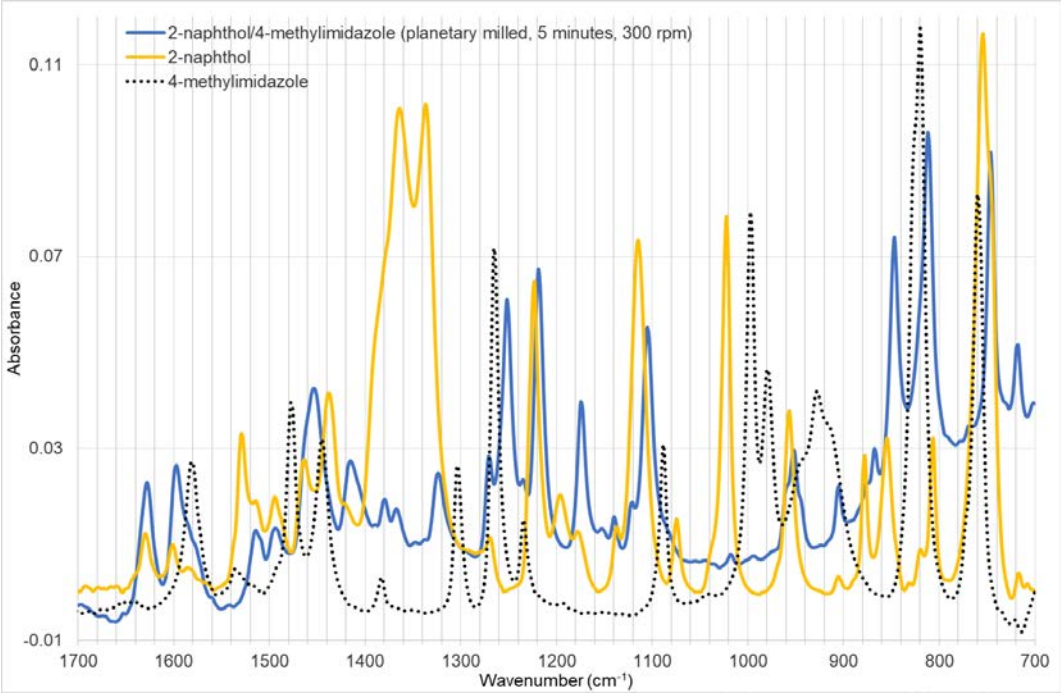

Figure B.58 – Infrared spectra of 2-naphthol/4-methylimidazole produced by planetary milling for 5 minutes at 300 rpm.

Table B.7 - Infrared spectra peak positions and heights of 2-naphthol/4-methylimidazole produced by planetary milling for 5 minutes at 300 rpm, with a 1:1 stoichiometry.

Peak Position (cm^{-1})	Peak Height (Absorbance)	Peak Position (cm^{-1})	Peak Height (Absorbance)
1627.94	0.02	1152.91	0.01
1597.27	0.03	1139.75	0.02
1514.18	0.01	1120.9	0.02
1493.59	0.01	1104.92	0.06
1453.65	0.04	952.31	0.03
1415.38	0.03	904.98	0.02
1389.27	0.01	875.23	0.02
1379.47	0.02	867.6	0.03
1367.43	0.02	846.89	0.07
1336.65	0.01	811.78	0.1
1323.58	0.02	776.83	0.03
1270.56	0.03	767.84	0.03
1251.63	0.06	746.28	0.09
1234.97	0.02	718.08	0.05
1218.76	0.07	701.56	0.04
1174.2	0.04		

B.33 2-naphthol/imidazol-2-amine

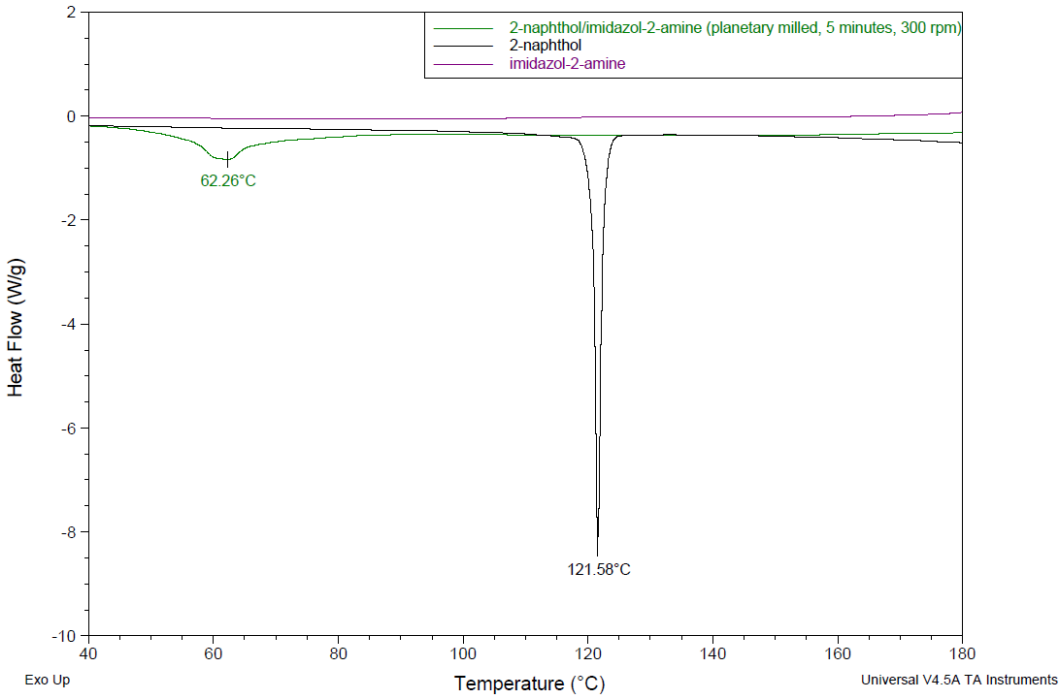

Figure B.59 - Thermal analysis of 2-naphthol/imidazol-2-amine produced by planetary milling for 5 minutes at 300 rpm. Imidazol-2-amine is a liquid and did not display a melt.

B.34 2-naphthol/2-bromoimidazole

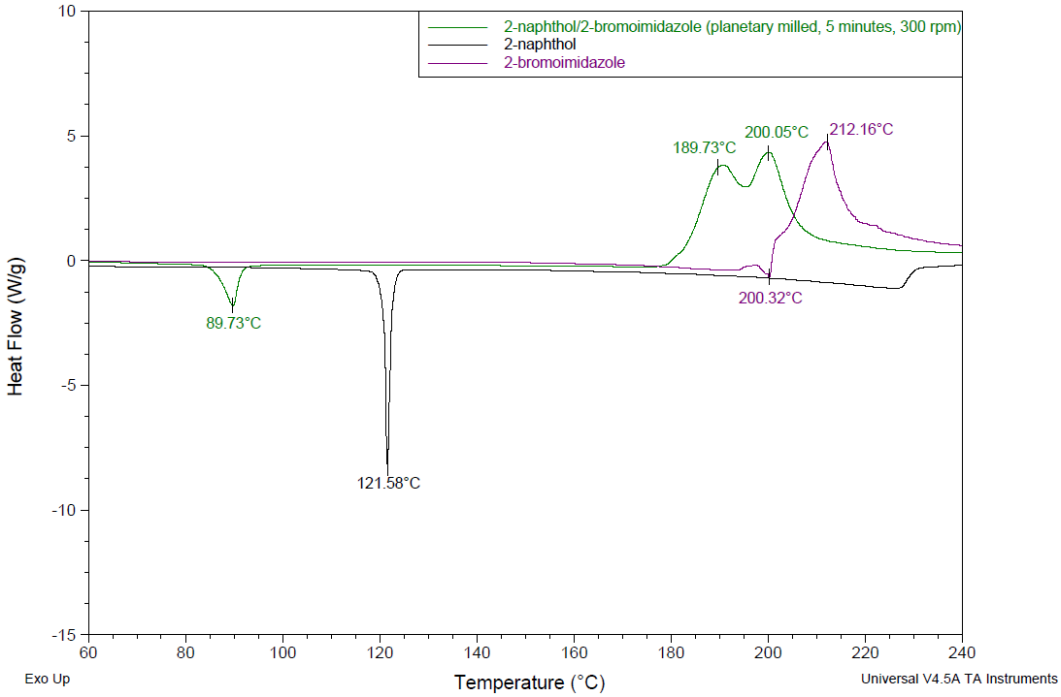

Figure B.60 - Thermal analysis of 2-naphthol/2-bromoimidazole produced by planetary milling for 5 minutes at 300 rpm.

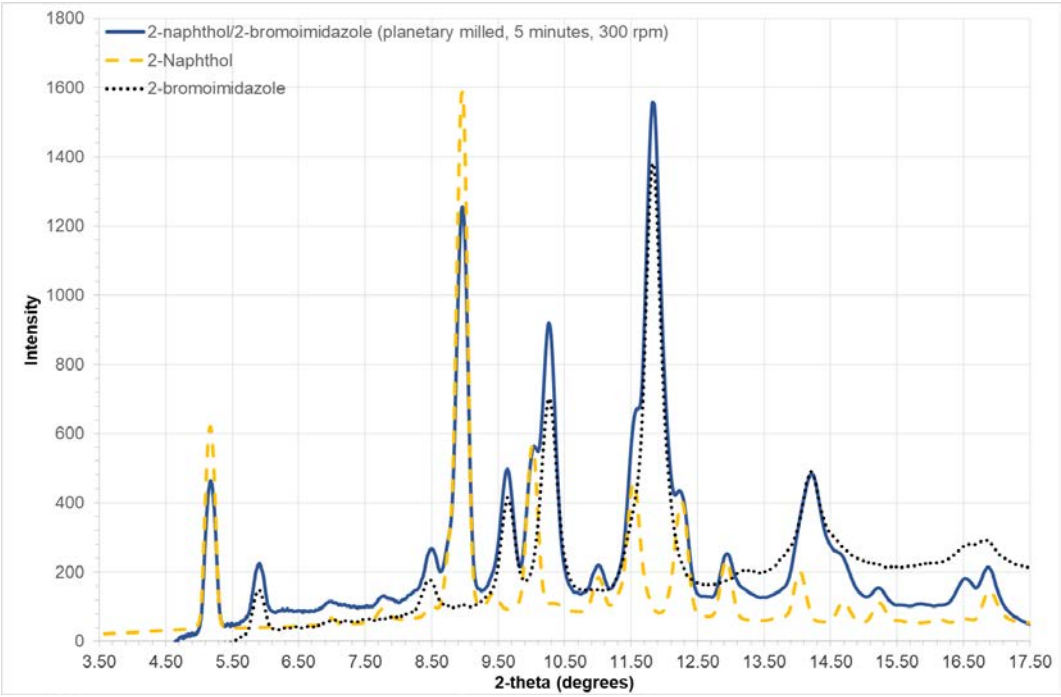

Figure B.61 – Powder x-ray pattern of 2-naphthol/2-bromoimidazole produced by planetary milling for 5 minutes at 300 rpm (λ = 0.7107 Å).

B.35 2-naphthol/4-bromoimidazole

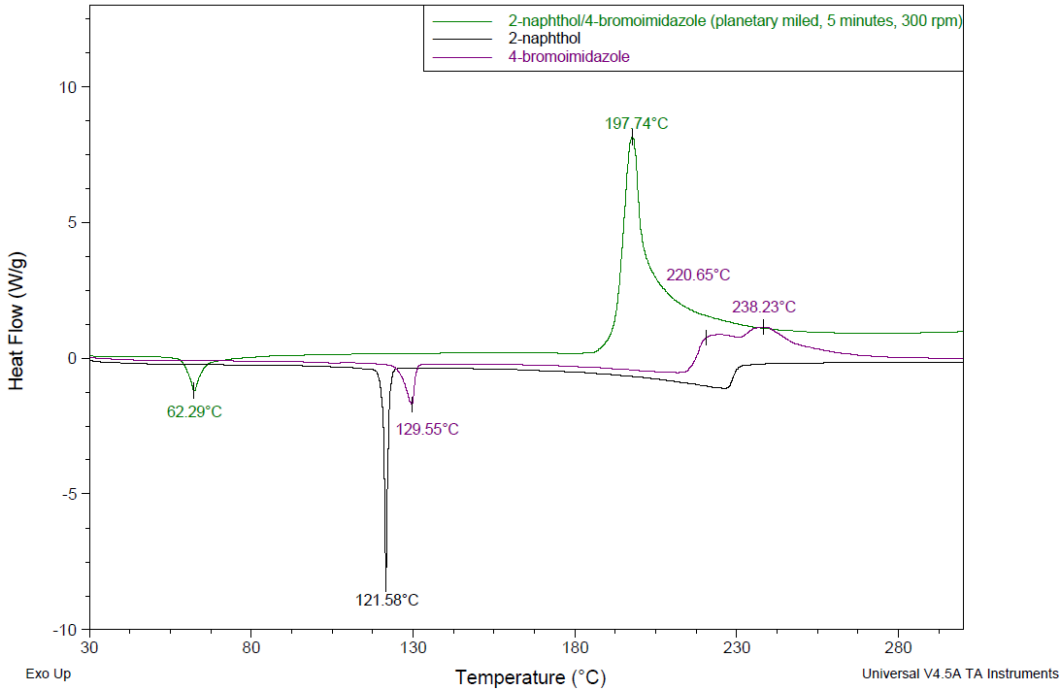

Figure B.62 - Thermal analysis of 2-naphthol/4-bromoimidazole produced by planetary milling for 5 minutes at 300 rpm.

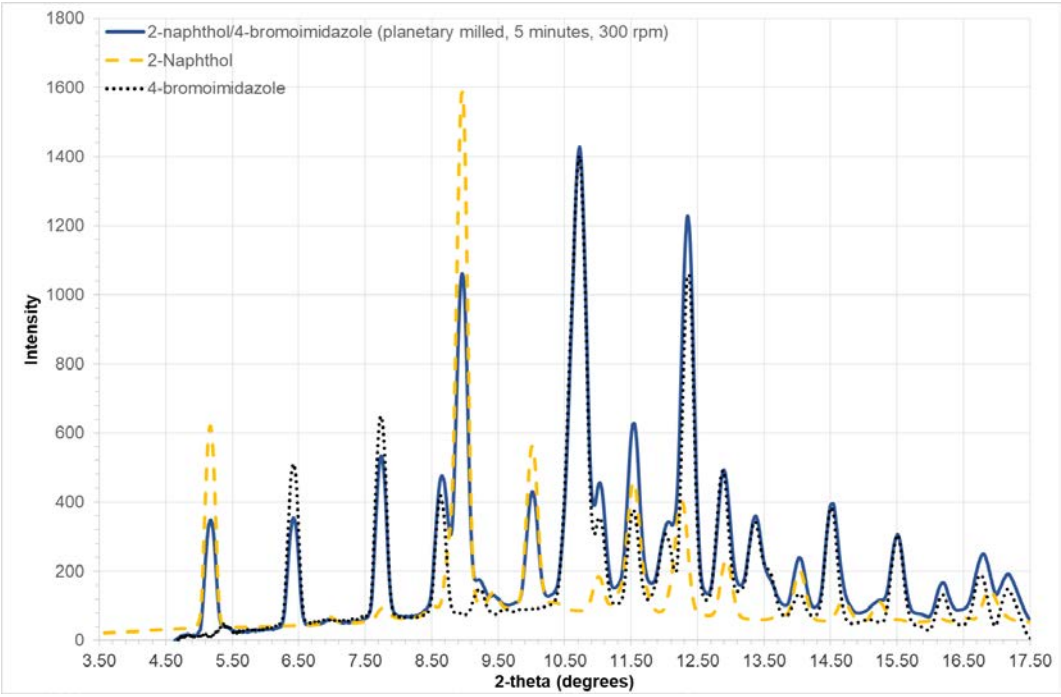

Figure B.63 – Powder x-ray pattern of 2-naphthol/4-bromoimidazole produced by planetary milling for 5 minutes at 300 rpm (λ = 0.7107 Å).

B.36 2-naphthol/2,4-dimethylimidazole

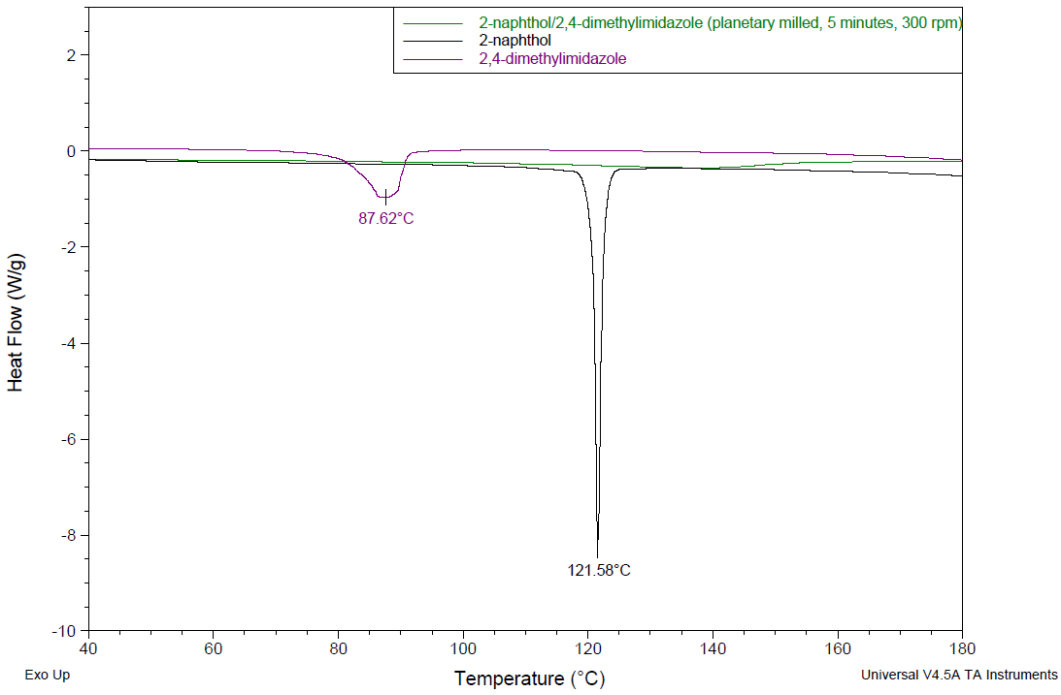

Figure B.64 - Thermal analysis of 2-naphthol/2,4-dimethylimidazole produced by planetary milling for 5 minutes at 300 rpm. The mixed system is a liquid and did not display a melt.

B.37 2-naphthol/4,5-dinitroimidazole

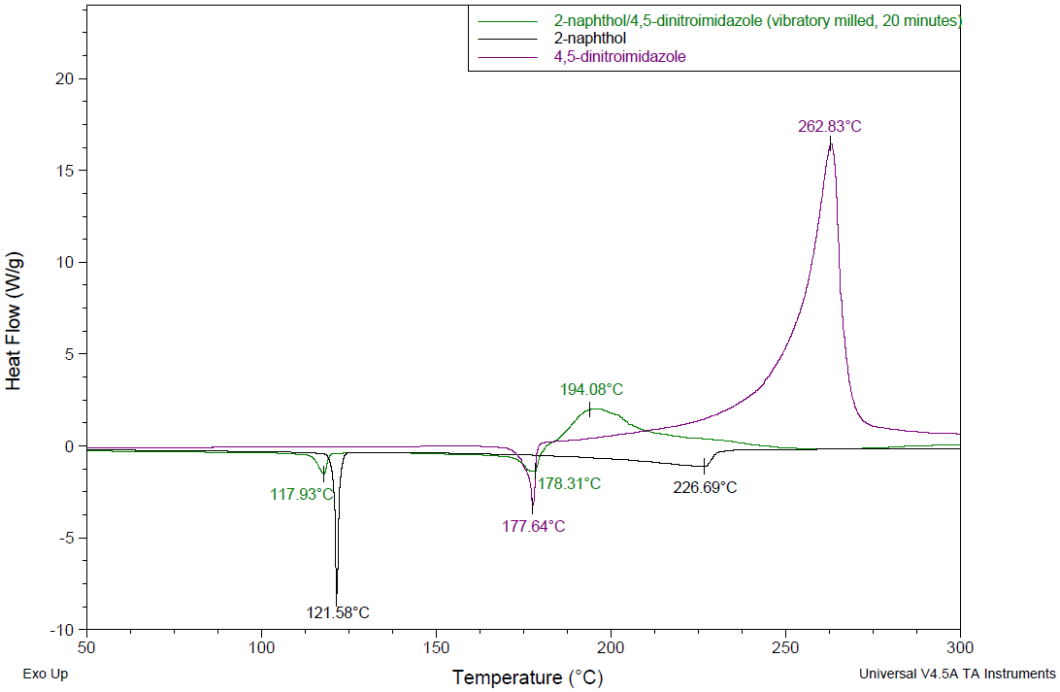

Figure B.65 - Thermal analysis of 2-naphthol/4,5-dinitrolimidazole produced by vibratory milling for 20 minutes.

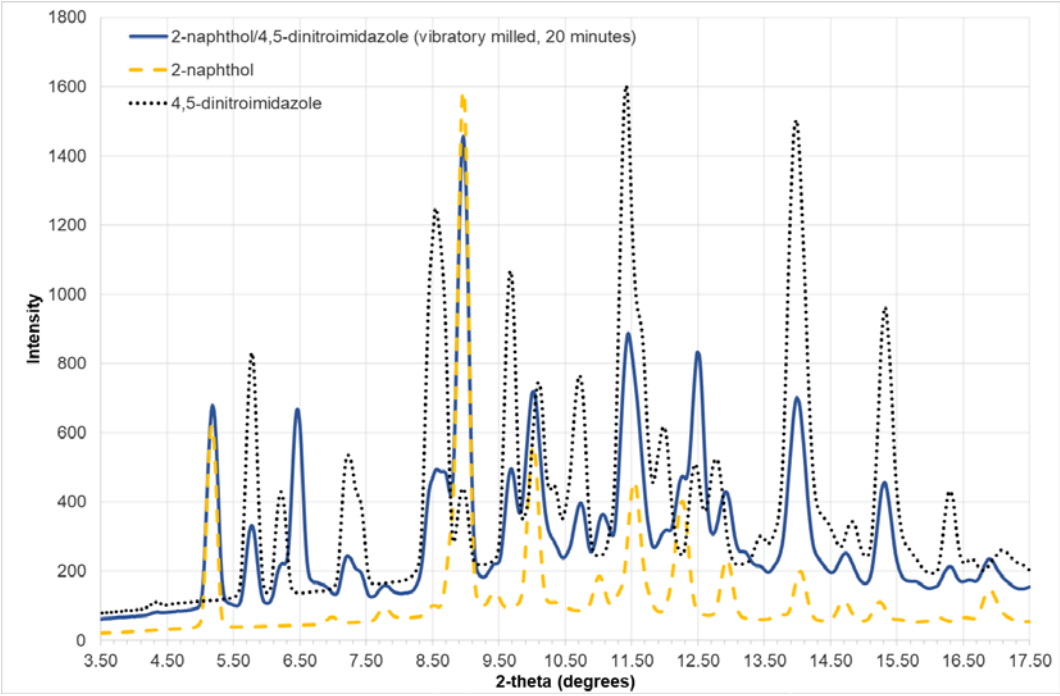

Figure B.66 – Powder x-ray pattern of 2-naphthol/4,5-dinitrolimidazole produced by vibratory milling for 20 minutes (λ = 0.7107 Å).

B.38 2-naphthol/4,5-dichlororimidazole

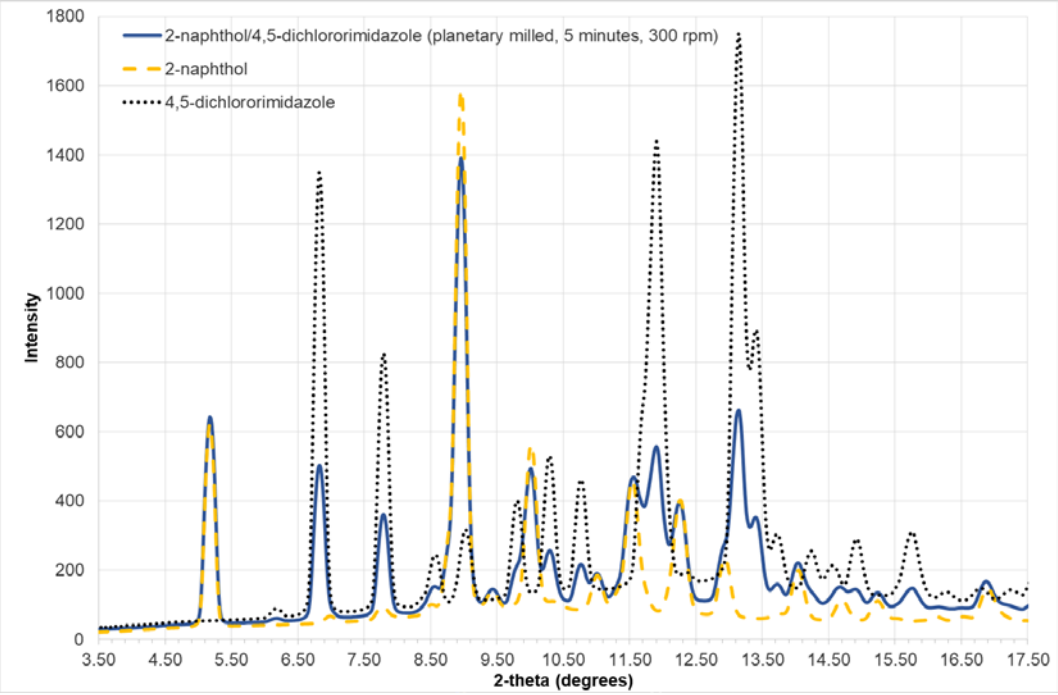

Figure B.67 - Powder x-ray pattern of 2-naphthol/4,5-dichlorolimidazole produced by planetary milling for 5 minutes at 300 rpm (λ = 0.7107 Å).

B.39 2-naphthol/2,4,5-tribromoimidazole

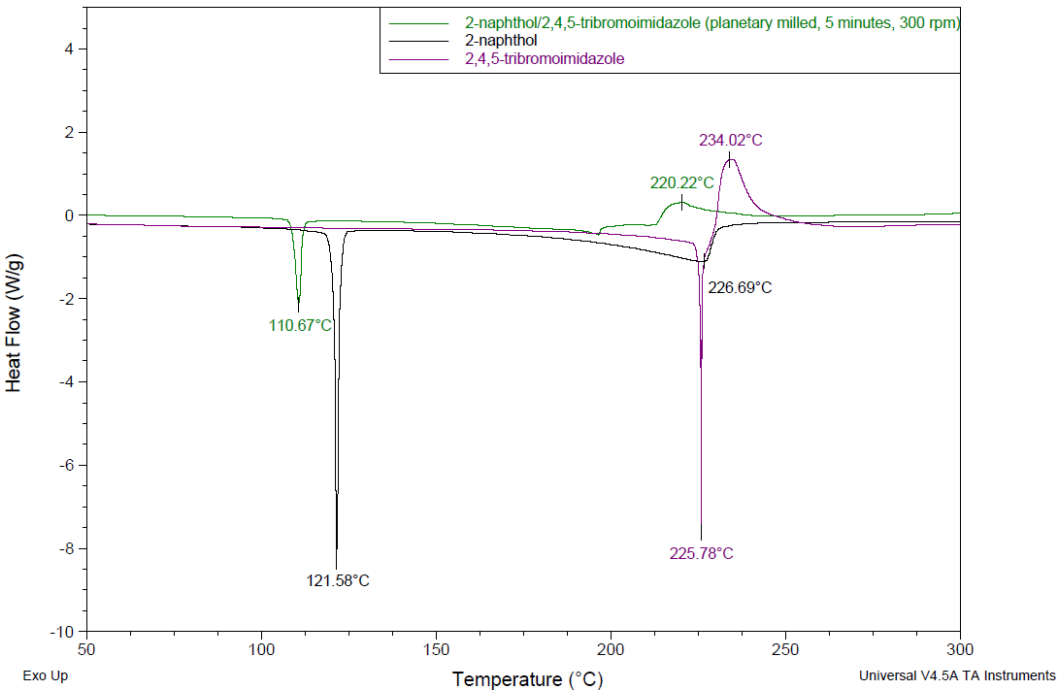

Figure B.68 – Thermal analysis of 2-naphthol/2,4,5-tribromolimidazole produced by planetary milling for 5 minutes at 300 rpm.

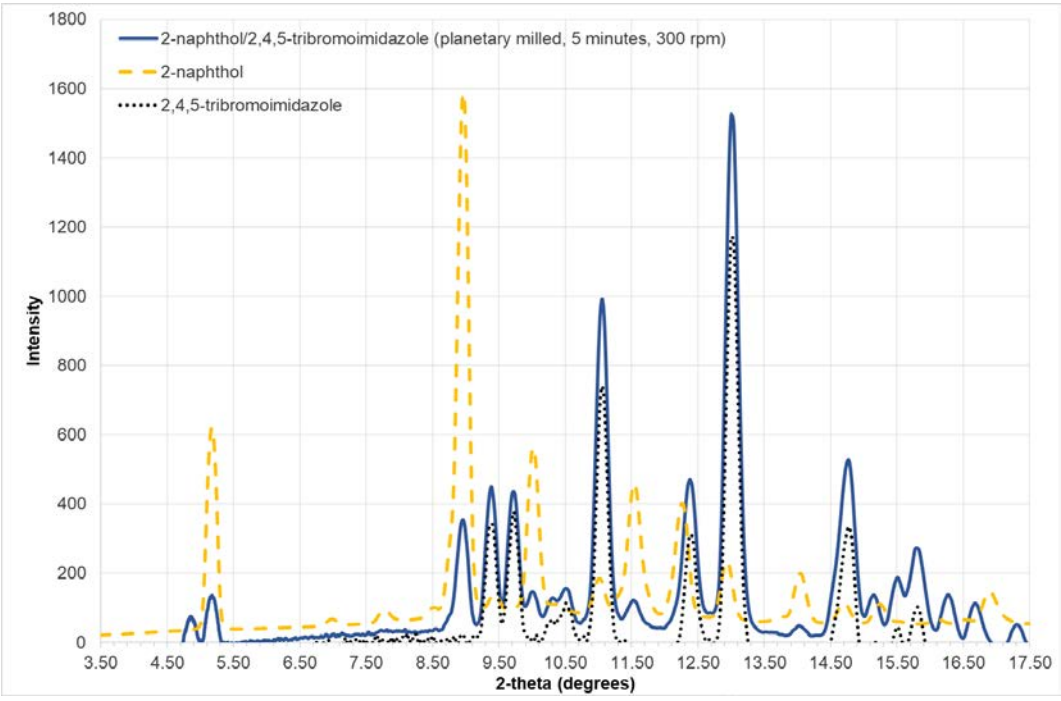

Figure B.69 - Powder x-ray pattern of 2-naphthol/2,4,5-tribromolimidazole produced by planetary milling for 5 minutes at 300 rpm (λ = 0.7107 Å).

B.40 2-naphthol/2-methyl-5-nitroimidazole

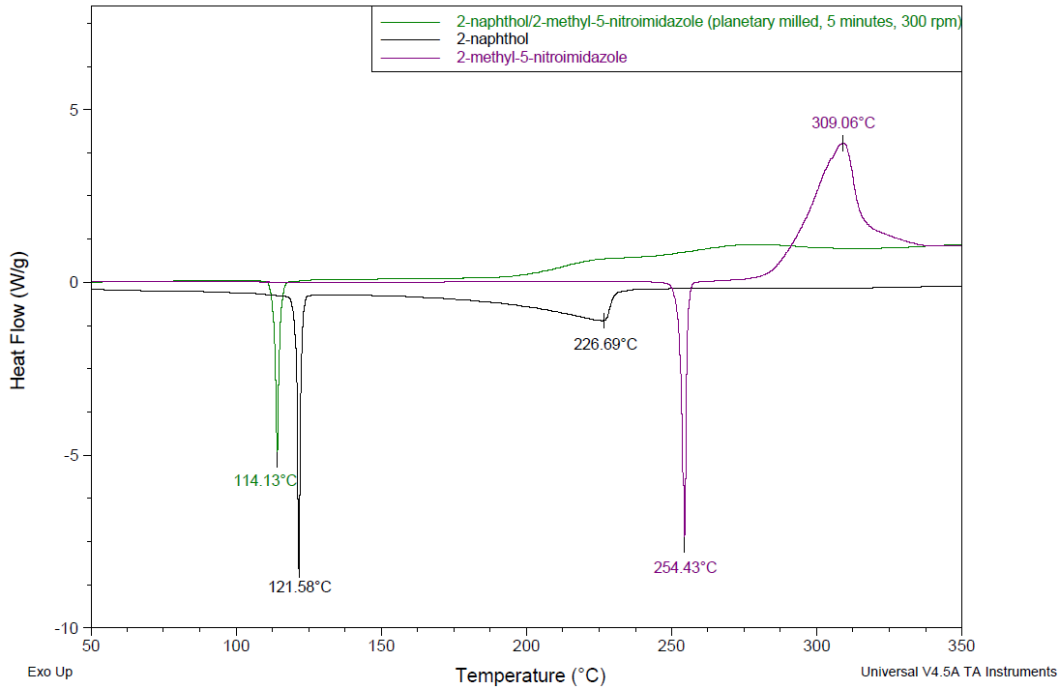

Figure B.70 - Thermal analysis of 2-naphthol/2-methyl-5-nitroimidazole produced by planetary milling for 5 minutes at 300 rpm.

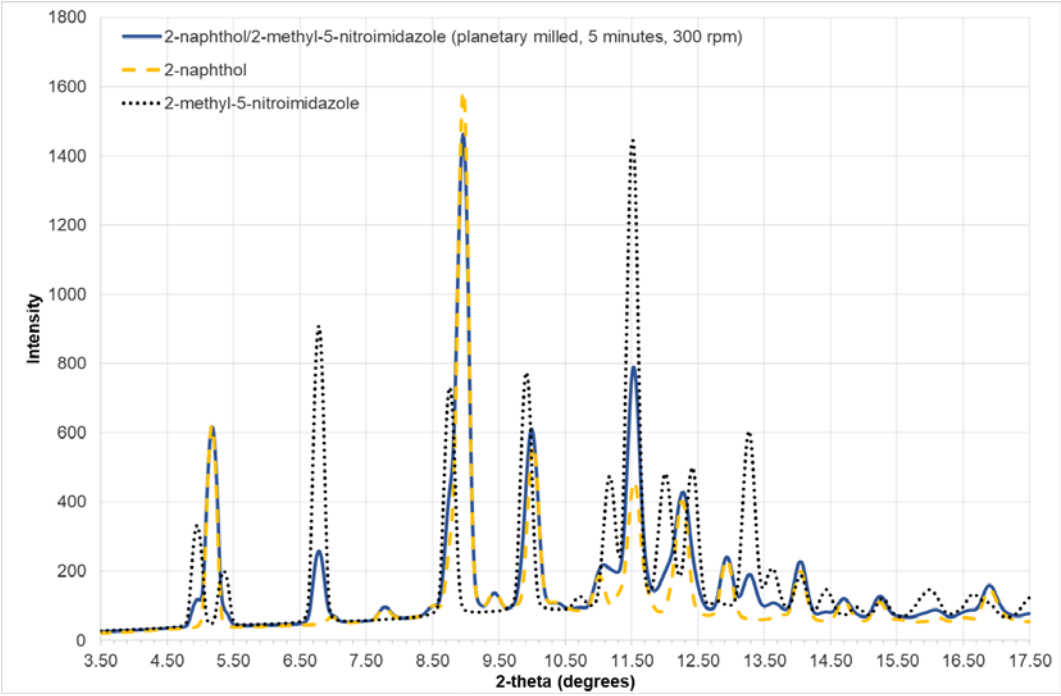

Figure B.71 – Powder x-ray pattern of 2-naphthol/2-methyl-5-nitroimidazole produced by planetary milling for 5 minutes at 300 rpm (λ = 0.7107 Å).

B.41 2-naphthol/4-methyl-5-nitroimidazole

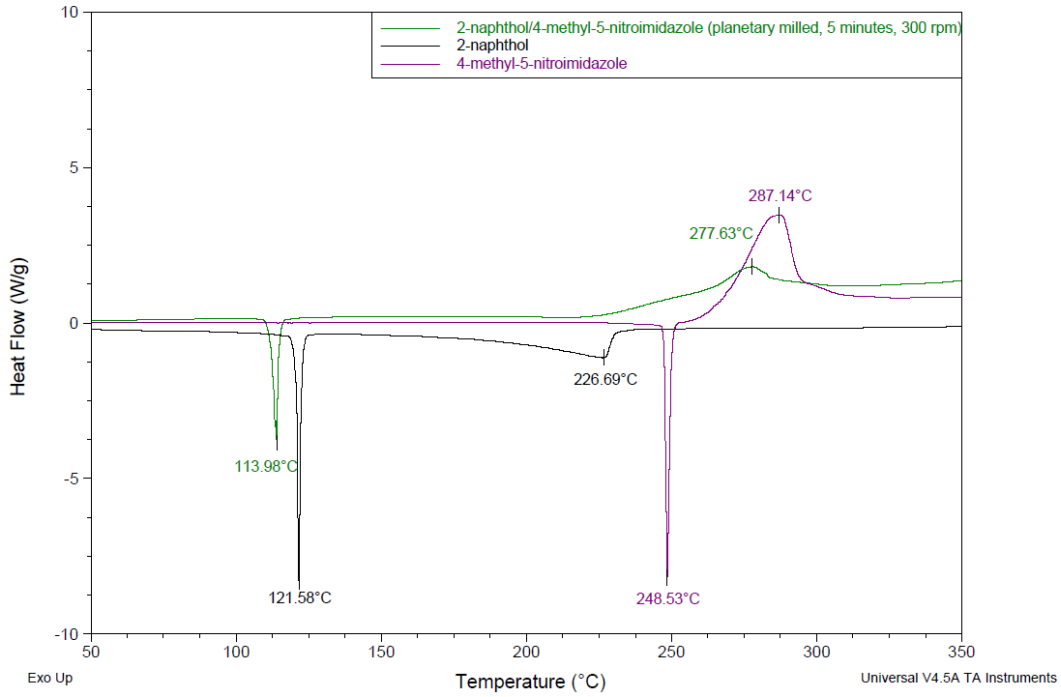

Figure B.72 - Thermal analysis of 2-naphthol/4-methyl-5-nitroimidazole produced by planetary milling for 5 minutes at 300 rpm.

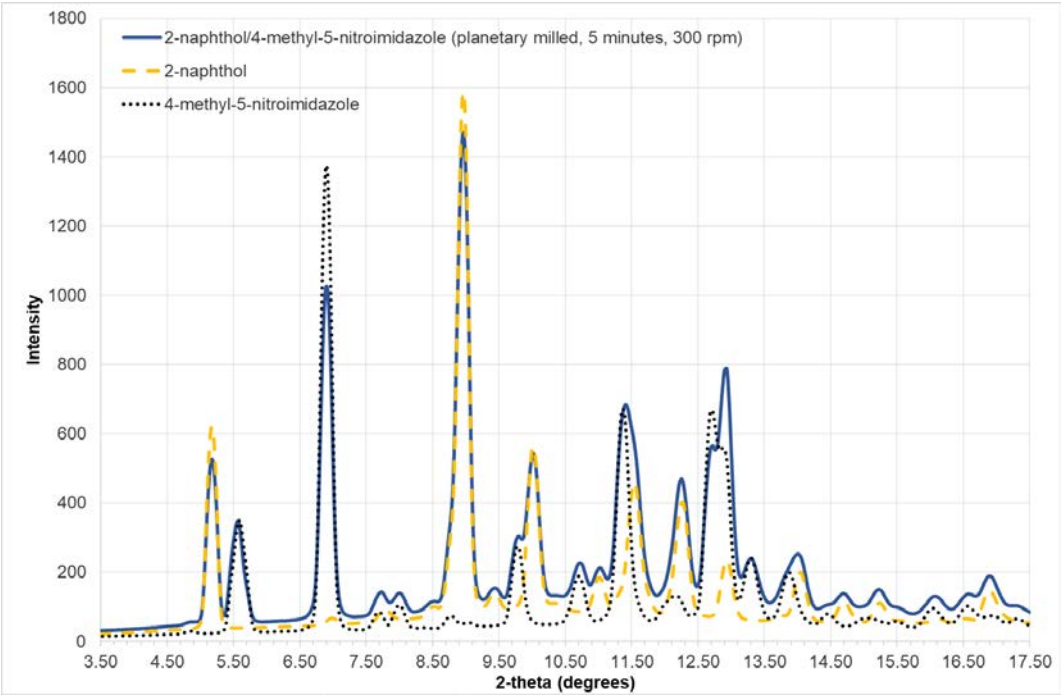

Figure B.73 – Powder x-ray pattern of 2-naphthol/4-methyl-5-nitroimidazole produced by planetary milling for 5 minutes at 300 rpm (λ = 0.7107 Å).

B.42 2-naphthol/2-bromo-5-nitroimidazole

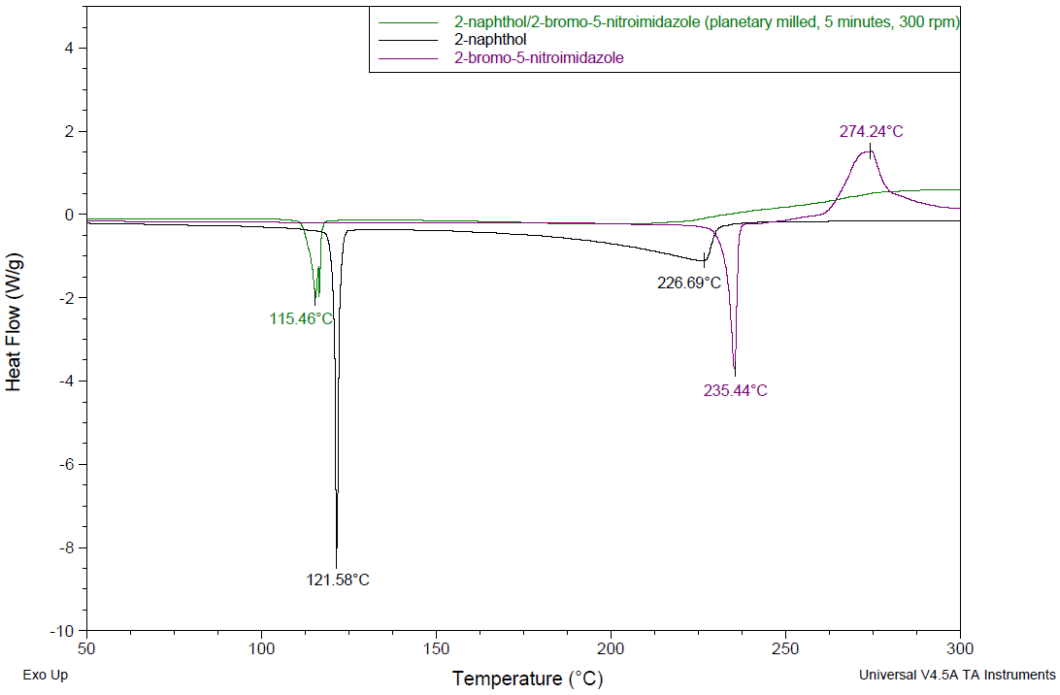

Figure B.74 - Thermal analysis of 2-naphthol/2-bromo-5-nitroimidazole produced by planetary milling for 5 minutes at 300 rpm.

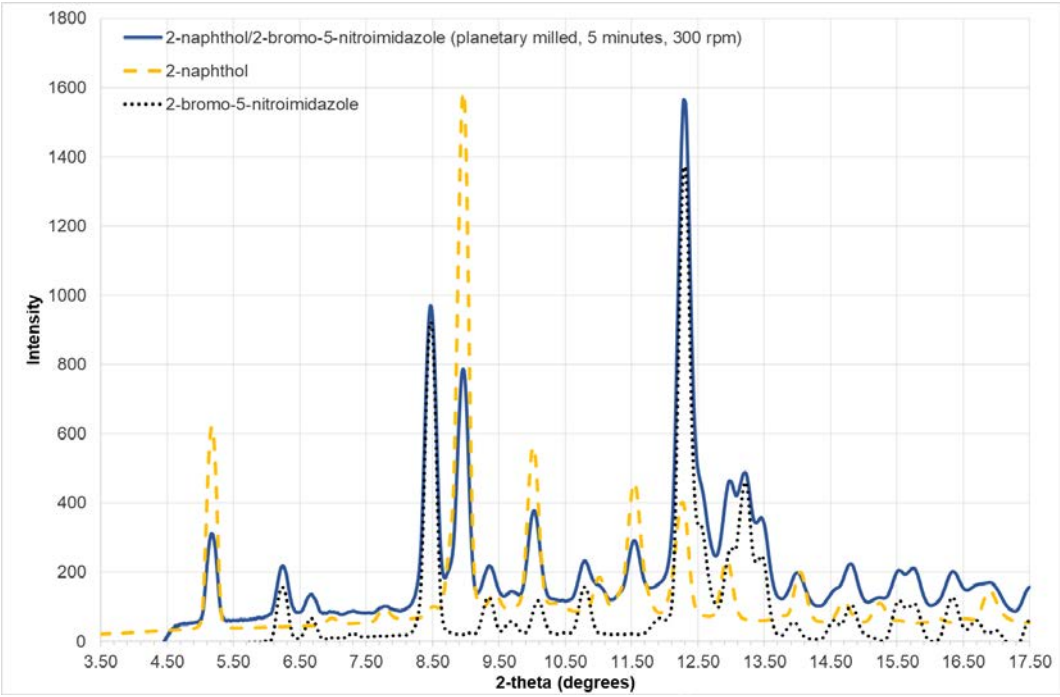

Figure B.75 – Powder x-ray pattern of 2-naphthol/2-bromo-5-nitroimidazole produced by planetary milling for 5 minutes at 300 rpm (λ = 0.7107 Å).

B.43 2-naphthol/4-bromo-2-methylimidazole

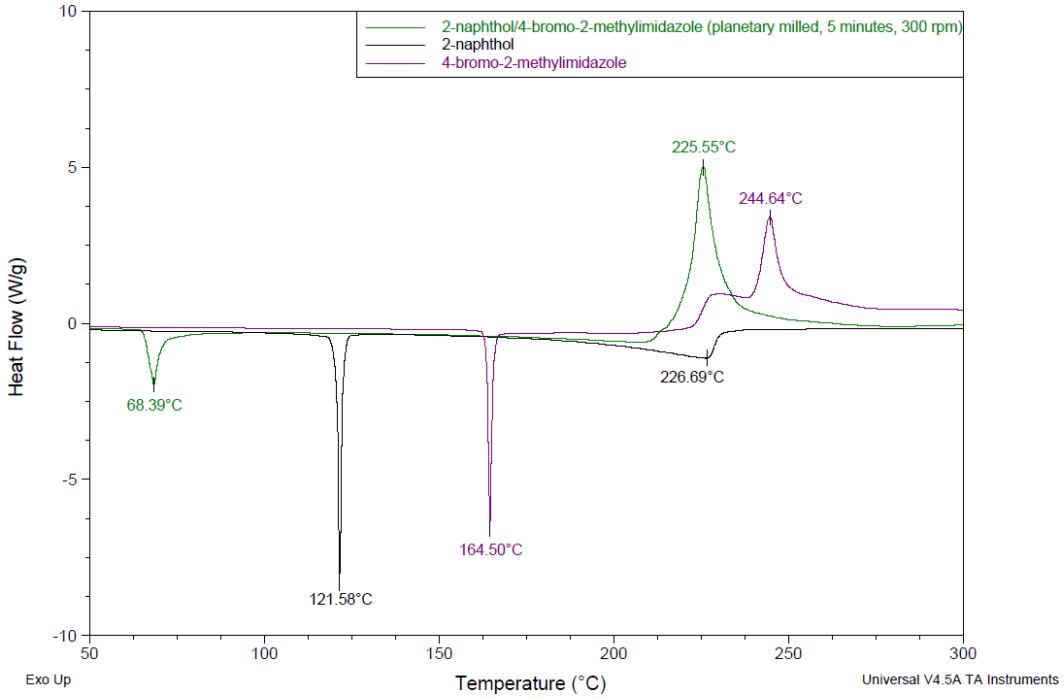

Figure B.76 – Thermal analysis of 2-naphthol/4-bromo-2-methylimidazole produced by planetary milling for 5 minutes at 300 rpm.

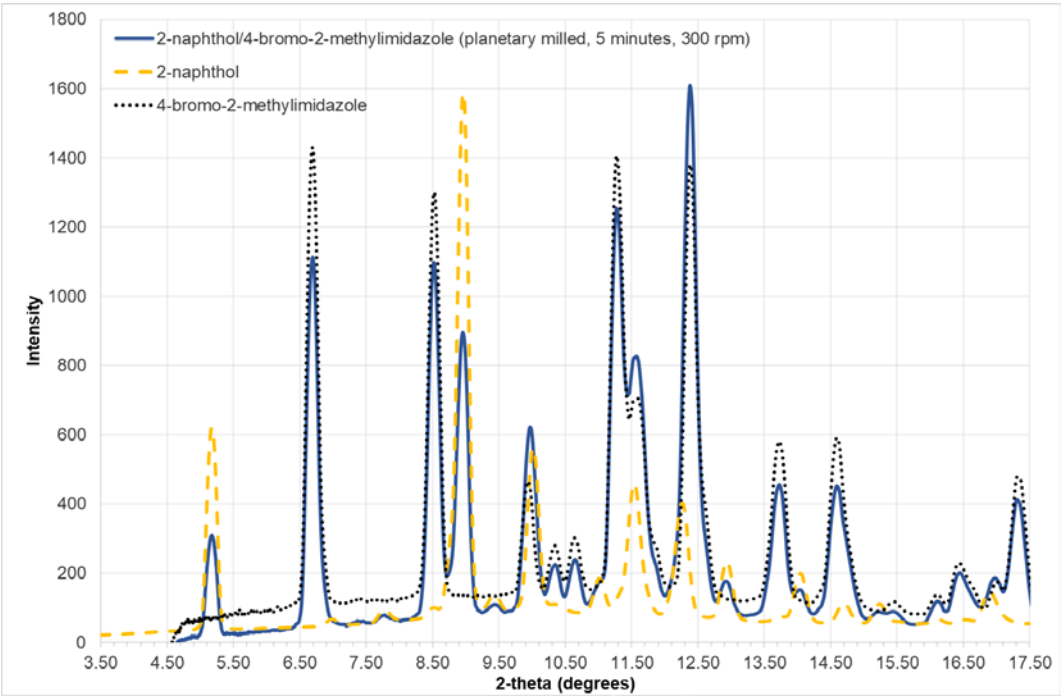

Figure B.77 - Powder x-ray pattern of 2-naphthol/4-bromo-2-methylimidazole produced by planetary milling for 5 minutes at 300 rpm (λ = 0.7107 Å).

B.44 2-naphthol/5-bromo-4-methylimidazole

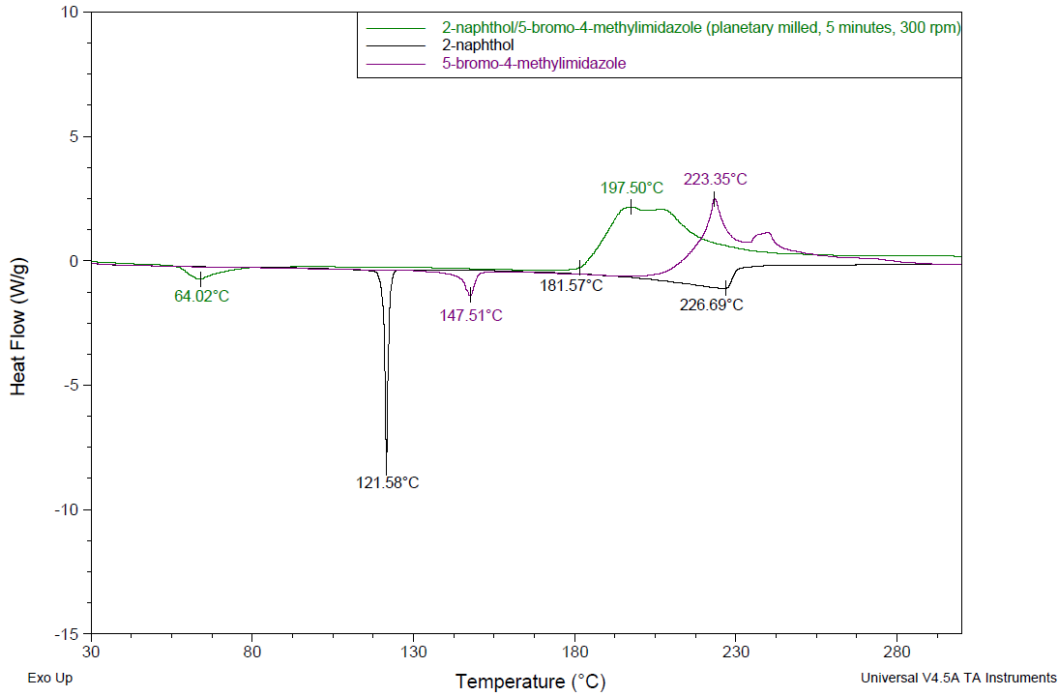

Figure B.78 - Thermal analysis of 2-naphthol/5-bromo-4-methylimidazole produced by planetary milling for 5 minutes at 300 rpm.

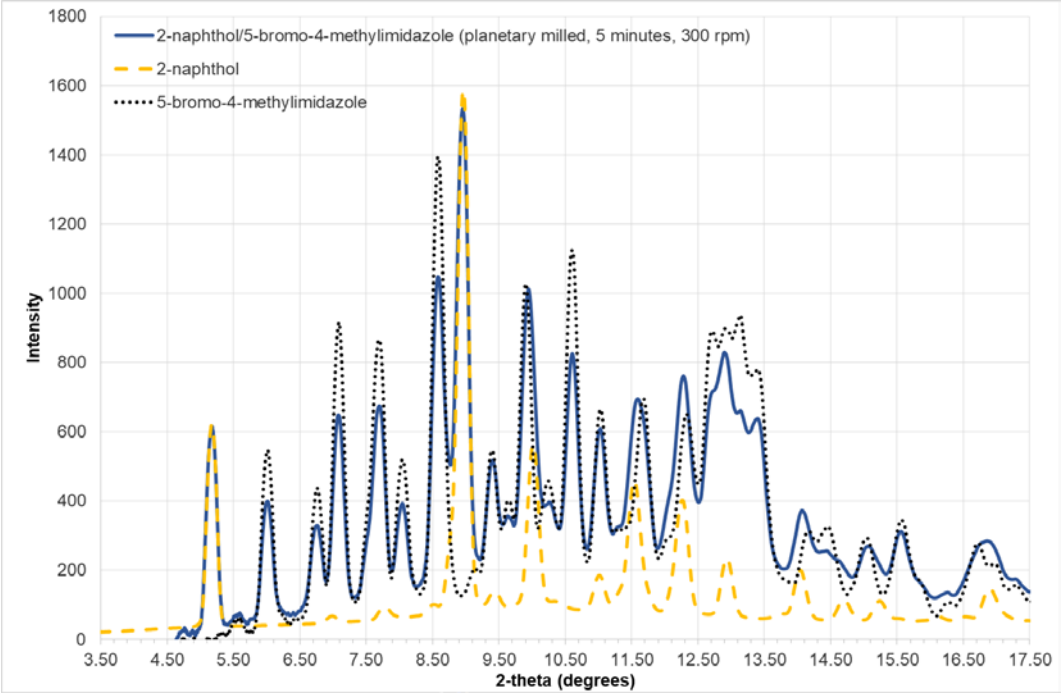

Figure B.79 – Powder x-ray pattern of 2-naphthol/5-bromo-4-methylimidazole produced by planetary milling for 5 minutes at 300 rpm (λ = 0.7107 Å).

B.45 2-naphthol/4,5-dibromo-2-methylimidazole

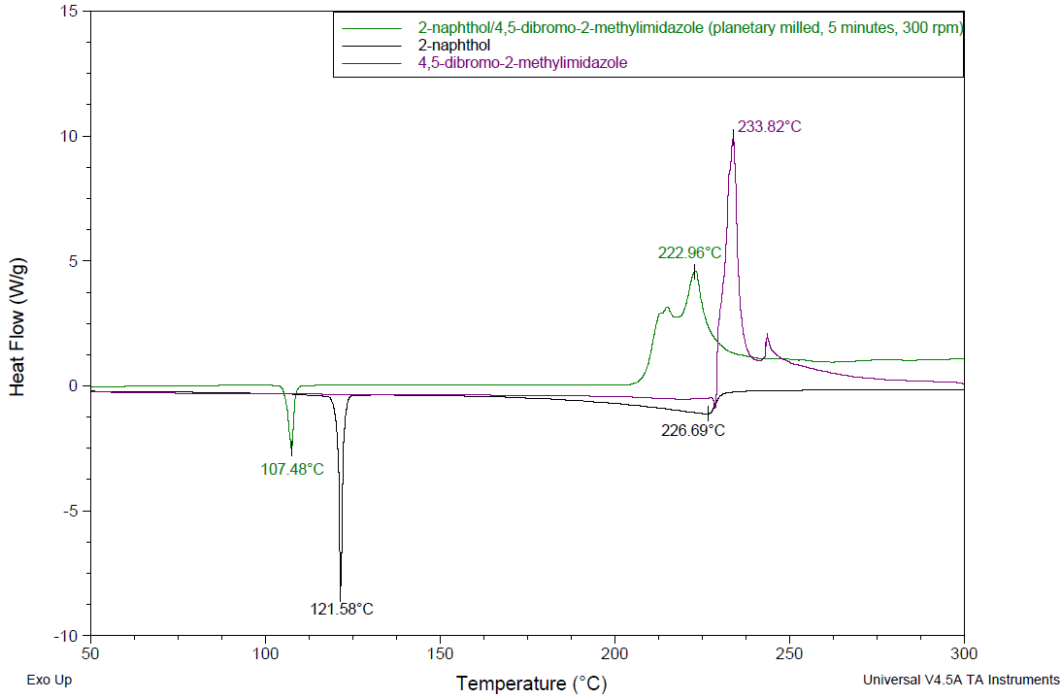

Figure B.80 - Thermal analysis of 2-naphthol/4,5-dibromo-2-methylimidazole produced by planetary milling for 5 minutes at 300 rpm.

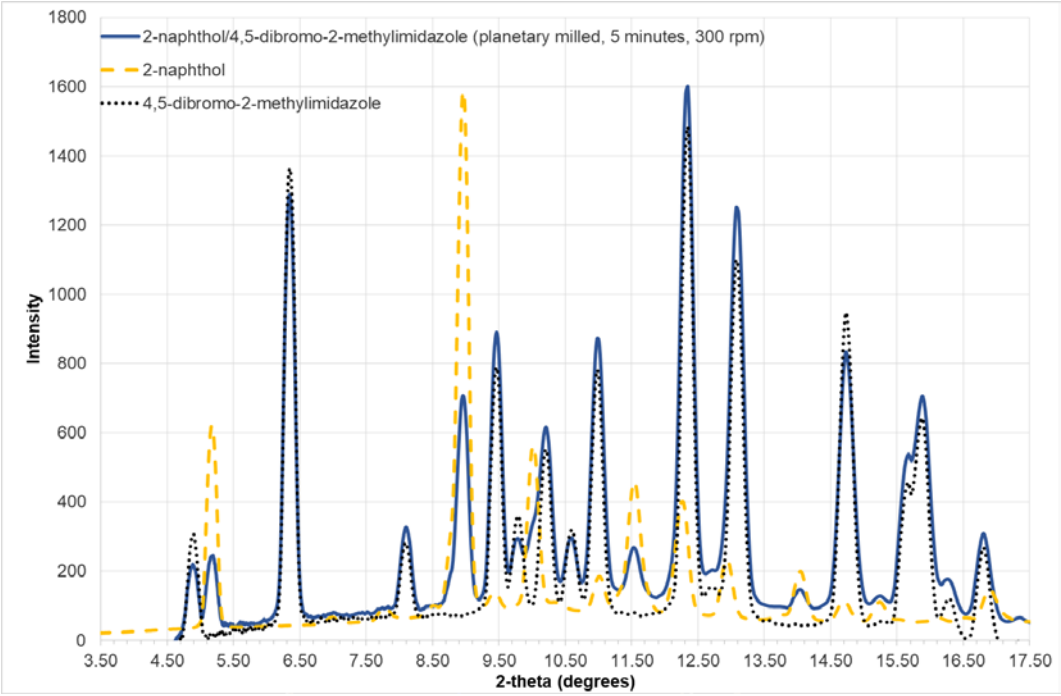

Figure B.81 – Powder x-ray pattern of 2-naphthol/4,5-dibromo-2-methylimidazole produced by planetary milling for 5 minutes at 300 rpm (λ = 0.7107 Å).

B.46 2-naphthol/2,5-dibromo-4-methylimidazole

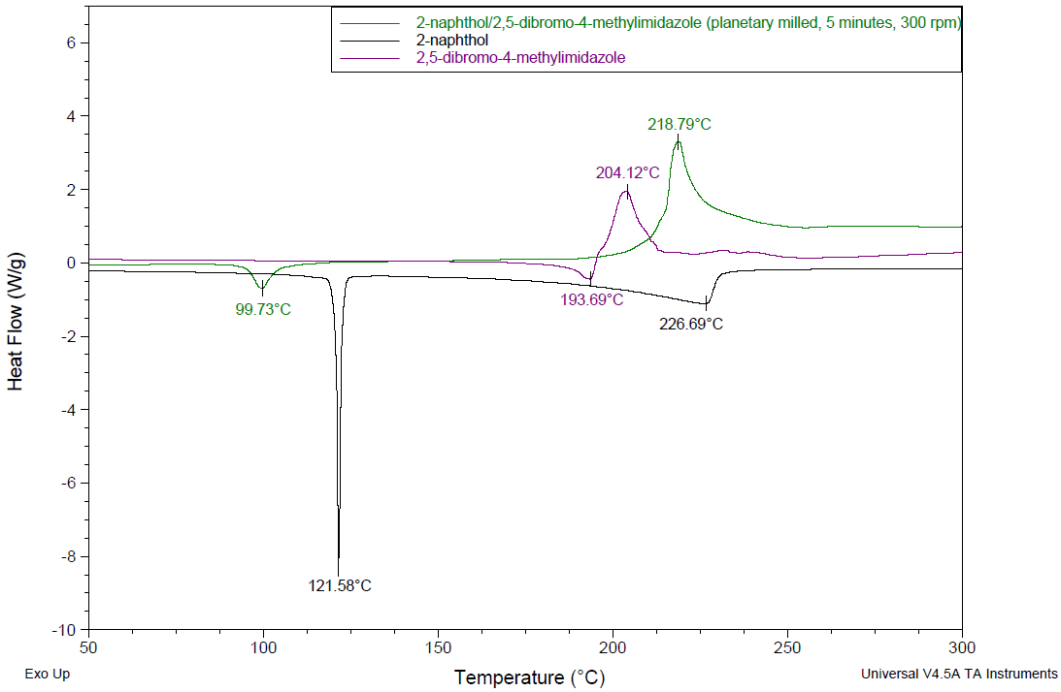

Figure B.82 - Thermal analysis of 2-naphthol/2,5-dibromo-4-methylimidazole produced by planetary milling for 5 minutes at 300 rpm.

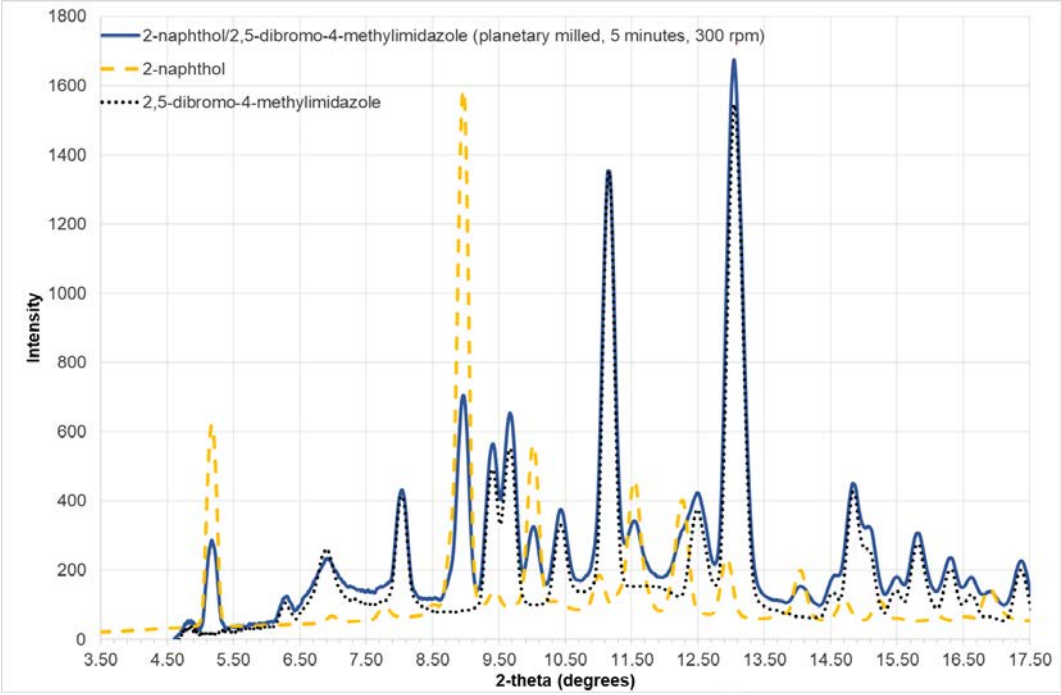

Figure B.83 – Powder x-ray pattern of 2-naphthol/2,5-dibromo-4-methylimidazole produced by planetary milling for 5 minutes at 300 rpm (λ = 0.7107 Å).

B.47 2-naphthol/1,2,3-triazole

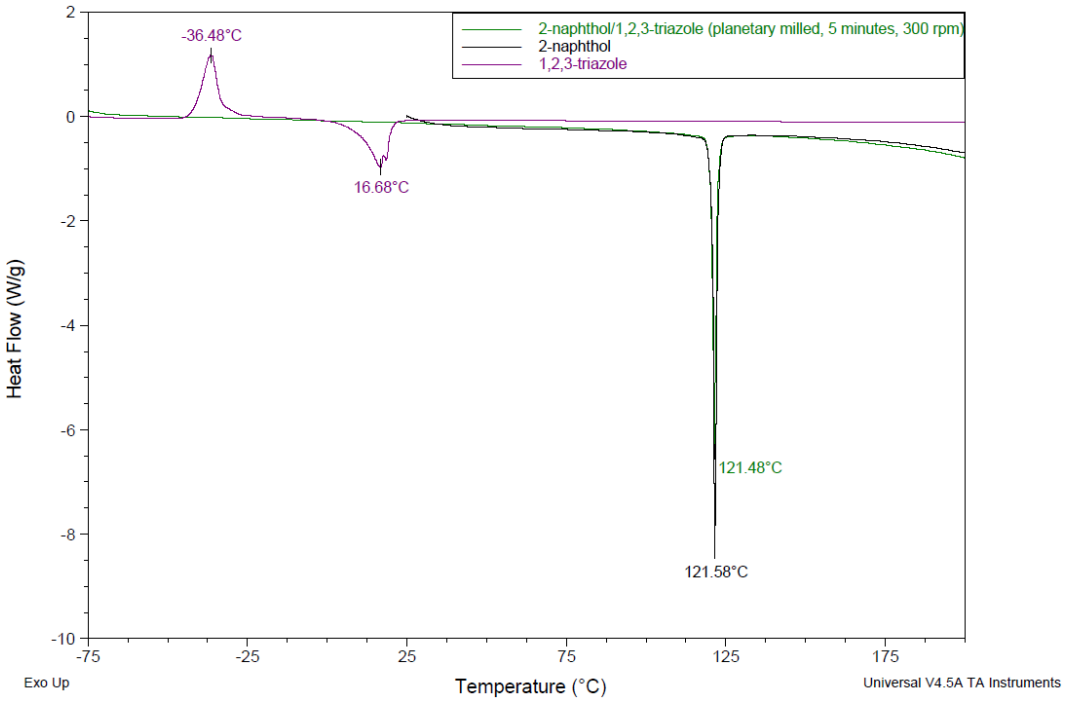

Figure B.84 - Thermal analysis of 2-naphthol/1,2,3-triazole produced by planetary milling for 5 minutes at 300 rpm.

B.48 2-naphthol/5-nitro-1,2,3-triazole

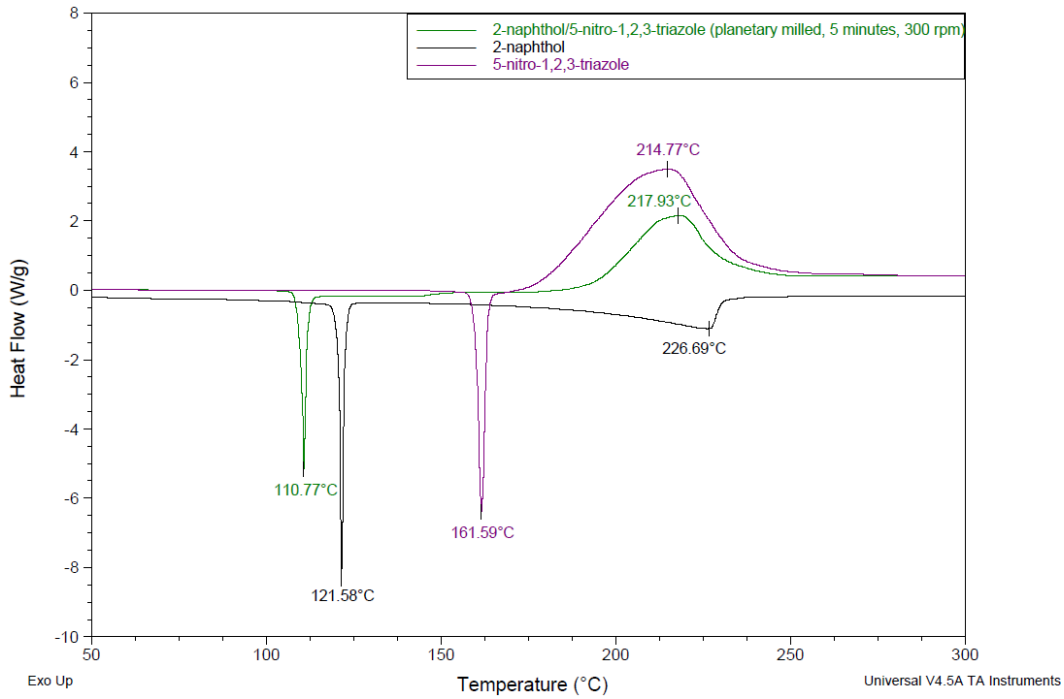

Figure B.85 - Thermal analysis of 2-naphthol/5-nitro-1,2,3-triazole produced by planetary milling for 5 minutes at 300 rpm.

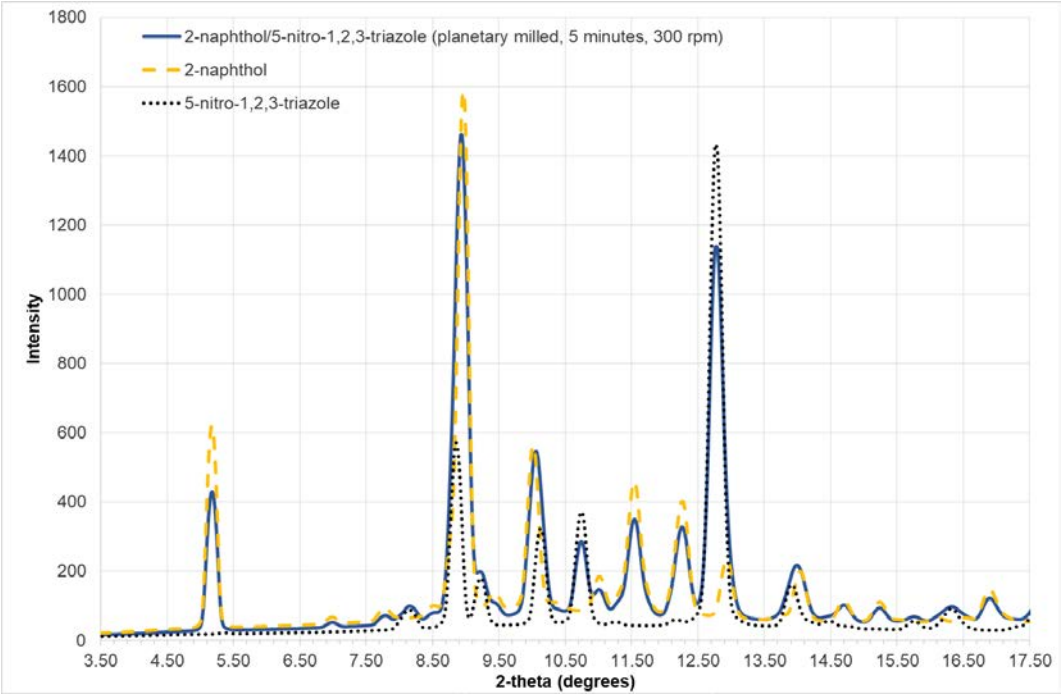

Figure B.86 – Powder x-ray pattern of 2-naphthol/5-nitro-1,2,3-triazole produced by planetary milling for 5 minutes at 300 rpm (λ = 0.7107 Å).

B.49 2-naphthol/1,2,4-triazole

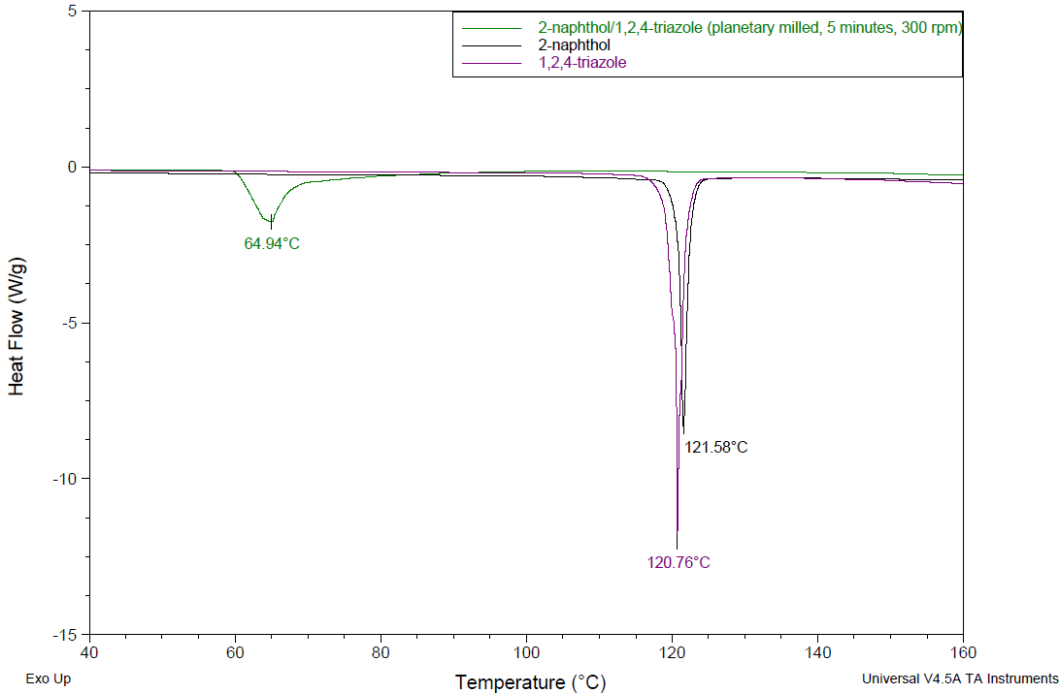

Figure B.87 - Thermal analysis of 2-naphthol/1,2,4-triazole produced by planetary milling for 5 minutes at 300 rpm.

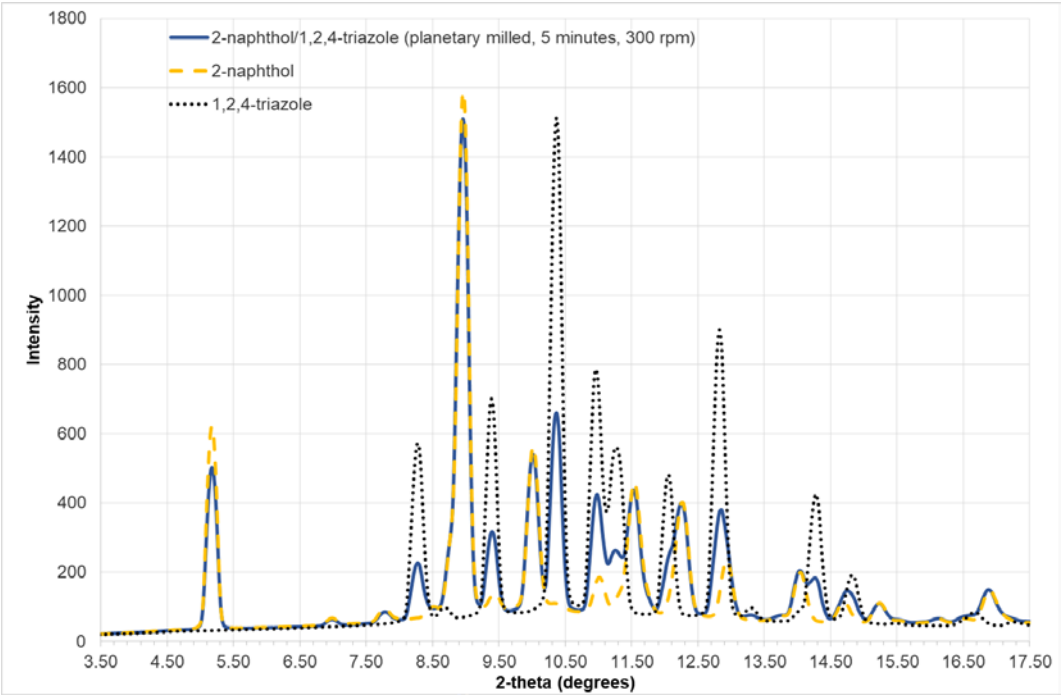

Figure B.88 – Powder x-ray pattern of 2-naphthol/1,2,4-triazole produced by planetary milling for 5 minutes at 300 rpm (λ = 0.7107 Å).

B.50 2-naphthol/3-methyl-1,2,4-triazole

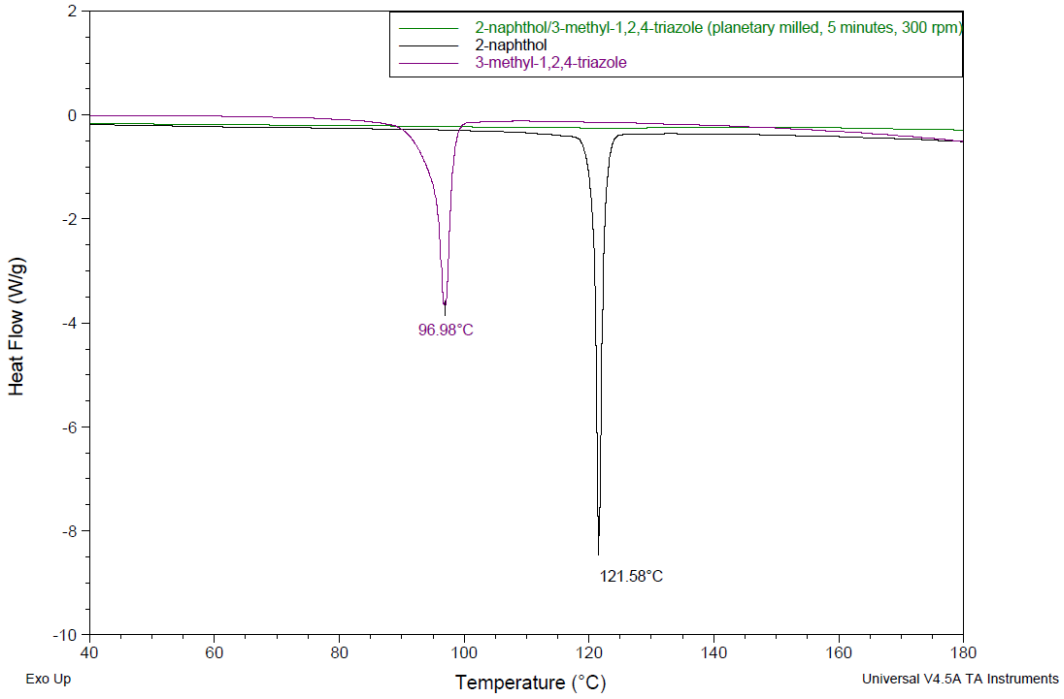

Figure B.89 - Thermal analysis of 2-naphthol/3-methyl-1,2,4-triazole produced by planetary milling for 5 minutes at 300 rpm.

B.51 2-naphthol/1,2,4-triazol-3-amine

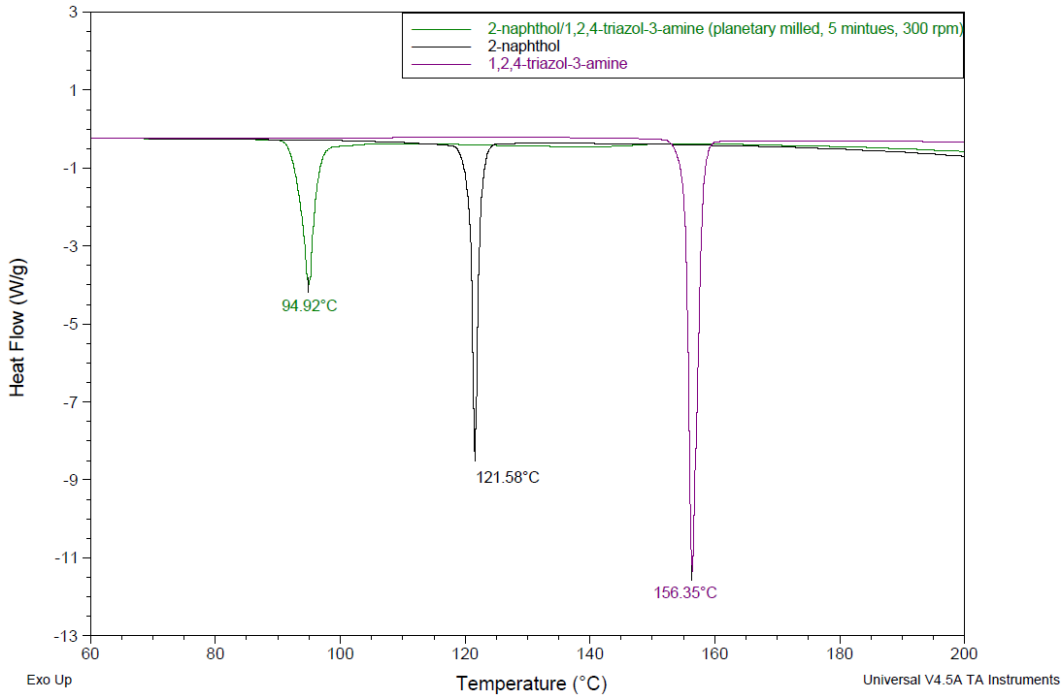

Figure B.90 - Thermal analysis of 2-naphthol/1,2,4-triazol-3-amine produced by planetary milling for 5 minutes at 300 rpm.

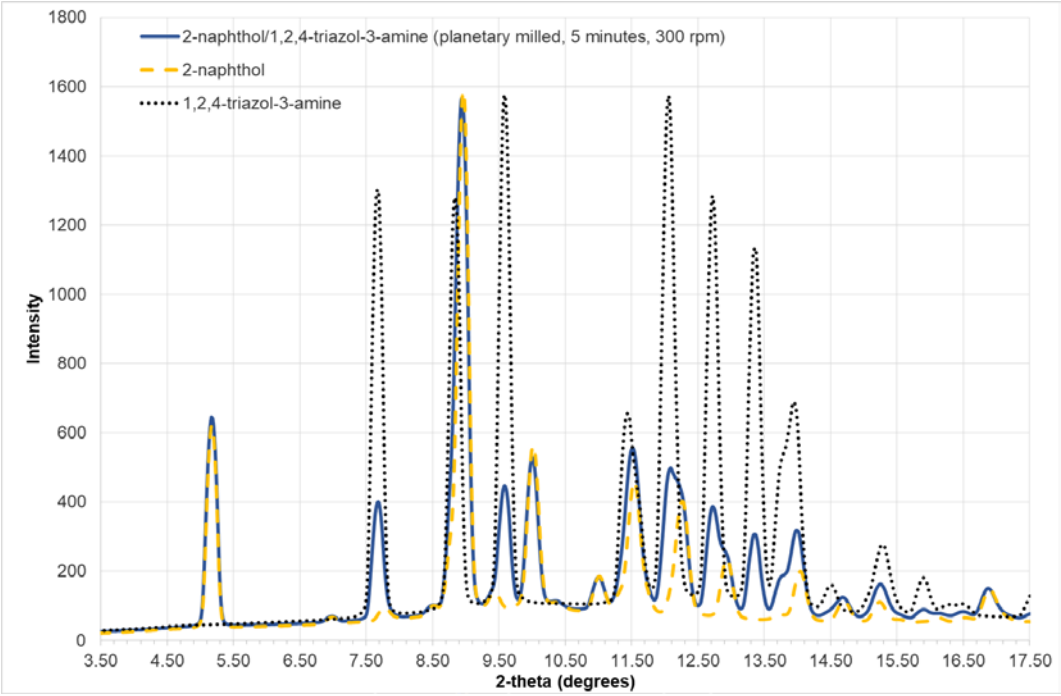

Figure B.91 – Powder x-ray pattern of 2-naphthol/1,2,4-triazol-3-amine produced by planetary milling for 5 minutes at 300 rpm (λ = 0.7107 Å).

B.52 2-naphthol/5-bromo-1,2,4-triazole

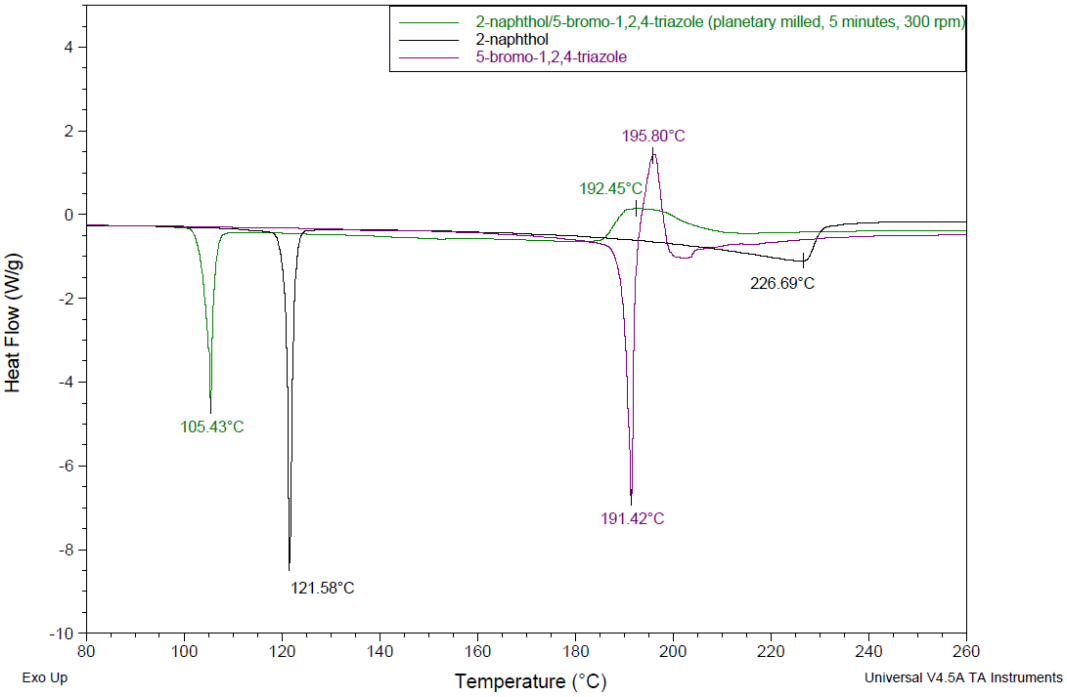

Figure B.92 - Thermal analysis of 2-naphthol/5-bromo-1,2,4-triazole produced by planetary milling for 5 minutes at 300 rpm.

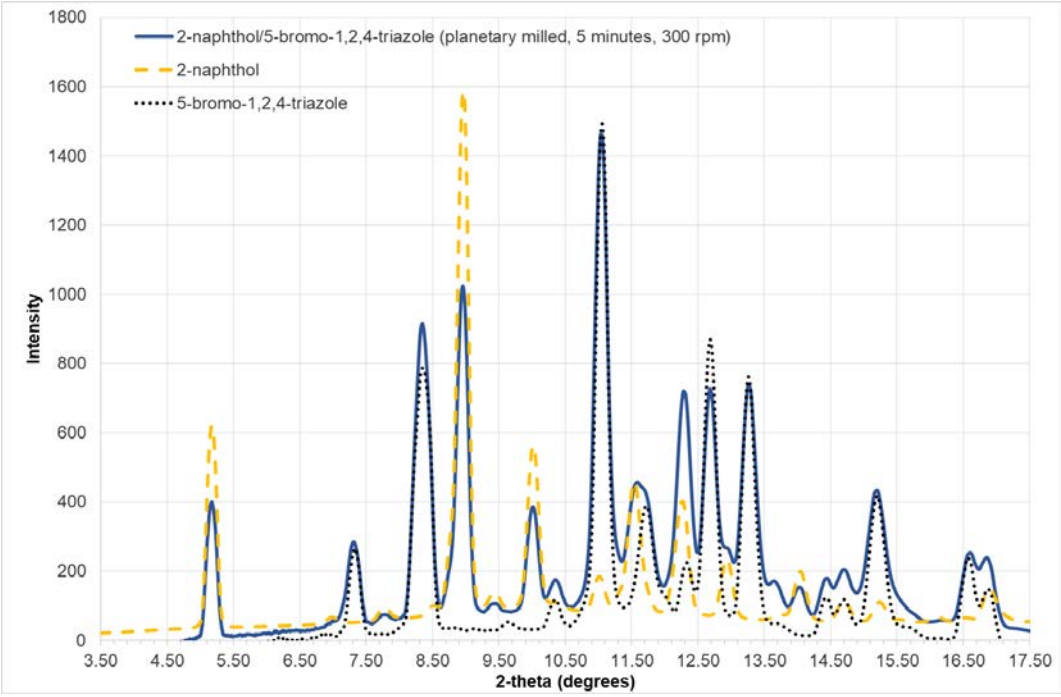

Figure B.93 – Powder x-ray pattern of 2-naphthol/5-bromo-1,2,4-triazole produced by planetary milling for 5 minutes at 300 rpm (λ = 0.7107 Å).

B.53 2-naphthol/1,2,4-triazol-3,5-diamine

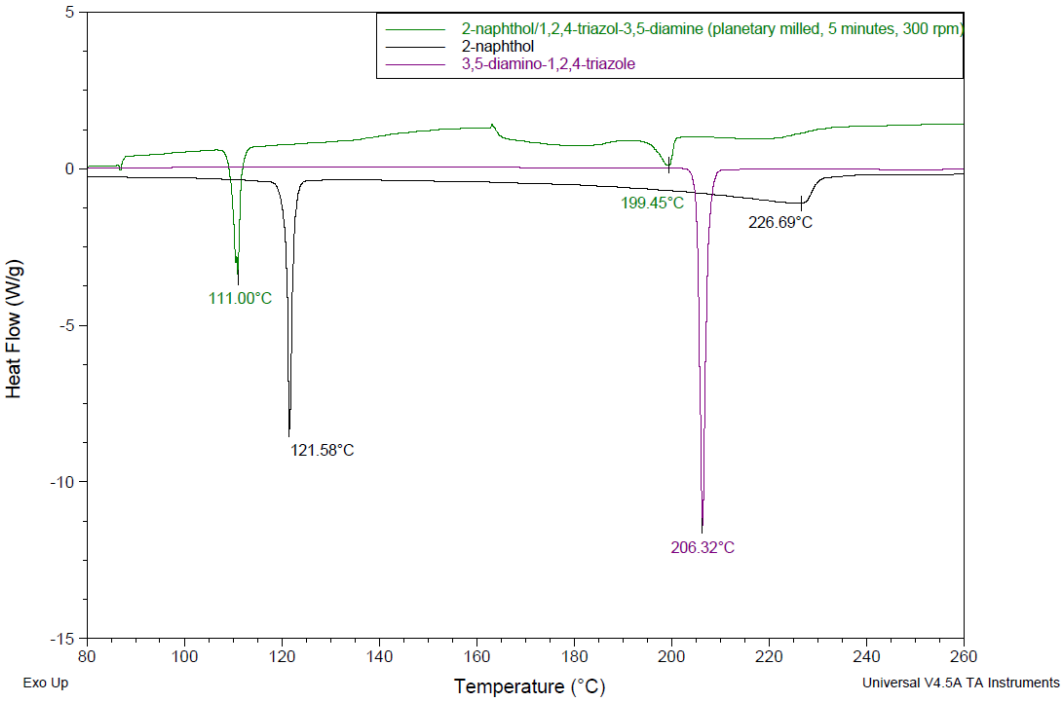

Figure B.94 - Thermal analysis of 2-naphthol/1,2,4-triazol-3,5-diamine produced by planetary milling for 5 minutes at 300 rpm.

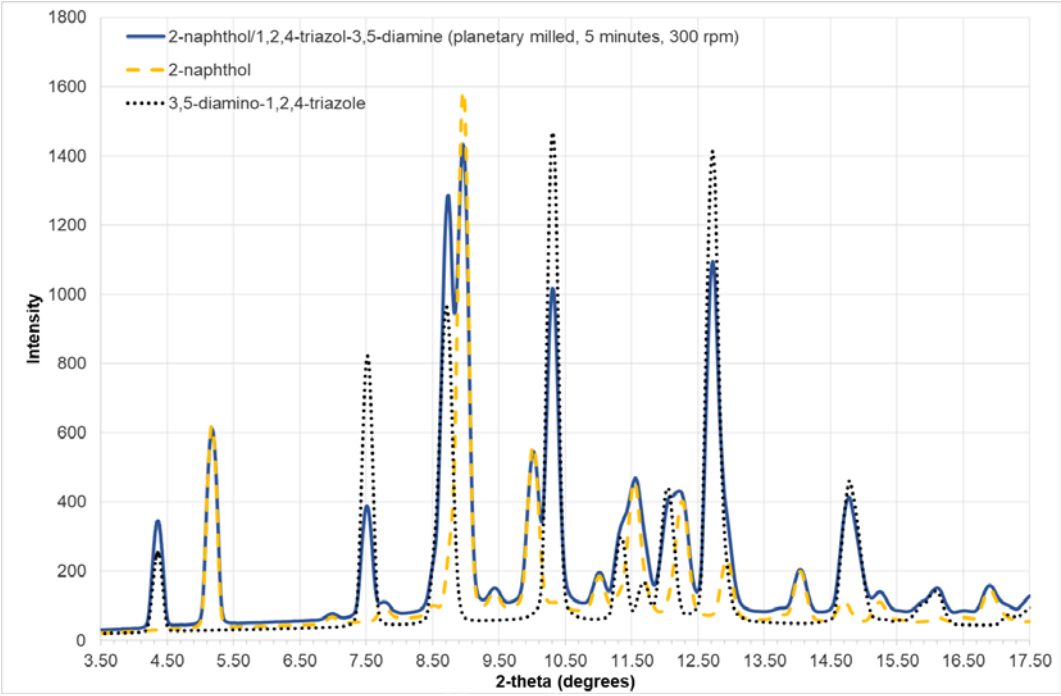

Figure B.95 – Powder x-ray pattern of 2-naphthol/1,2,4-triazol-3,5-diamine produced by planetary milling for 5 minutes at 300 rpm (λ = 0.7107 Å).

B.54 2-naphthol/3,5-dimethyl-1,2,4-triazole

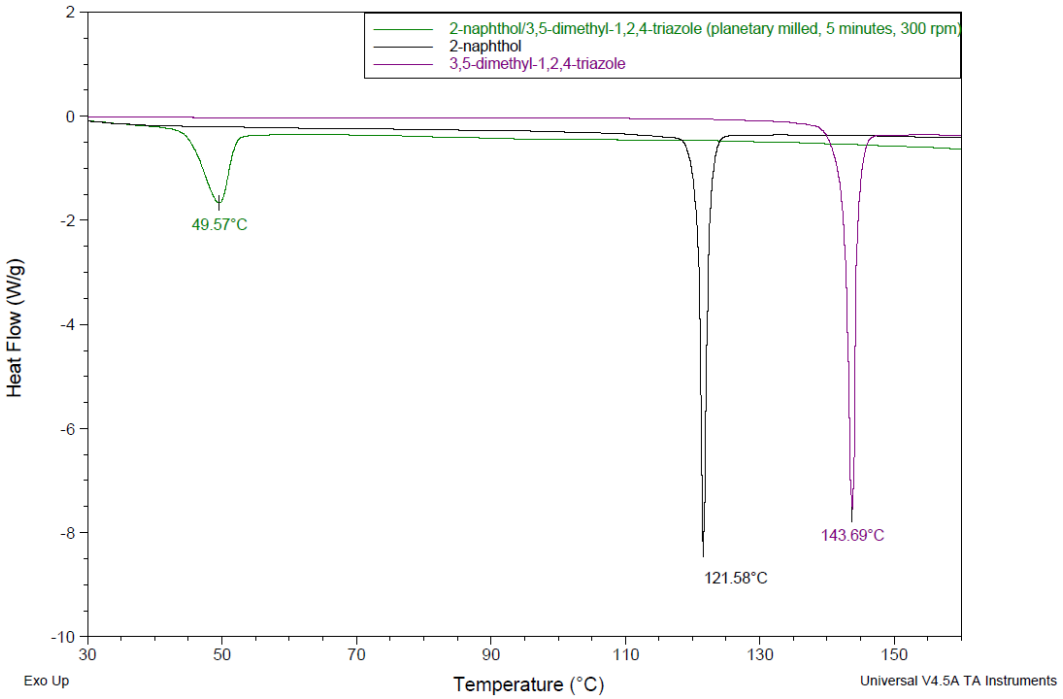

Figure B.96 - Thermal analysis of 2-naphthol/3,5-dimethyl-1,2,4-triazole produced by planetary milling for 5 minutes at 300 rpm.

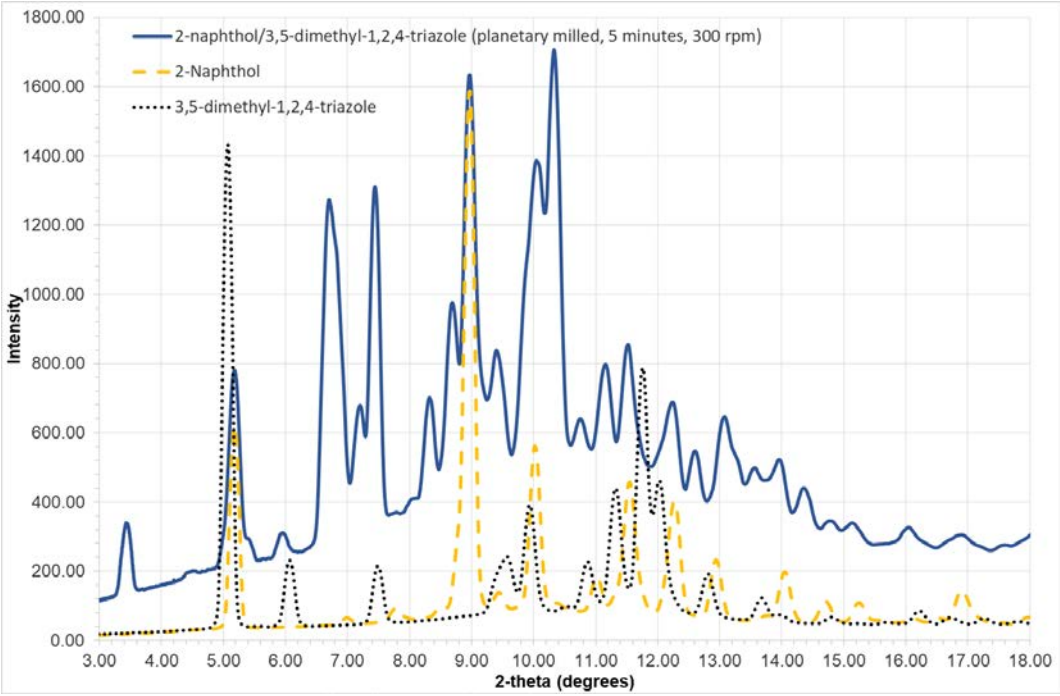

Figure B.97 – Powder x-ray pattern of 2-naphthol/3,5-dimethyl-1,2,4-triazole produced by planetary milling for 5 minutes at 300 rpm (λ = 0.7107 Å).

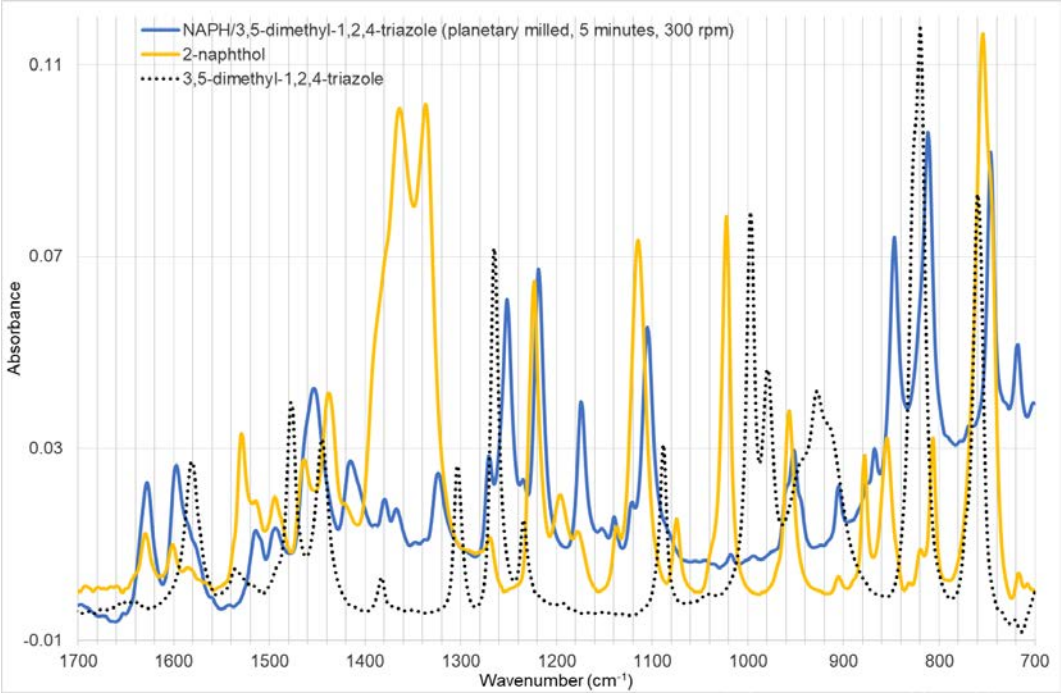

Figure B.98 – Infrared spectra of 2-naphthol/3,5-dimethyl-1,2,4-triazole produced by planetary milling for 5 minutes at 300 rpm.

Table B.8 - Infrared spectra peak positions and heights of 2-naphthol/3,5-dimethyl-1,2,4-triazole produced by planetary milling for 5 minutes at 300 rpm, with a 1:1 stoichiometry.

Peak Position (cm^{-1})	Peak Height (Absorbance)	Peak Position (cm^{-1})	Peak Height (Absorbance)
2769.14	0.01	1241.63	0.03
2764.09	0.01	1218.64	0.05
2758.97	0.01	1176.13	0.02
2700.52	0.01	1119.32	0.01
2661.94	0.01	1063.34	0.04
2604.43	0.01	1043.24	0.03
2552.35	0.01	1018.01	0.01
1629.64	0.03	960.14	0.02
1601.01	0.02	937.66	0.01
1589.25	0.02	906.06	0.02
1512.17	0.03	872.04	0.02
1457.43	0.02	852.05	0.08
1431.12	0.01	817.99	0.04
1409.91	0.03	796.78	0.03
1400.15	0.03	749.1	0.09
1381.64	0.02	729.07	0.02
1366.81	0.01	718.16	0.03
1305.91	0.05	702.62	0.02
1275.71	0.01		

B.55 2-naphthol/3,5-dibromo-1,2,4-triazole

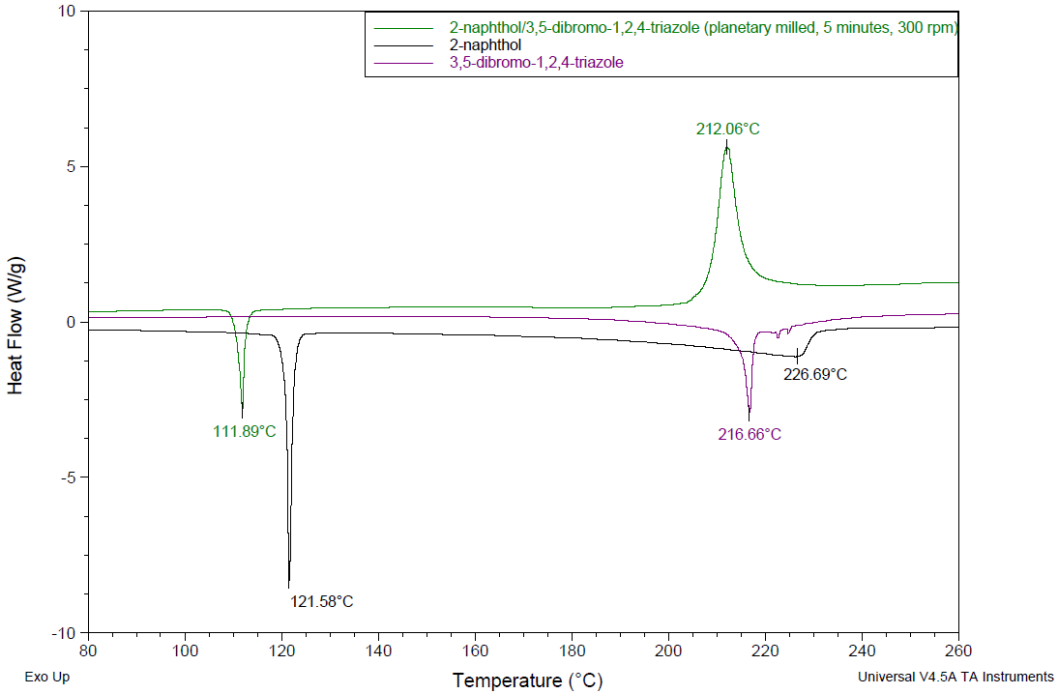

Figure B.99 - Thermal analysis of 2-naphthol/3,5-dibromo-1,2,4-triazole produced by planetary milling for 5 minutes at 300 rpm.

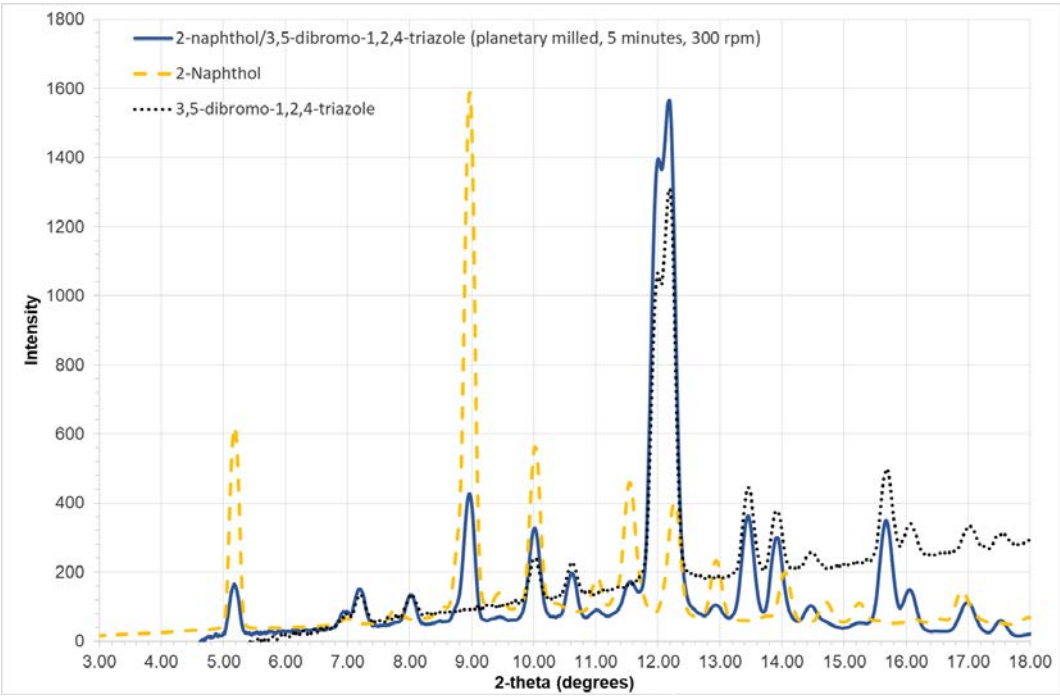

Figure B.100 – Powder x-ray analysis of 2-naphthol/3,5-dibromo-1,2,4-triazole produced by planetary milling for 5 minutes at 300 rpm (λ = 0.7107 Å).

B.56 2-naphthol/1,2,3,4-tetrazole

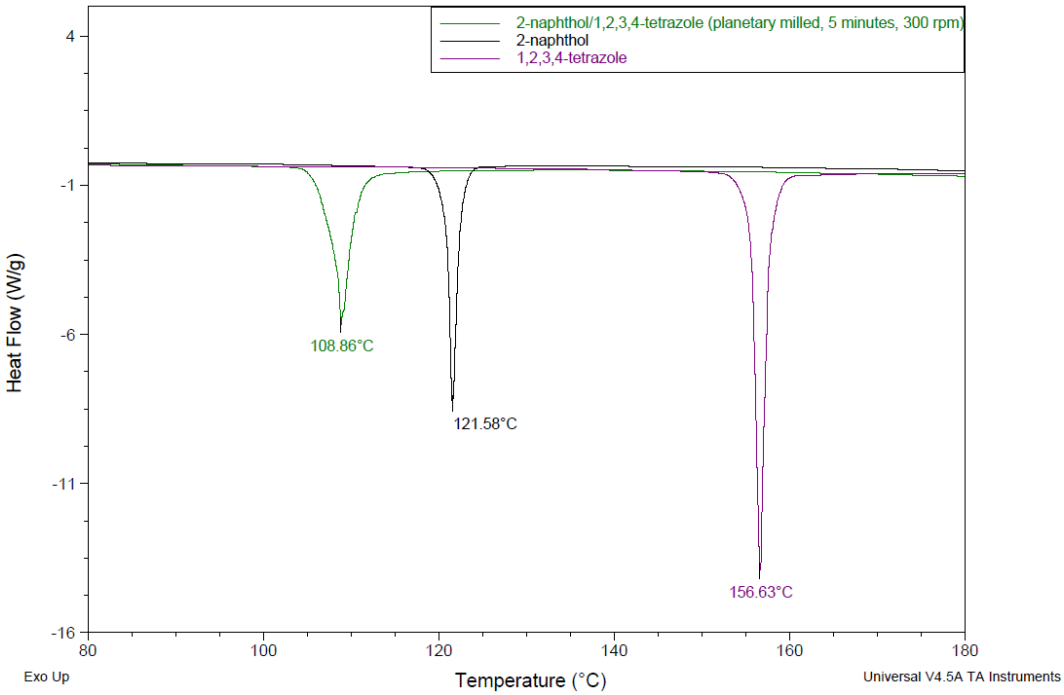

Figure B.101 - Thermal analysis of 2-naphthol/1,2,3,4-tetrazole produced by planetary milling for 5 minutes at 300 rpm.

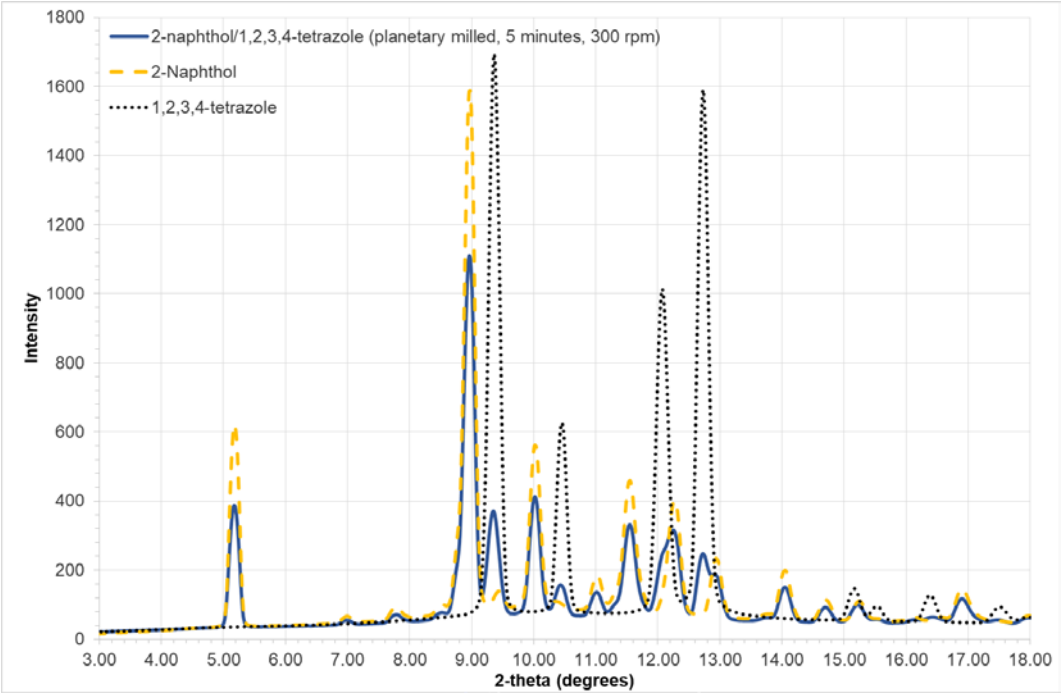

Figure B.102 – Powder x-ray pattern of 2-naphthol/1,2,3,4-tetrazole produced by planetary milling for 5 minutes at 300 rpm (λ = 0.7107 Å).

B.57 2-naphthol/1,2,3,4-tetrazol-5-amine

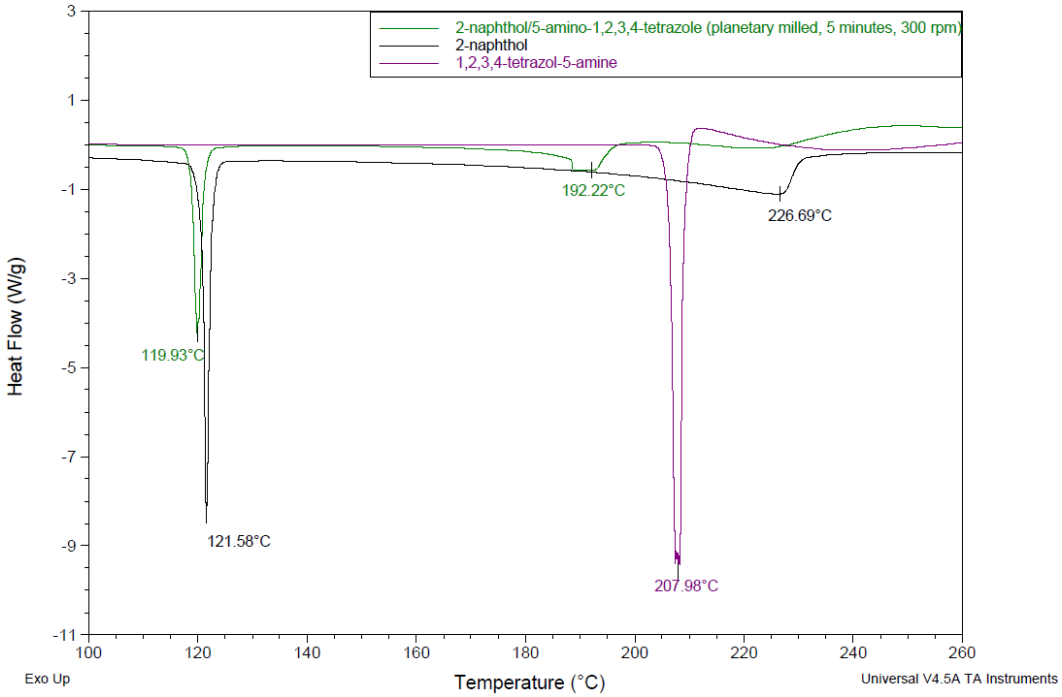

Figure B.103 - Thermal analysis of 2-naphthol/1,2,3,4-tetrazol-5-amine produced by planetary milling for 5 minutes at 300 rpm.

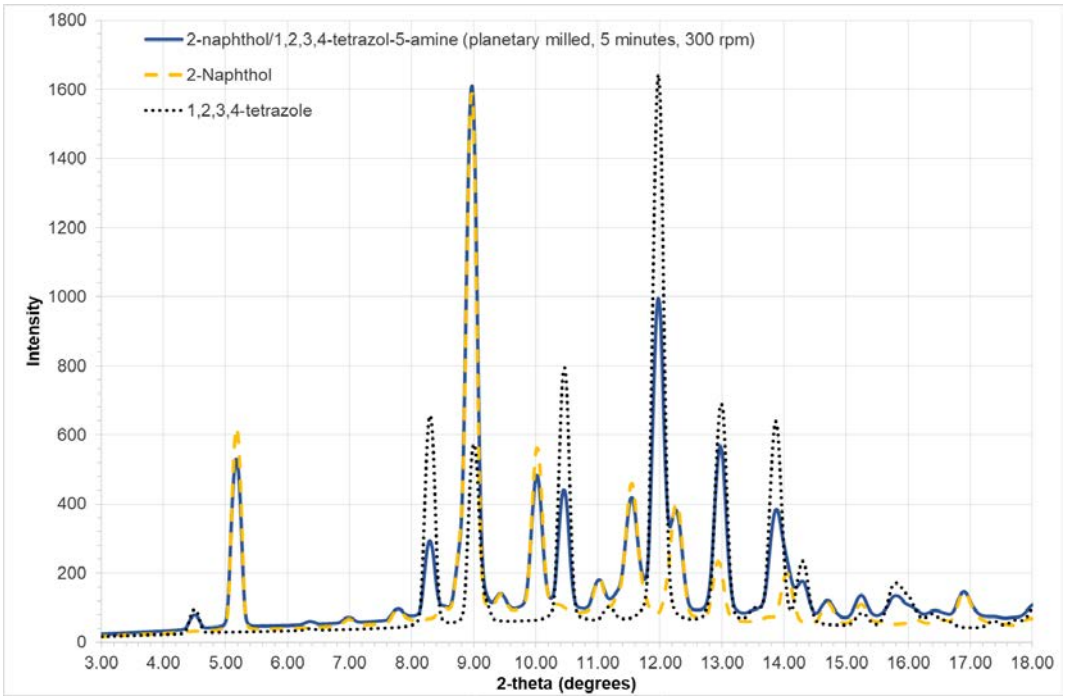

Figure B.104 – Powder x-ray pattern of 2-naphthol/1,2,3,4-tetrazol-5-amine produced by planetary milling for 5 minutes at 300 rpm (λ = 0.7107 Å).

B.58 2-naphthol/5-methyl-1,2,3,4-tetrazole

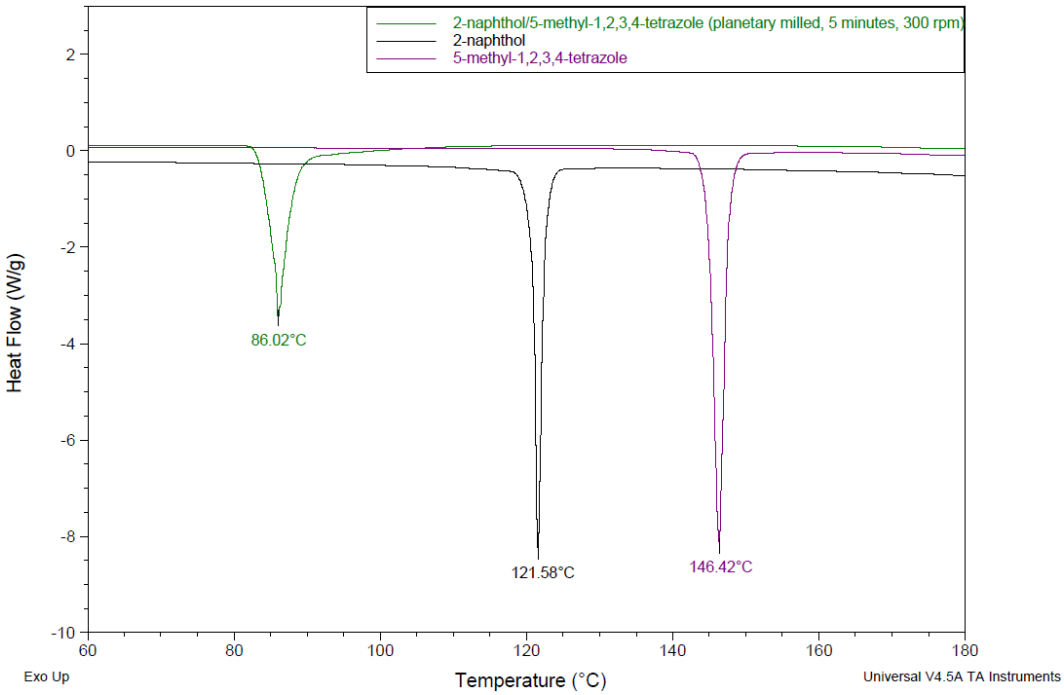

Figure B.105 - Thermal analysis of 2-naphthol/5-methyl-1,2,3,4-tetrazole produced by planetary milling for 5 minutes at 300 rpm.

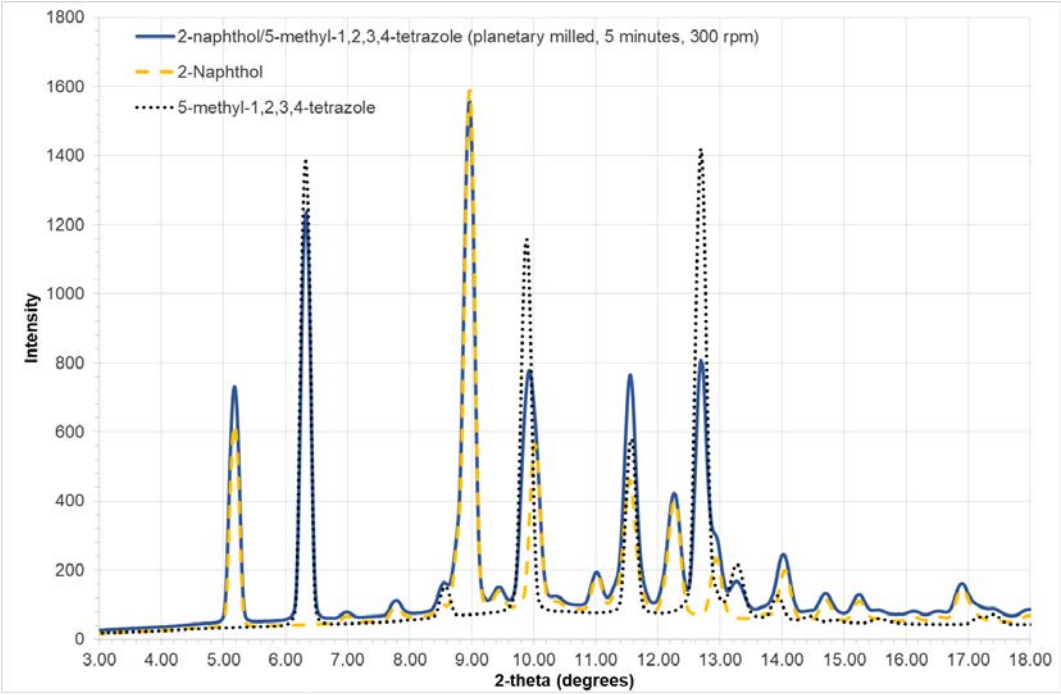

Figure B.106 – Powder x-ray pattern of 2-naphthol/5-methyl-1,2,3,4-tetrazole produced by planetary milling for 5 minutes at 300 rpm (λ = 0.7107 Å).

B.59 2-naphthol/3-nitro-1,2,4-triazol-5-one

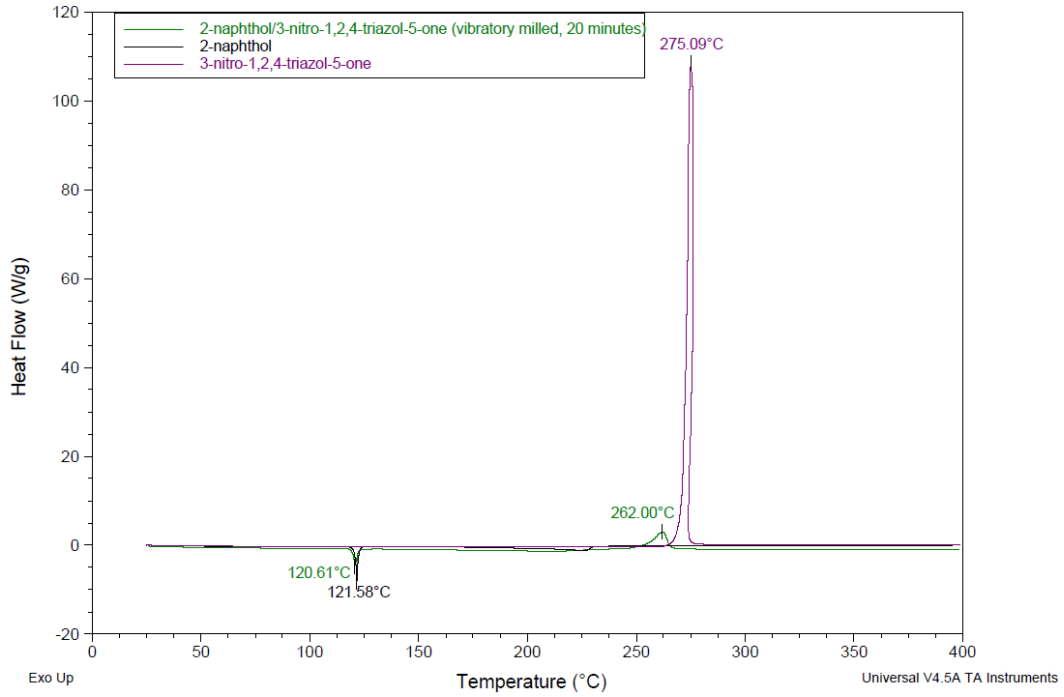

Figure B.107 - Thermal analysis of 2-naphthol/3-nitro-1,2,4-triazol-5-one produced by planetary milling for 5 minutes at 300 rpm.

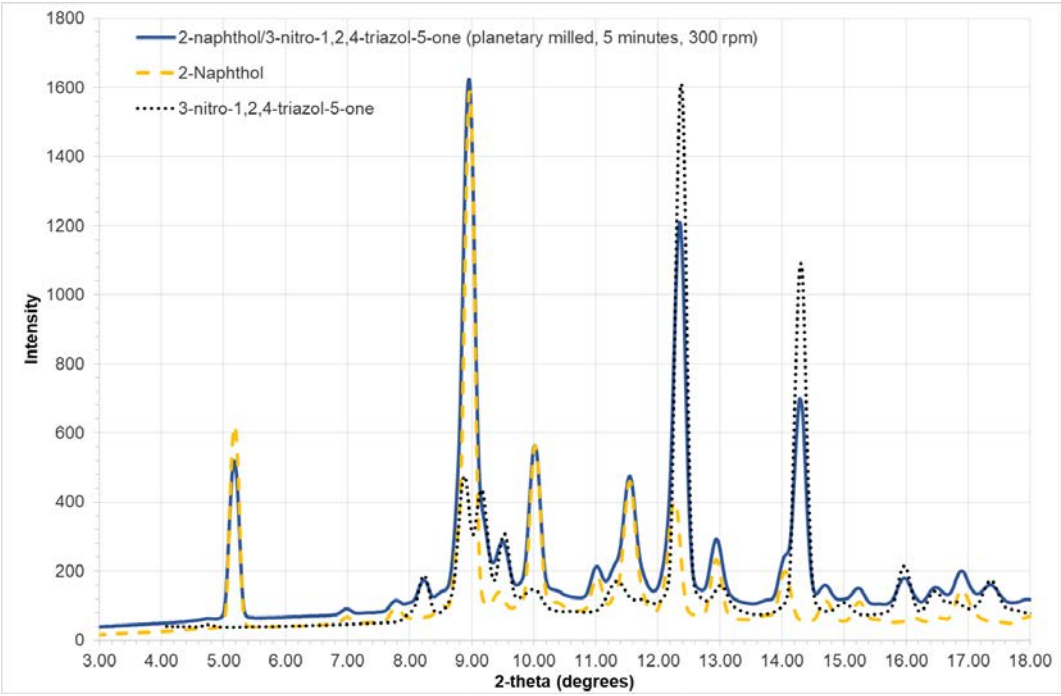

Figure B.108 – Powder x-ray analysis of 2-naphthol/3-nitro-1,2,4-triazol-5-one produced by planetary milling for 5 minutes at 300 rpm (λ = 0.7107 Å).

B.60 Molecular Electrostatic Potentials

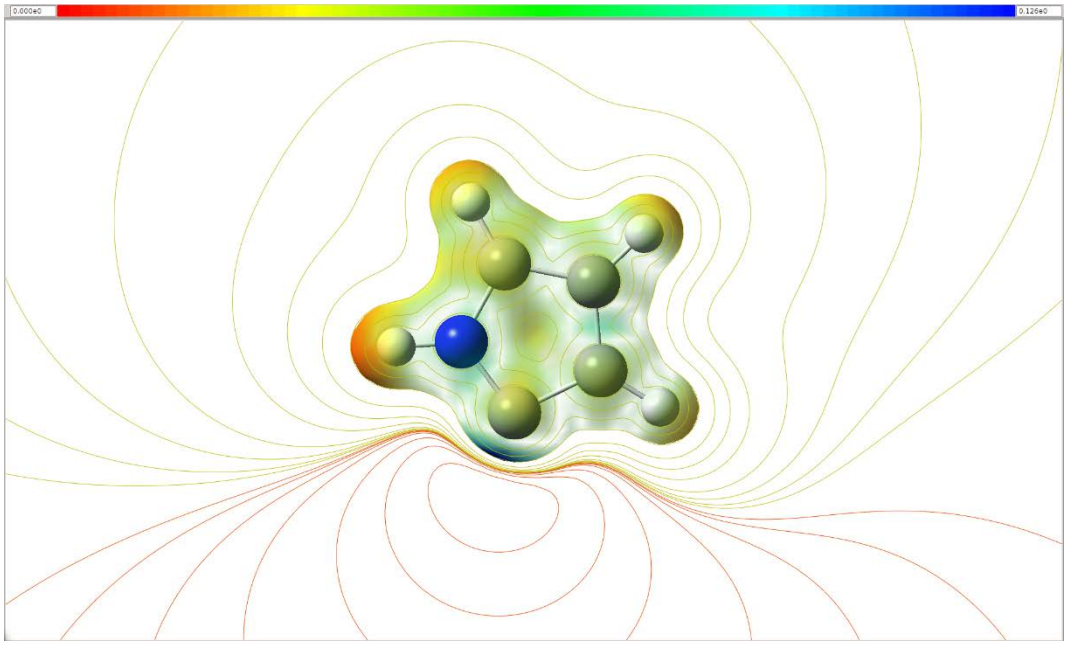

Figure B.109 - Molecular electrostatic potential map of pyrrolidine.

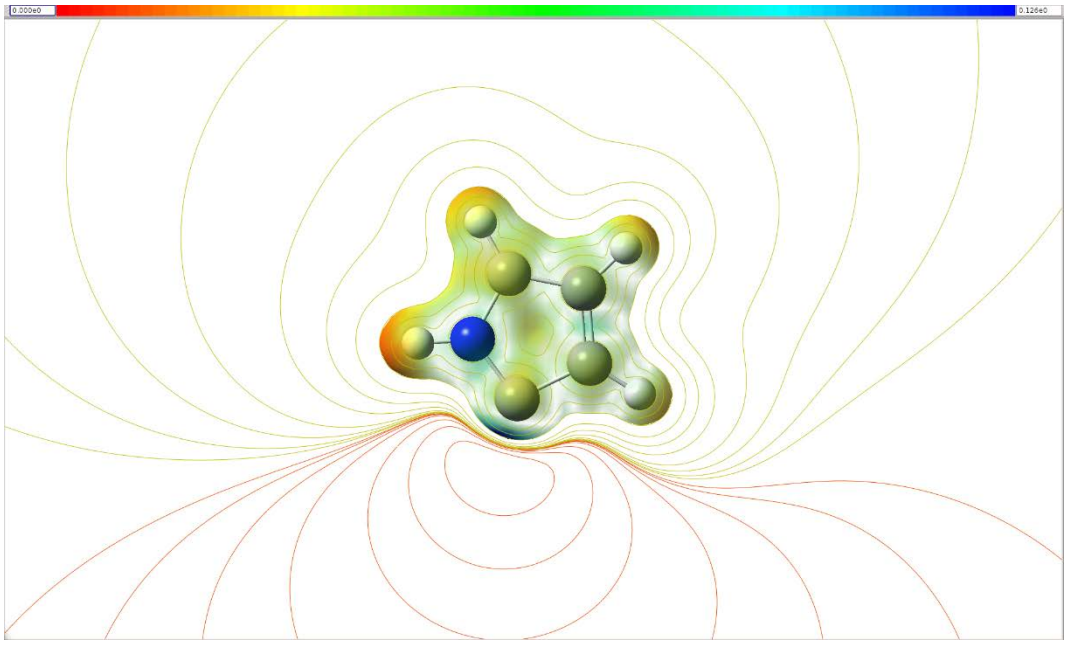

Figure B.110 - Molecular electrostatic potential map of 3-pyrroline.

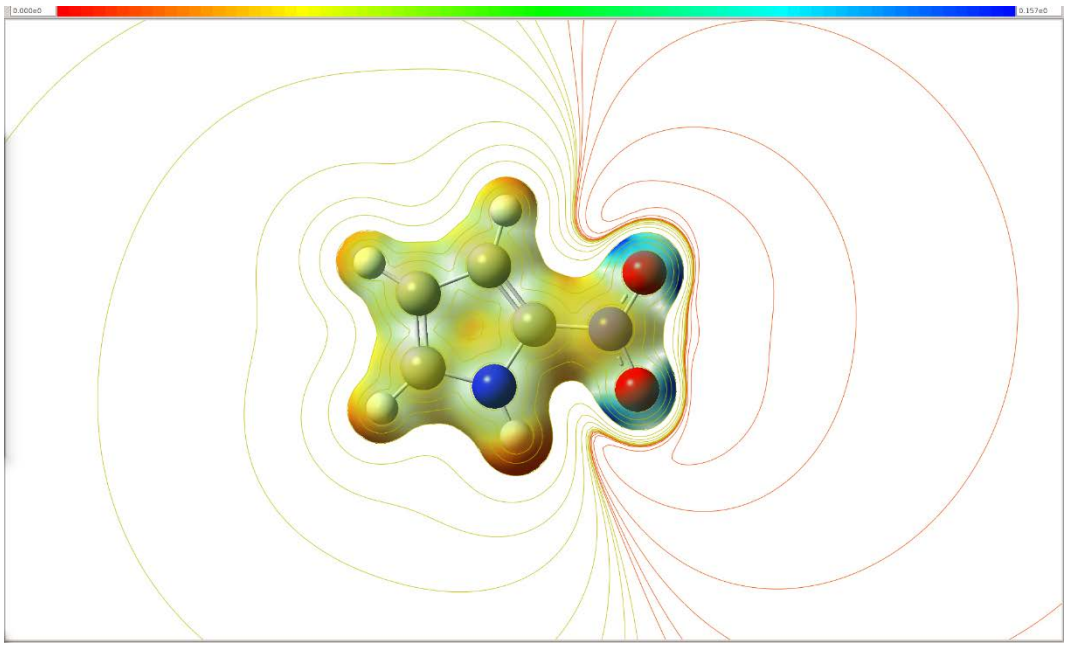

Figure B.111 - Molecular electrostatic potential map of 2-nitropyrrole.

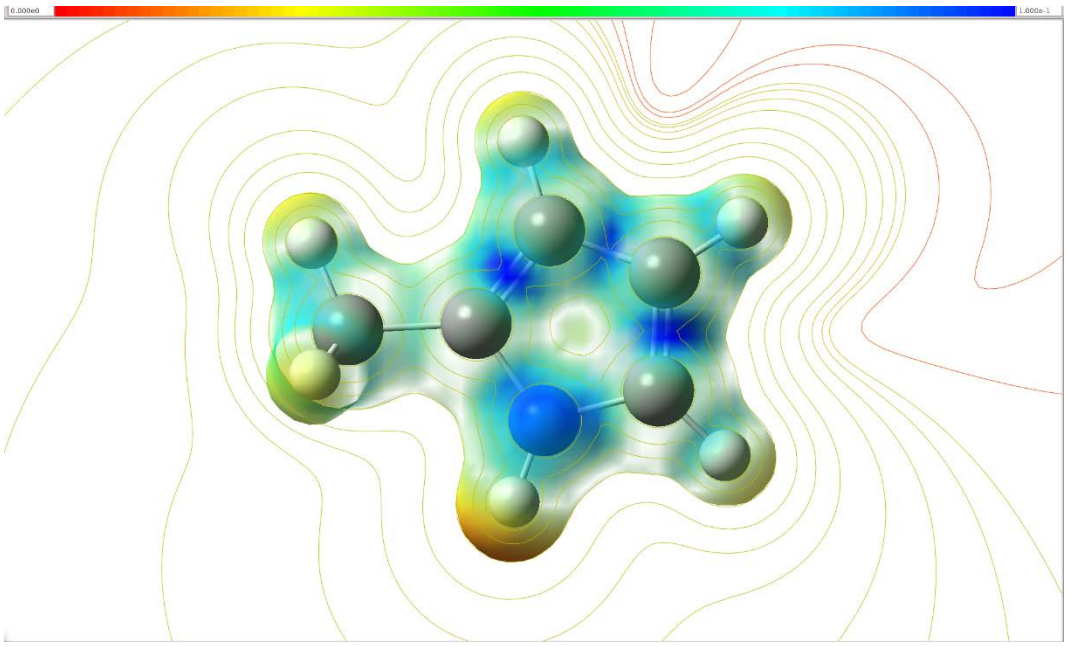

Figure B.112 - Molecular electrostatic potential map of 2-methylpyrrole.

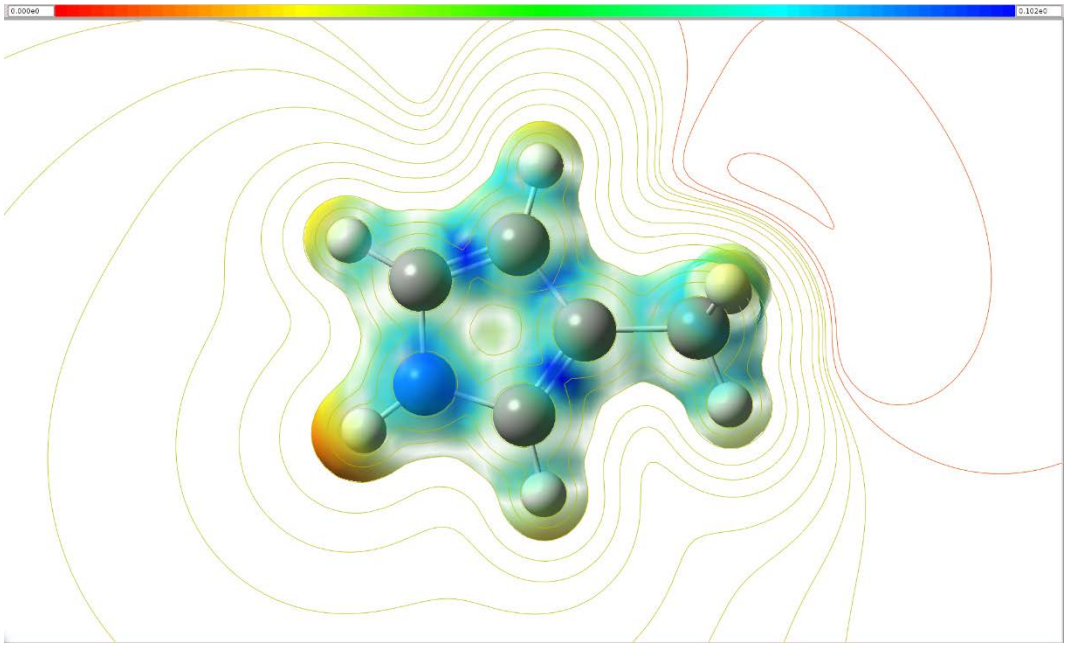

Figure B.113 - Molecular electrostatic potential map of 3-methylpyrrole.

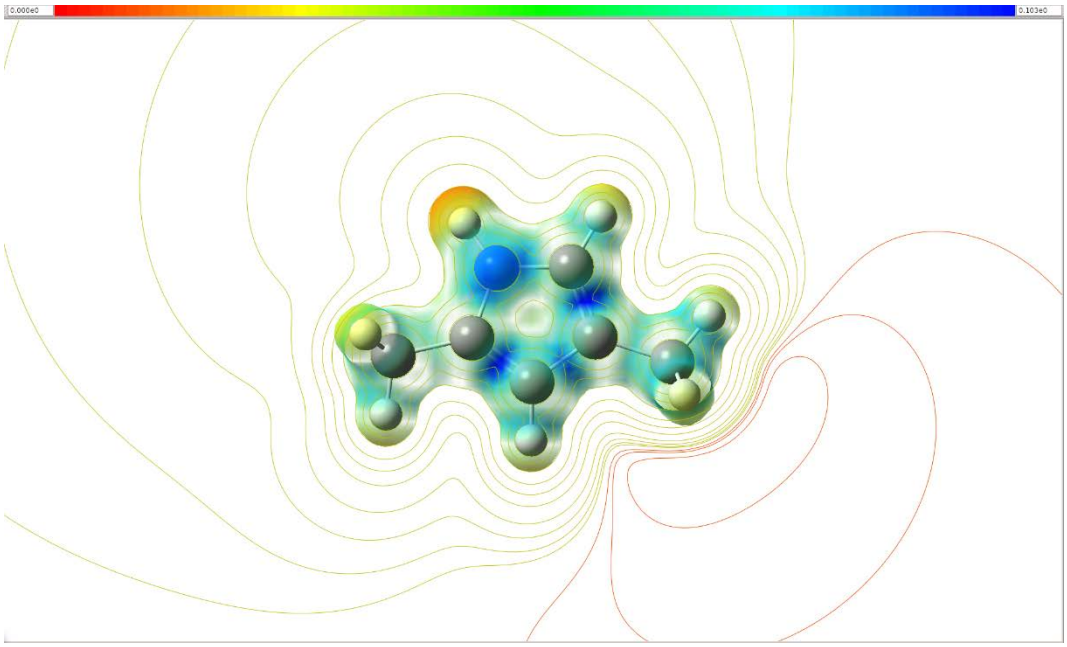

Figure B.114 - Molecular electrostatic potential map of 2,4-dimethylpyrrole.

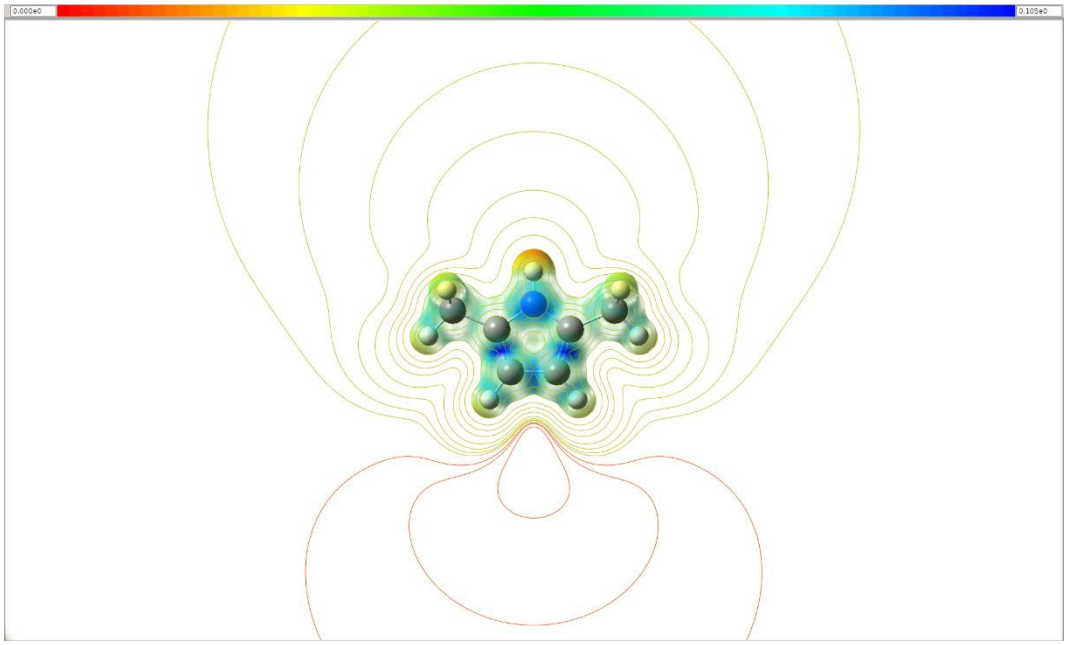

Figure B.115 - Molecular electrostatic potential map of 2,5-dimethylpyrrole.

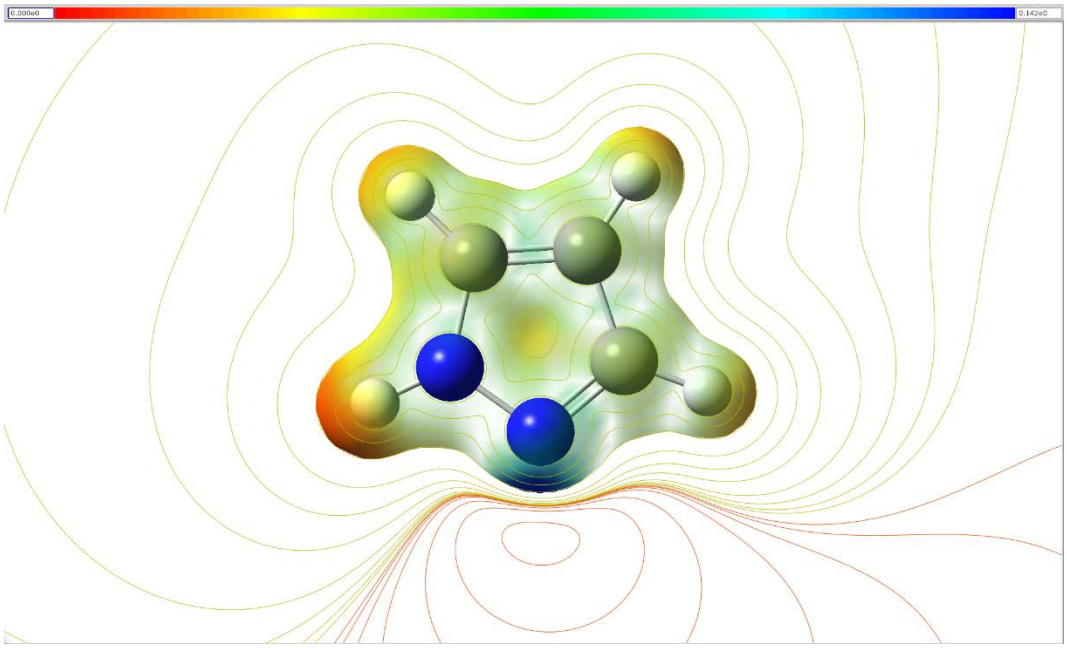

Figure B.116 - Molecular electrostatic potential map of pyrazole.

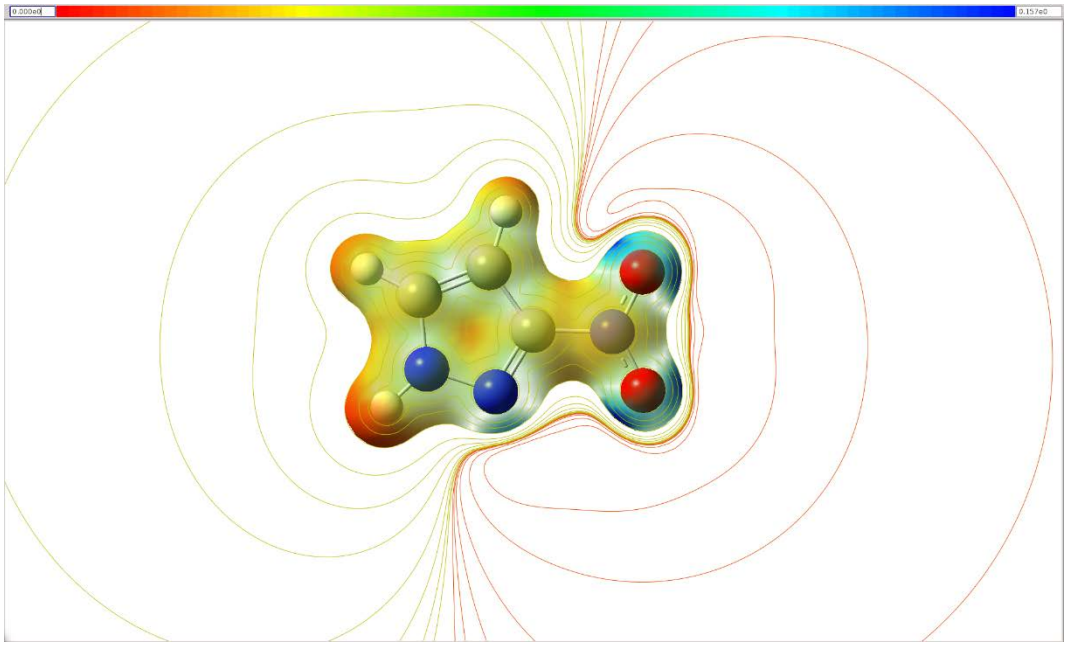

Figure B.117 - Molecular electrostatic potential map of 3-nitropyrazole.

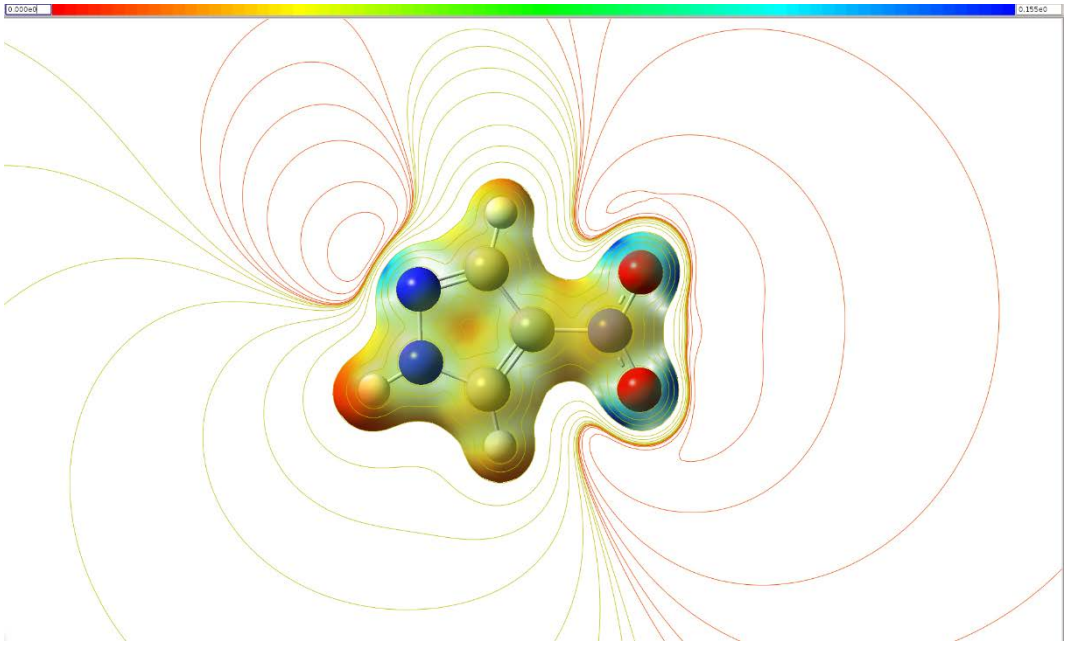

Figure B.118 - Molecular electrostatic potential map of 4-nitropyrazole.

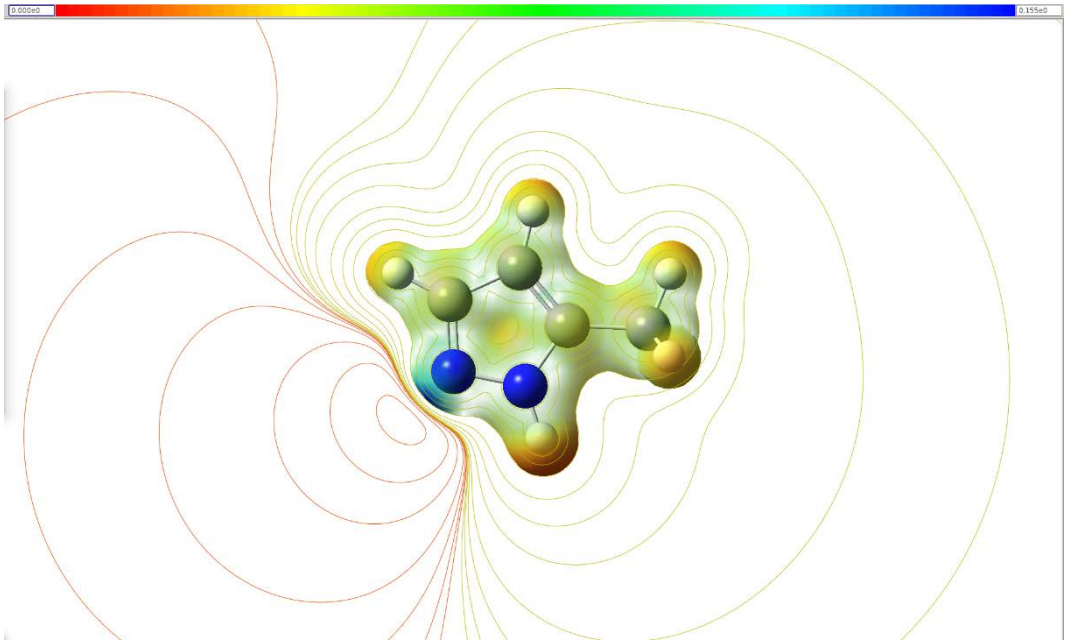

Figure B.119 - Molecular electrostatic potential map of 5-methylpyrazole.

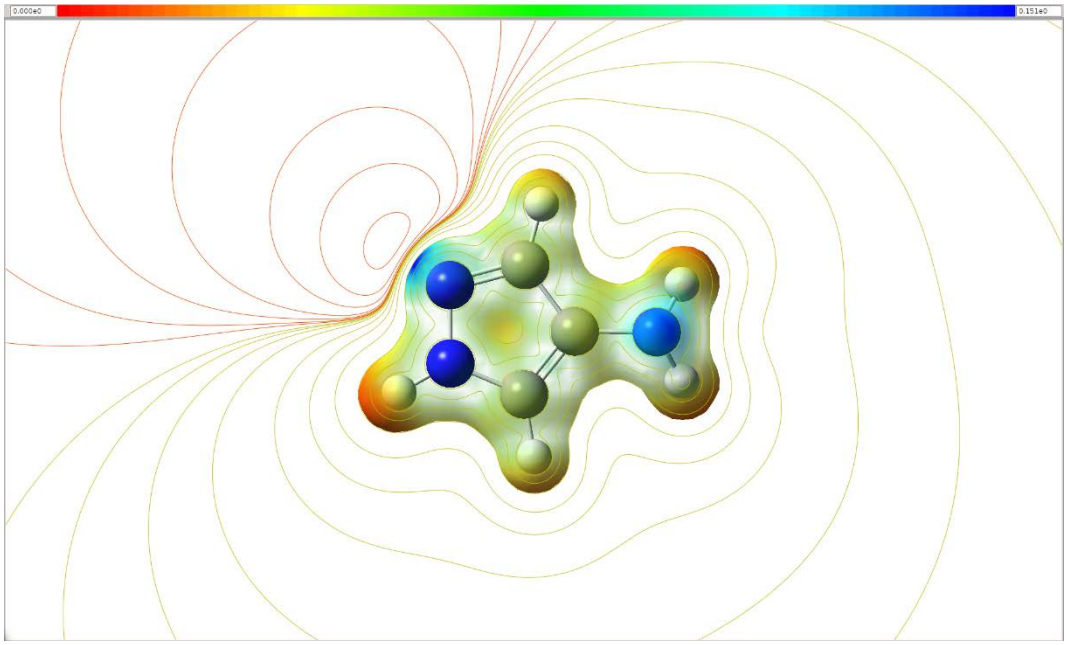

Figure B.120 - Molecular electrostatic potential map of pyrazol-4-amine.

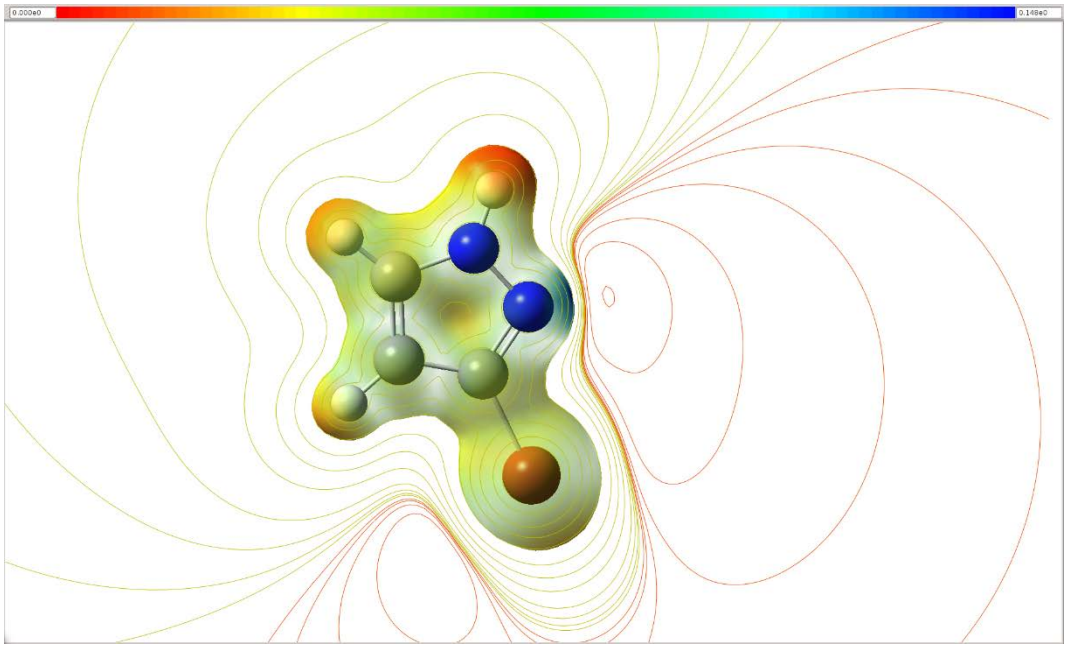

Figure B.121 - Molecular electrostatic potential map of 3-bromopyrazole.

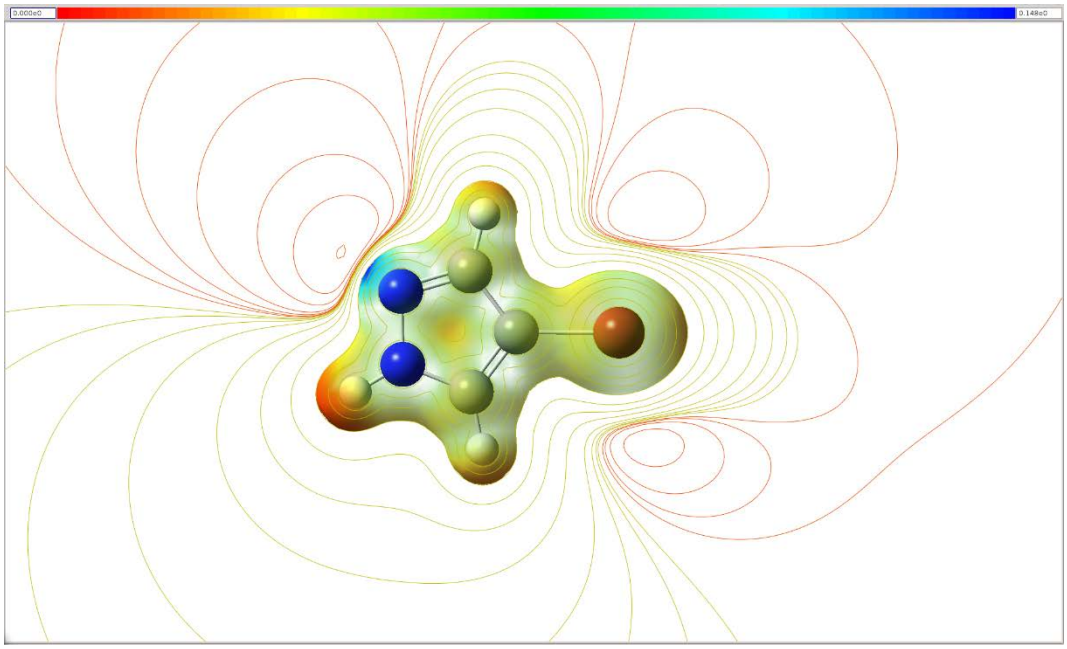

Figure B.122 - Molecular electrostatic potential map of 4-bromopyrazole.

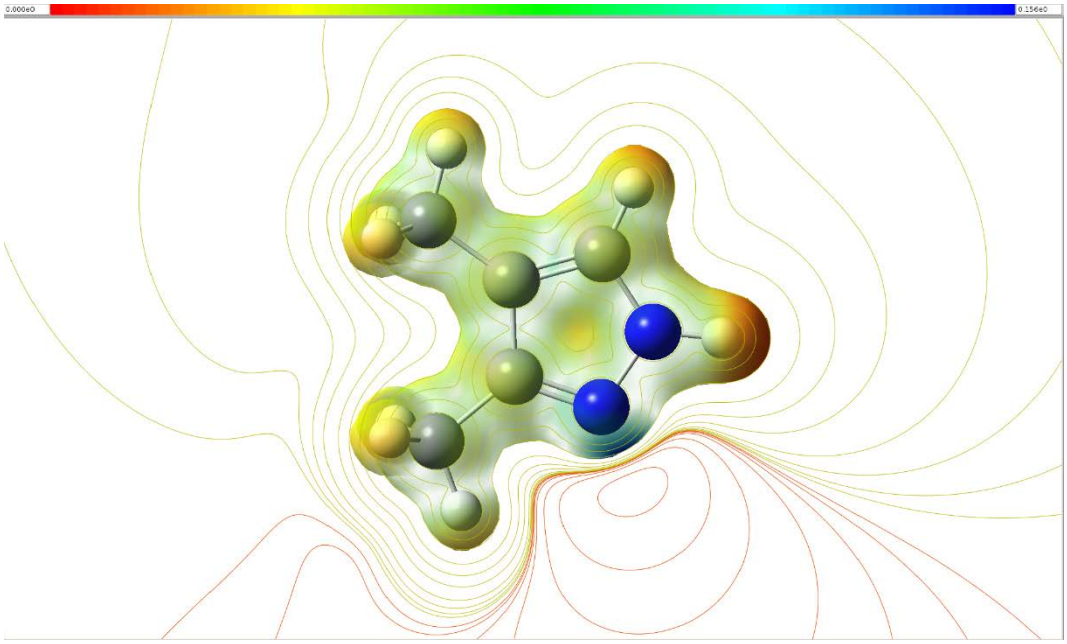

Figure B.123 - Molecular electrostatic potential map of 3,4-dimethylpyrazole.

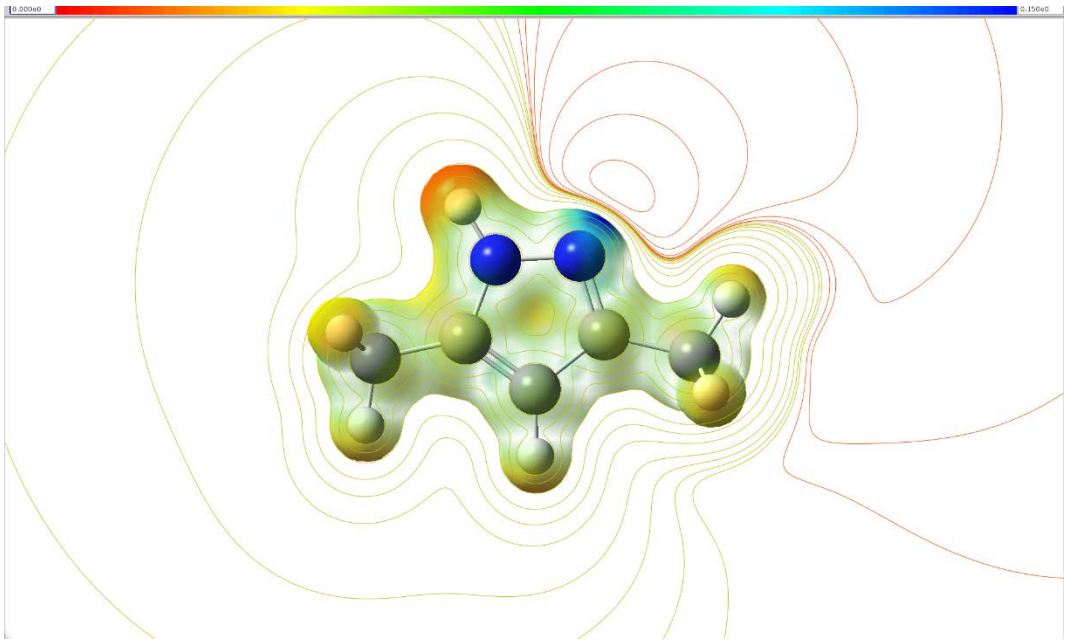

Figure B.124 - Molecular electrostatic potential map of 3,4-dimethylpyrazole.

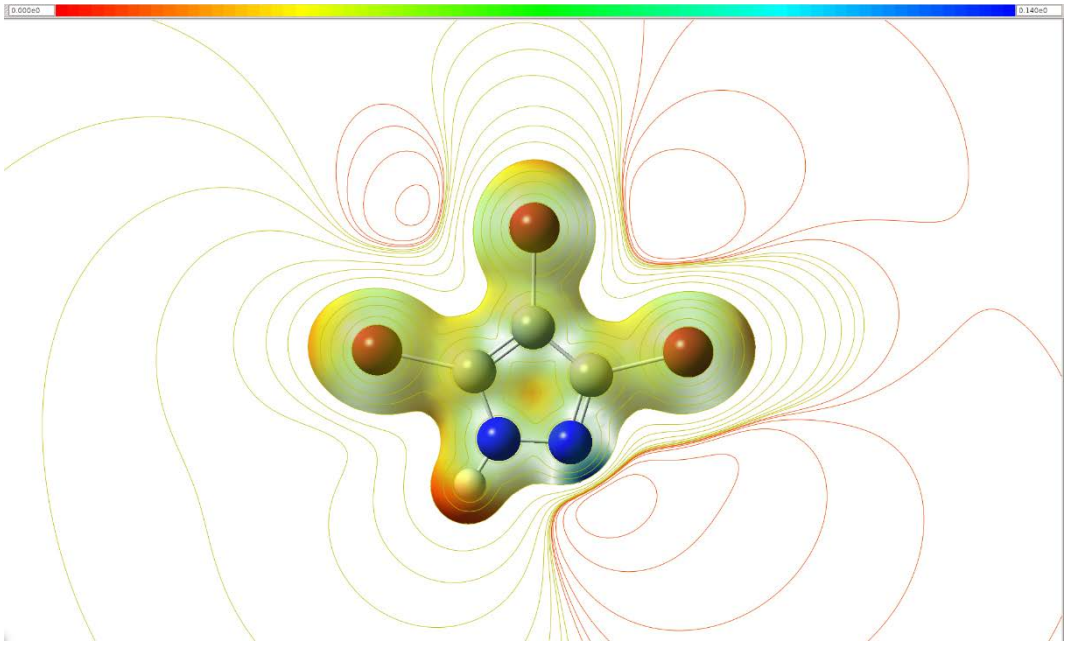

Figure B.125 - Molecular electrostatic potential map of 3,4,5-tribromopyrazole.

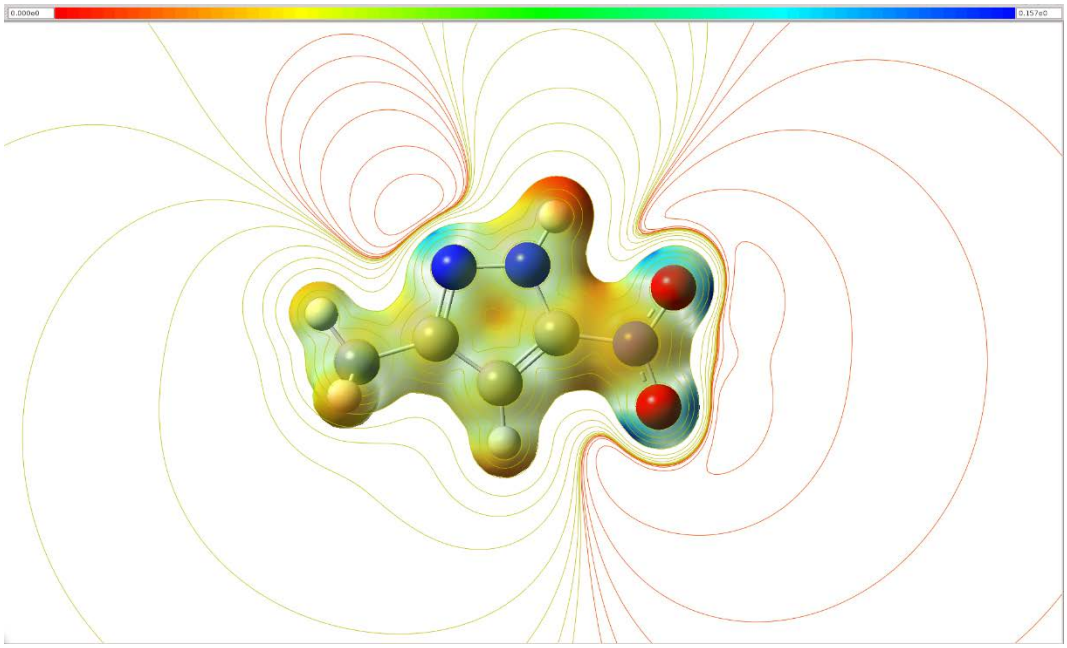

Figure B.126 - Molecular electrostatic potential map of 3-methyl-5-nitropyrazole.

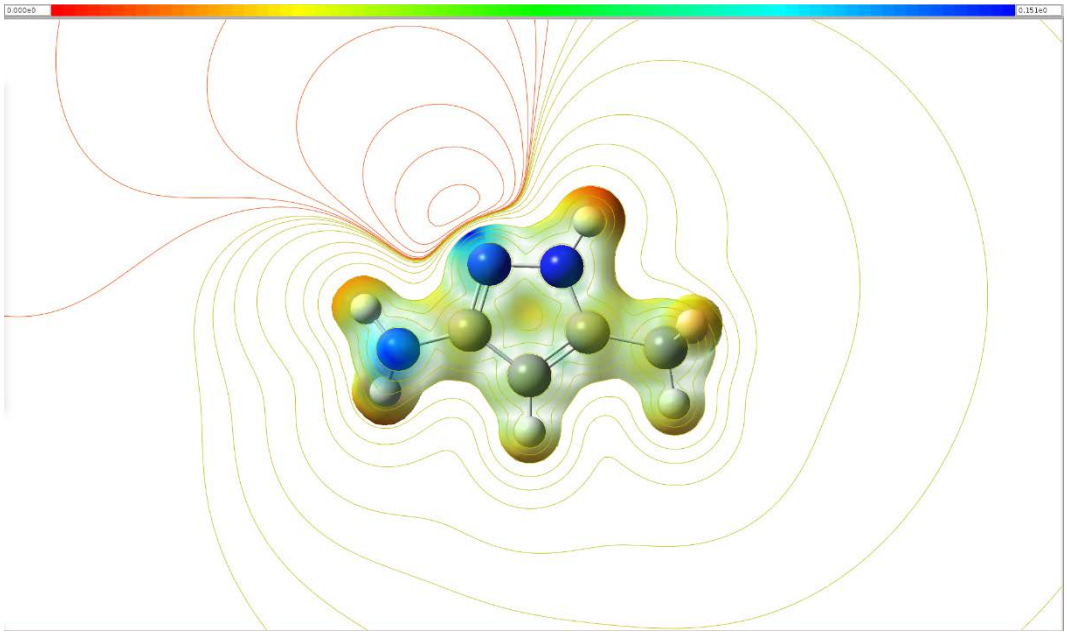

Figure B.127 - Molecular electrostatic potential map of 5-methylpyrazol-3-amine.

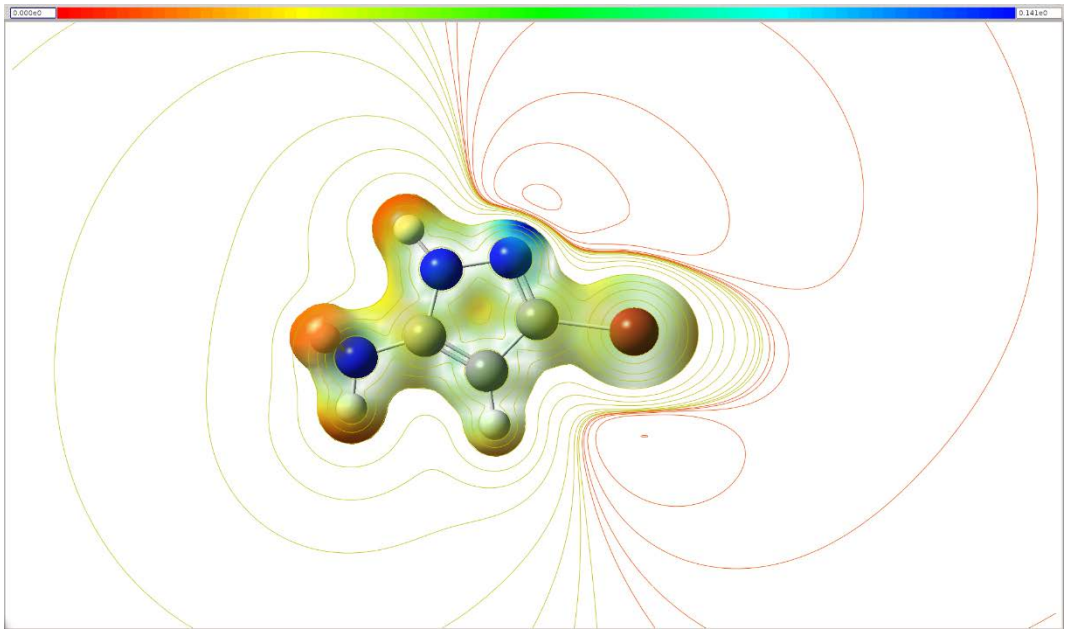

Figure B.128 - Molecular electrostatic potential map of 3-bromopyrazol-5-amine.

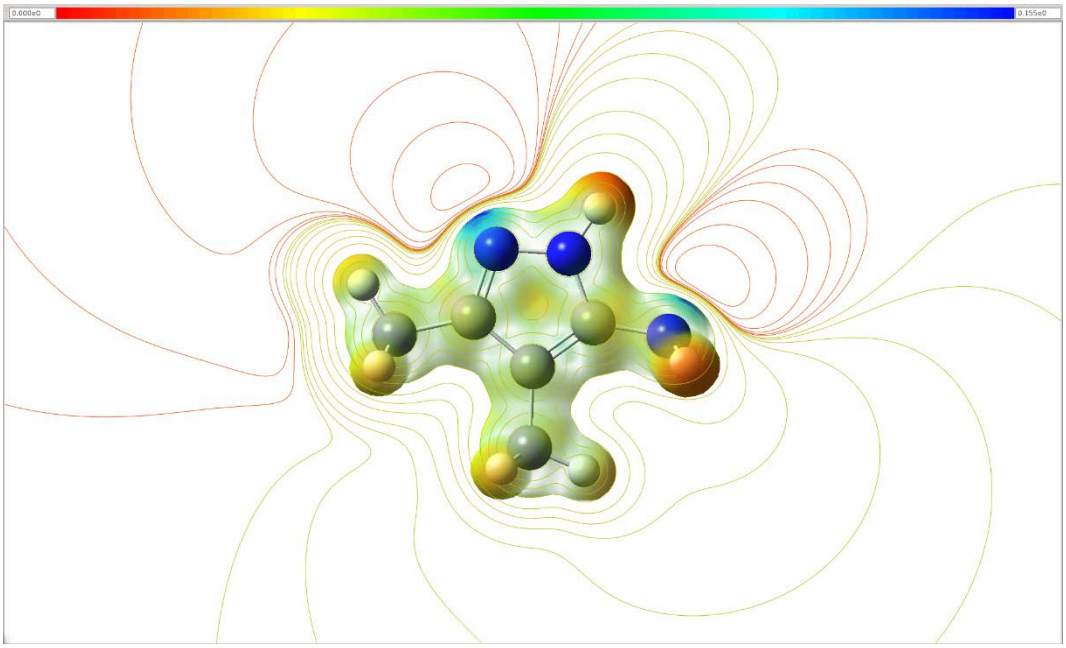

Figure B.129 - Molecular electrostatic potential map of 3,4-dimethylpyrazol-5-amine.

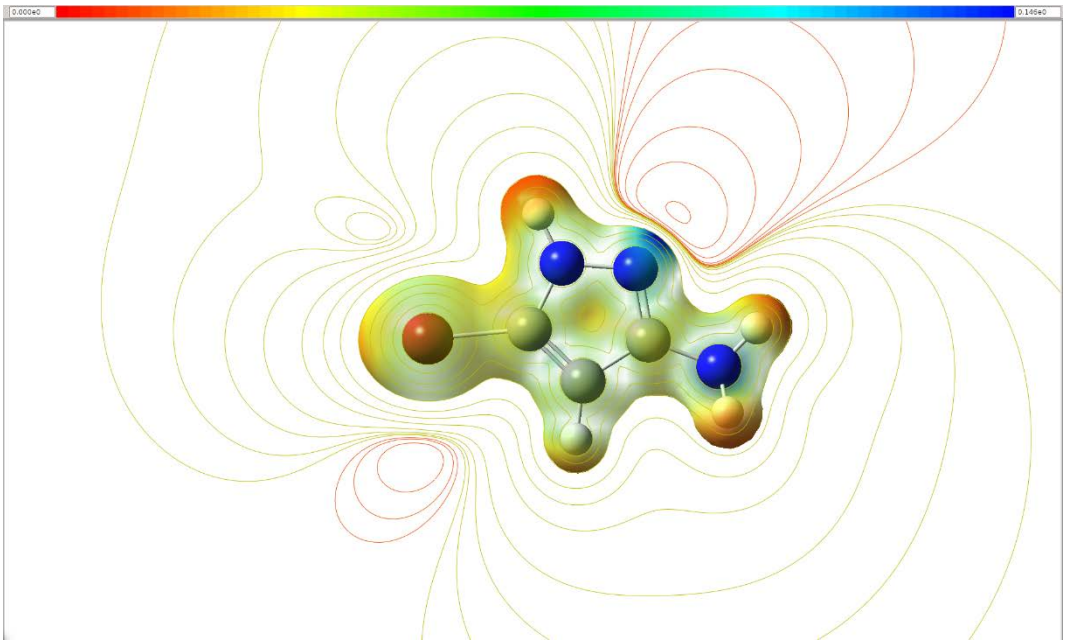

Figure B.130 - Molecular electrostatic potential map of 3-methyl-4-bromopyrazole.

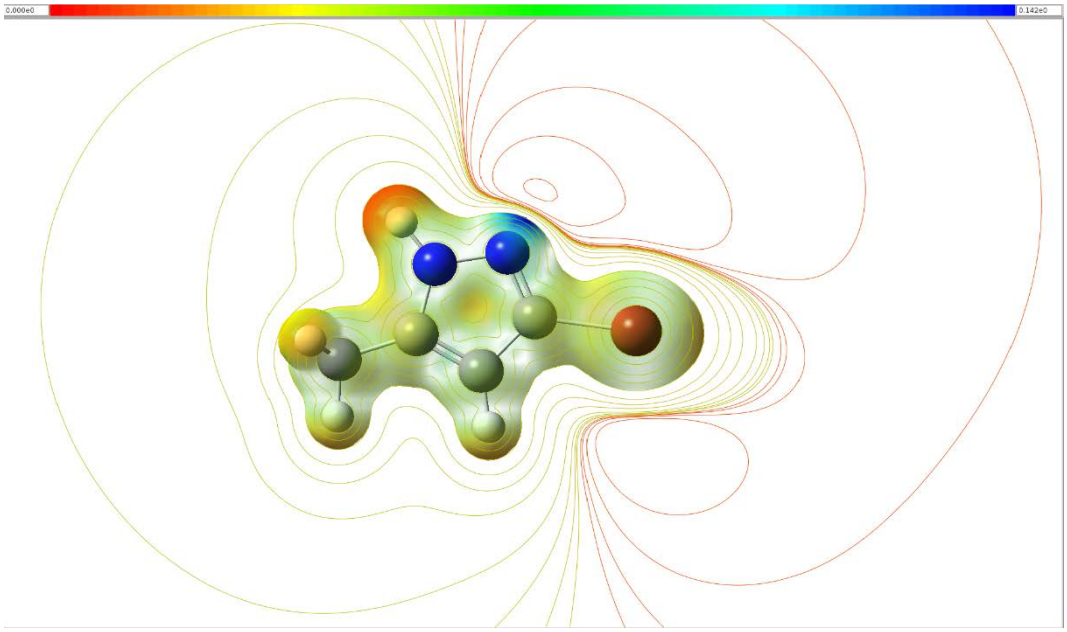

Figure B.131 - Molecular electrostatic potential map of 3-bromo-5-methylpyrazole.

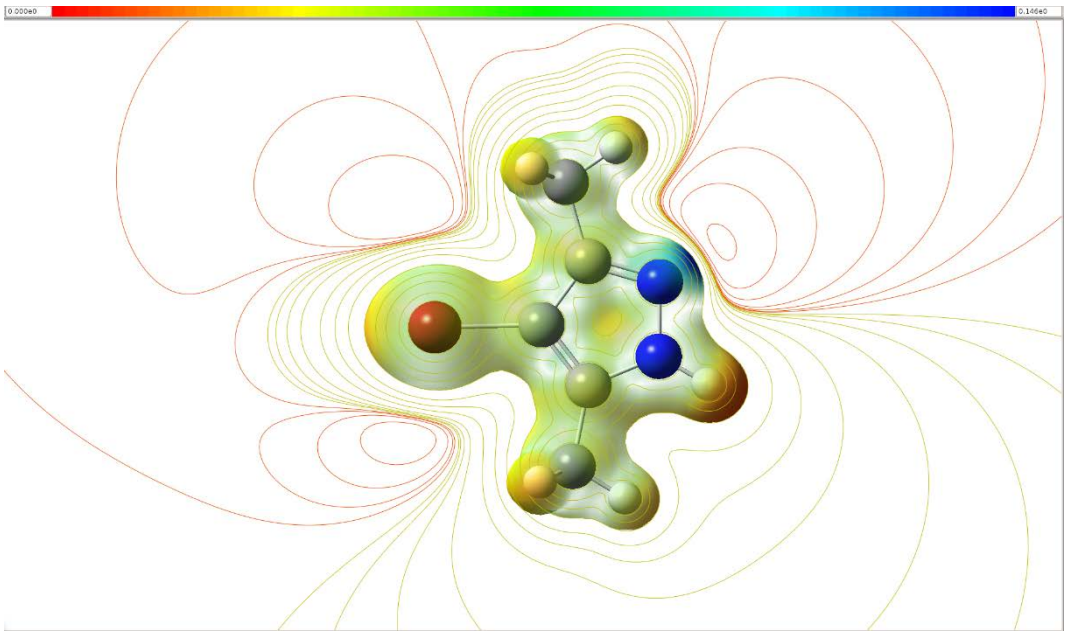

Figure B.132 - Molecular electrostatic potential map of 4-bromo-3,5-dimethylpyrazole.

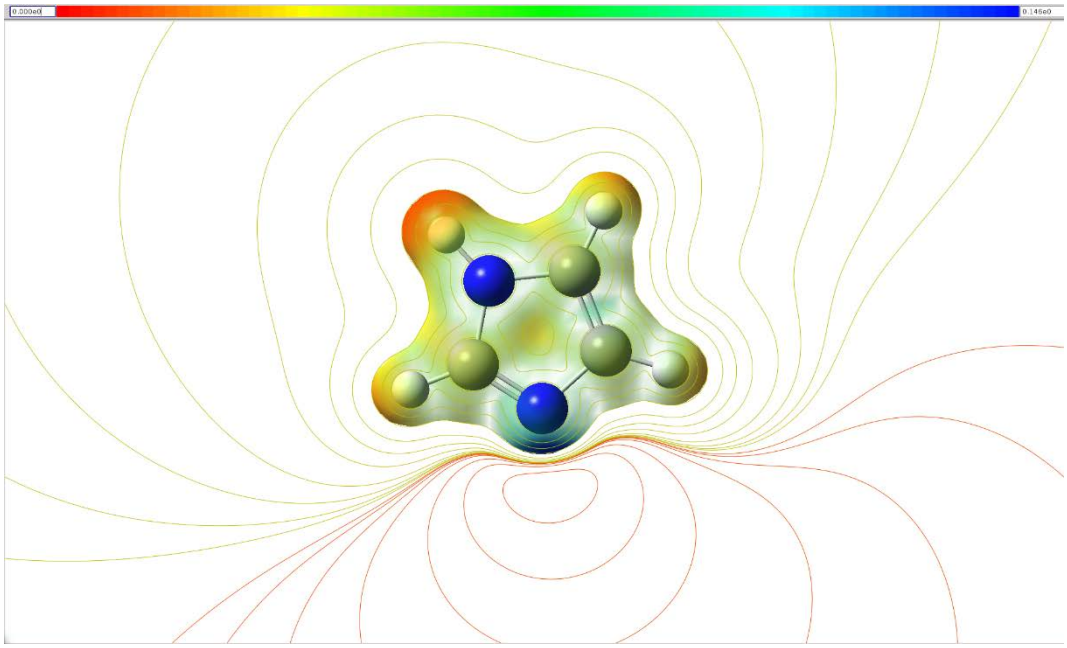

Figure B.133 - Molecular electrostatic potential map of imidazole.

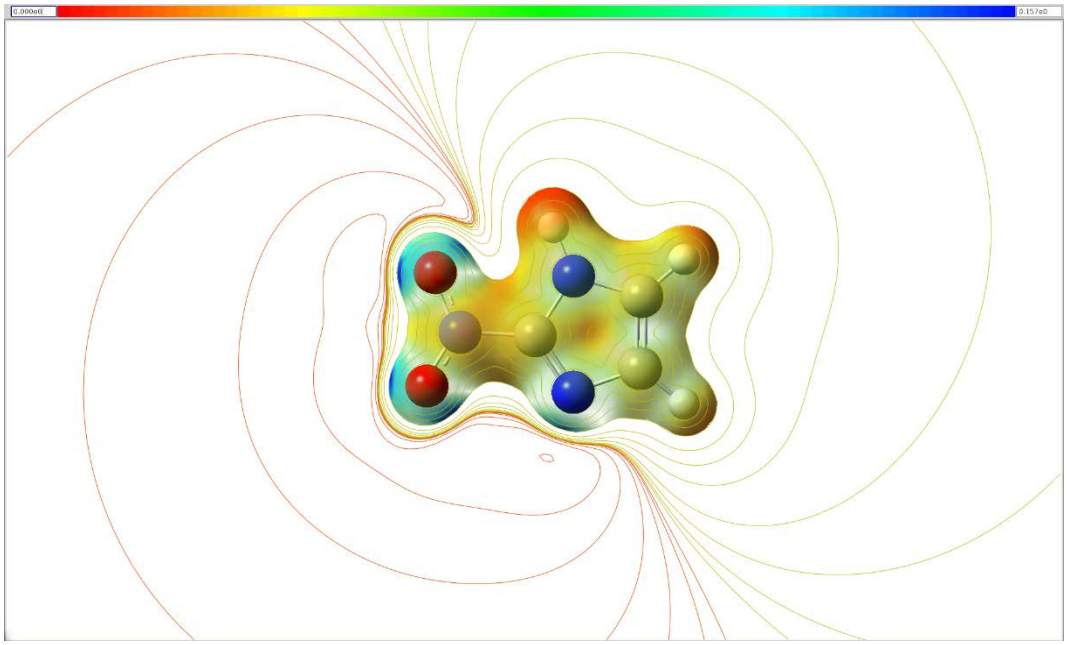

Figure B.134 - Molecular electrostatic potential map of 2-nitroimidazole.

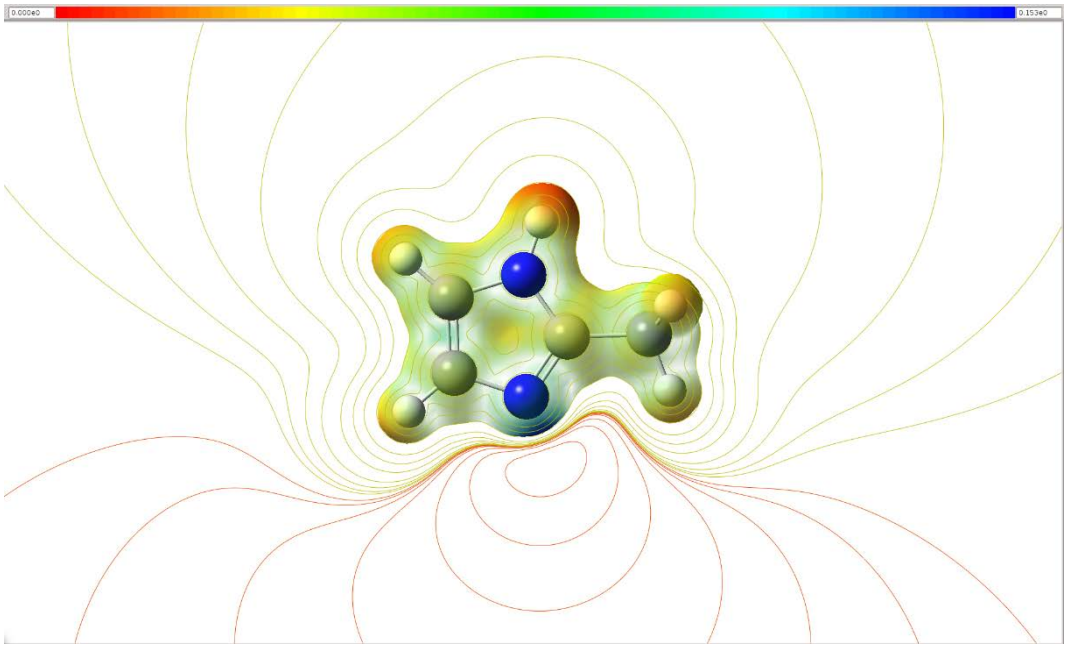

Figure B.135 - Molecular electrostatic potential map of 2-methylimidazole.

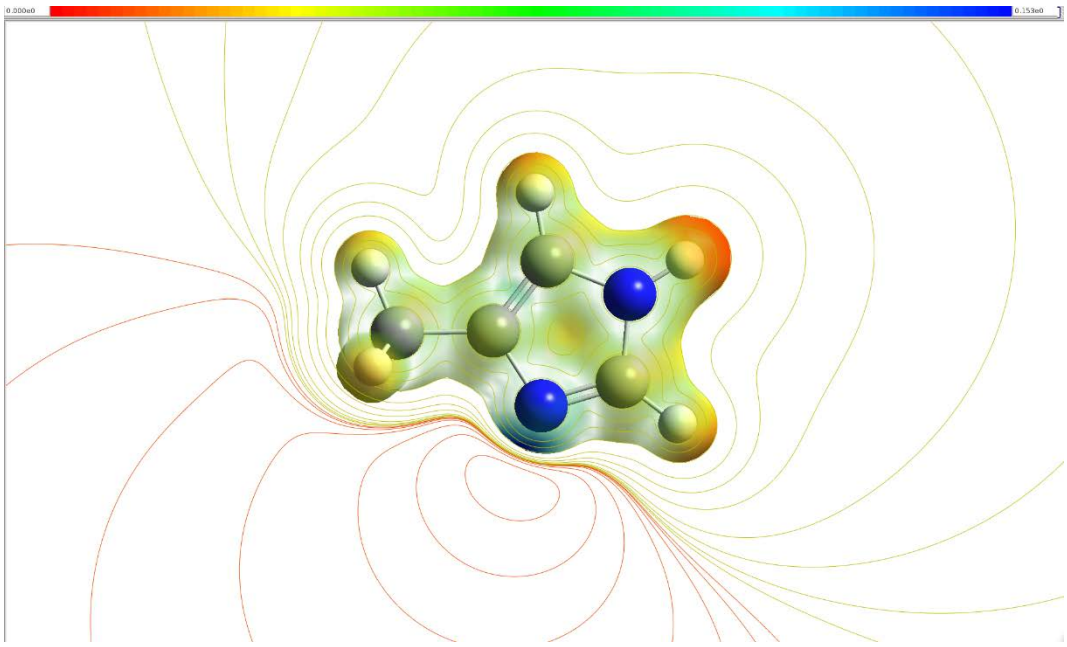

Figure B.136 - Molecular electrostatic potential map of 4-methylimidazole.

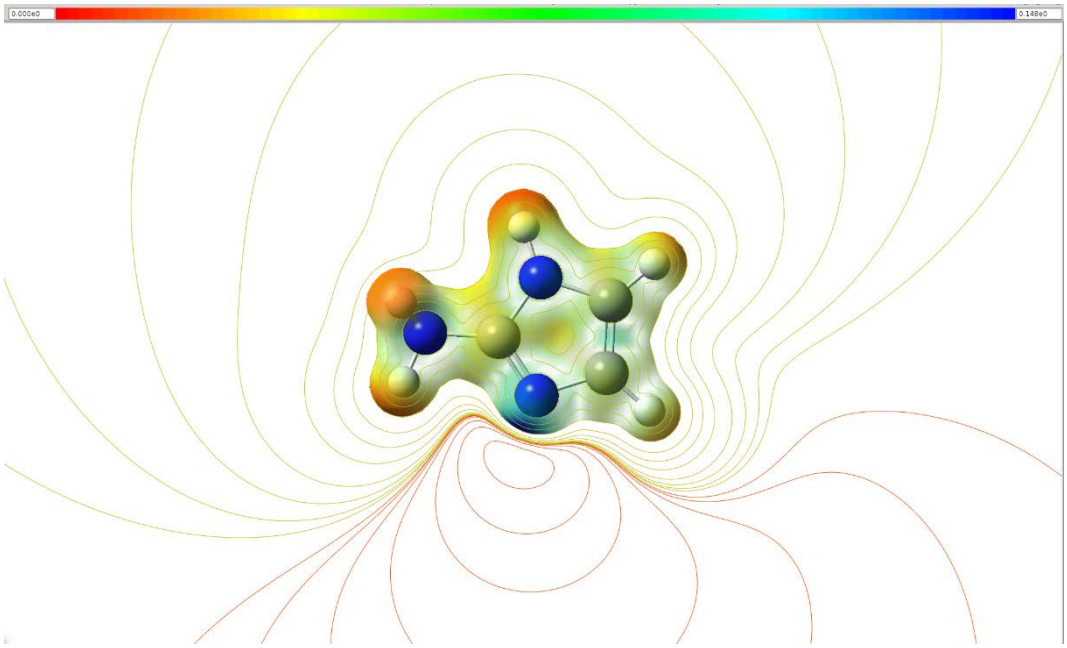

Figure B.137 - Molecular electrostatic potential map of imidazol-2-amine.

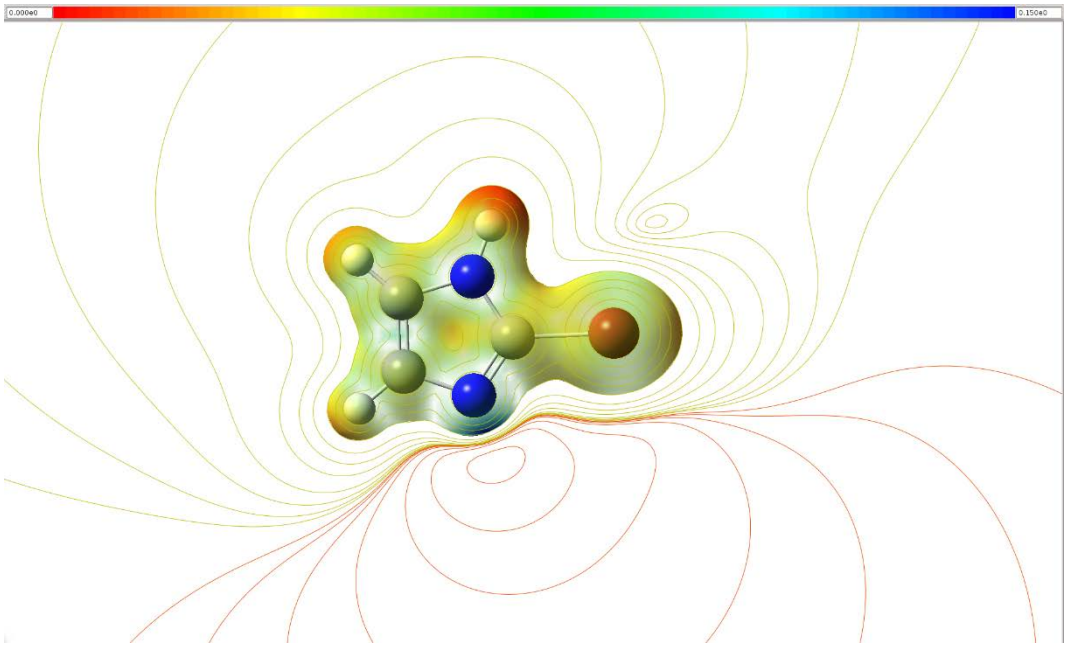

Figure B.138 - Molecular electrostatic potential map of 2-bromoimidazole.

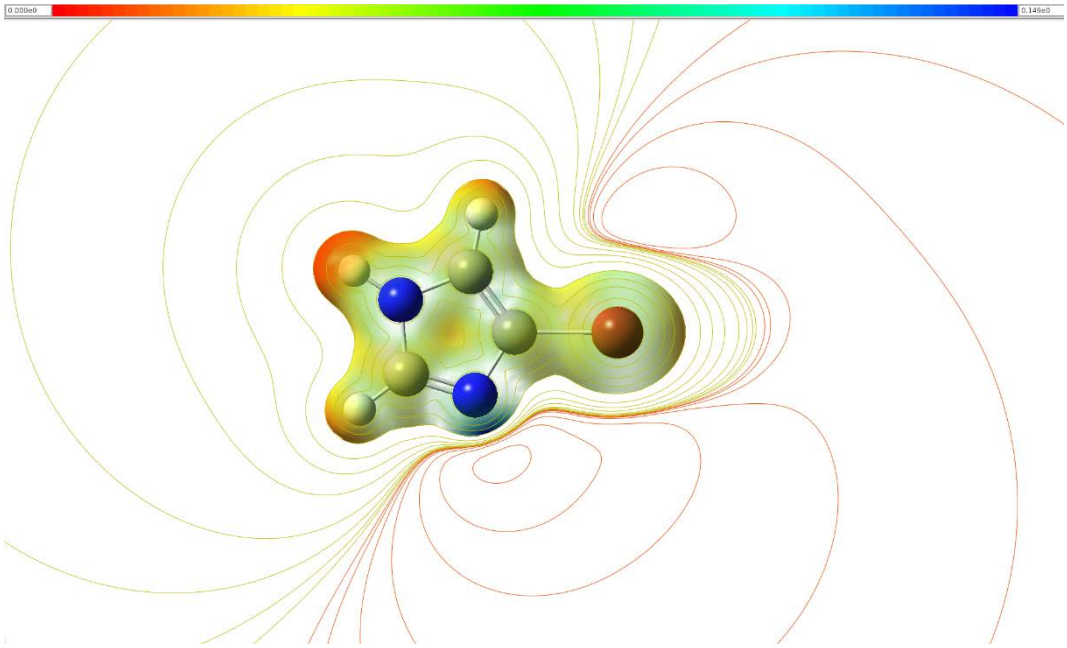

Figure B.139 - Molecular electrostatic potential map of 4-bromoimidazole.

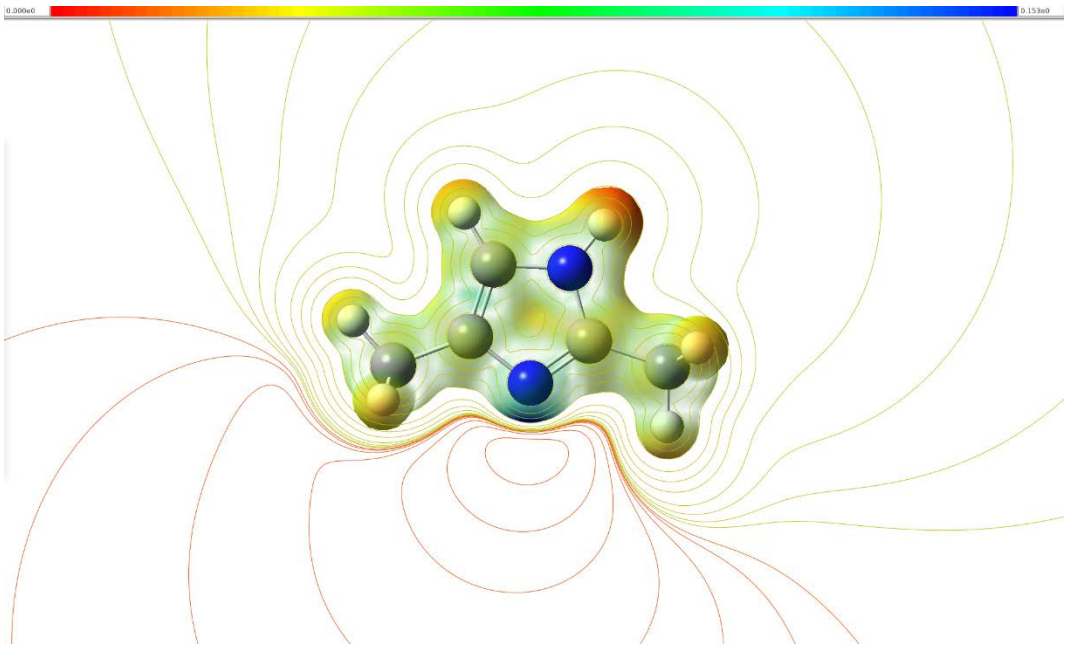

Figure B.140 - Molecular electrostatic potential map of 2,4-dimethylimidazole.

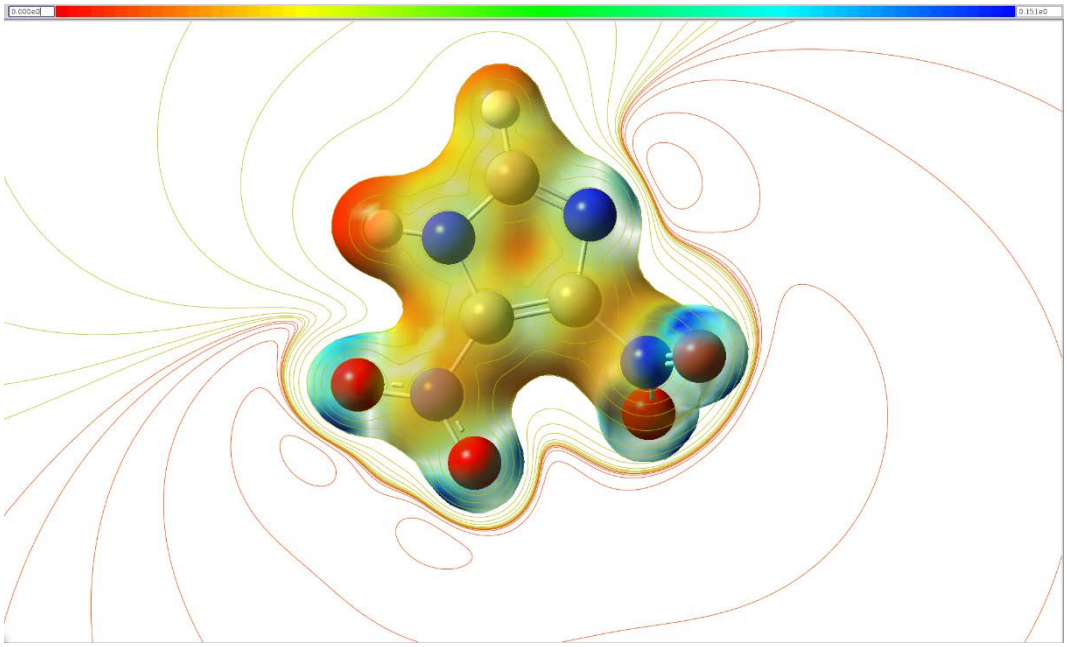

Figure B.141 - Molecular electrostatic potential map of 4,5-dinitroimidazole.

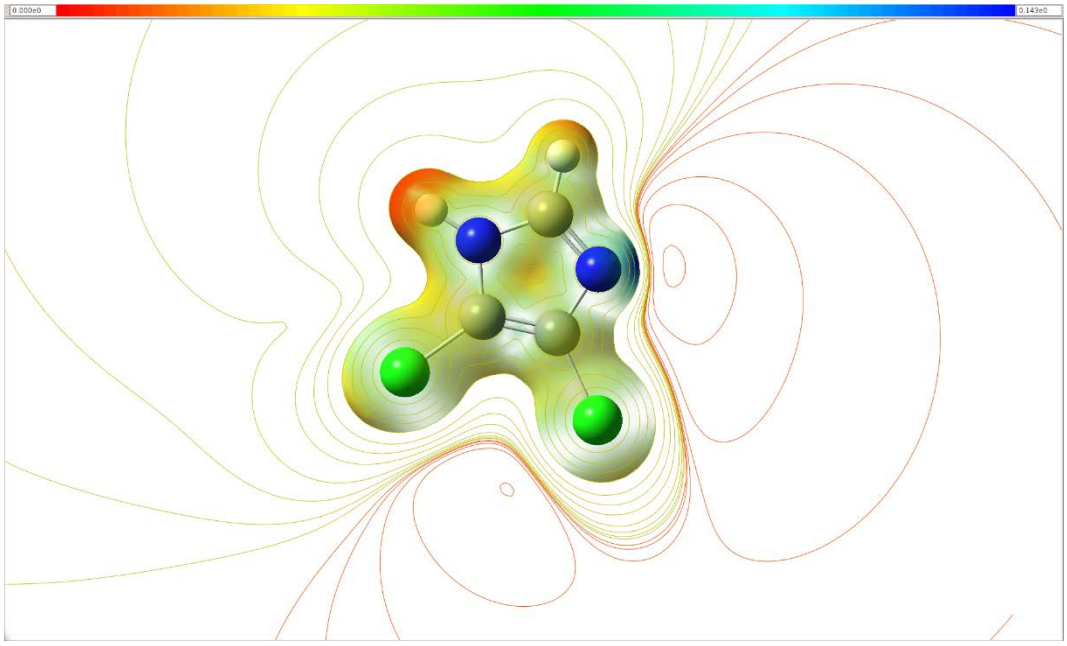

Figure B.142 - Molecular electrostatic potential map of 4,5-dichloroimidazole.

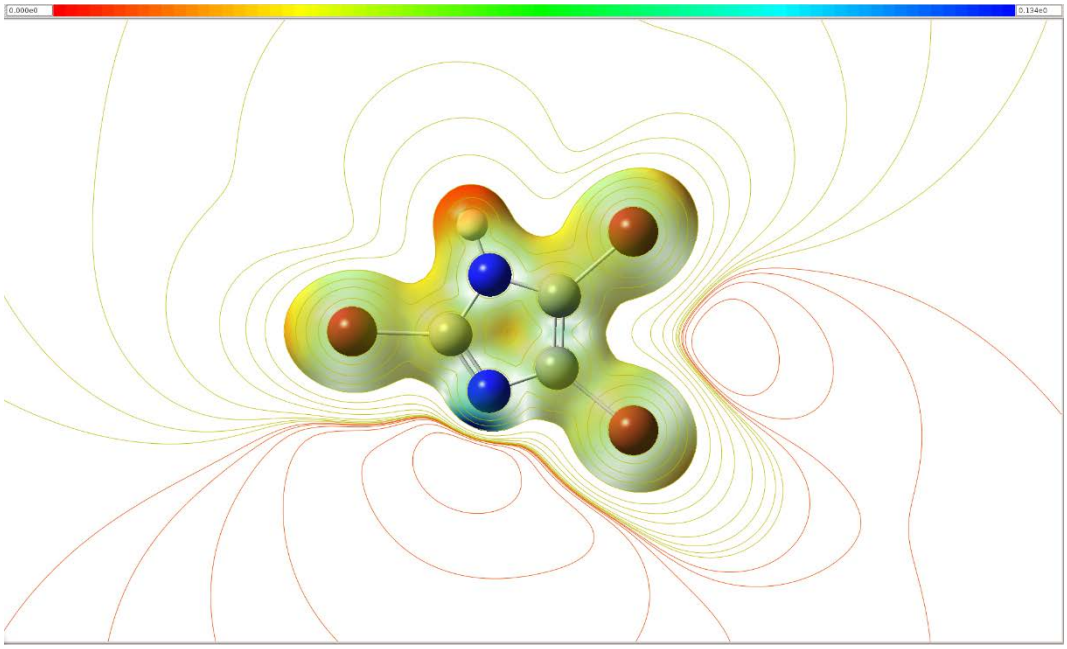

Figure B.143 - Molecular electrostatic potential map of 2,4,5-tribromoimidazole.

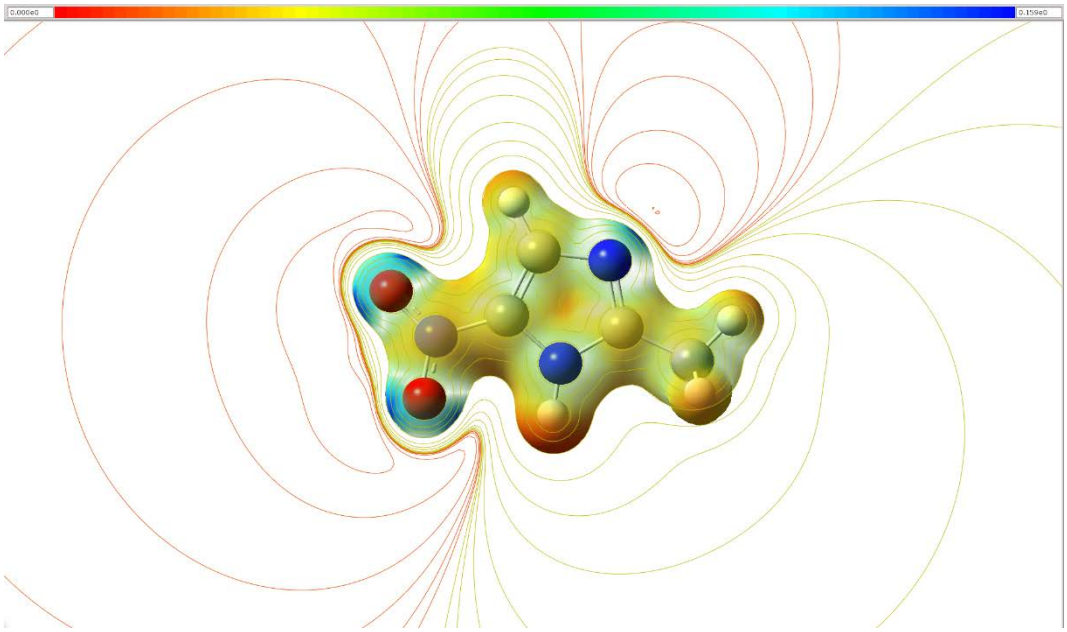

Figure B.144 - Molecular electrostatic potential map of 2-methyl-5-nitroimidazole.

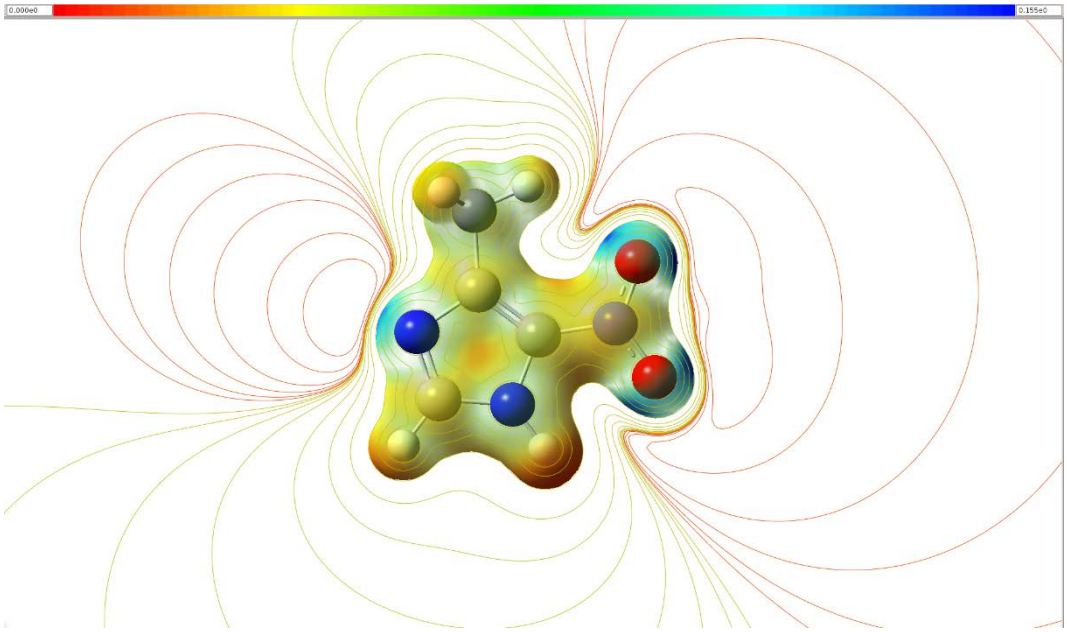

Figure B.145 - Molecular electrostatic potential map of 4-methyl-5-nitroimidazole.

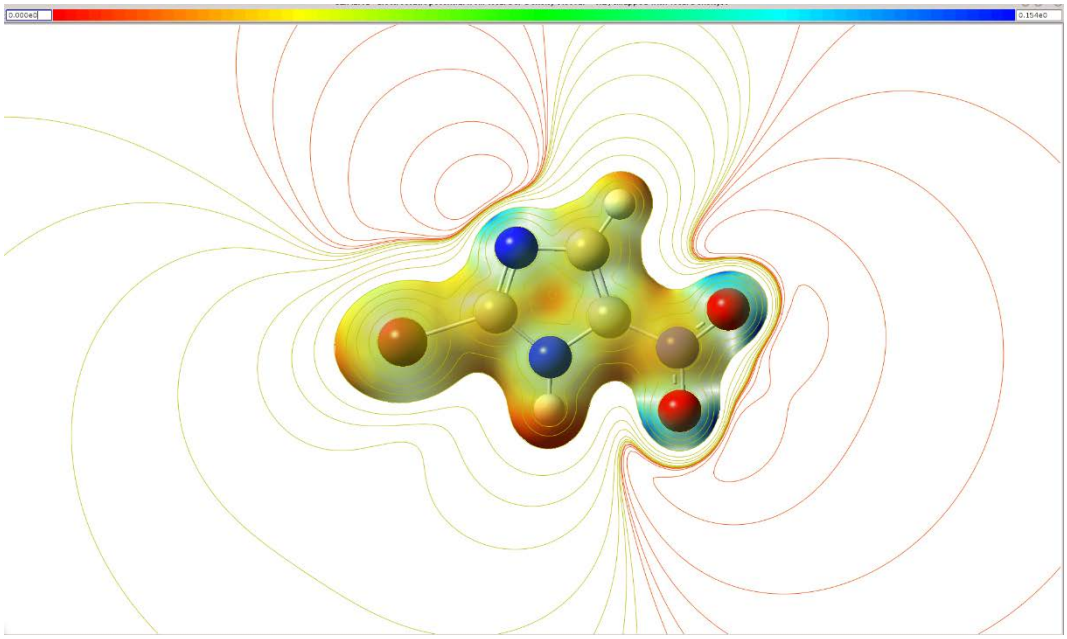

Figure B.146 - Molecular electrostatic potential map of 2-bromo-5-nitroimidazole.

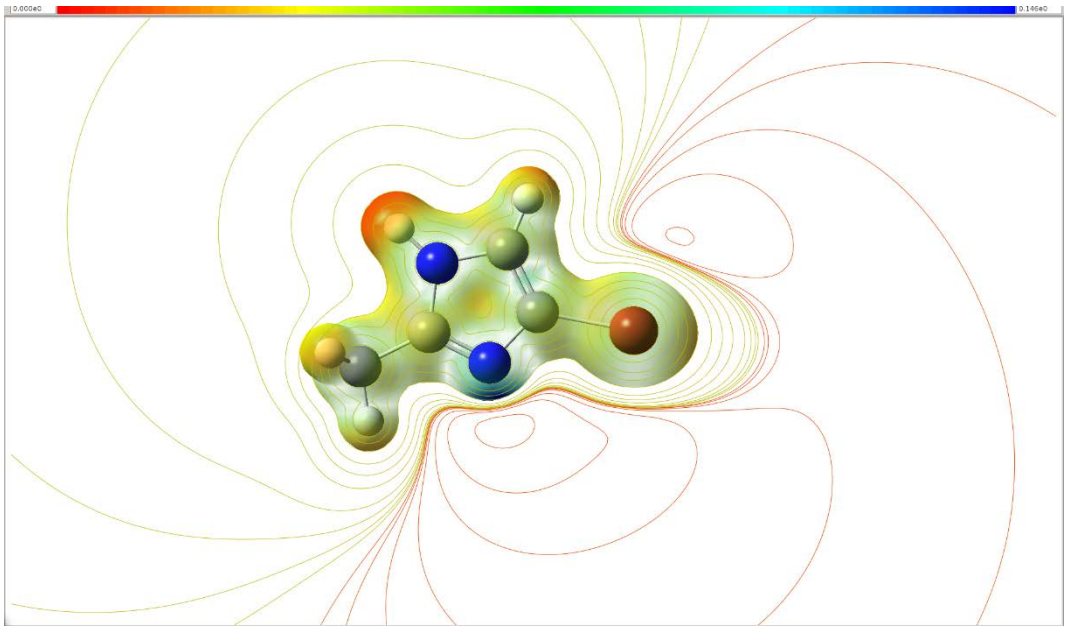

Figure B.147 - Molecular electrostatic potential map of 4-bromo-2-methylimidazole.

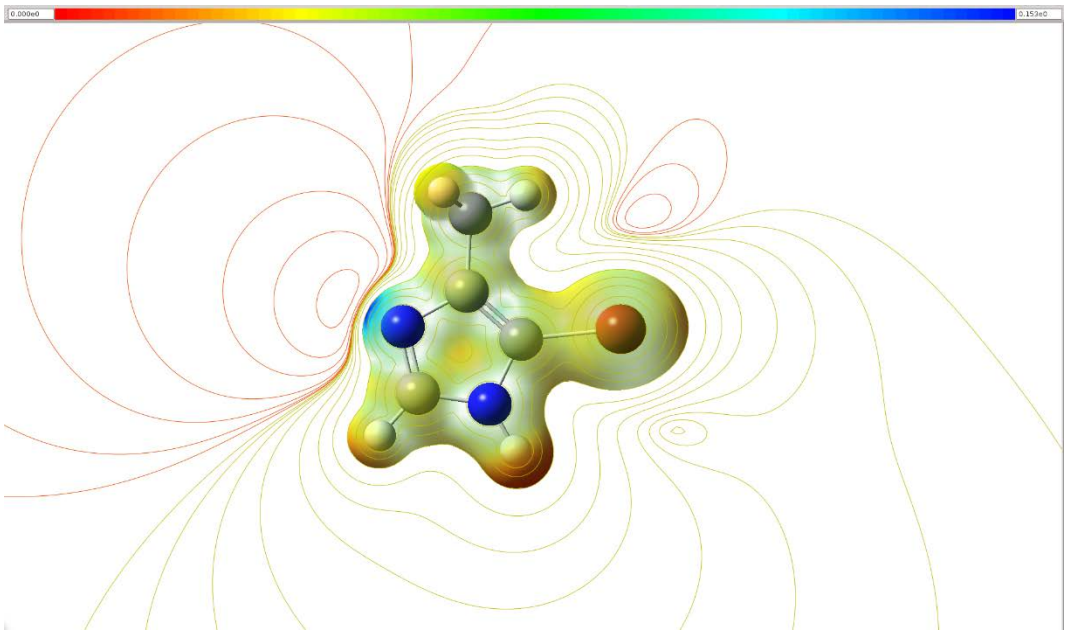

Figure B.148 - Molecular electrostatic potential map of 5-bromo-4-methylimidazole.

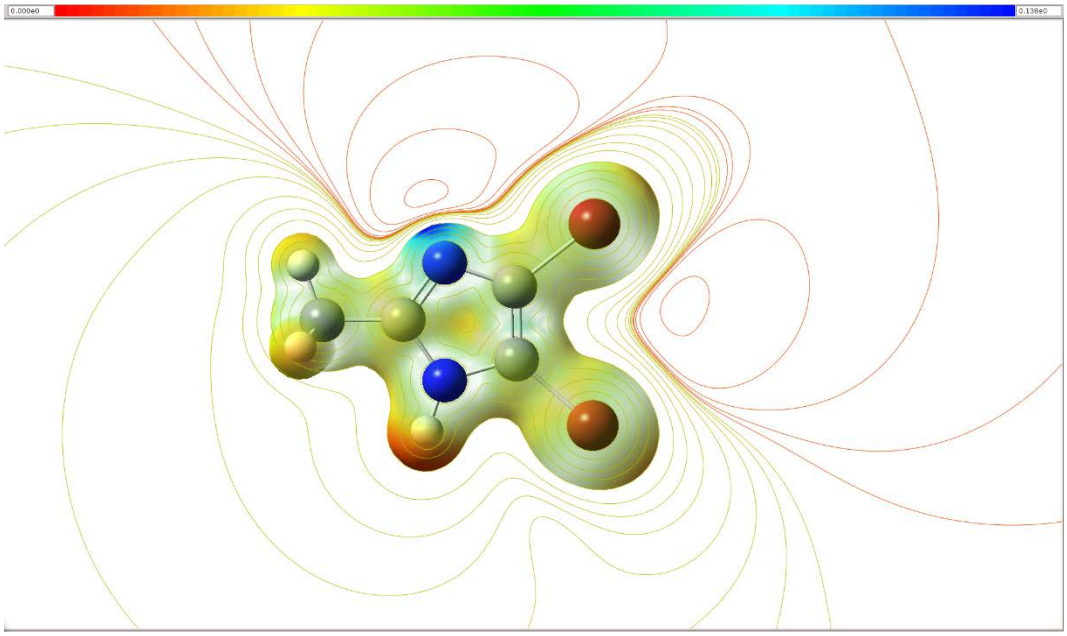

Figure B.149 - Molecular electrostatic potential map of 4,5-dibromo-2-methylimidazole.

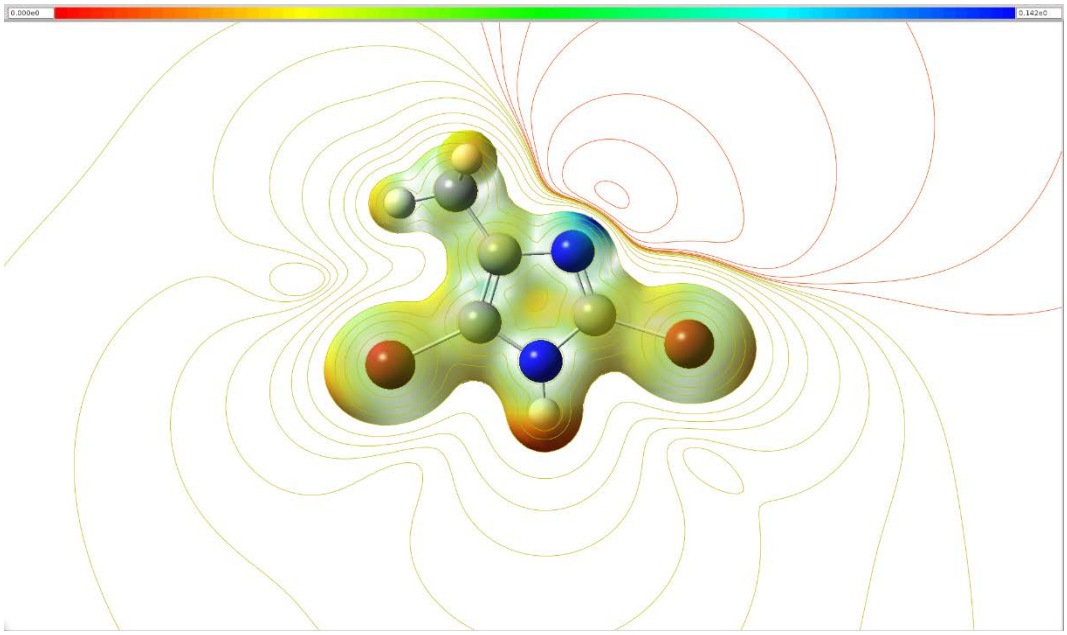

Figure B.150 - Molecular electrostatic potential map of 2,5-dibromo-4-methylimidazole.

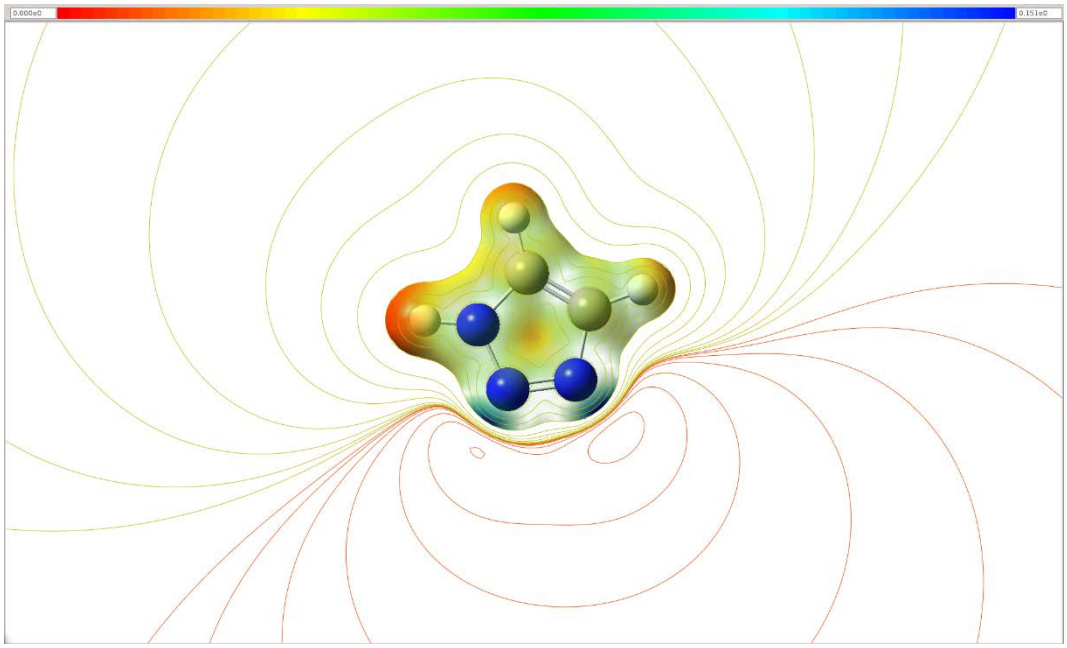

Figure B.151 - Molecular electrostatic potential map of 1,2,3-triazole.

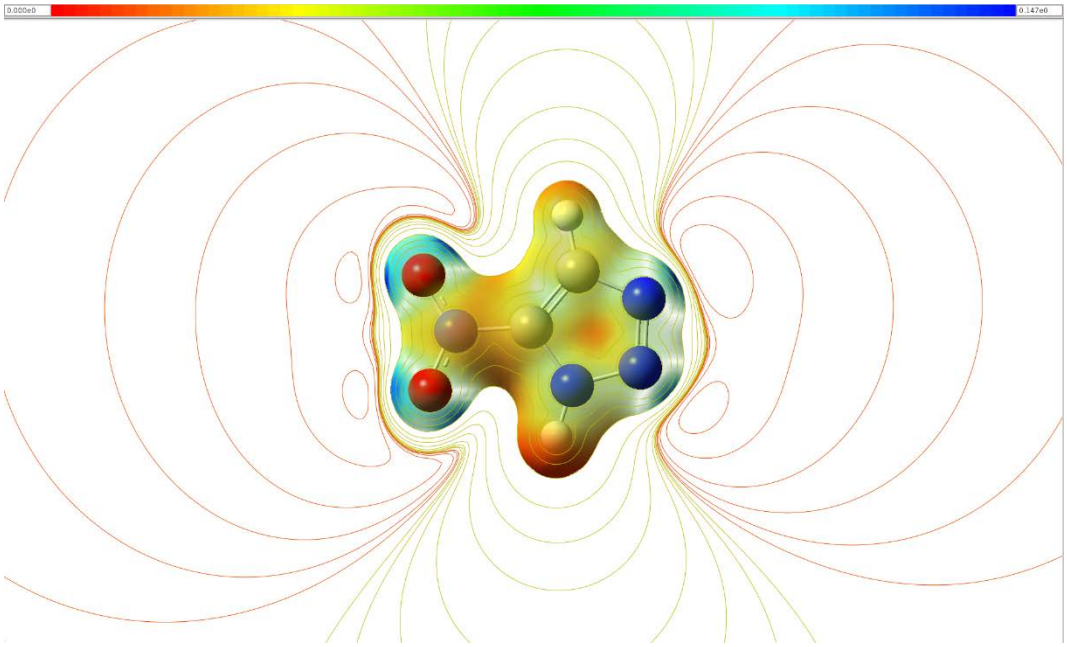

Figure B.152 - Molecular electrostatic potential map of 5-nitro-1,2,3-triazole.

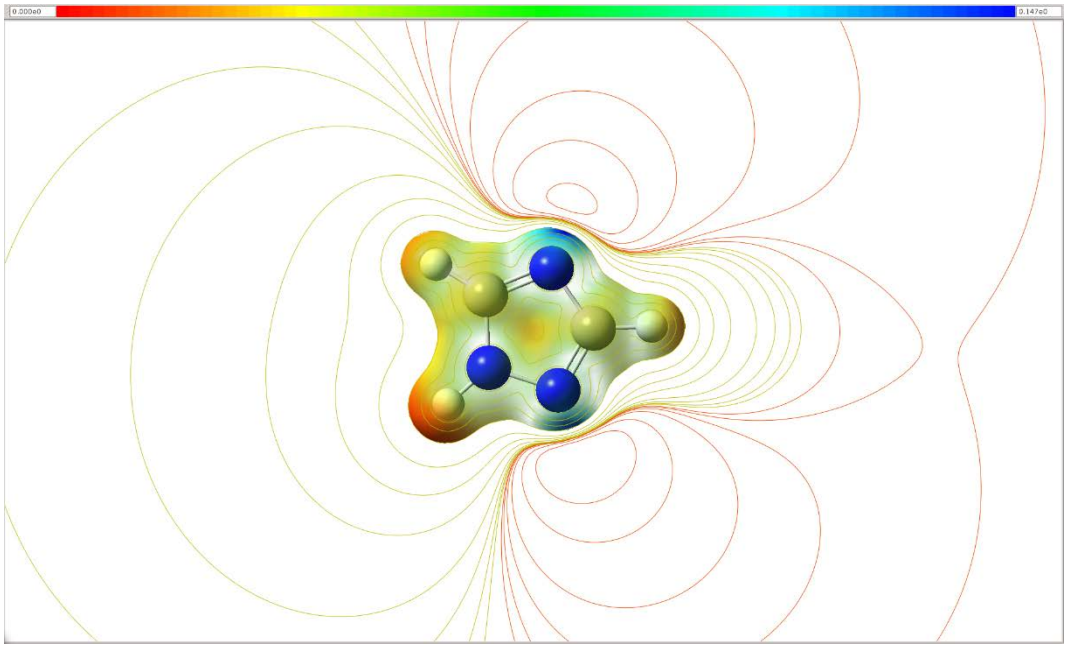

Figure B.153 - Molecular electrostatic potential map of 1,2,4-triazole.

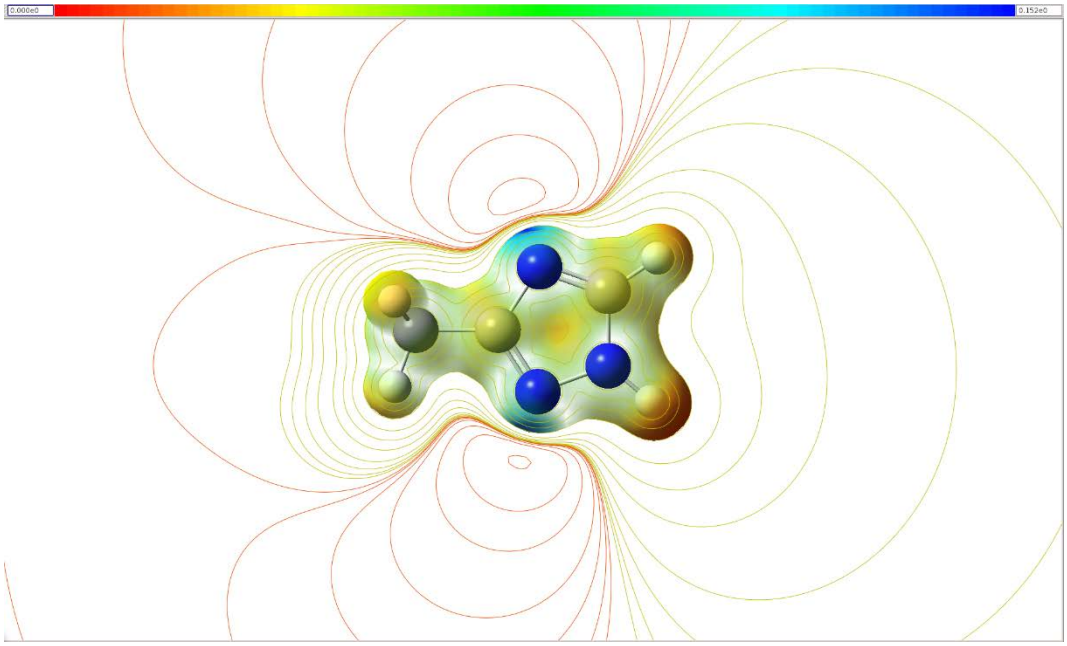

Figure B.154 - Molecular electrostatic potential map of 3-methyl-1,2,4-triazole.

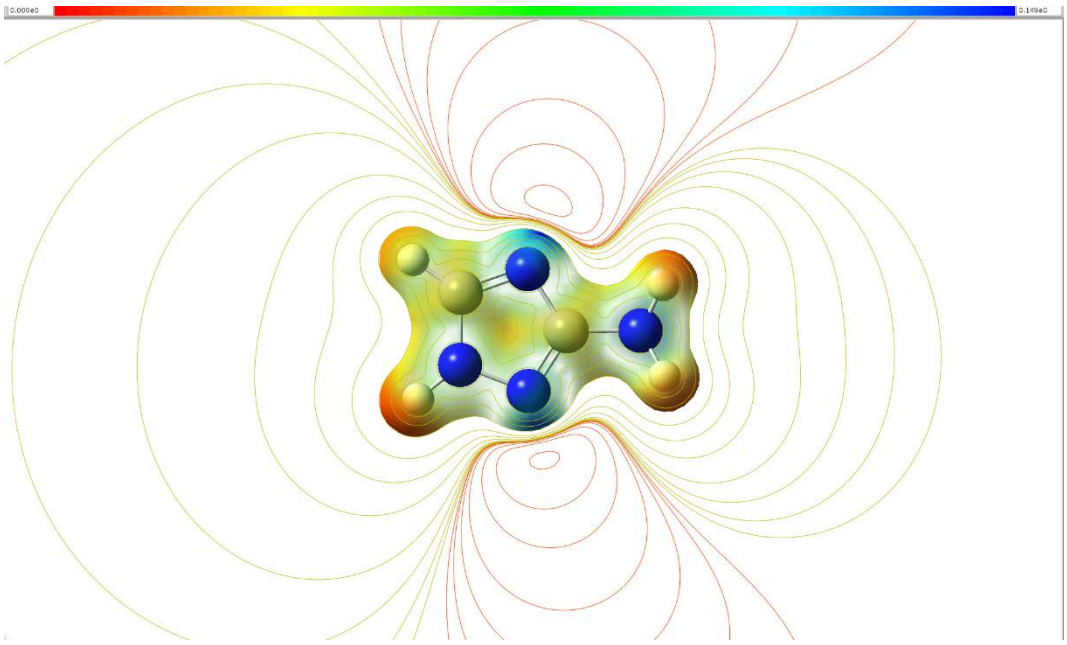

Figure B.155 - Molecular electrostatic potential map of 1,2,4-triazol-3-amine.

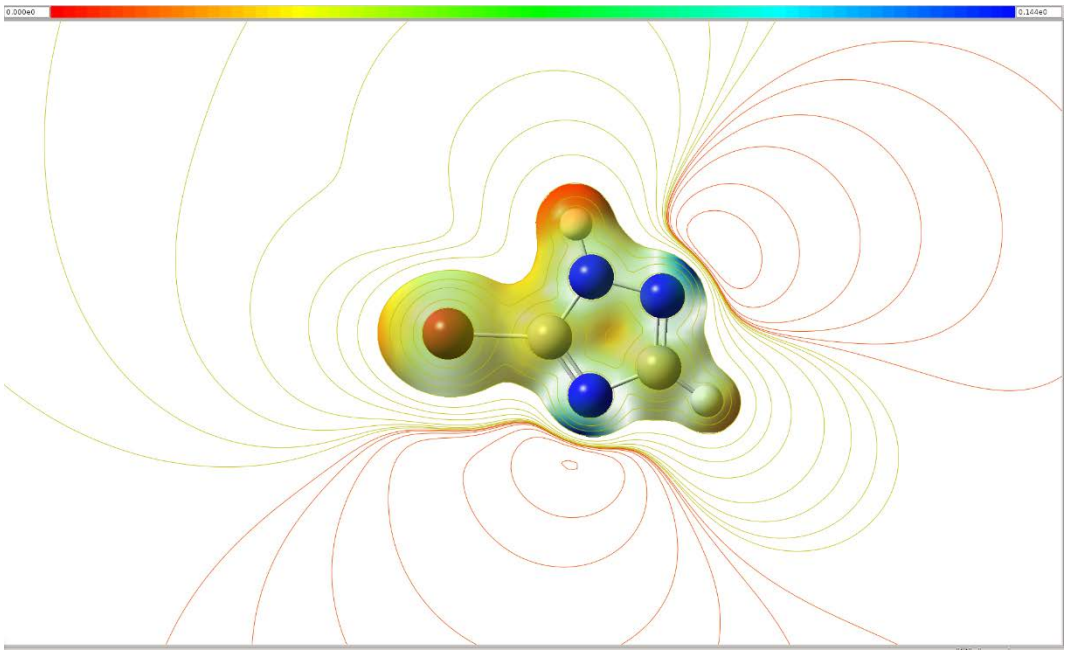

Figure B.156 - Molecular electrostatic potential map of 5-bromo-1,2,4-triazole.

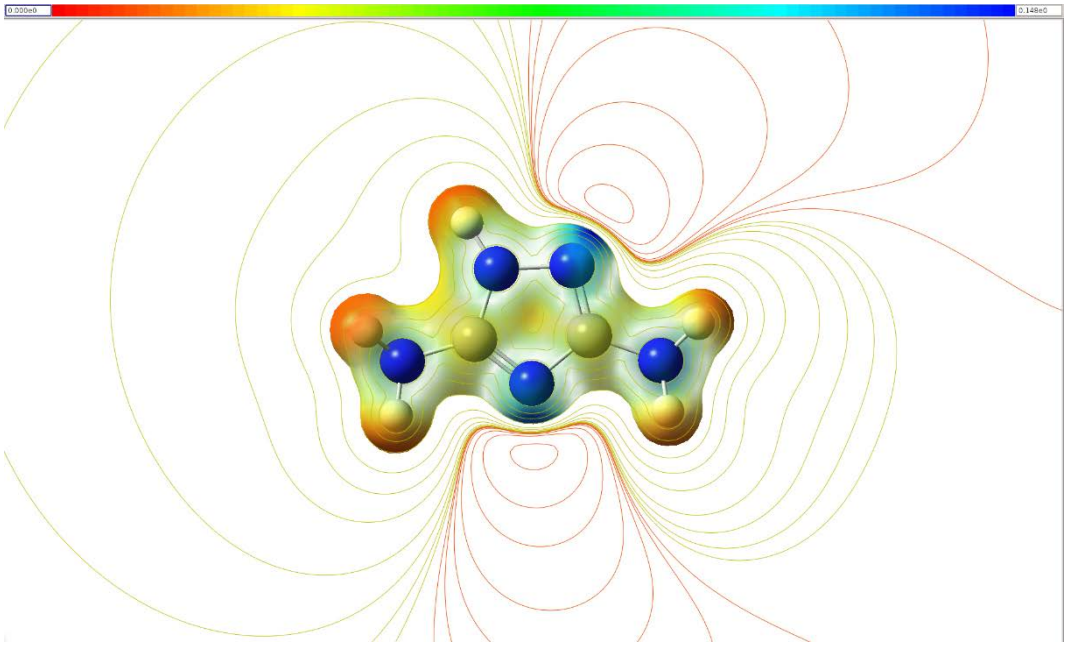

Figure B.157 - Molecular electrostatic potential map of 1,2,4-triazol-3,5-diamine.

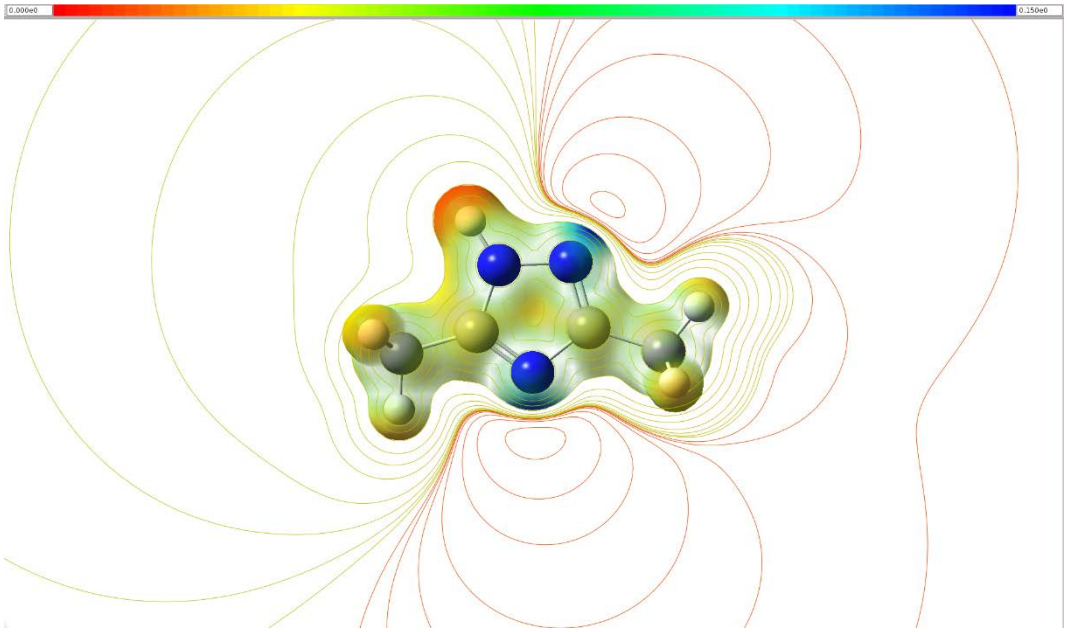

Figure B.158 - Molecular electrostatic potential map of 3,5-dimethyl-1,2,4-triazole.

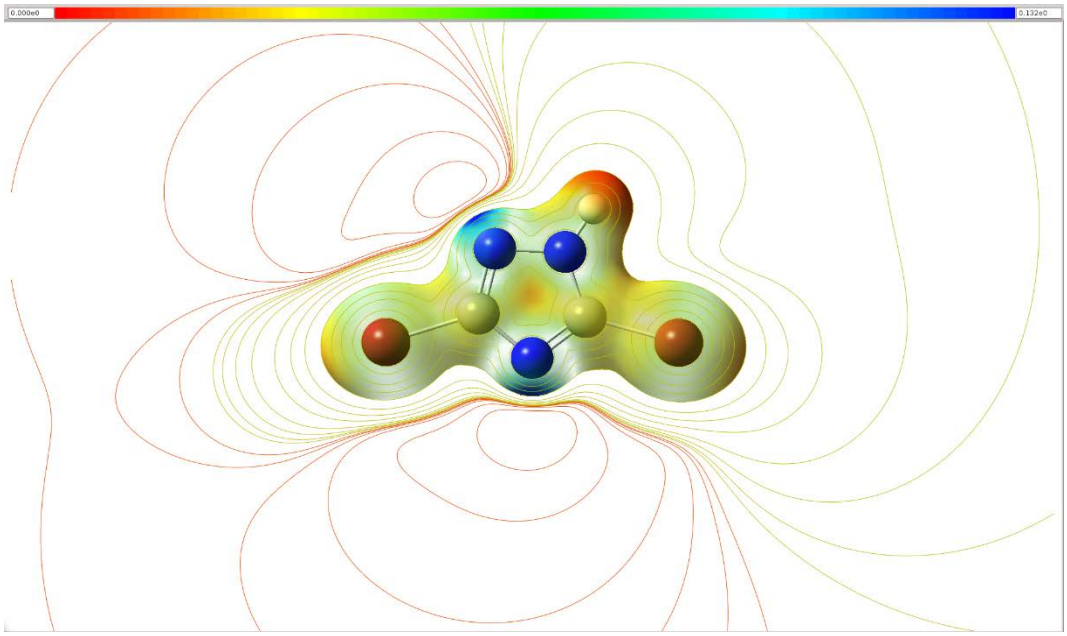

Figure B.159 - Molecular electrostatic potential map of 3,5-dibromo-1,2,4-triazole.

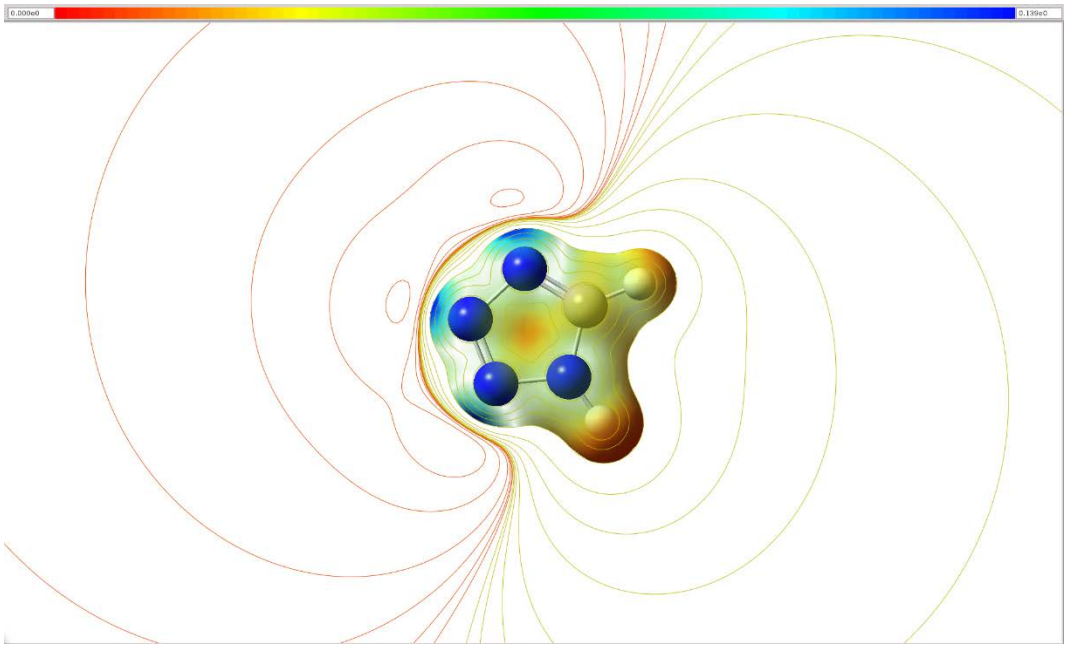

Figure B.160 - Molecular electrostatic potential map of 1,2,3,4-tetrazole.

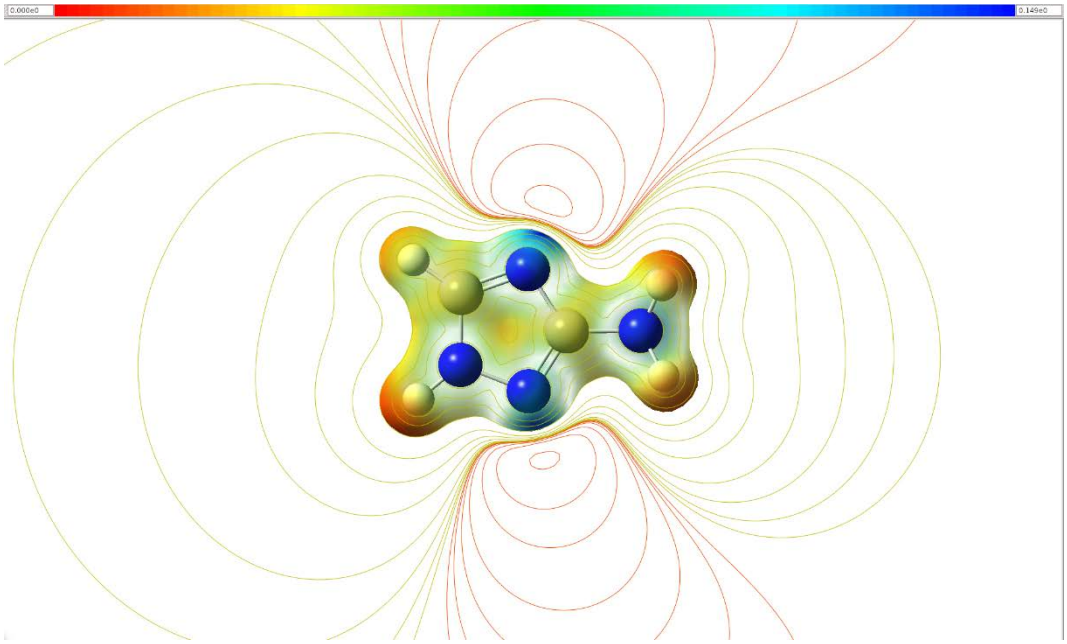

Figure B.161 - Molecular electrostatic potential map of 1,2,3,4-tetrazol-5-amine.

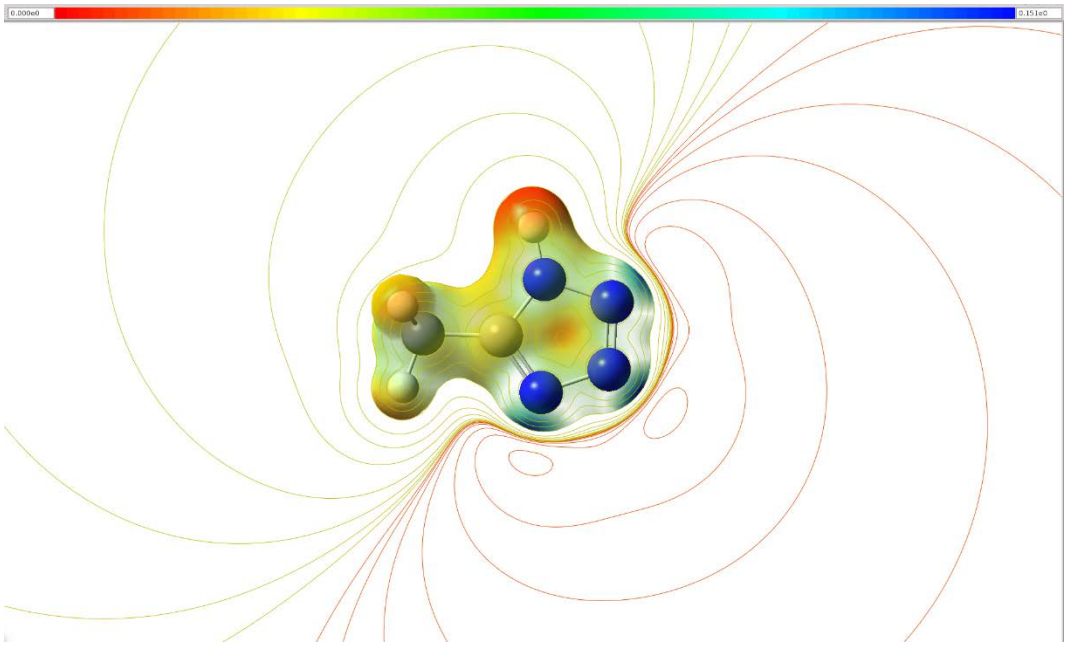

Figure B.162 - Molecular electrostatic potential map of 5-methyl-1,2,3,4-tetrazole.